Unnatural Amino Acids for Protein Modification by Oxime Ligation

Dissertation

Submitted for the Degree of

Doctor of Natural Sciences (Dr.rer.nat.)

Presented by

Vanessa Radtke

at the

Universität Konstanz

Faculty of Science

Department of Chemistry

Day of the Oral Examination:	29th November 2019
1st Referee:	Prof. Dr. Andreas Marx
2nd Referee:	Prof. Dr. Martin Scheffner

Danksagung

Die vorliegende Arbeit entstand von Januar 2015 bis Juni 2019 in der Arbeitsgruppe für Organische und Zelluläre Chemie von Prof. Dr. Andreas Marx an der Universität Konstanz.

Zuallererst bedanke ich mich bei Prof. Dr. Andreas Marx für die Aufnahme in seine Arbeitsgruppe und für die Bereitstellung des interessanten Themas. Darüberhinaus bin ich ihm sehr dankbar für sein Vertrauen, seine Unterstützung und die wissenschaftlichen Diskussionen. Auch in herausfordernden Projektphasen konnte ich daraus immer wieder neue Motivation ziehen.

Prof. Dr. Martin Scheffner danke ich für die Erstellung des Zweitgutachtens, für die spannende Kooperation und die wissenschaftlichen Diskussionen. Prof. Dr. Jörg Hartig danke ich für die Übernahme des Prüfungsvorsitzes.

Der Konstanz Research School Chemical Biology und dem SPP1623 danke ich für die guten Bildungsangebote.

Moritz Schmidt und Prof Dr. Daniel Summerer danke ich für die Hilfestellung beim Screening von PylRS Bibliotheken und die Bereitstellung dieser.

Bei Simon Geigges und Alexandra Julier bedanke ich mich für die produktive und spannende Zusammenarbeit. Allen Mitgliedern der AG Marx, besonders denen in Chemie Box 5 und Bio Box 1, danke ich für die schöne Arbeitsatmosphäre und die große Hilfsbereitschaft im Labor.

Mein Dank gilt auch meinen Praktikanten während meiner Protomtionszeit. Giuliano Bayer danke ich für die große Hilfe bei der Generierung und dem Testen vieler PylRS Mutanten. Hanna Bähr und Iljas Müller danke ich für die Synthese von Aminosäuren.

Martina Adam danke ich für die Generierung verschiedener PylRS Mutanten und Meike Liebmann und Anke Gerull danke ich für die Synthese von Aminosäuren.

Ein großes Dankeschön gilt Alexandra Julier, Joachim Lutz, Heike Kropp, Maite Mißun und Simon Geigges für das schnelle Korrekturlesen von Teilen dieser Arbeit.

All meinen Freunden danke ich für die wundervolle Zeit in Konstanz und bei meinen Heimatbesuchen. Besonders die 15 Uhr-Pausen und die Unternehmungen mit den „Freizeitfreunden“ und den „AG-Marx-Mädels“ waren ein perfekter Ausgleich zum Laboralltag.

Mein ganz besonderer Dank gilt meinem Freund Fritz für seine bedingungslose Unterstütztung, seine Aufmunterung, wenn es mal nicht so gut lief, und die wunderschöne Zeit, die wir immer miteinander haben. Ebenso danke ich meiner Familie, besonders meinen Eltern, Helmut und Gabi, für ihre volle Unterstützung in allen Lebenslagen.

Zusammenfassung

Monoubiquitinierung ist eine posttranslationale Modifikation, die in der Natur bei einer Vielzahl von Proteinen vorkommt. Verschiedene Forschungsergebnisse ergaben, dass die Eigenschaften von Proteinen, darunter die subzelluläre Lokalisation[1-2], die biologische Funktion[3] und Protein–Protein-Wechselwirkungen[4], durch Monoubiquitinierung verändert werden können. Allerdings ist bisher nur wenig darüber bekannt, welchen Einfluss die Position der Ubiquitinierung auf die Eigenschaften des entsprechenden Proteins hat. Ein Grund dafür könnte die eingeschränkte Verfügbarkeit von ortsspezifisch monoubiquitinierten Proteinen sein.

Ubiquitin ist durch eine Isopeptidbindung zwischen seinem C-Terminus und einer Lys-Seitenkette des Substrats mit dem Protein verknüpft. Diese Isopeptidbindung kann durch in Zellen vorhandene DUBs gespalten werden. Die biochemische Untersuchung von Protein–Ub-Konjugaten in Zellen und im Zelllysat kann durch ein Isopeptid-Mimetikum, das gegen DUBs stabil ist, ermöglicht werden. Triazole, die durche kupferkatalysierte Azid-Alkin-Cycloaddition generiert werden, wurden bereits erfolgreich als Isopeptid-Mimetikum für Protein–Ub-Konjugate vergewendet.[5-6] Allerdings kann die Behandlung von Proteinen mit Kupfer unter physiologischen Bedingungen problematisch sein, da z.B. reaktive Sauerstoffspezies gebildet werden können.[7] Daher werden mildere Reaktionen für die Imitierung einer Isopeptid-Bindung benötigt.

In diesem Projekt sollte die Oximligation – die Reaktion zwischen einer Aminooxygruppe und einer Carbonylspezies – als milde Ligationsmethode zur ortsspezifischen Ubiquitinierung von Proteinen untersucht werden. Daher wurden neue, aminooxy-modifizierte Aminosäuren synthetisiert und durch Stop-Codon-Suppression in Proteine eingebaut. Damit das beteiligte Enzym, PylRS, diese Aminosäuren als Antwort auf ein Stop-Codon in die Proteinkette einbaut, wurden verschiedene Mutationen in dessen Aminosäure-Bindungstasche eingefügt. Aus diesem Pool wurden Mutanten identifiziert, die diesen Vorgang begünstigen. Die aminooxy-modifizierten Aminosäuren wurden mit Carbamat-basierten Schutzgruppen versehen, die als Erkennungsmerkmal für die jeweiligen PylRS-Mutanten dienten und um Nebenreaktionen mit endogenen Carbonylverbindungen zu verhindern. Diese Schutzgruppen konnten auf dem Protein nach der Expression abgespalten werden.

Ausgewählte Proteine wurden ortsspezifisch mit diesen Aminosäuren modifiziert und die Reaktionspartner wurden mit einer Carbonylfunktionalität ausgestattet. Daraufhin wurde die Oximligation für die Generierung von ortsspezifisch verknüpften Protein–Protein-Konjugaten DNA Pol β–Ub, H1.2–Ub und p53–Ub untersucht. Die Ergebnisse deuten darauf hin, dass DNA Pol β und H1.2 durch Oximligation ubiquitiniert wurden. Außerdem wurde in Kooperation mit Alexandra Julier (AG Scheffner, Universität Konstanz) das erste Mal ein

funktionales, positionsspezifisch ubiquitiniertes p53-Konjugat synthetisiert. Die oxim-verknüpften p53–Ub-Konjugate waren gegen Hydrolyse durch DUBs stabil. Wie auch p53 wurde dieses Konjugat von Interaktionspartnern erkannt, was auf die korrekte Faltung von p53 nach der Oximligation hindeutet.

Folglich wurden unterschiedliche Aminosäuren erfolgreich durch Stop-Codon-Suppression mit in dieser Arbeit identifizierten PylRS Mutanten in Proteine eingebaut, um diese ortsspezifisch mit Aminooxygruppen zu funktionalisieren und durch Oximligation zu ubiquitinieren. Diese Ergebnisse lassen auf die Eignung der Oximligation für die ortsspezifische Imitierung der Ubiquitinierung unter milden Bedingungen schließen und stellen die Grundlage für weitere Untersuchungen dieser Konjugate dar.

Abstract

Mono-ubiquitination is a post-translational modification that has been observed and studied for various proteins. The properties of a protein, such as the subcellular location[1-2], the biological function[3], and protein–protein interactions[4] can be altered by protein mono-ubiquitination. However, only few is known about the influence of the site of ubiquitination on the protein's fate. That might be due to the restricted accessibility of site-specifically mono-ubiquitinated proteins.

Ub is connected to proteins by an isopeptide bond between the C-terminus of Ub and a Lys side chain of the substrate. These isopeptide bonds can be cleaved in cells by DUBs. An isopeptide bond mimic that is stable against DUBs enables the biochemical characterization of Ub–protein conjugates in cells and cell lysates. Triazoles formed by copper-catalyzed azide-alkyne cycloaddition have been successfully used for isopeptide bond mimicry.[5-6] However, treatment of proteins with copper can be problematic, e.g. because of the formation of reactive oxygen species.[7] Hence, milder ligation strategies for the mimicry of ubiquitination are necessary.

In this project, oxime ligation – the reaction between an aminooxy group and a carbonyl compound – should be investigated as a mild tool for site-specific protein-ubiquitination. To meet this challenge, new aminooxy-modified amino acids were synthesized and their incorporation into proteins by stop-codon suppression was established. To urge the acceptance of these amino acids by the participating enzyme, PylRS, mutations were introduced in the amino acid binding pocket of that enzyme. From that pool those mutants were identified that enhance that process. The aminooxy groups of the amino acids were equipped with different carbamate-based protection groups as recognition elements for respective PylRS mutants, and to prevent the aminooxy group from reacting with endogenous carbonyl compounds. These protection groups could be removed on the protein after expression.

Desired proteins were site-specifically functionalized with these aminooxy-modified amino acids, and the reaction partners were equipped with a carbonyl compound. Hence, oxime ligation was studied in order to generate site-specifically linked DNA Pol β–Ub, H1.2–Ub, and p53–Ub conjugates. The results indicate, that DNA Pol β and H1.2 were ubiquitinated by oxime ligation. Furthermore, functional and site-specifically ubiquitinated p53 was generated for the first time and by means of oxime ligation in a cooperation project with Alexandra Julier (Scheffner group, Universität Konstanz). It was demonstrated that the oxime-linked p53–Ub conjugate is stable against DUBs. Furthermore, like p53, p53–Ub was recognized by interaction partners, which indicates correct folding of the protein after oxime ligation.

Thus, different amino acids were successfully incorporated into proteins by stop-codon suppression with PylRS mutants identified in this thesis for the modification of proteins with aminooxy groups and oxime ligation was applied to generate protein–Ub conjugates. These results indicate the feasibility of oxime ligation for the site-specific mimicry of ubiquitination under mild conditions, and are the basis for further functional studies of the generated conjugates.

Table of Contents

Abbreviations

aaRS	Aminoacyl-tRNA synthetase
AcK	Acetyl lysine
AhA	Azidohomoalanine
AMP	Adenosine monophosphate
ATP	Adenosine triphosphate
AOAA/U	Aminooxy-modified amino acid
BER	Base excision repair
Bn	Benzyl
Boc	*tert*-Butyl oxycarbonyl
BocK	Boc lysine
Carb	Carbenicillin
Cbz	Carboxybenzyl
CD	Circular dichroism
CuAAC	Copper-catalyzed azide alkyne cycloaddition
CouK	Coumarin-lysine
CV	Column volume
DBU	1,8-Diazabicyclo[5.4.0]undec-7-en
DCM	Dichloromethane
DIPEA	*N*,*N*-Diisopropylethylamine
DMAP	4-Dimethylaminopyridine
DNA	Deoxyribonucleic acid
DNA Pol β	DNA polymerase β
DBO	Dibenzocyclooctyne
DFO	Difluorocyclooctyne
EtBr	Ethidium bromide
HRMS	High-resolution mass spectra
TCO	*trans*-Cyclooctene
DPT	Dipyridyl-tetrazine
MAT	Monoaryl-tetrazine
EDC	1-Ethyl-3-(3-dimethylaminopropyl)carbodiimide
EMSA	Electromobility shift assay
EPL	Expressed protein ligation
DCM	Dichloromethane
DMF	Dimethylformamide
DTT	Dithiothreitol
DUB	Deubiquitinating enzyme
eq	Equivalents
IEDDA	Inverse-electron demand Diels-Alder
ft	Freeze-thaw
FPLC	Fast protein liquid chromatography
FT	Flow-through
IPTG	Isopropyl-β-D-thiogalactopyranosid
Kan	Kanamycin
KeK	Keto-lysine
LB	Lysogeny Broth
M	Marker
MOM	Methyloxymethyl

mRNA	Messenger RNA
MsCl	Methanesulfonyl chloride
MQ H2O	Milli-Q water
NCl	Native chemical ligation
NMM	New minimal medium
NMR	Nuclear magnetic resonance
o.n.	Overnight
PBS	Phosphate-buffered saline
Plk	Propargyl-lysine
PP	Pyrophosphate
Pyl	Pyrrolysine
PylRS	Pyrrolysyl tRNA synthatase
PTM	Post-translational modification
POI	Protein of interest
ppm	Parts per million
p-TSOH	*p*-Toluenesulfonic acid
Rt	Room temperature
RNA	Ribonucleic acid
RL	Rabbit reticulocyte lysate
RP-MPLC	Reversed-phase medium-pressure liquid chromatography
SCS	Stop-codon suppression
SDS	Sodium dodecyl sulfate polyacrylamide
SDS-PAGE	Sodium dodecyl sulfate polyacrylamide gel electrophoresis
SEC	Size exclusion chromatography
SPAAC	Strain-promoted azide alkyne cycloaddition
SPI	Selective pressure incorporation
SPPS	Solid-phase peptide synthesis
TCEP	Tris(2-carboxyethyl)phosphine
TES	Triethyl silane
TFA	Trifluoroacetic acid
THF	Tetrahydrofuran
tRNA	transfer RNA
U/AOAA	Aminooxy-modified amino acid
UAA	Unnatural amino acid
Ub	Ubiquitin
UbCHL3	Ubiquitin C-terminal hydrolase L3
wt	Wild-type

The one- and three-letter codes for amino acids were used according to the IUPAC-IUB commission's recommendation for biochemical nomenclature.[8]

1. Introduction

1.1 Ubiquitination in Nature

Ubiquitin (Ub) is a highly conserved protein that consists of 76 amino acids (8.5 kDa), and it is found in all eukaryotic cells (ubiquitous). Post-translational modification (PTM) of substrate proteins with Ub alters their biological functionalities.[9]

Ub is connected to a target protein by an isopeptide bond between a Lys side chain of the substrate and the C-terminal Gly of Ub. Ubiquitination is a reversible modification – the respective isopeptide bond can be cleaved by deubiquitinating enzymes (DUBs).[10-12] The process of ubiquitination is mediated by a three-step enzymatic cascade (Figure 1).[9],[13-17]

First, Ub-activating enzyme E1 binds Ub and adenosine triphosphate (ATP) and adenylates the C-terminus of Ub. This is followed by the formation of a Ub–thioester–E1 intermediate between the E1-active-site Cys side chain and the C-terminal carboxyl group of Ub. Adenosine monophosphate (AMP) is released during that process.[9],[13-14] Second, the Ub–thioester–E1 intermediate is transferred to the active-site Cys of E2 by a transthioesterification. This is catalyzed by the ubiquitin-conjugating enzyme E2, which binds E1 and Ub.[15] Third, Ub is transferred to the substrate protein and an isopeptide bond is formed between a substrate Lys and the Ub C-terminus. This process is catalyzed by E3 ligases, which can be divided into three classes.[15] RING-domain E3 ligases directly transfer activated Ub from E2 to the substrate by serving as scaffold to bring the involved molecules in close proximity. HECT-domain E3 ligases bind Ub in a transthioesterification before Ub is conjugated with the substrate protein.[16] RING-in-between-RING ligases exhibit a RING-HECT hybrid mechanism[17].

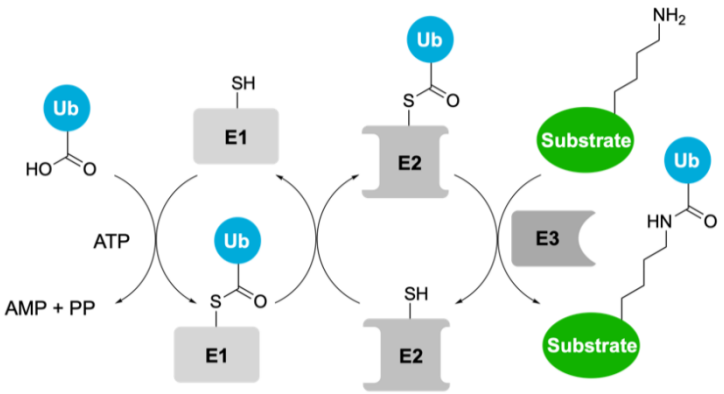

Figure 1: Depiction of the E1–E2–E3 ubiquitination cascade. PP: Pyrophosphate. This scheme was reproduced and modified from D. Rösner[18].

The simplest form of protein ubiquitination is the attachment of one Ub monomer (mono-ubiquitination). The conjugation of multiple Ub monomers to several substrate Lys residues is termed multiple mono-ubiquitination. Ubiquitin itself can serve as target of ubiquitination, which results in the formation of Ub chains. These chains can be anchored to a substrate protein (poly-ubiquitination). An elongation factor E4 can extend the formation of Ub chains of more than three monomers by transferring Ub from E2–Ub intermediates to previously poly-ubiquitinated substrates.[19] The single monomers are connected to each other by an isopeptide bond between one of the seven Lys side chains or the N-terminal Met of one Ub monomer and the C-terminus of another Ub monomer. The number of Ub monomers in Ub chains and the linkage type between these monomers most likely determine the functional properties of proteins that are conjugated to these chains.[20]

Probably, the best characterized function of protein poly-ubiquitination is the proteolytic degradation of the substrate by the 26S proteasome with subsequent release of reusable ubiquitin.[21] “For the discovery of ubiquitin-mediated protein degradation” the Nobel Prize in Chemistry was awarded to Aaron Ciechanover, Avram Hershko, and Irwin Rose in 2004.[22]

The ubiquitin proteasome pathway is involved in the degradation of various ubiquitinated substrates. In this context, the pathogenesis of several diseases is connected either with the stabilization of a protein due to reduced activity of a participating enzyme or with the accelerated degradation of a certain protein.[9] Additionally, poly- and mono-ubiquitination were found to have an impact on the protein’s fate other than only proteolytic degradation. For example, mono-ubiquitination was found to affect the function[3], protein–protein interactions[4], and subcellular localization[1-2] of the target protein. Furthermore, it can have an impact the protein trafficking, endocytosis[23], and gene expression[24], and was reported to regulate DNA repair[25-28].[29]

1.2 Substrates of Ubiquitination

A series of proteins are known targets of ubiquitination, e.g. DNA polymerase β (DNA Pol β), linker histone H1, or p53.[9],[28]

DNA Pol β is a eukaryotic 39 kDa protein and plays a pivotal role in gap-filling deoxyribonucleic acid (DNA) synthesis and base excision repair (BER) of DNA.[30-34] It consists of two domains, which are connected to each other by a hinge region.[35-37] The C-terminus (8 kDa) has a high binding affinity to single-stranded DNA and harbors a lyase activity. The polymerase domain (31 kDa) contains a nucleotidyl tranferase activity and binds double-stranded DNA. In BER, DNA Pol β executes both of these functions to fill single-nucleotide gaps. The precise regulation of DNA Pol β is crucial, since over- and under-expression have been associated with an increased rate of mutagenesis and DNA repair deficiency, respectively.[38-39] One pathway of regulating the nuclear level of DNA Pol β is the ubiquitin proteasome proteolytic pathway, and in this context mono-ubiquitination was found to promote poly-ubiquitination.[28] DNA Pol β modification with ubiquitin was reported in several positions throughout the protein, e.g. in positions 41, 61, and 81, when E3 ligase MULE is involved.[28] However, it is not clear, whether all positions are equally ubiquitinated, or if mono-ubiquitination can have another impact on DNA Pol β than its proteolytic degradation.

Linker histone H1 promotes the compaction of nucleosomes (DNA wrapped around two copies of four core histones) and thus forms chromatosomes[40] and chromatin[41]. In eukaryotes, DNA is compacted in chromatin. The chromatin structure regulates the accessibility of the DNA and is associated with processes like transcription, replication, and repair.[42] H1 consists of an N-terminal tail, a globular domain, and a disordered C-terminal domain. Histone H1.2 is a somatic subtype of H1.[43] H1.2 can repress p53-dependent transcription of chromatin[44] or trigger the release of proapoptotic factors as answer to DNA strand breaks[45-46]. PTMs of histones and distinct modification patterns can influence the chromatin state and hence the biological consequences.[47-48] Ubiquitination of H1.2 can be carried out by E3 ligase RNF168 in complex with Rad6[49] or by UBC18 with RNF8[50] in response to DNA damage. Several H1.2 positions were reported as ubiquitination targets[51-54]. However, the fate of mono-ubiquitinated H1.2 and the link between function and site of ubiquitination could not be determined so far.

p53, often referred to as the “guardian of the genome”[55], is a tumor suppressor protein that regulates the transcription of many genes, which are involved in cell cycle arrest, DNA repair mechanism, autophagy, senescence, apoptosis, and cell metabolism.[56] Hence, it is not surprising that in the vast majority of human cancers p53 is mutated or not tightly regulated.[57-58] p53 consists of an N-terminal transactivation domain, a DNA-binding domain, and a C-terminal domain (regulatory region and oligomerization domain).[57] The active form

of p53 is a tetramer and the oligomerization state is mediated by the oligomerization domain. The DNA-binding domain is responsible for site-specific binding of double-stranded DNA, which proceeds cooperatively by tetrameric p53.[59] The disordered N-terminal transactivation domain binds to transcriptional coactivators and parts of the transcription machinery, and thus, links gene recognition and gene expression.[60-61] Alternatively, it binds to HDM2 that is involved in p53 ubiquitination, and hence, marks p53 for proteolytic degradation or nuclear export.[62-64] Degradation of p53 by the ubiquitin proteasome pathway can also occur in the course of p53 targeting by high-risk HPV oncoprotein E6, which recruits HECT-domain E3 ligase E6AP.[65-67] Ubiquitination of p53 has been suggested for all p53 Lys residues that are present in all domains of the protein. For example, position 120 in the DNA-binding domain was identified as ubiquitination site in different studies.[53],[68-69] Multiple mono-ubiquitination of p53 has been shown to contribute to its nuclear export[1-2],[69] and mitochondrial translocation[70]. Moreover, an influence on DNA binding was suggested.[71] However, the question still remains which fate p53 has upon mono-ubiquitination and if the effect of ubiquitination depends on the modification site.

Most likely, the reason why the link between the position and the effect of protein ubiquitination has not been identified yet, is because site-specifically ubiquitinated proteins are not easily enzymatically accessible.

1.3 Site-specific Protein Ubiquitination in vitro

1.3.1. Ligation Chemistries for Isopeptide Bond Mimicry

The generation of site-specifically mono-ubiquitinated proteins of interest (POI) has gained more and more interest in recent years. This is, because the availability of these conjugates is the basis to investigate the possible impact of the ubiquitination site on the fate of the modified protein. Protein–Ub conjugates cannot be consecutively expressed, since protein substrates are connected to Ub by an isopeptide bond between a Lys side chain of the substrate and the C-terminal Gly of Ub. Therefore, ligation chemistries have been developed that lead to the generation of a site-specific amide bond or an amide bond mimic. These reactions should proceed chemoselectively, mildly, under aqueous conditions, in good yields, with reasonable kinetics, and without or with only minor by-product formation. Reactions meeting most of these requirements are often referred to as biocompatible "click reactions"[72].

About 40 years after the observation by Wieland *et al.* that Cys and a C-terminal Val thioester form a Val–Cys dipeptide *via* a thioester intermediate[73], Kent *et al.* developed native chemical ligation (NCL, Figure 2) in 1994.[74] NCL is performed between a C-terminal thioester of one protein and an N-terminal Cys of a second protein, and proceeds by a reversible transthioesterification, followed by an irreversible S,N-acyl shift, which yields a native amide bond.[75] Isopeptide bonds can be formed with this method, e.g., by introducing mercaptolysine at the ligation site, followed by desulfurization.[76-78] In 2000, the traceless Staudinger ligation between a C-terminal phosphinothioester and an N-terminal azide was established.[79-80] Additionally, several methods relying on enzymatic processes for ligation of proteins or peptide fragments upon amide bond formation have been developed.[75]

However, with respect to protein–Ub conjugation, these isopeptide bonds can be cleaved by DUBs in cells and cell lysates. Hence, for the biochemical characzerization of protein–ubiquitin conjugates, the use of a stable isopeptide mimic may be necessary. A suiting isopeptide bond mimic resembles an isopeptide bond in atom count and electronic properties, and mimics the original structure and orientation of the substrate and Ub to each other.

A multitude of ligation chemistries for the mimicry of protein PTMs, including ubiquitination, have been developed (Figure 2). Probably, the most prominent example is copper-catalyzed azide alkyne cycloaddition (CuAAC).[81] In the presence of Cu(I) the 1,3-dipolar cycloaddition between an alkyne and a terminal azide selectively yields 1,4-disubstituted triazoles.[82-83] The reaction proceeds in high yields in aqueous medium in a wide pH range.[81] Like an amide bond, the triazole bond was found to adopt a planar structure and to participate in hydrogen bonding, and has a similar electrophoretic dipole.[81],[84-85] However, the use of Cu(I) is not always beneficial, since difficulties in the removal of copper from protein–Ub conjugates have

been observed.[86] Moreover copper is toxic to cells[87] and can form reactive oxygen species under physiological conditions[7].

An alternative to copper-catalysis is the introduction of ring strain to the alkyne. In the strain-promoted variant of azide alkyne cycloaddition (SPAAC) alkynes derived from cyclooctyne are employed.[88-89] However, due to the large size of fast-reacting cyclooctyne derivatives (Figure 2) the formed bond most likely does not represent an optimal isopeptide bond mimic.

Inverse-electron demand Diels-Alder (IEDDA) reaction is another prominent cycloaddition reaction, which provides fast kinetics, high biorthogonality and does not require catalysts. The reaction proceeds between an electron-rich dienophile (alkene/alkyne) and an electron-poor diene (often 1,2,4,5-tetrazine) yielding a pyridazine.[90] To enhance the reaction rate, tetrazines are often substituted with electron-withdrawing groups to decrease the $LUMO_{diene}$–$HOMO_{dienophile}$ gap and dienophiles with ring strain, e.g. *trans*-cyclooctene, are empoyled (Figure 2).[90] This strategy is very efficient for the labelling of biomolecules, however, the resulting linkage is very bulky and hence, probably not an optimal choice for isopeptide bond mimicry. That limitation can also be observed for various bioothogonal reactions with fast kinetics.[91]

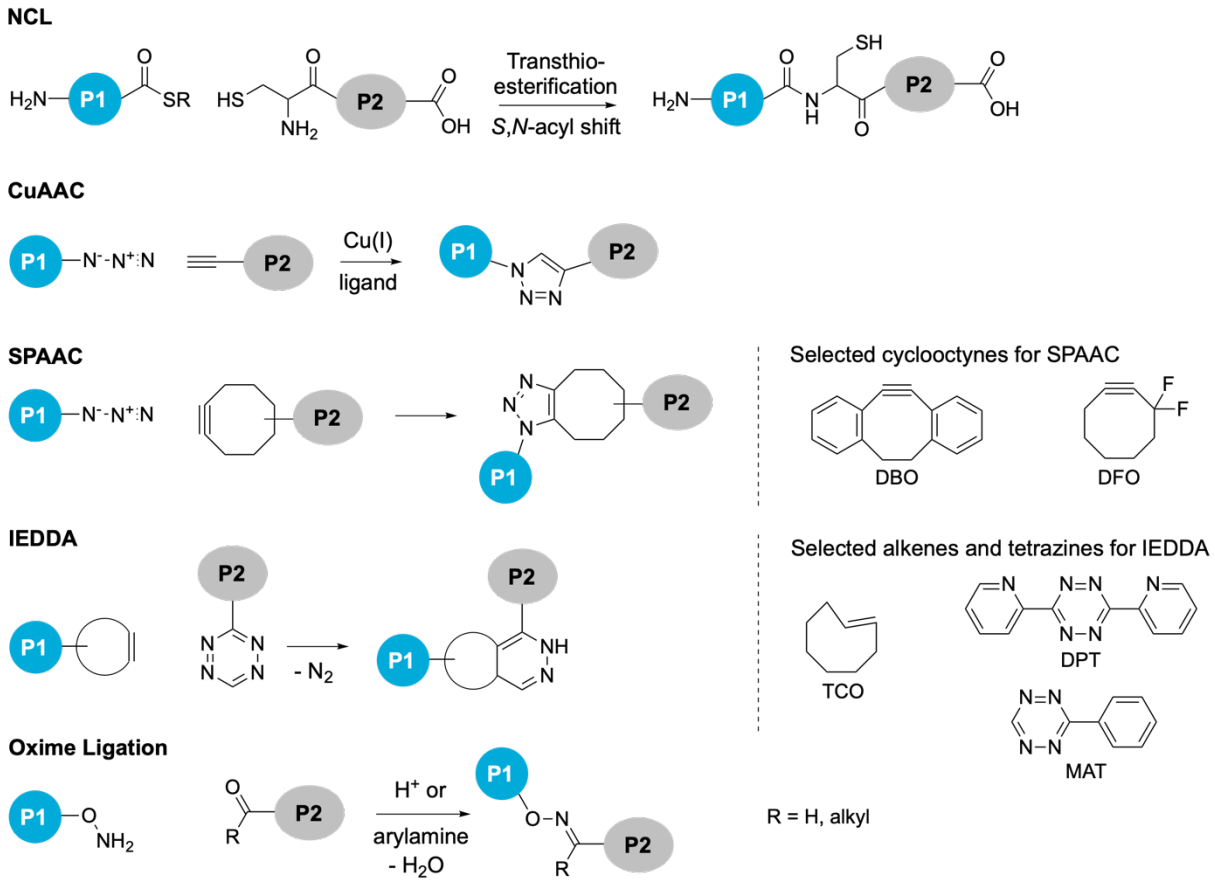

Figure 2: Selected biocompatible ligation methods. DBO: Dibenzocyclooctyne. DFO: Difluorocyclooctyne. TCO: *trans*-Cyclooctene. DPT: Dipyridyl-tetrazine. MAT: Monoaryl-tetrazine. P1/P2: Protein 1/2.

Oxime ligation (Figure 2) has already been described in the early 1880s[92-95] but only gained more and more interest for applications in bioconjugation in recent years.[96-97] The reaction proceeds between a carbonyl functionality (aldehyde or ketone) and an aminooxy group, which is an excellent nucleophile due to the α-effect of the oxygen atom. The only by-product is water, and the oxime bond is small in size and can act as hydrogen acceptor. Hence, the oxime bond might be a suiting isopeptide bond mimic. The reaction rate of oxime ligation is moderate – especially when less than millimolar concentrations of reaction partners are applied – but can be enhanced by acidic (3 < pH < 7) or aryl amine catalysis.[96-97]

Mechanistic studies revealed that the formation of oximes starts with the acid-catalyzed nucleophilic attack of the aminooxy group at the carbonyl carbon atom to yield a tetrahedral intermediate (Figure 3). In the next step, the hydroxyl group abstracts a proton and water is eliminated. The oxime bond is then formed by deprotonation.[98] At pH 3–7, the dehydration usually is the rate-determining step.[99] At lower pH (pH < 3) the reaction rate is decreased because the aminooxy group is protonated at the amine, which results in a decreased nucleophilicity. In this case, the nucleophilic attack of the aminooxy group is the rate-limiting step.[99]

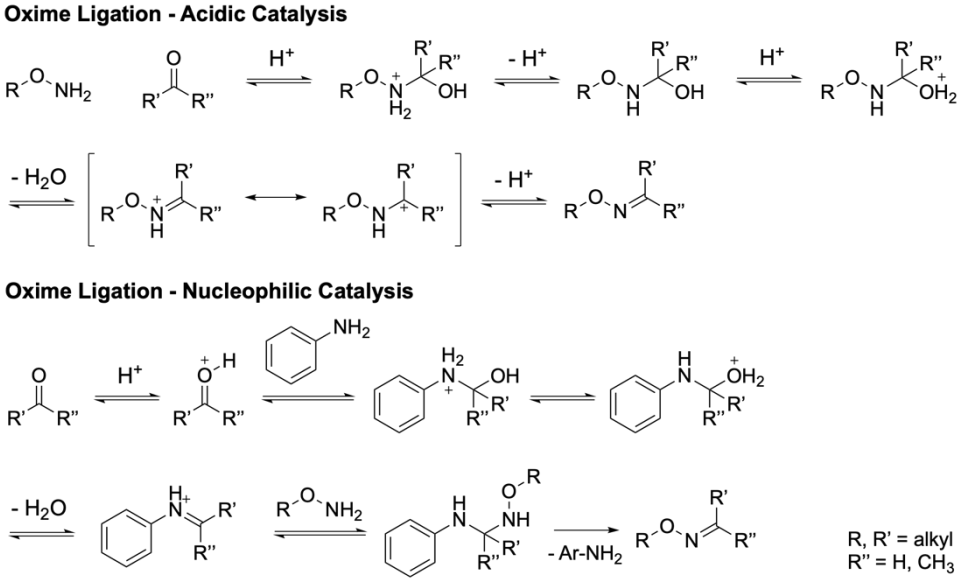

Figure 3: Acidic and nucleophilic catalysis (exemplified with aniline) of oxime ligation.

Nucleophilic aryl amine catalysis was first described with aniline[100] and proceeds best at acidic or neutral pH[101]. Aniline nucleophilically attacks the carbonyl carbon atom, and a tetrahedral intermediate is formed. Upon release of water, a Schiff base is produced, which is nucleophilically attacked by the aminooxy group. That leads to the formation of a tetrahedral intermediate. Finally, the oxime is formed, and aniline is released. Also here, the breakdown of the tetrahedral intermediate is rate-limiting.[96],[100] A lot of research was done in order to identify more efficient oxime ligation catalysts that are suitable for typical bioconjugation

conditions (µM range of reactants and pH close to 7, Figure 4).[102-104] Therefore, aniline was modified with different substituents that enhance the amine nucleophilicity. For example *p*-anisidine[105] and *p*-phenylenediamine[106] were found to display enhanced reaction rates compared to aniline.[102] Additionally, for anthranilic acid, the carboxy group in *ortho* position to the amine was suggested to participate in acidic catalysis and catalyze the rate-determining water elimination.[102] This concept was transferred to different proton-donating substituents.[102],[107] Substitution on the aromatic ring with electron-donating groups was found to further enhance catalysis (2-amino-5-methoxybenzoic acid).[103] Furthermore, oxime ligation was reported to be accelerated by freeze-thaw catalysis[108] and in the presence of saline[109].

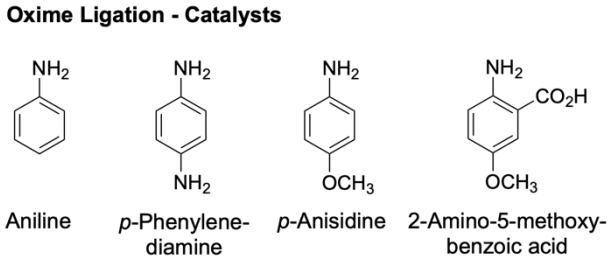

Figure 4: Selection of nucleophilic catalysts for oxime ligation.

Oxime ligation is reversible and hydrolysis of the oxime is enhanced under acidic conditions and at high temperatures.[96],[110-111] To add stability, the oxime bond can be reduced to the respective aminooxy compound.[112] The nature of the carbonyl (aldehyde or ketone), as well as steric and electronic properties of the reaction partners do not only have a great influence on the reaction rate and turnover, but also on the stability of the oxime product.[111],[113] Generally, aldehydes react faster but oxime products derived from aldehydes are more prone to hydrolysis than their ketone counterparts. Moreover, due to the elevated reactivity, aldehydes can form imines with Lys side chains. However, the oxime bond is more stable towards hydrolysis than corresponding imines or hydrazones. The high electronegativity of the oxygen atom leads to a diminished basicity of the sp^2-hydridized nitrogen with respect to the imine or hydrazone amine.[111] Additionally, due to electron delocalization the electrophilicity of the sp^2 carbon is reduced, which results in a lower susceptibility towards nucleophilic attacks.[97]

Hence, oxime ligation might be a powerful tool for protein–protein conjugation.

1.3.2 Site-Specific Modification of Proteins with Functional Handles

1.3.2.1 Synthetic and Semi-Synthetic Methods

In order to perform site-selective reactions on proteins as described in chapter 1.3.1, the proteins of interest need to be equipped with the respective functional handles.

Several chemical or enzymatic approaches have been used to do so. Peptides and small proteins like Ub can be generated by solid-phase peptide synthesis (SPPS), which facilitates the incorporation of any desired modified amino acid at any position.[114] Alternatively, orthogonal protection group chemistry in SPPS can be exploited to selectively modify an amino acid after chain elongation. By combination with NCL, even larger proteins can be synthesized by SPPS and thus, be modified.[74] Expressed protein ligation (EPL) addresses the size-limitations of SPPS.[115],[116] The thioester-bearing protein is generated by expression of the protein fused to an intein, followed by an intein-catalyzed S,N-acyl shift and a transthioesterification. NCL can then be performed with a synthetic, modified peptide. However, SPPS is very time-consuming and cost-intensive, and NCL/EPL limits the number of possible ligation sites and, therefore, of sites for protein modification.

As an alternative, chemistries for the selective modification of natural amino acids have been developed.[117] This enables the expression of a protein that contains the amino acid to be modified at any desired position. However, the protein of interest should not naturally contain that amino acid to ensure site-specificity of the modification and to prevent perturbation of the protein structure upon mutation to another canonical amino acid. As an example, Cys is one of the least abundant amino acids in proteins and there is no other canonical amino acid that bears a primary thiol group. This thiol can be employed in thioether formation or as nucleophile in nucleophilic substitutions. Choosing an appropriate pH, which depends on the protein environment, can prevent side reactions with amines.[118-121] Nevertheless, this approach is limited by the natural abundance of the amino acid to be modified in the desired protein.

1.3.2.2 Genetic Incorporation of Unnatural Amino Acids

Methods relying on the genetic incorporation of unnatural amino acids enable the modification of a protein during expression and are based on the natural translational machinery. The two most commonly used approaches are selective pressure incorporation (SPI) and stop-codon suppression (SCS).

The central dogma of molecular biology describes the transfer of information from DNA to ribonucleic acid (RNA) to protein in living systems. Information is stored as DNA, which is transcribed to messenger RNA (mRNA). The mRNA nucleotide sequence is then translated into a protein amino acid sequence. In that process, three nucleotides consisting of A, C, G, or T/U encode for one amino acid (codon). Thus, 64 different codons exist. Three of these codons are stop codons and terminate protein expression: UAG (amber), UAA (ochre), and UGA (opal). Most organisms use 20 canonical amino acids. Hence, one amino acid can be encoded by several base triplets, but one base triplet always encodes one of the 20 amino acids (except stop codons). Translation starts with an AUG (Met) codon and proceeds from the protein N-terminus to the C-terminus. During translation, transfer RNA (tRNA) is charged by a specific aminoacyl-tRNA synthetase (aaRS) with its cognate amino acid in an ATP-dependent process. The charged tRNA is shuttled to the ribosome, which mediates the binding of the anticodon of the charged tRNA to the respective mRNA codon and catalyzes amino acid polymerization. Instead of tRNA, upon termination of translation release factors can bind to the stop codon, disassemble the ribosome, and release the nascent protein.[122-123]

SPI takes advantage of the structural similarity of an unnatural amino acid to a canonical amino acid and the promiscuity of the respective aaRS/tRNA pair. In the absence of the natural amino acid the unnatural variant is incorporated in response to the respective codon instead. The incorporation of azidohomoalanine in place of Met by using Met auxotrophic bacterial strains is one among various examples for SPI[5],[124],[91].

SCS in rare cases occurs naturally for the incorporation of selenocysteine in response to an opal codon, and of pyrrolysine (Pyl) in response to an amber codon.[125] That concept has been exploited for the incorporation of designer amino acids into any desired position in any protein of interest (Figure 5). This is enabled by the reassignment of a stop codon to an orthogonal aaRS/tRNA pair.[91] The most commonly used stop codon in bacterial SCS is the amber codon, because it is least used by *E. coli* (~7%).[126-127] An alternative approach is the engineering of an orthogonal ribosome that decodes quadruplet codons.[128-129]

The aaRS/$tRNA_{CUA}$ pairs are most commonly designed to incorporate the unnatural amino acid (UAA) in response to the amber codon. However, it must not recognize endogenous amino acids and aaRS must only charge the suppressor $tRNA_{CUA}$ with the unnatural amino acid. This specificity is commonly achieved by introducing aaRS/$tRNA_{CUA}$ pairs from another

domain of life to the expression host, but there were also examples for the *de novo* design of such pairs. Four orthogogal types of aaRS/$tRNA_{CUA}$ pairs were developed for SCS: The *M. jannaschii* TyrosylRS/$tRNA_{CUA}$ (TyrRS) pair (orthogonal in *E. coli*), the *E. coli* TyrosylRS/$tRNA_{CUA}$ pair (orthogonal in eukaryotic cells), the *E. coli* LeucylRS/$tRNA_{CUA}$ (LeuRS) pair (orthogonal in eukaryotic cells), and *Methanosarcinae* PyrrolysylRS/$tRNA_{CUA}$ (PylRS) pairs (orthogonal in bacteria, eukaryotic cells, and animals).[91]

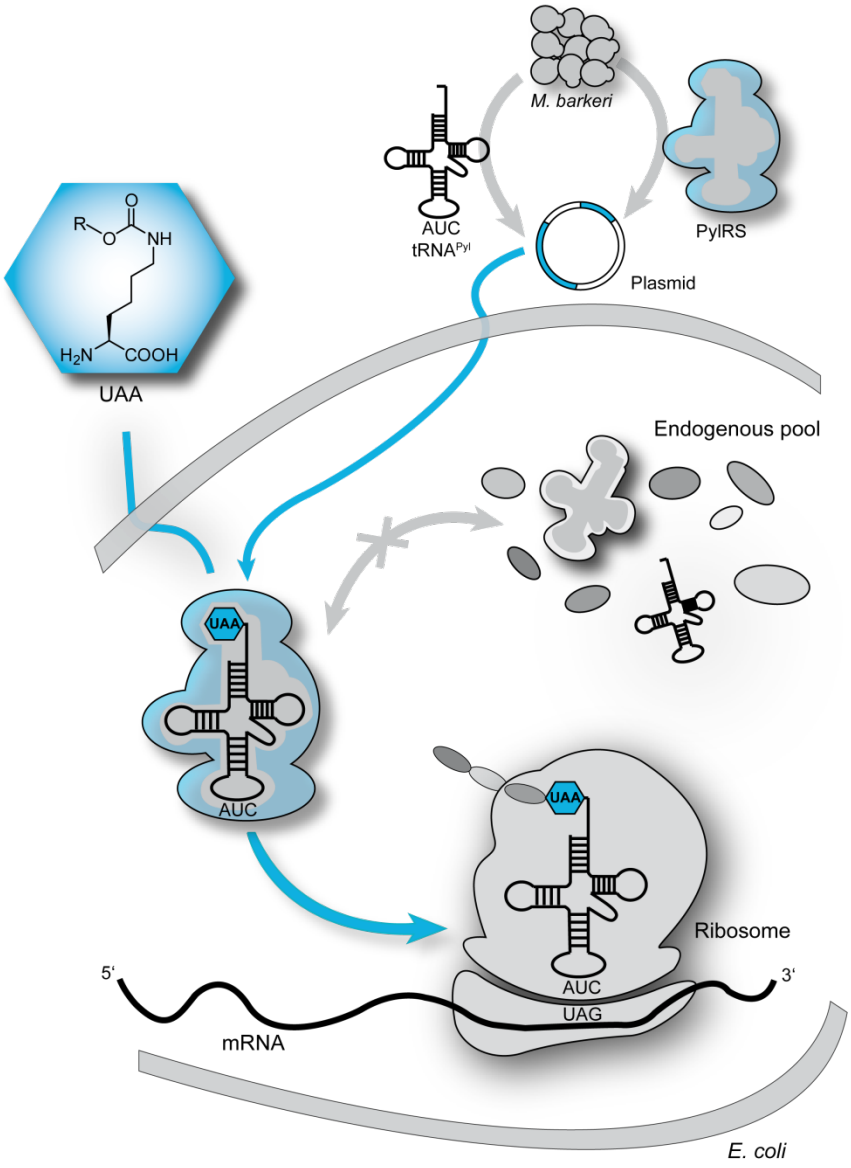

Figure 5: Schematic depiction of amber stop-codon suppression with PylRS. The ability of a PylRS mutant to incorporate UAA is usually determined by the organic rest R. This scheme was modified from D. Rösner *et al.*[130] by M. Mißun and V. Radtke.

For the first three mentioned pairs active-site manipulation to remove recognition of canonical amino acids is necessary. The PylRS/$tRNA_{CUA}$ pairs bind pyrrolysine but none of the natural amino acids, and its cognate $tRNA_{CUA}$ is a natural amber suppressor. PylRS contains a highly conserved C-terminal class II aaRS signature core domain that catalyzes

aminoacylation of $tRNA_{CUA}$ and an N-terminal domain that is involved in binding of the $tRNA_{CUA}$. The two domains are connected to each other by a linker region that differs in amino acid length and sequence for PylRS variants.[131] For example, the linker region of PylRS from *M. barkeri* contains 35 amino acids less than that from *M. mazei*. Crystallization of a C-terminal fragment of PylRS from *M. mazei* in complex with Pyl gave insight into the binding of amino acids in the binding pocket.[132] Residue N346 (*M. mazei* numbering) forms a hydrogen bond with the N_ε-carbonyl oxygen atom and Y384 acts as a cap for binding of Pyl. These residues were suggested to play an important role in the substrate specificity of PylRS. The pyrrole ring is buried in a large hydrophobic pocket.[133]

By mutations in the PylRS binding pocket, the substrate scope can be further expanded. In the following, PylRS positions are numbered with respect to PylRS from *M. barkeri*, if not stated otherwise. The directed evolution of PylRS mutants from a genetically encoded library is often used to identify suiting PylRS/tRNA pairs for new UAAs. This screening consists of a positive selection to identify PylRS mutants able to incorporate the desired UAA and a negative selection to exclude variants that bind to natural amino acids.[134] Such experiments led to the generation of PylRS Y349F and PylRS Y271A Y349F (PylRS AF). Mutation Y349F was suggested to increase the general aminoacylation activity of PylRS by affecting the opening and closure of the amino acid binding pocket. The size of the PylRS hydrophobic pocket can be increased by Y271A. PylRS variants harboring a Y271A mutation were found to accept amino acids with bulky side chains.[135] In general, the N_ε-carbamate group has proven as valuable recognition motif for acceptance of Lys derivatives by PylRS.[132],[135-136]

Based on these findings, a series of Lys-based amino acids have been incorporated into proteins by SCS, bearing functional handles or different protection groups for chemoselective reactions or for the deprotection of a specific Lys residue, respectively.[91] Among them, there are amino acids equipped with ketones, alkynes or azides, which have been applied in oxime/hydrazone ligations and in CuAAC (Figure 6). At the start of the project, no aminooxy-modified amino acid with a suiting RS/tRNA pair had been published. In 2016, Virdee and coworkers reported the incorporation of an aminooxy-modified Boc lysine derivative by a PylRS mutant (see chapter 1.3.3 and 3.1.1).[137]

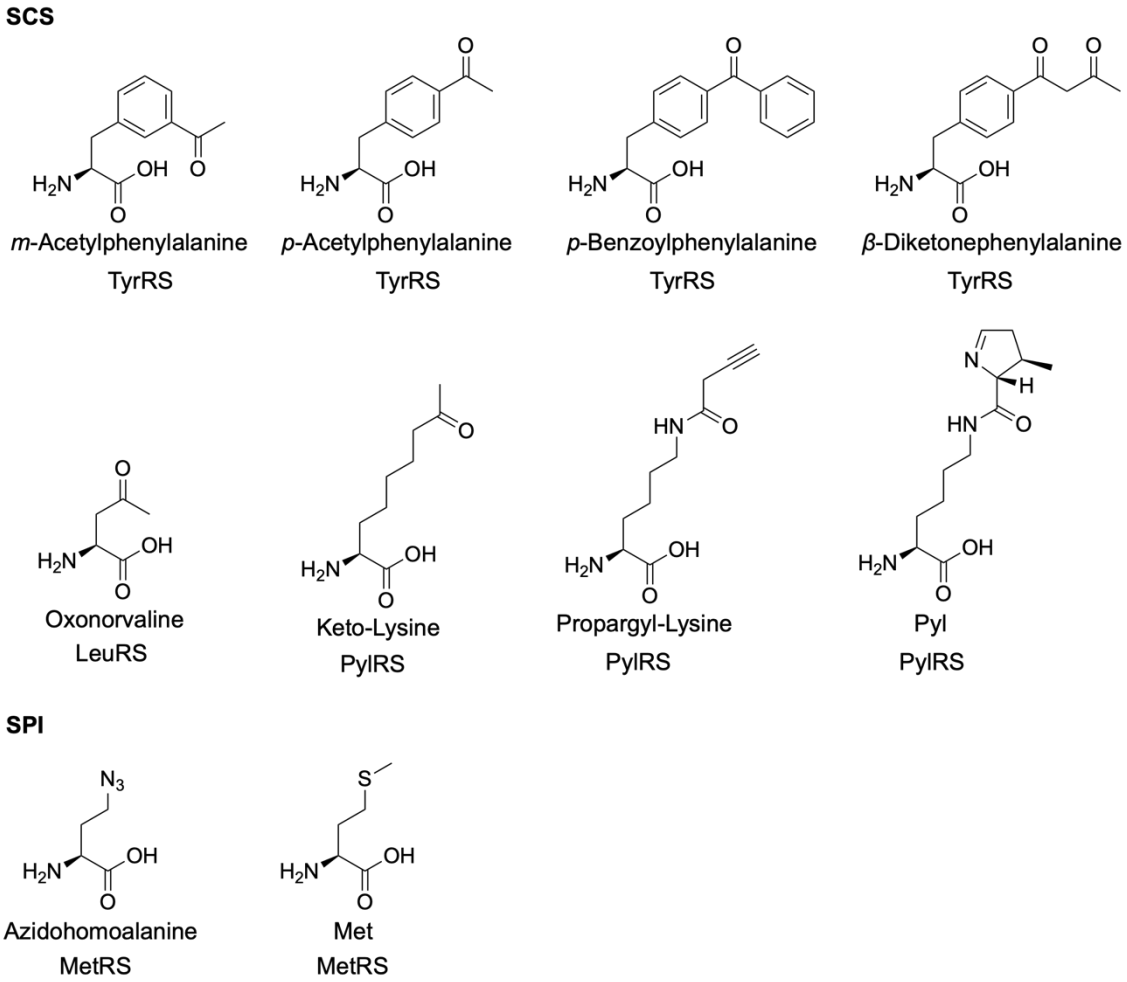

Figure 6: Selected amino acids that have been incorporated into proteins by SCS or SPI and can be used for oxime ligation or CuAAC, and type of RS used for their incorporation.[91]

Compared to the expression of native proteins, expression in combination with SCS is less efficient because the suppressor tRNA competes with release factors for binding at the amber codon[138]. That results in partial termination of translation instead of amino acid incorporation, and hence in a reduced protein yield. To circumvent that, release factor 1-deficient *E. coli* cells were generated.[127] Moreover, the incorporation efficiency depends on the sequence context[139] of the amber codon and on the activity of the PylRS. Several approaches to increase the general PylRS activity independent from alterations in the amino acid binding pocket have been described. The D. R. Liu lab identified four mutations at the PylRS N-terminus (V31I, T56P, H62Y, A100E, denoted as IPYE) by phage-assisted continuous evolution to enhance PylRS activity, and thereby improve SCS.[140] For example, 9.7-fold more protein was expressed for incorporation of acetyl lysine (AcK) with AcKRS-IPYE than with AcKRS. W. Liu and coworkers published mutations R19H H29R T122S (denoted as HRS) for an enhanced PylRS activity.[141] The use of AcKRS-HRS instead of AcKRS led to a 4.4-fold enhanced incorporation of AcK at an amber codon.

1.3.3 Previous Strategies for Protein Ubiquitination

Several strategies for the site-specific ubiquitination of proteins – including Ub–Ub conjugation – have been investigated.

Site-specifically linked Ub polymers (except for linkage type K27) can be enzymatically synthesized.[142] However, this method is limited by its unproductivity and the availability of the respective enzymes. Therefore, synthetic or semi-synthetic methods were required for the generation and the investigation of site-specifically linked Ub dimers, chains, and other ubiquitinated proteins (Figure 7).

Przybylski *et al.* reported about the generation of diubiquitin by employing SPPS to synthesize K63-linked C-terminal Ub fragments, which is followed by conjugation to N-terminal, bacterially expressed Ub by thioether ligation.[120] An approach by Strieter *et al.* was based on thiol-ene coupling for the generation of isopeptide-linked Ub chains.[143-145] Furthermore, protein ubiquitination was achieved by SPPS together with NCL.[146] This was later combined with EPL and the use of a photo-cleavable thiol auxiliary[147] for the site-specific ubiquitination of histone H2B peptides.[148] The desulfurization of Cys to Ala after NCL to increase the number of possible ligation sites[149] was combined with photocleavable auxiliary-mediated EPL for the generation of ubiquitinated full-length H2B[3]. Other methods for the generation of Ub dimers relied on SPPS and mercaptolysine-mediated NCL followed by desulfurization.[76-78],[150] NCL was extended to the synthesis of defined Ub polymers – as free chains or coupled to a substrate. Various advances have been made regarding the generation of thioesters, the incorporation and the kind of the thiol/amine handle and auxiliary, as well as the combination with different ligation strategies.[141],[151-163] Alternatively, Chin *et al.* used a technique they named GOPAL. They combined intein chemistry and genetic code expansion to generate Ub variants with orthogonally protected Lys residues and then performed site-specific isopeptide coupling.[164] This was also used by other groups by using silver-mediated isopeptide bond formation and different protection groups.[165-166]

The methods mentioned above are useful for the generation of isopeptide-linked Ub–protein derivatives. However, for the application of such conjugates in cell lysates, proteolytically stable linkages are more suitable (Figure 8).

Recently, Lang *et al.* published a method for the in vitro and in vivo ubiquitination of proteins by connecting genetic-code expansion with sortase function.[167] The generated ubiquitinated proteins are stable against DUBs, due to two point mutations at the Ub C-terminus.

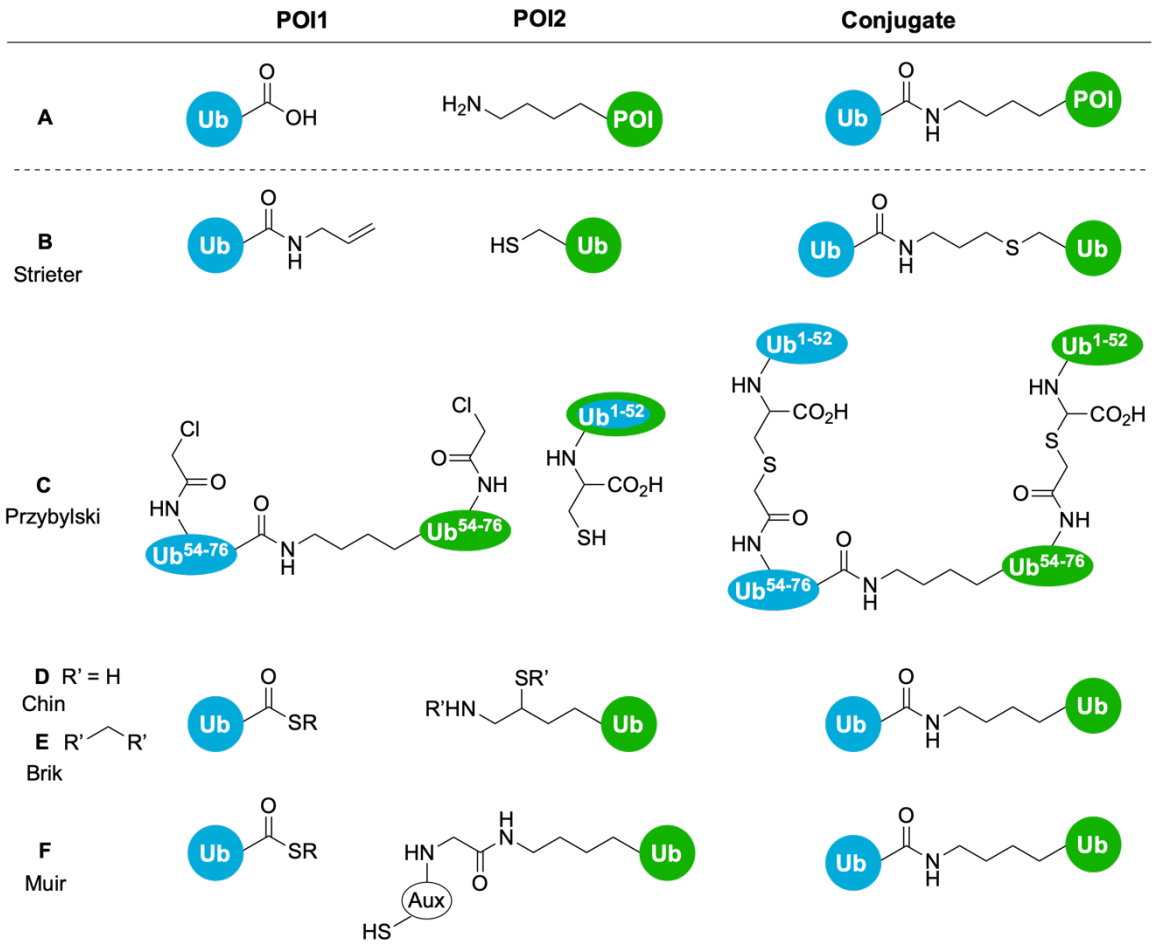

Figure 7: Schematic depiction of selected methods for the generation of isopeptide-linked ubiquitinated proteins. **A)** Native linkage. **B)**[120] **C)**[143-145] **D)**[156] **E)**[150] **F)**[148]. This figure was reproduced and modified from X. Zhao[168].

Different groups exploited thiol nucleophilicity of Cys-modified Ub mutants to connect different monomers to each other[119],[169] or to a protein substrate[170-171]. A disulfide exchange was employed by Muir *et al.*[172-173] and Zhuang and coworkers[174] to synthesize ubiquitinated histone H2B and PCNA, respectively. This method was also applied for the generation of mono-ubiquitinated α-synuclein.[175-176]

In 2010, Marx *et al.* and Mootz *et al.* independently reported on protein ubiquitination by CuAAC.[5-6] The Mootz group incorporated the alkyne functionality by reacting propargylamine with a C-terminal intein-generated thioester and the azide was site-specifically installed at a Cys mutation. For the application to proteins that contain a natural Cys, they optimized the method by incorporation of the azide by genetic code expansion.[177-178] Marx and coworkers modified both proteins by the genetic incorporation of an azide- and an alkyne-modified amino acid into desired protein positions. They not only applied this method for the generation of Ub dimers of all Lys connectivities[5] and of Ub chains[179], but also for the ubiquitination of PCNA[4], DNA Pol β[180], and histone H1.2[18]. For the generation of Ub chains, this method was further enhanced by site-specific installation of the alkyne

functionality by nucleophilic attack of a mutated Cys thiol[121]. This way, Ub chains of all connectivities were synthesized in large quantities, since dual incorporation of unnatural amino acids in one protein could be circumvented. Nuclear magnetic resonance (NMR) analysis of respective 48-linked dimers later confirmed structural and dynamic similarity towards isopeptide-linked dimers[181]. Another approach combined SPPS with UAAs for CuAAC in order to synthesize Ub chains.[182-183]

Oxime ligation was applied by Ovaa *et al.*[184] for the isosteric mimicry of an isopeptide bond. The C-terminus of Ub was in situ aldehyde-modified from a diethyl acetal, which was generated by reverse tripsinolysis and aminobutyraldehyde diethyl acetal. The Ub peptide reaction partner was site-specifically aminooxy-modified by the incorporation of a respective amino acid by SPPS. Brik *et al.* used oxime ligation for the ubiquitination of α-globulin and β-globulin and combined it with NCL for Ub chain elongation.[185] Here, a mutated Cys residue was used to install chloroacetaldehyde at the POI, and Ub was modified with an aminooxy group by nucleophilic attack of 1,2-bis(aminooxy)ethane at a C-terminal thioester.[185]

Concurrently to this work, the group of Virdee published the incorporation of a Boc-protected aminooxy-modified lysine derivative by SCS into Ub and SUMO.[137] They showed that they can release the free aminooxy group by treating the protein with TFA and applied these proteins in oxime ligations with an aldehyde-modified Ub to generate Ub–Ub, Ub–SUMO, and Ub polymers. The Ub dimers generated with this method were stable against DUBs, and crystallography revealed that they display the same structure as native Ub dimers.

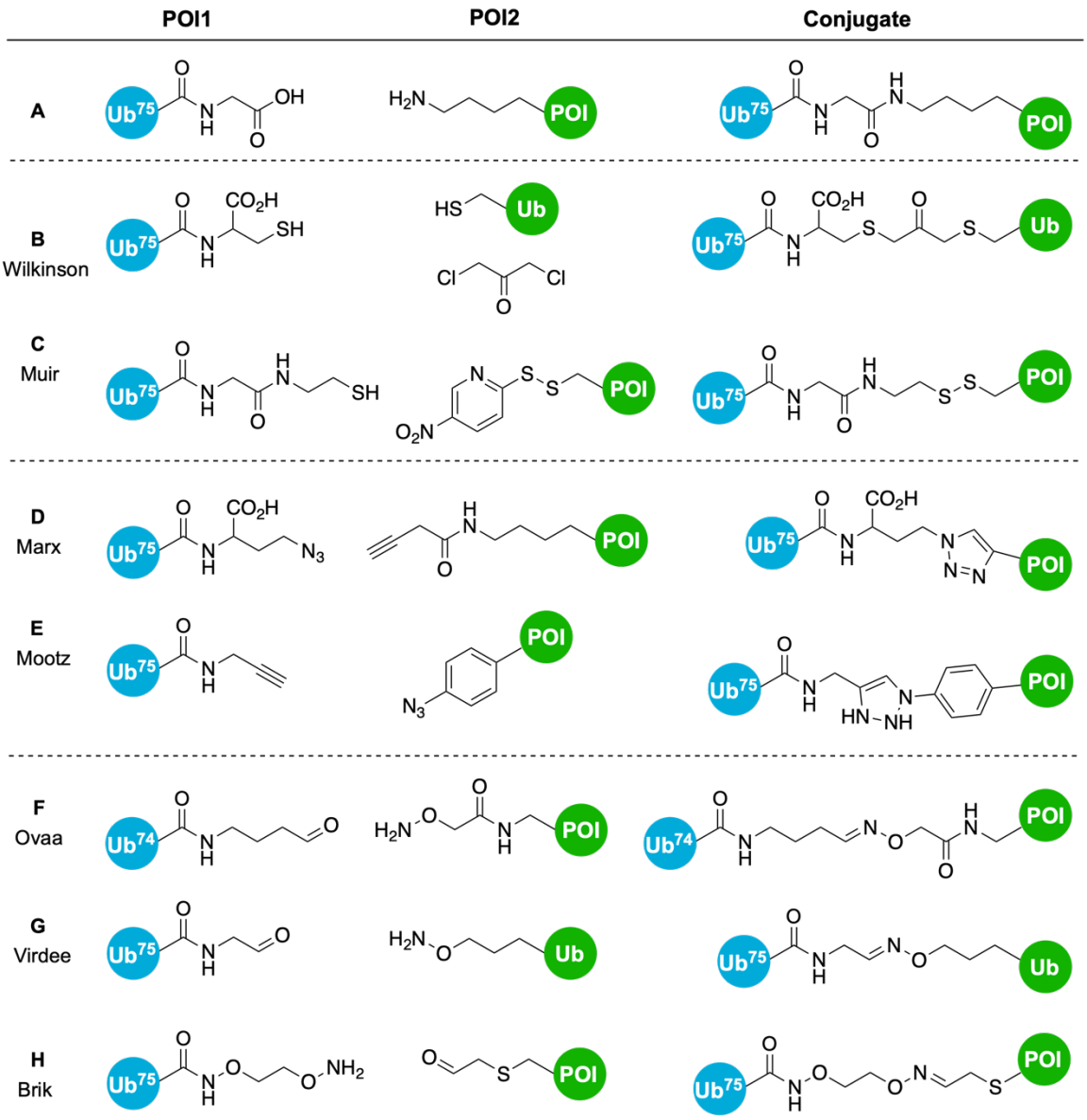

Figure 8: Schematic depiction of selected methods for the mimicry of protein ubiquitination. **A)** Native linkage. **B)**[119], **C)**[172] Cys-mediated strategies. **D)**[4-5],[18],[179-180], **E)**[177] CuAAC. **F)**[184], **G)**[137], **H)**[185] Oxime ligation. This figure was reproduced and modified from X. Zhao[168].

2. Aim

The aim of this thesis was the synthesis and the genetic incorporation of aminooxy-modified amino acids (AOAAs) into proteins, and the investigation of oxime ligation as mild tool for protein ubiquitination.

Oxime ligation proceeds between a carbonyl compound and an aminooxy group. Hence, POIs should be modified with the respective functional handles. Suiting PylRS/$tRNA_{CUA}$ pairs should be identified to site-specifically incorporate the AOAAs into proteins by SCS. These PylRS/$tRNA_{CUA}$ pairs should be employed to introduce these AOAAs into histone H1.2 and DNA Pol β. To investigate ubiquitination by oxime ligation with these proteins a carbonyl functionality should be incorporated into Ub by selectively installing a linker at a mutated Cys residue. For investigation of p53 ubiquitination, a keto-modified amino acid should be incorporated into p53 by SCS, and Ub should be modified with an AOAA by SCS.

These carbonyl- and aminooxy-modified proteins should then be applied in oxime ligation for protein ubiquitination. Here, the focus was set on optimizing reaction conditions regarding turnover and protein solubility. Successfully synthesized protein-Ub conjugates should be isolated and the effect of oxime ligation on the proteins' function and on the proteolytic stability of the conjugates should be assessed. Furthermore, first studies to characterize the effect of POI ubiquitination should be performed. Particularly, the DNA binding ability of p53–Ub was of high interest.

3. Results and Discussion

3.1 General Considerations

3.1.1 Design of Aminooxy-Modified Amino Acids

In this work, site-specific protein-ubiquitination should be mimicked by means of oxime ligation. Therefore, one POI needs to be site-specifically modified with an aminooxy group (Figure 9), the other POI with a ketone or an aldehyde. The modification of a protein with an aminooxy functionality should be realized by SCS. The advantage of this method is that the AOAA can be installed in nearly any protein at any position.

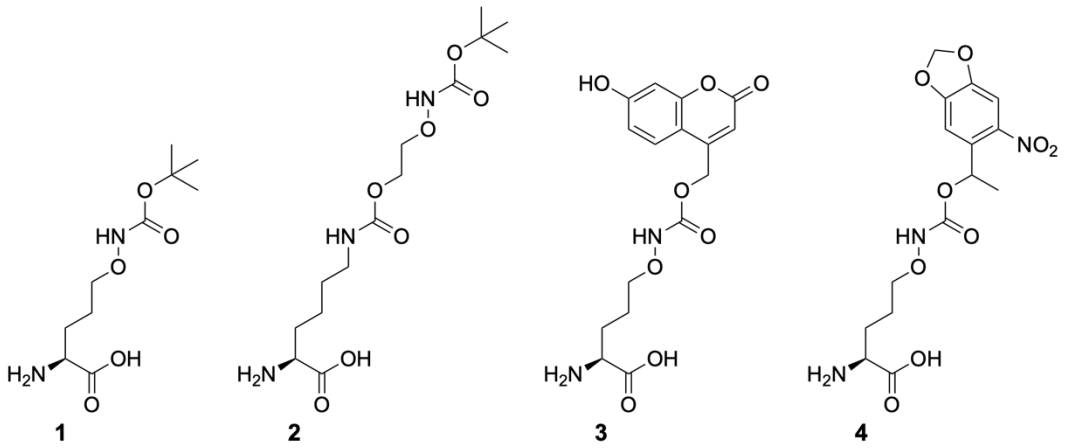

Figure 9: Aminooxy-modified amino acids investigated within this work.

The natural bond formed between Ub and its substrates is an isopeptide bond between a Lys side chain of the POI and the C-terminus of Ub. Lys derivatives modified with an ε-amine carbamate, e.g. Boc lysine, are known to be accepted by the PylRS/$tRNA_{CUA}$ pair. Therefore, the structures of AOAAs **1**–**4** are based on the structure of Lys. The aminooxy groups in **1**, **3**, and **4** are integrated into the Lys side chain by replacing the ε-methylene group with an oxygen atom. In **2**, the aminooxy group is connected to Lys by a carbamate. This way, the atom count of the Lys side chain, and thus the position of the carbamate, is maintained for all AOAAs. All AOAAs bear protecting groups to prevent the free aminooxy group from reacting with endogenous carbohydrates during protein biosynthesis in *E. coli* cells. Furthermore, the presence of carbamate groups in ε-position has been shown to be important for the recognition of unnatural amino acids by PylRS.[132],[135-136]

The Boc protection groups of amino acids **1** and **2** are acid labile and can only be used in proteins that can withstand acid-treatment. Amino acids **3** and **4** are protected by light-sensitive protection groups that can be removed by irradiation at 365 nm.

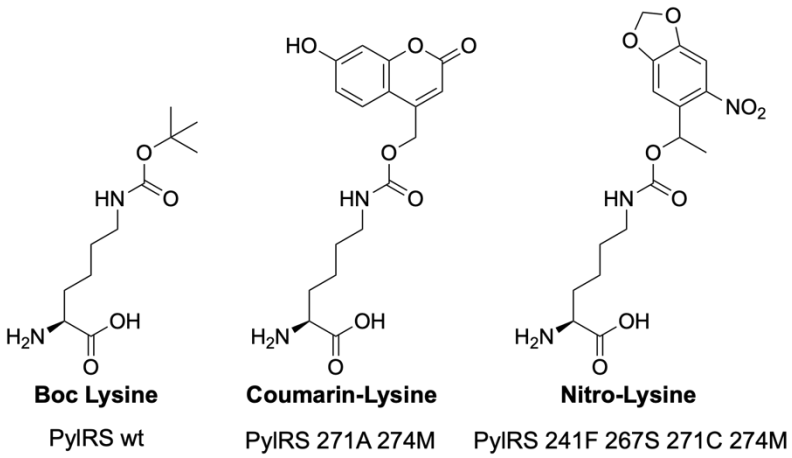

Figure 10: Lys derivatives of **1**, **3**, and **4** (Boc lysine, Coumarin-lysine, and Nitro-lysine) and published PylRS mutants for their incorporation by SCS.[135],[186-187]

In the following, PylRS mutations are numbered with respect to PylRS from *M. barkeri*, if not stated otherwise. For the incorporation of Boc lysine, Coumarin-lysine, and Nitro-lysine, the respective Lys variants of **1**, **3**, and **4**, potent PylRS mutants have been published (Figure 10).[135],[186-187] Because of the high promiscuity of PylRS for amino acid acceptance and because **1**, **3**, and **4** are isoelectronic to the respective Lys variants, it was assumed that AOAAs **1**, **3**, and **4** might be efficiently incorporated into POIs by these PylRS mutants. A series of carbamate-modified lysine derivatives with an elongated side chain are accepted by the PylRS AF mutant (Y271A Y349F).[135] Therefore, it was anticipated that **2** might be accepted by the PylRS AF mutant as well.

In the course of this thesis, Virdee *et al.* identified a suiting PylRS Y349W/tRNA$_{CUA}$ pair for AOAA **1**. They also investigated the incorporation of AOAA **4** with the PylRS/tRNA$_{CUA}$ pair for Nitro-lysine, which resulted in poor SCS.[137]

3.1.2 Carbonyl-Modification of Proteins

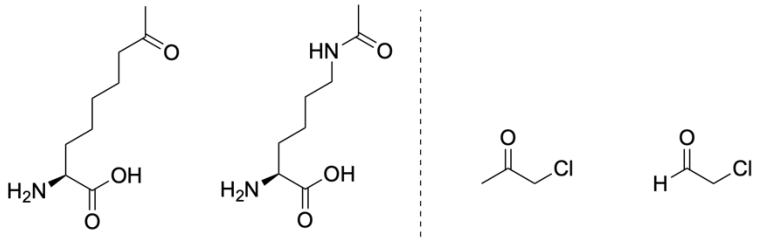

Figure 11: Keto-lysine and acetyl lysine and published PylRS mutants for their incorporation.[188-189] Chloroacetone and chloroacetaldehyde shall be site-specifically attached to a Cys residue by nucleophilic substitution.

To modify a POI with a carbonyl functionality two methods were considered. The first was the incorporation of a ketone-bearing amino acid into a protein by SCS. Keto-lysine (KeK **5**) is an acetyl lysine (AcK) analog with the carbamate nitrogen of AcK replaced by a methylene group (Figure 11). Both amino acids have been described to be incorporated by a PylRS/$tRNA_{CUA}$ pair (D76G L266V L270I Y271F L274A C313F, denoted as AcKRS).[188-189] Other ketone-functionalized amino acids with literature-known aaRS/$tRNA_{CUA}$ pairs are mostly based on Tyr/Phe (see chapter 1.3.2.2, Figure 6).[91] However, an oxime bond that involves an aromatic environment was not considered to be desirable for isopeptide bond mimicry. Therefore, KeK with its Lys-based structure was the keto-modified amino acid of choice with a known PylRS/$tRNA_{CUA}$ pair for the mimicry of an isopeptide bond upon oxime ligation.

Another approach for the site-specific carbonyl-functionalization of proteins was based on the enhanced thiol nucleophilicity of Cys over the amine nucleophilicity of Lys in a defined pH range, which depends on the protein environment.[118-121] Hence, a keto- or an aldehyde-modified alkyl halide linker should be site-specifically attached to a mutated Cys by nucleophilic substitution.

3.2. Chemical Syntheses

3.2.1 Synthesis of Boc-Protected AOAA 1

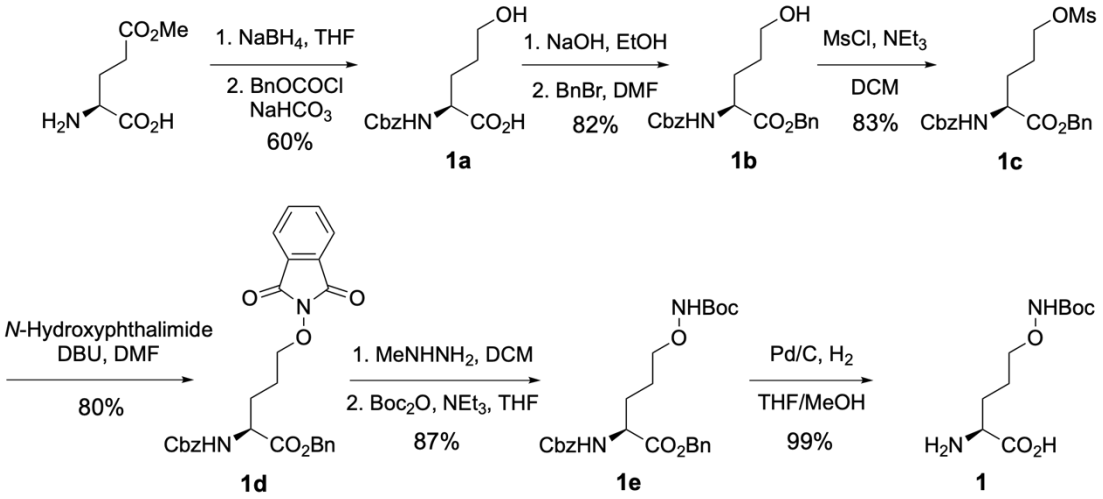

Scheme 1: Synthesis of AOAA **1**. Boc: *tert*-Butyl oxycarbonyl. Bn: Benzyl. Cbz: Carboxybenzyl. DCM: Dichloromethane. MsCl: Methanesulfonyl chloride.

The synthesis of AOAA **1** was accomplished in a 6-step route. The syntheses of compounds **1a**–**e** have been published.[190-191] The route for the preparation of **1b** as depicted in Scheme 1 was preferred over the reduction of commercially available N_{α}-Cbz-L-glutamic acid 1-benzyl ester[192], because up-scaling to > 20 mmol reactions proceeded well, whereas the yield for the latter route was strongly reduced. Different to literature, the attachment of the Cbz protection group to prepare **1a** was performed in saturated $NaHCO_3$, because the use of 0.2 M $NaHCO_3$ did not result in product formation. The removal of the benzyl ester and the Cbz group were performed with 20 mol% Pd/C by hydrogenolysis with a yield of 99%.

Alternatively, the reaction between *N*-Boc hydroxylamine and **1c** (or modified with tosylate or iodide as leaving group) was investigated (data not shown). Reaction time and temperature (room temperature (rt), 55 °C), bases (NaH, 1,8-diazabicyclo[5.4.0]undec-7-en (DBU)) and solvents (dimethylformamide (DMF), tetrahydrofuran (THF)) were varied. However, the best condition (tosylate as leaving group, 2 equivaents (eq) DBU, 2 eq *N*-Boc hydroxylamine, DMF, 2 d, rt) with a yield of 35% was not transferable to a > 5 mmol reaction scale. The low yields might be caused by the low nucleophilicity of *N*-Boc hydroxylamine. In the course of this thesis, a similar synthesis route was published by Virdee *et al.*[137]

3.2.2 Synthesis of Side-Chain Elongated AOAA 2

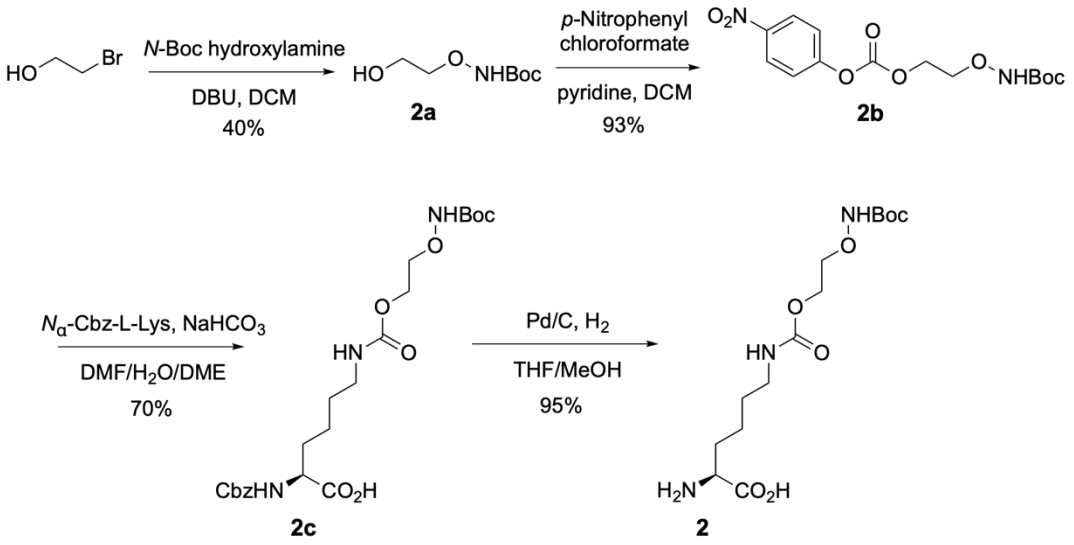

Scheme 2: Synthesis of AOAA **2**. DME: Dimethoxyethane.

Amino acid **2** was synthesized in 4 steps (Scheme 2). The synthesis of **2a** has been described in literature.[193] Compound **2a** was activated as a *p*-nitrophenyl carbonate (93% yield) and the ε-amine of N_α-Cbz-L-Lys was reacted with **2b** in a nucleophilic substitution (70% yield). The Cbz protection group was removed with 10 mol% Pd/C by hydrogenolysis to furnish **2** in 95% yield.

3.2.3 Synthesis of Coumarin-Protected AOAA 3

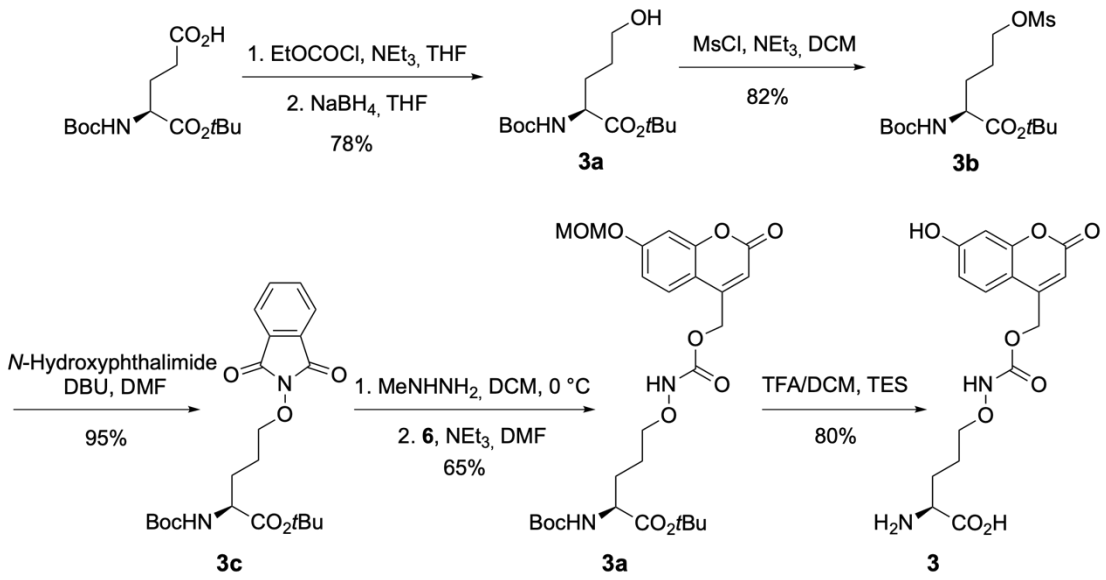

Scheme 3: Synthesis of AOAA **3**. TES: Triethylsilane. TFA: Trifluoroacetic acid.

Amino acid **3** was synthesized in 5 steps (Scheme 3). The preparation of compounds **3a**–**b** has been described in literature.[194-195] The coumarin protection group was introduced by hydrazinolysis of **3c**, followed by a nucleophilic attack of the free aminooxy group at the carbonate carbon atom of *p*-nitrophenyl carbonate **6** (65% yield). Treatment of **3a** with TFA/DCM 1:1 in the presence of 1.1 eq triethylsilane furnished **3** in 80% yield. The synthesis, characterization, and work with compounds **3d**–**3** and **6** was performed in the dark.

p-Nitrophenyl carbonate **6** was synthesized as reported (Scheme 4).[196],[186]

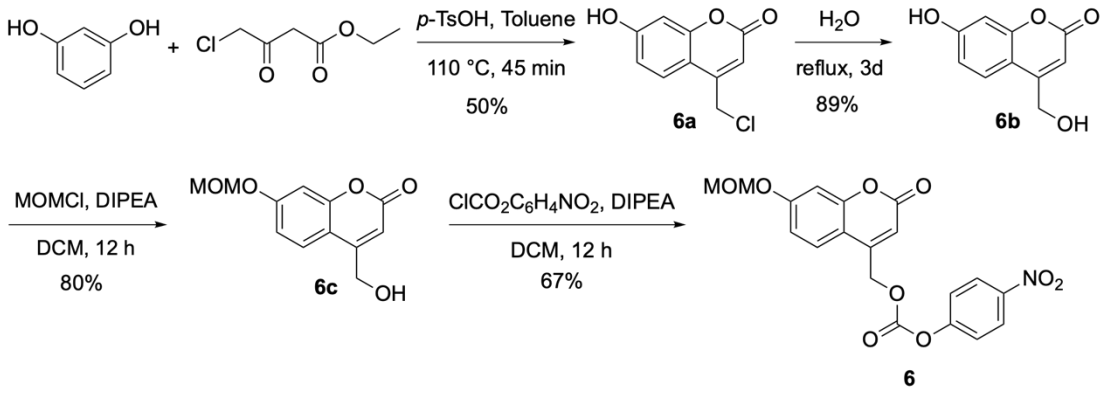

Scheme 4: Synthesis of compound **6**. MOM: Methyloxymethyl. DIPEA: *N*,*N*-Diisopropylethylamine. *p*-TSOH: *p*-Toluenesulfonic acid**.**

3.2.4 Synthesis of Nitro-Aryl-Protected AOAA 4

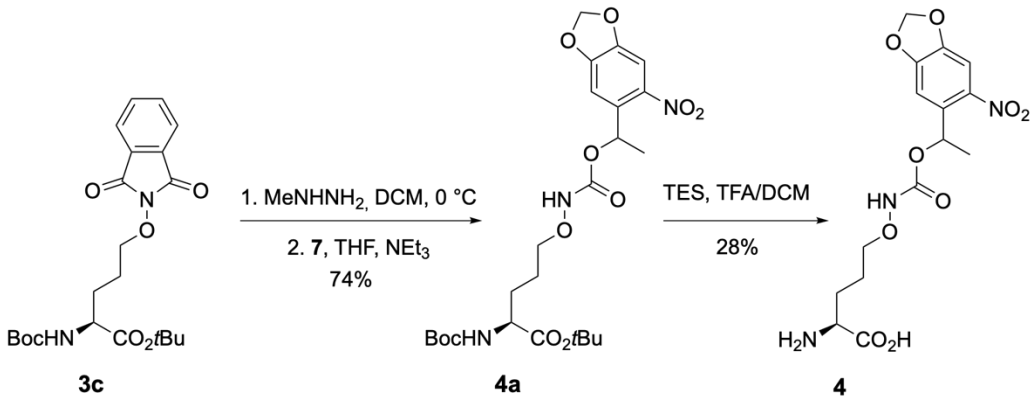

Scheme 5: Synthesis of AOAA **4**.

The synthesis of **4** was performed in 5 steps (Scheme 5). The first three steps are equivalent to the synthesis of **3**.[194-195] The aminooxy group was introduced by a nucleophilic attack of *N*-hydroxyphthalimide at the δ-carbon atom of **3c** (74% yield). Hydrazinolysis with methylhydrazine and protection with *p*-nitrophenyl carbonate **7** (Scheme 6) yielded **4a** in 74%. Amino acid **4** was furnished by treatment with TFA/DCM 1:1, 1.1 eq triethylsilane (28% yield). The low yield in the last step might be attributed to the acid-lability of the nitro protection group. The nitro substituent on the aromat and the benzylic methyl group could stabilize a positive charge, which is formed during an acid-catalyzed deprotection mechanism. In the course of this thesis, a similar synthesis route was published by Virdee *et al.*[137]

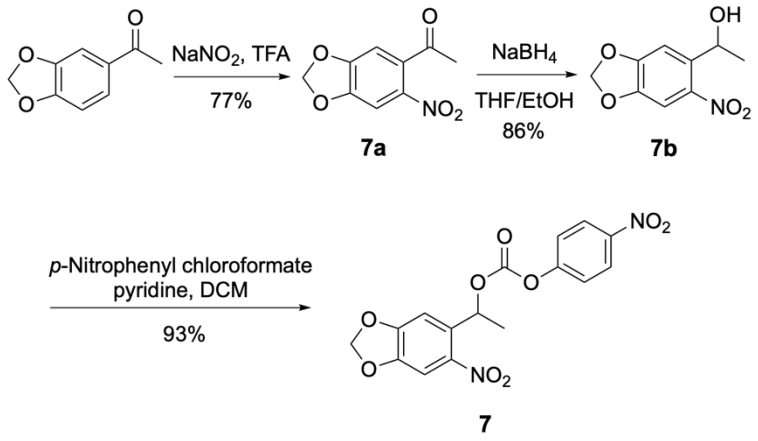

Scheme 6: Synthesis of *p*-nitrophenyl carbonate **7**.

p-Nitrophenyl carbonate **7** was synthesized in three steps (Scheme 6). The preparation of **7a**–**b** has been described.[197] Compound **7** was synthesized for the first time by a nucleophilic attack of the hydroxyl group of **7b** at *p*-nitrophenyl chloroformate (2 eq) in the

presence of pyridine in 93% yield. The synthesis, characterization, and work with compounds **4a**–**4** and **7** was performed in the dark.

3.2.5 Synthesis of Keto-Lysine KeK

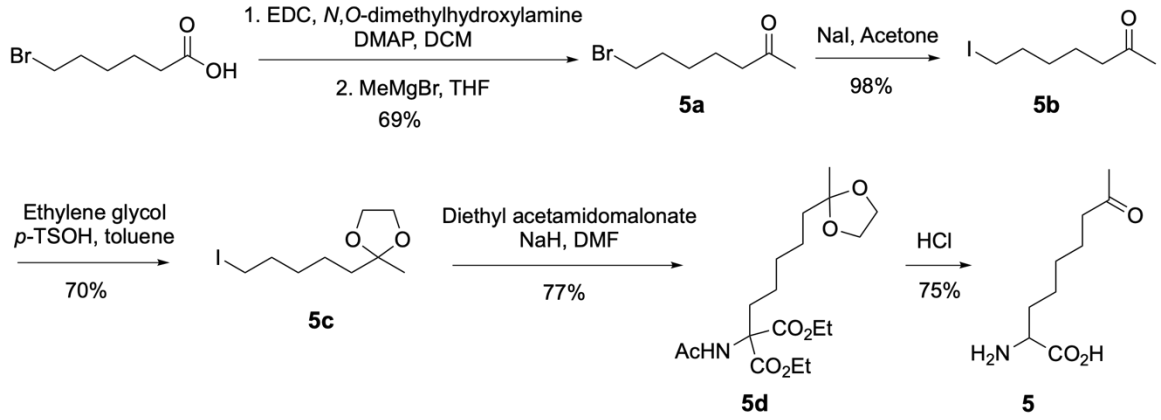

Scheme 7 : Synthesis of KeK **5**.[189]. EDC: 1-Ethyl-3-(3-dimethyl-aminopropyl)carbodiimide. DMAP: 4-Dimethylaminopyridine.

The synthesis of **5** (KeK) was performed as described in literature (Scheme 7).[189] Up-scaling to reaction batches of > 100 mmol of starting material was achieved while published yields were approximately maintained. During acidic deprotection of **5d** a brown oil was formed as side product, which could be removed from amino acid **5** by reversed-phase medium-pressure liquid chromatography (RP-MPLC), however, not as described with ion exchange chromatography.

3.2.6 Synthesis TAMRA–Ketone

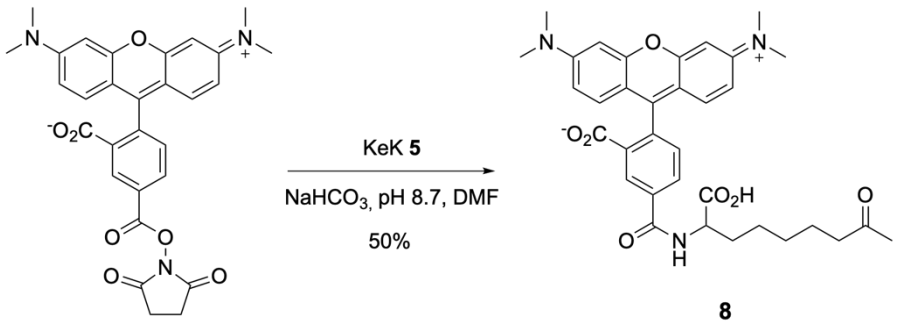

Scheme 8: Synthesis of TAMRA-Ketone **8**.

Before protein ubiquitination, the feasibility of oxime ligation involving aminooxy-modified proteins should be assessed with a keto-modified TAMRA dye (TAMRA-Ketone **8**). The labelling of aminooxy-functionalized proteins with TAMRA-Ketone can be followed by fluorescence readout after sodium dodecyl sulfate polyacrylamide gel electrophoresis (SDS-PAGE).

TAMRA-Ketone **8** was synthesized in one step from KeK **5** and TAMRA-NHS ester (1.5 eq, kindly provided by Maike Lehner[198-199]) at pH = 8.7 in 50% yield for the first time (Scheme 8). The compound was purified by RP-MPLC and stored at −20 °C. Reaction conditions were adapted from Buntz *et al*.[200]

3.3. Identification of PylRS Mutants for the Incorporation of UAAs

3.3.1 General Workflow for Test Incorporations into DNA Pol β

In order to investigate the potency of a *M. barkeri* PylRS mutant to incorporate an unnatural amino acid in response to an amber codon, test expressions of DNA Pol β 41TAG were performed. DNA Pol β served as model system for test incorporations because its expression is well established. Moreover, the level of expressed DNA Pol β can be analyzed by SDS-PAGE of the respective cell lysate and is a measure for UAA incorporation. This means, the more DNA Pol β is expressed, the better the unnatural amino acid is incorporated into the protein. PylRS mutants were generated by site-directed mutagenesis. The general protocol for DNA Pol β expression with unnatural amino acid incorporation was established and optimized by Tatjana Schneider.[130] Therefore, PylRS mutant and DNA Pol β 41TAG/$tRNA_{CUA}$ were co-expressed in a 6 mL expression medium. UAA of desired concentration was added at OD_{600} = 0.2–0.3. At OD_{600} = 0.6–0.9 a 1 mL sample was taken (-IPTG or -I) and expression was induced by addition of isopropyl-β-D-thiogalactopyranosid (IPTG, 1 mM). After 16 h at 37 °C, another 1 mL sample was taken. The OD_{600} values of both samples were adjusted to 2.5 and subjected to SDS-PAGE. The same procedure was applied to the incorporation of Boc lysine (BocK, final concentration 1 mM) into DNA Pol β 41TAG by PylRS wt (wild-type) as positive control.[135]

3.3.2 Test Incorporations of UAAs

3.3.2.1 Boc-Protected AOAA 1

The structural similarity of BocK and AOAA **1** led to the assumption, that amino acid **1** might also be an efficient substrate of PylRS wt.[135] The incorporation efficiency of AOAA **1** increased with higher concentration of amino acid during expression. However, in comparison to the positive control the incorporation efficiency was very low even when a final concentration of 10 mM **1** was used (Figure 12). A screening for suiting PylRS/$tRNA_{CUA}$ pairs was performed in collaboration with Moritz Schmidt from AG Summerer (data not shown). The screening consisted of consecutive positive (identify synthetases that incorporate UAA) and negative (exclude canonical amino acids) selection rounds and was performed on Agar plates.[201] All PylRS libraries were based on PylRS Y306A Y384F from *M. mazei* (AF mutant, *M. barkeri* numbering: Y271A Y349F) and contained additional mutations as shown in Table 1.

Table 1: *M. mazei* PylRS libraries used for the screening of PylRS mutants for incorporation of AOAAs **1** and **2**.

Library Name	Randomized Positions
AF	A302, L309, C348, M350, W417
LR	C348, M350, I413, R415
RE	M276, L407, D408, W411, W417
MoSI	Y306, L309, N346, C348, W411, I413
MoSII	A302, L309, N346, C348, Y384

That screening did not furnish a suiting synthetase. It has been reported that a Y349F mutation in PylRS increased overall aminoacylation of $tRNA_{CUA}$ independent of amino acid structure.[135] Since AOAA **1** was accepted by PylRS to a small extent, it was tested, if the Y349F mutation increased the aminoacylation of $tRNA_{CUA}$ with AOAA **1**. The incorporation of AOAA **1** by PylRS Y349F was very efficient, particularly, it was nearly as efficient as the positive control BocK (Figure 12 B).

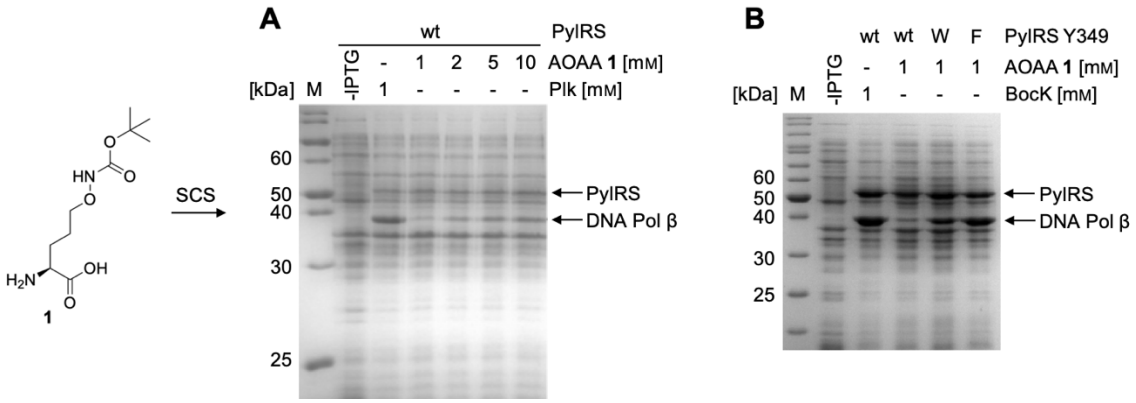

Figure 12: SDS-PAGE analysis of test incorporations as described in 3.3.1. **A)** Incorporation of AOAA **1** by PylRS wt. Here, propargyl-lysine (Plk), which is incorporated with similar efficiency by PylRS wt as BocK, served as positive control.[202] **B)** Incorporation of AOAA **1** by PylRS Y349F and PylRS Y349W. M: Marker.

Around the time of that finding, the incorporation of AOAA **1** with PylRS Y349W was published by Virdee *et al*.[137] The authors figured this mutant would be suiting for amino acid **1** because it was reported to incorporate a Boc lysine derivative that bears a polar hydroxyl or thiol group at the Lys δ-position.[156] The incorporation efficiency with this mutant is very similar, if not slightly reduced, to that with PylRS Y349F identified in this thesis (Figure 12 B). Analysis of a crystal structure of PylRS with pyrrolysine in the binding pocket indicated that residue Y349 might be important for substrate specificity.[132] The acceptance of AOAA **1** by PylRS mutants with aromatic unpolar amino acids F and W in position 349 might not only be attributed to an overall enhanced aminoacylation, but these mutations might favor interactions between AOAA **1** and the binding pocket. Moreover, the good acceptance of AOAA **1** by these PylRS 349 mutants might explain the unsuccessful screening for PylRS synthetases since all mutants screened for contained mutation Y271A in addition to Y349F. Mutation Y271A has been found to enlarge the PylRS binding pocket for binding of UAAs with bulky side chains, however, that is not necessary for AOAA **1**.[135]

3.3.2.2 Side-Chain Elongated AOAA 2

It was envisioned that the prolonged side chain of AOAA **2** and the Lys carbamate bond might favor the acceptance of AOAA **2** by PylRS AF, which is known to accept a broad scope of Lys derivatives with bulky side chains.[135] Additionally, PylRS AF was varied by combining Y271A with Y349W instead of Y349F, since both 349 mutants have been shown to incorporate AOAA **1**.[137] However, the incorporation of AOAA **2** was very inefficient with these PylRS mutants (Figure 13 and Figure 14 B) and even less efficient than that with PylRS wt (Figure 13 A).

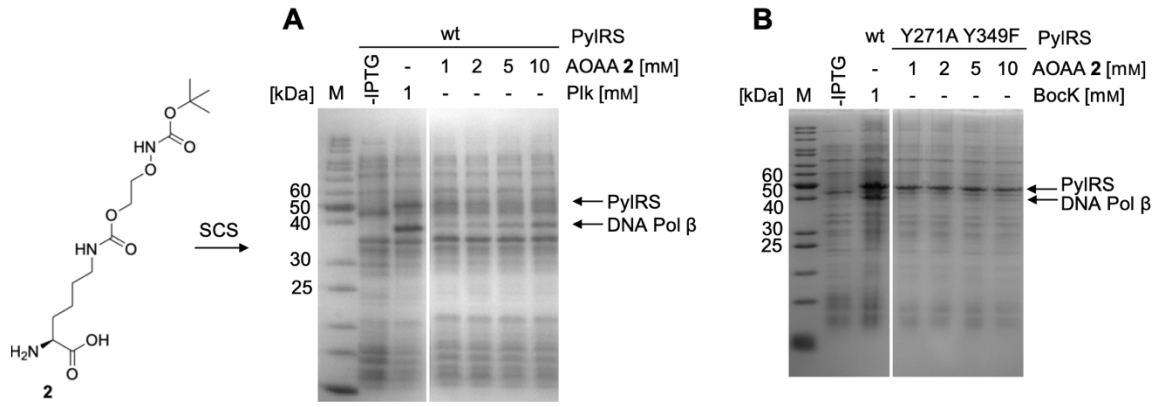

Figure 13: SDS-PAGE analysis of AOAA **2** incorporation into DNA Pol β with **A)** wt PylRS and **B)** PylRS AF. M: Marker. In A), propargyl-lysine (Plk), which is incorporated with similar efficiency by PylRS wt as BocK, served as positive control.[202]

A screening for PylRS mutants as described in chapter 3.3.2.1 did not lead to the discovery of an enhanced synthetase for the incorporation of AOAA **2**. Nevertheless, since PylRS wt aminoacylates $tRNA_{CUA}$ with AOAA **2** at least to some extent, it was expected that distinct mutations of PylRS will lead to a good acceptance of **2**. Therefore, AOAA **2** was modeled into the binding pocket of PylRS wt (by Karin Betz, based on PDB entry: 2ZIN[135]), and residues 274 and 315 were identified to be in close proximity to the elongated Lys side chain (Figure 14). Because these residues might sterically hinder binding of AOAA **2** in the binding pocket, they were mutated to Ala, which resulted in PylRS L274A, PylRS M315A, and PylRS L274A M315A. The generation of these PylRS mutants and respective test incorporations were performed by Giuliano Bayer.

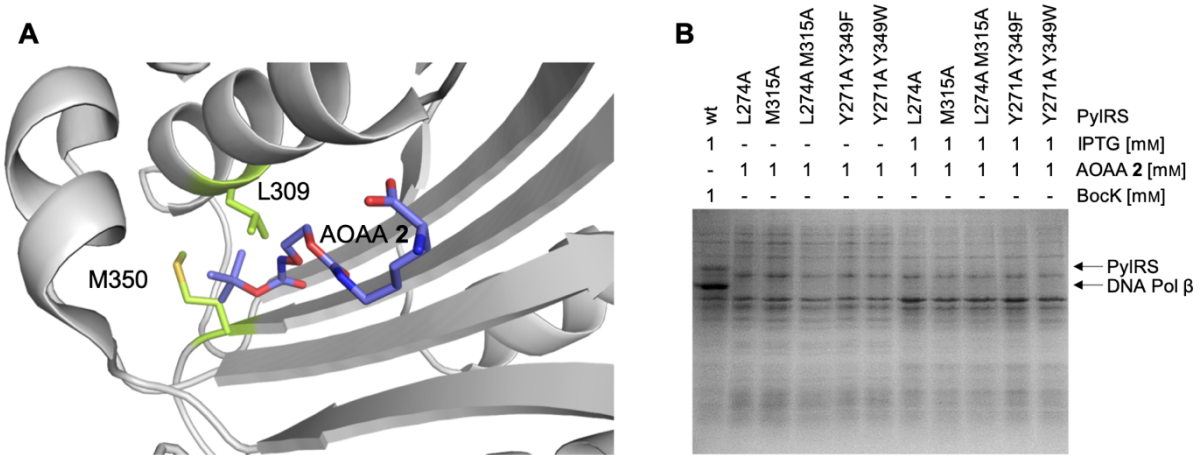

Figure 14: **A)** AOAA **2** was modeled into the binding pocket of *M. mazei* PylRS wt (amino acid numbering for *M. barkeri* was used for description of mutated residues) complexed with Boc lysine and an ATP analog (PDB: 2ZIN[135]). Structurally similar parts of AOAA **2** and BocK were superimposed. The binding mode of AOAA **2** was arbitrarily chosen in a way that as little as possible PylRS side chains were in close proximity. **B)** SDS-PAGE analysis of test incorporations with 1 mM AOAA **2** and PylRS mutants identified as described in A) and PylRS Y271A Y349F and PylRS Y271A Y349W.

However, AOAA **2** was no suiting substrate for any of these mutants (Figure 14 B). It can only be hypothesized that mutation to Ala was not beneficial and/or that AOAA **2** has a different orientation in PylRS than assumed for modeling.

In general, the polarity of the second, aminooxy-modified carbamate group and the large size of the amino acid side chain might make the identification of a suiting PylRS/$tRNA_{CUA}$ pair for AOAA **2** difficult, and a broad screening for PylRS mutants is necessary.

3.3.2.3 Coumarin-Protected AOAA 3

Coumarin-protected amino acid **3** is isosteric to Coumarin-lysine. Hence, PylRS Y271A L274M, which has been published for the incorporation of Coumarin-lysine[186], was tested for aminoacylation of $tRNA_{CUA}$ with AOAA **3** (Figure 15). After SDS-PAGE analysis of test incorporations, a clear band of DNA Pol β could be observed, which indicates AOAA **3** incorporation. Compared to the positive control and the incorporation of Coumarin-lysine, the incorporation of AOAA **3** was less efficient, yet sufficient (Figure 15 B). Increasing the amino acid concentration from 1 mM to 2 or 5 mM during expression did not enhance aminoacylation of $tRNA_{CUA}$ by AOAA **3** to a great extent (Figure 15 A).

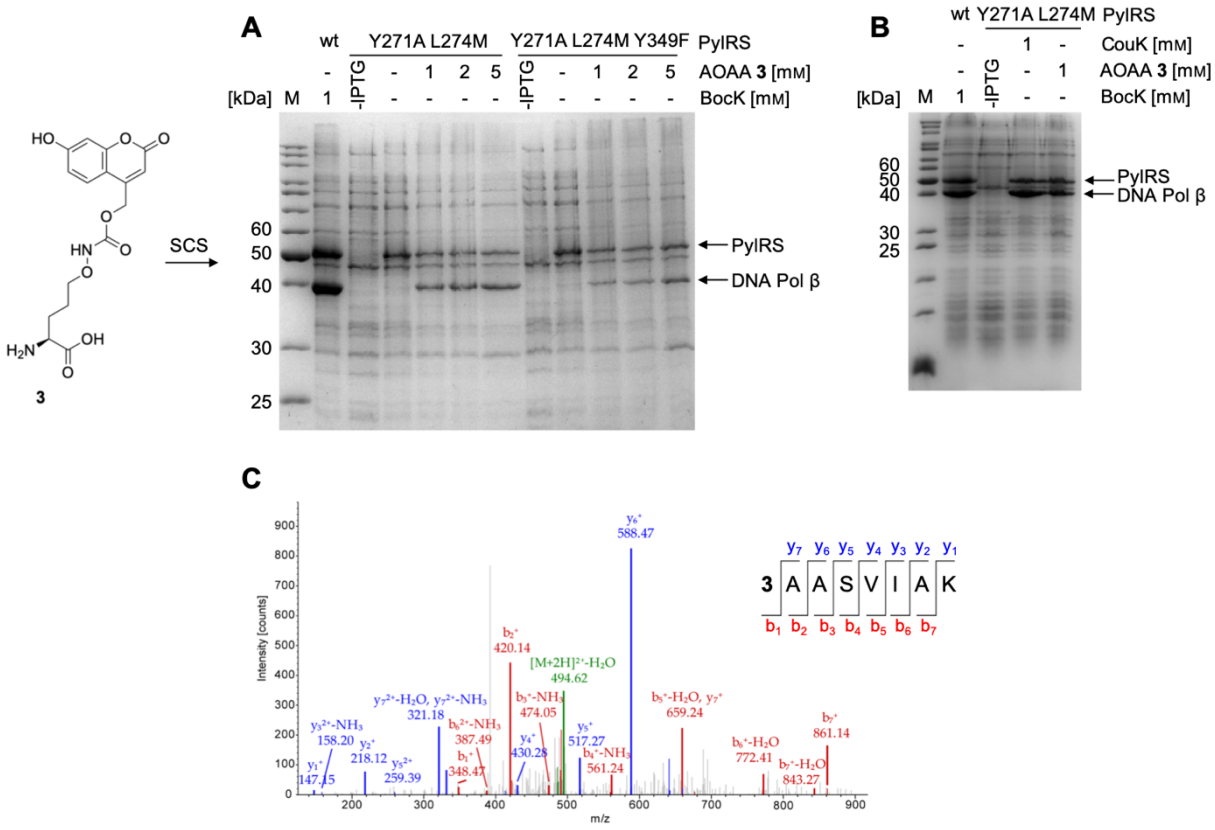

Figure 15: SDS-PAGE analysis of test incorporation of AOAA **3** into DNA Pol β **A)** by PylRS Y271A L274M and PylRS Y271A L274M Y349F **B)** in comparison to Coumarin-lysine (CouK). M: Marker. **C)** LC-MS/MS analysis supports the presence of DNA Pol β 41U**3** generated with PylRS Y271A L274M. Note: AOAA is abbreviated as U to describe position in POI.

Because a Y349F mutation led to a significantly enhanced acceptance of amino acid **1** by PylRS in comparison to PylRS wt (chapter 3.3.2.1), it was hypothesized that this mutation might generally enhance the acceptance of δ-position aminooxy-modified amino acids. Therefore, this mutation was combined with PylRS Y271A L274M. However, the incorporation efficiency of AOAA **3** into DNA Pol β was decreased with PylRS Y271A L274M Y349F (Figure 15 A). Virdee *et al.* reported a similar finding, when they attempted to enhance AOAA **4** incorporation by combining PylRS Y349W, which they identified for the

acceptance of amino acid **1**, with mutations that enabled incorporation of the Lys derivative of AOAA **4**.[137] Thus, PylRS Y349W/F mutations do not seem to generally increase the acceptance of Lys derivatives modified with an aminooxy group at the δ-position, but the interplay between PylRS and amino acid appears to be much more complex.

Notably, both mutants investigated for the incorporation of AOAA **3** (PylRS Y271A L274M and PylRS Y271A L274M Y349F) showed only traces of DNA Pol β when only canonical amino acids were present (Figure 15 A). Hence, a suiting PylRS Y271A L274M/$tRNA_{CUA}$ pair for the incorporation of AOAA **3** into proteins was identified in this work.

3.3.2.4 Nitro-Aryl-Protected AOAA 4

The incorporation of AOAA **4** by PylRS M241F A267S Y271C L274M, which has been known to incorporate the respective Lys variant[187], was reported to be very inefficient.[137] Combination of this mutant with Y349W, a mutation the authors identified for an efficient incorporation of AOAA **1** by PylRS, led to an even decreased acceptance of AOAA **4**.[137] In order to identify an efficient PylRS mutant, AOAA **4** was modeled into the PylRS binding pocket (by Karin Betz, based on PDB entry: 2ZIN[135]), and amino acid side chains that might sterically hinder binding of AOAA **4** were mutated to Ala. Selected positions depending on the orientation of the amino acid in the binding pocket were a) L274A, W382A or b) Y271A, L274A, I378A (Figure 16).

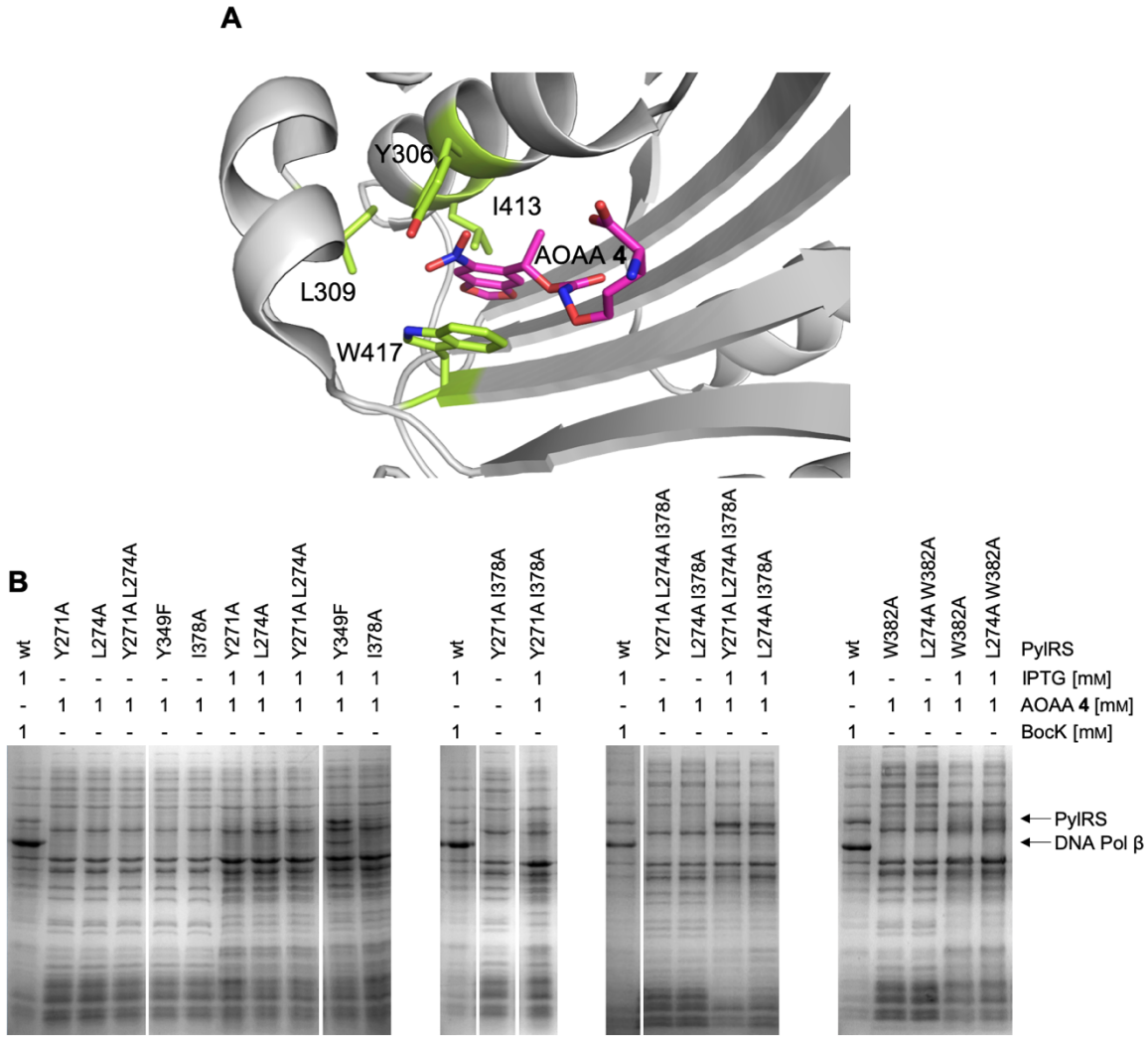

Figure 16: **A)** AOAA **4** was modeled into the binding pocket of *M. mazei* PylRS wt (amino acid numbering for *M. barkeri* was used for description of mutated residues) complexed with BocK and an ATP analog (PDB: 2ZIN[135]). Structurally similar parts of AOAA **4** and BocK were superimposed. The binding mode of AOAA **4** was arbitrarily chosen in a way that as little as possible PylRS side chains were in close proximity**. B)** SDS-PAGE analysis of test incorporations of AOAA **4** in DNA Pol β performed with PylRS mutants identified as described in A).

However, in Figure 16 B it is shown that none of these mutants incorporated AOAA **4** at 1 mM into DNA Pol β. Additionally, test incorporation was performed with PylRS Y349F. After SDS-PAGE analysis a weak band of DNA Pol β could be observed (Figure 17 B), which indicates inefficient incorporation of AOAA **4** with this mutant. Therefore, mutants identified by modeling were combined with Y349F and test incorporations were performed. The generation of PylRS mutants and respective test incorporations as shown in Figure 16 B and Figure 17 A were performed by Giuliano Bayer.

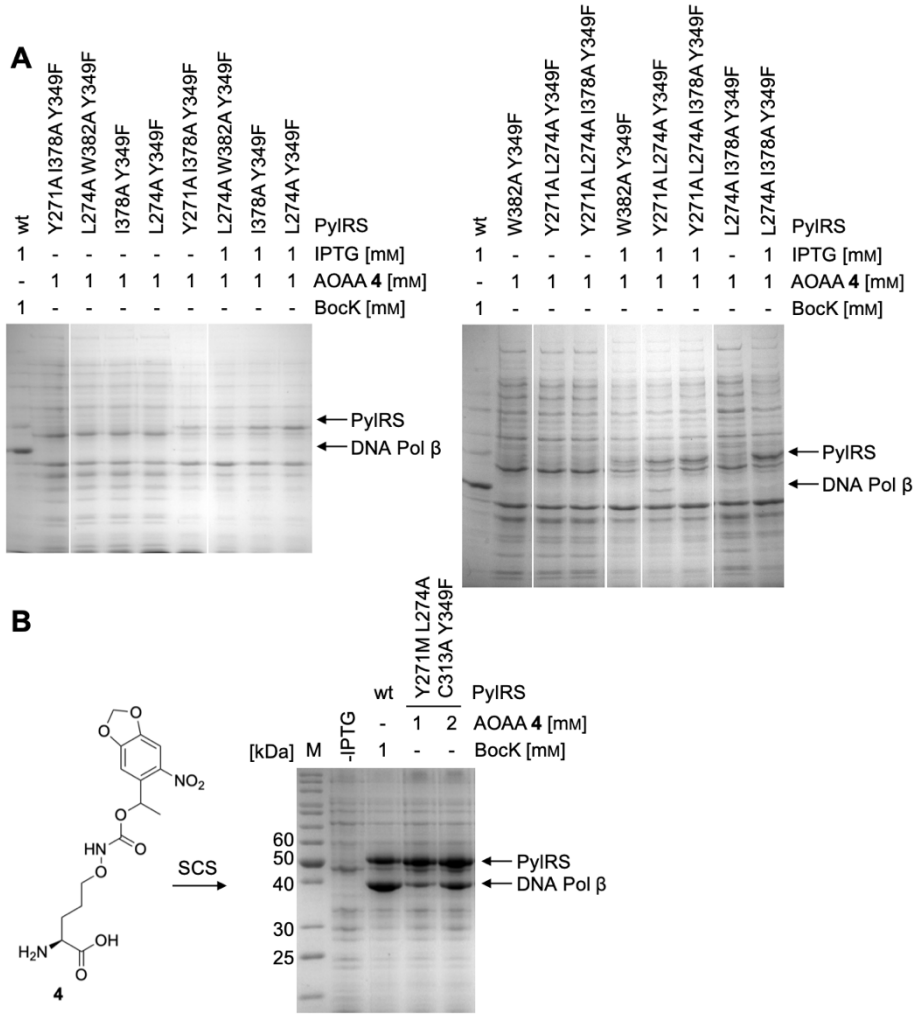

Figure 17: SDS-PAGE analysis of test incorporations of AOAA **4** with **A)** PylRS mutants identified by modeling combined with Y349F and **B)** with literature-known PylRS Y271A L274A C313A Y349F[203] into DNA Pol β. M: Marker.

The only mutant that could aminoacylate $tRNA_{CUA}$ with AOAA **4** was PylRS Y271A L274A Y349F. PylRS Y271M L274A C313A Y349F contains two of these mutations and has been reported to accept *o*-nitrobenzyl-oxycarbonyl-N_ε-L-Lys.[203] Hence, this mutant was generated and tested for acceptance of AOAA **4**. SDS-PAGE revealed that AOAA **4** (final concentration 1 mM) could be incorporated into DNA Pol β by PylRS Y271M L274A C313A Y349F and the incorporation efficiency was strongly enhanced by the use of AOAA **4** at a final concentration

of 2 mM (Figure 17 B). The incorporation efficiency of AOAA **4** with the PylRS mutant published by Virdee *et al.*[187] and with that identified in this thesis cannot be compared to each other with the experiments described above. This is because the published PylRS mutant was used for SCS in a different protein and only for AOAA **4** at a final concentration of 1 mM. Nevertheless, a suiting PylRS mutant for the incorporation of AOAA **4** was identified in this thesis.

3.3.2.5 Keto-Lysine KeK

The incorporation of KeK has been described with AcKRS (D76G L266V L270I Y271F L274A C313F).[188-189] Therefore, this mutant was generated and tested for the incorporation of KeK at a final concentration of 2, 5, and 10 mM into DNA Pol β (Figure 18, note: KeK was used as racemate). SDS-PAGE revealed that the expression of DNA Pol β increased with increasing concentrations of KeK, however, the level of DNA Pol β remained very low even with the use of KeK at a final concentration of 10 mM. Therefore, KeK can be incorporated into proteins with AcKRS, but it is not an efficient substrate. Also, the use of PylRS wt did not lead to a more efficient aminoacylation of $tRNA_{CUA}$ (Figure 18 right).

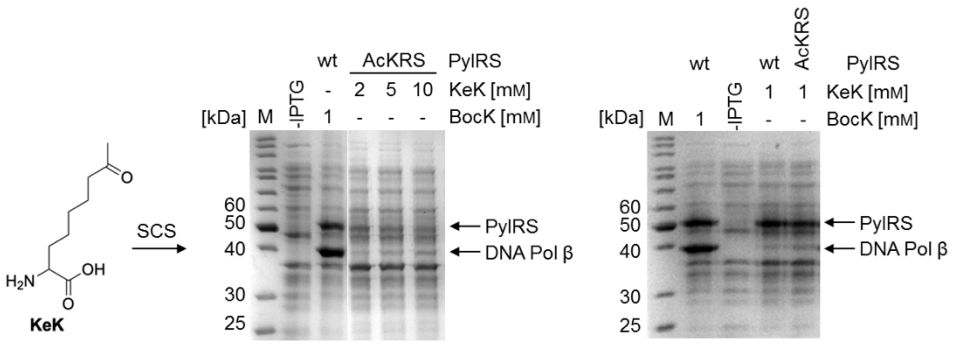

Figure 18: SDS-PAGE analysis of test incorporations of KeK with AcKRS and PylRS wt into DNA Pol β. M: Marker.

The codon usage and sequence (14 mutations) of the PylRS used in this thesis differed from that published by Liu *et al.*[189] Since this could have an influence on the expression of PylRS and its acceptance of KeK, a gene fragment encoding for exactly the published synthetase was ordered (Integrated DNA Technologies) and cloned into pRSF Duet-1, which yielded AcKRS Liu. However, test incorporations with AcKRS Liu did not lead to an enhanced stop-codon suppression in the presence of KeK (Figure 19 A). Deacetylase inhibitor nicotinamide is usually added during incorporation of AcK into proteins by AcKRS to prevent deacetylation of AcK.[188] If KeK was bound to deacetylase CobB, the availability for aminoacylation of $tRNA_{CUA}$ might be reduced. Therefore, test incorporation of KeK with AcKRS Liu was performed in the presence of 20 mM nicotinamide. However, the presence of nicotinamide during expression even decreased the amount expressed DNA Pol β (Figure 19 A). However, it is still unclear, whether the presence of nicotinamide does not lead to an enhanced incorporation of KeK because KeK is a similarly potent deacetylase inhibitor or because KeK is not involved in deacetylase inhibition. Test incorporation in an *E. coli* CobB knockout strain might give insight into that question.[204]

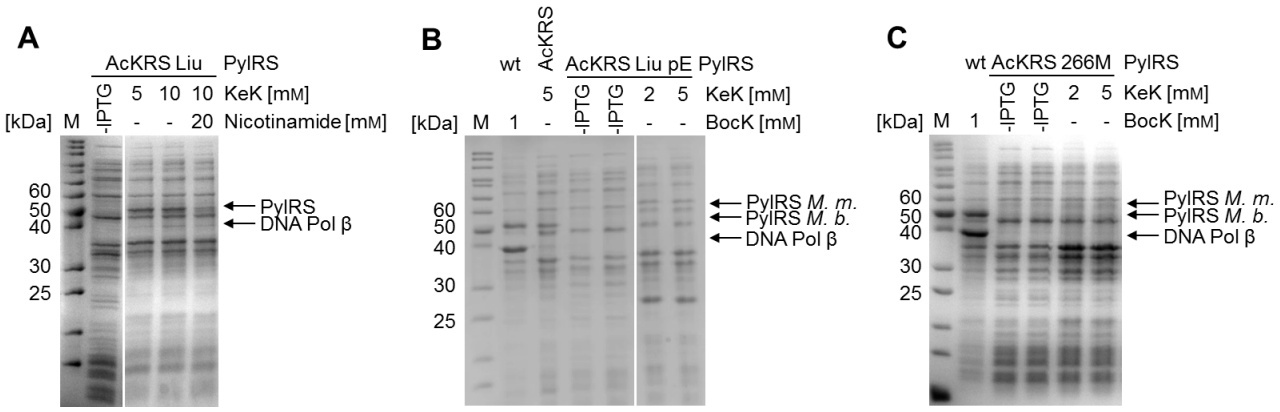

Figure 19: SDS-PAGE analysis of test incorporations of KeK into DNA Pol β with **A)** AcKRS Liu in presence or absence of nicotinamide, **B)** with AcKRS Liu pE, and **C)** with AcKRS L266M. M: Marker.

The group of Prof. W. Liu (Texas A&M University), who published the incorporation of KeK by AcKRS[189], provided an AcKRS variant they optimized in their lab (from *M. mazei*, pEvol vector, denoted as AcKRS Liu pE). Additionally, an AcKRS variant containing L266M – a mutation published to enhance AcK incorporation with respect to AcKRS[205] – was generated by Alexandra Julier (Scheffner group) (from *M. mazei*, pRSF Duet-1, denoted as AcKRS 266M). In Figure 19 B/C, it is shown that both AcKRS variants did not enhance aminoacylation of $tRNA_{CUA}$ with KeK compared to the initial AcKRS investigated in this thesis. Therefore, although generally inefficient compared to the positive control, from all PylRS mutants tested, AcKRS with KeK at a final concentration of 10 mM as described in Figure 18 was the most efficient synthetase for the incorporation of KeK.

The low incorporation efficiency of KeK by AcKRS variants might be attributed to the lack of a N_{ε}-carbamate group as present in AcK, and which has been shown to interact with PylRS.[132],[135-136] Alternatively, KeK might inhibit Lys deacetylase CobB, which could result in poor availability of KeK during expression.

3.3.3 Attempts to Enhance PylRS Activity

D. R. Liu *et al.* reported the introduction of four mutations (V31I, T56P, H62Y, A100E, denoted as IPYE) into PylRS for the general enhancement of PylRS activity.[140] Thus, the incorporation of AcK was improved 9.7-fold by the introduction of these mutations into AcKRS.[140] Since the results of that publication suggested that PylRS activity can be generally enhanced by these IPYE mutations and does not alter binding specificity towards distinct amino acids, these mutations were added to PylRS Y349F, PylRS Y271M L274A C313A Y349F, and AcKRS for the incorporation of AOAA **1**, AOAA **4**, and KeK, respectively. The generation of these mutants was performed by Martina Adam. Test incorporations of these amino acids into DNA Pol β with PylRS IPYE mutants were performed as described above and compared to test incorporations with the respective PylRS mutants that lack IPYE.

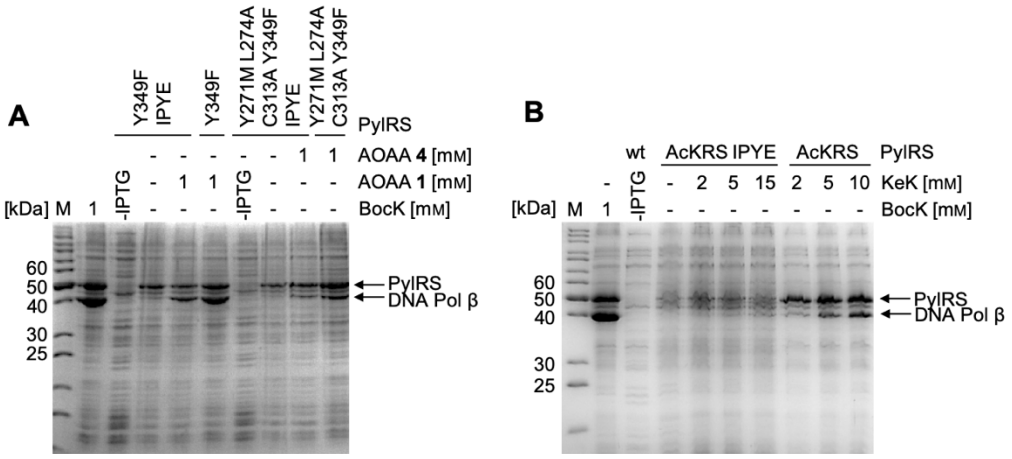

Figure 20: Test incorporations of **A)** AOAA **1**, AOAA **4**, and **B)** KeK with PylRS Y349F +/-IPYE, PylRS Y271M L274A C313A Y349F +/-IPYE, and AcKRS +/-IPYE, respectively, into DNA Pol β. M: Marker.

Test incorporations revealed that the introduction of IPYE mutations did not lead to an increased but to a decreased expression of DNA Pol β (Figure 20). This indicates a less efficient incorporation of these amino acids by IPYE-containing PylRS mutants compared to IPYE-lacking PylRS mutants.

3.3.4 Overall Discussion on the Identification of PylRS Mutants for the Incorporaton of UAAs

In this thesis, PylRS Y349F, PylRS Y271A L274M, and PylRS Y271M L274A C313A Y349F were identified for the efficient incorporation of AOAAs **1**, **3**, and **4**, respectively. No investigated PylRS/$tRNA_{CUA}$ pair genetically encoded AOAA **2**. Several attempts were made to further increase incorporation efficiency of KeK by known synthetase AcKRS[189], however, none of them were successful.

When discussing amino acid incorporation efficiencies by PylRS mutants, it should be kept in mind that single mutations in PylRS might affect PylRS expression due to unfavorable codon usage or alterations in mRNA secondary structures.[206] However, in this work no consistent, direct link between expression level of PylRS – when interpreted from band intensity after SDS-PAGE analysis – and incorporation efficiency could be observed for test incorporations into DNA Pol β.

Synthetases published for Lys variants were tested for the incorporation of respective isoelectronic AOAAs. It was striking that the incorporation efficiency was strongly reduced for all δ-aminooxy-modified amino acids tested in this work. That finding was unexpected because PylRS mutants are known to tolerate a variety of amino acid modifications.[91],[135] Probably, by replacing the ε-methylene group with an oxygen atom electronic properties are changed in a way that binding between AOAA and PylRS mutant is affected.

Mutation Y349F was suggested to accelerate the general $tRNA_{CUA}$ aminoacylation by PylRS.[135] Moreover, position 349 was suggested to play an important role in modulating PylRS substrate specificity.[132] In this work, addition of Y349F to a potent PylRS mutant for an AOAA did not further enhance the PylRS incorporation efficiency. This finding contradicts the assumption that Y349F generally increases the acceptance of δ-aminooxy-modified amino acids by PylRS mutants. This hypothesis was made in this work because AOAA **1** was accepted by PylRS Y349F whereas isoelectronic BocK is incorporated by PylRS wt.[135] Virdee *et al.* observed a similar effect.[137] Additionally, the introduction of IPYE mutations to PylRS has been reported to generally increase PylRS activity and thus incorporation efficiency.[140] However, the results of this thesis do not corroborate these data, since incorporation efficiencies of AOAAs **1**, **4**, and KeK were reduced upon addition of IPYE to respective PylRS mutants. These results illustrate that it is extremely difficult to transfer the knowledge gained about PylRS mutations for the incorporation of one amino acid to a structurally similar second amino acid.

Furthermore, the modeling of AOAAs **2** and **4** into the PylRS binding pocket, the subsequent identification of potentially sterically hindering PylRS residues, and their mutation to Ala did not lead to the generation of suiting PylRS/$tRNA_{CUA}$ pairs. Thus, interactions between amino acid and PylRS tend to be much more complex than just determined by sterical hindrance.

Modeling can be used to explain a known amino acid/PylRS interaction and to identify residues to be randomized for a screening, rather than to determine distinct mutations to a specific amino acid.

Overall, suiting PylRS/$tRNA_{CUA}$ pairs for the incorporation of AOAAs **1**, **3**, and **4** were identified.

3.4. Analysis of Incorporation of Photo-Protected AOAAs into Ub 48TAG

3.4.1 Coumarin AOAA 3

3.4.1.1 Incorporation of Coumarin AOAA 3 into Ub 48TAG

The results of the test incorporations performed in chapter 3.3.2.3 suggested the successful incorporation of AOAA **3** by PylRS Y271A L274M. In order to verify the incorporation by mass analysis, Ub was chosen as model protein. Hence, Ub 48TAG with a C-terminal His tag/$tRNA_{CUA}$, and PylRS Y271A L274M were co-expressed into *E. coli* BL21 (DE3) cells. At OD_{600} = 0.2–0.3 AOAA **3** (final concentration 1 mM) was added and expression was induced at OD_{600} = 0.6–0.9 by addition of IPTG (final concentration 1 mM). After overnight (o.n.) expression at 37 °C the cell pellet was harvested by centrifugation, resuspended in 20 mM Tris, 300 mM NaCl, 0.1% Triton x-100, pH 7.5, and sonicated. After centrifugation, the supernatant was incubated with imidazole (final concentration 5 mM) and cOmplete His-tag purification resin (Roche) for at least 2 h at 4 °C. The protein was eluted with increasing concentrations of imidazole (5–500 mM) in 20 mM Tris, 300 mM NaCl, pH 7.5 (Figure 21 A). For His-tag cleavage, pure fractions were incubated with Ubiquitin C-terminal hydrolase L3 (UbCHL3) and dialyzed against 0.1 x phosphate-buffered saline (PBS) o.n., followed by dialysis against 20 mM NaOAc, pH 4.5. The protein was applied to SP Sepharose® Fast Flow resin and eluted with increasing concentrations of NaCl (0–500 mM) in 20 mM NaOAc, pH 4.5 (Figure 21 B). Pure fractions were pooled and dialyzed against phosphate-buffered saline (PBS) pH 7.2. A 500 mL expression yielded 1.4 mg Ub 48U**3** (note: AOAA is abbreviated as U to describe position in POI).

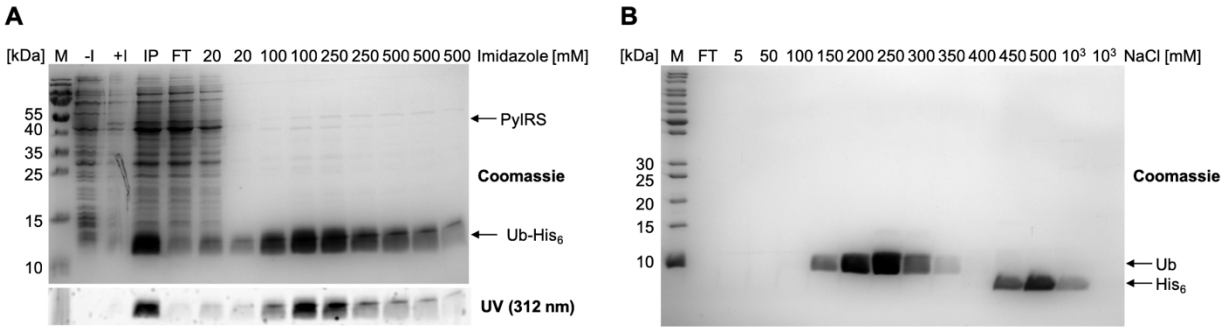

Figure 21: SDS-PAGE analysis after **A**) purification of Ub 48U**3** by immobilized metal ion chromatography followed by **B**) cation exchange after His-tag cleavage. The fluorescence readout in A) was performed by transilluminating the gel with 312 nm (Amersham Gel Reader Imager 600, EtBr filter). M: Marker. -I/+I: Sample before induction of expression and after expression. IP: Sample before addition of His-tag purification resin. FT: Flow-through, M: Marker. Note: No band for UbCHL3 was detected due to precipitation of the protein at pH 4.5. Only supernatant was used for purification.

The expression and purification protocols for His-tagged Ub were adapted from Katrin Stuber[207].

3.4.1.2 Mass Analysis of Ub 48U3

The mass spectrum of Ub 48U**3** showed a mass that can be assigned to Ub 48U**3** (Figure 22 A, calc.: 8784.9 Da, found: 8784.6 Da). However, an additional mass with a mass shift of +18 Da was observed (8802.8 Da). This additional mass was not observed in mass measurements of Ub wt and cannot be assigned to misincorporation of a canonical amino acid (Figure 22 B). The mass spectrum of free AOAA **3** (Figure 22 C) and the respective NMR spectrum were pure (see attachments, note: AOAA **3** can withstand harsh acidic conditions. The last step of AOAA **3** synthesis is performed in 50% TFA/DCM at rt). This indicates that the additional mass was not just a random impurity in the protein sample and that AOAA **3** used in this experiment did not contain an impurity that would explain the additional species.

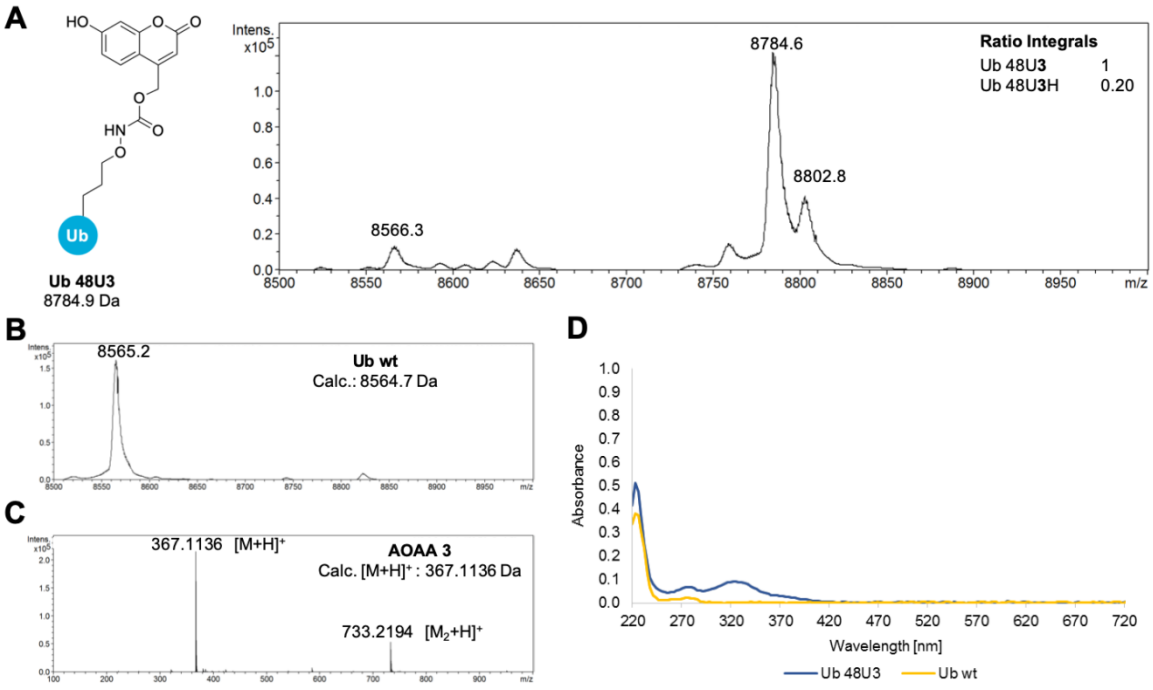

Figure 22: LC-MS Data with respective expected mass values of **A)** Ub 48U**3, B)** Ub wt, and **C)** AOAA **3**. Signal with 8566.3 Da might derive from misincorporation of Lys in response to TAG or from deprotected Ub 48U**3**. **D)** UV/vis spectrum of Ub wt and Ub 48U**3** (180 µM each) in PBS pH 7.2.

For further investigations LC-MS analysis was used to study the deprotection of the coumarin group on Ub and the origin of the +18 Da species. It was assumed that Ub 48U**3**, its deprotected form and the +18 Da variant have approximately similar properties in ESI-ToF measurements. Thus, the integrals of mass signals that are compared to each other in the following do not represent exact ratios of respective compounds to each other, but they represent trends of those.

The UV/vis spectrum of Ub 48U**3** in PBS pH = 7.2 (Figure 22 D) shows an absorption band from 300–420 nm with a local maximum at 325 nm, which is not observed for Ub wt and can

therefore be assigned to the coumarin group. These values are in accordance with reported absorption bands for coumarin dyes.[186] To investigate, if the coumarin group can be photochemically removed, protein samples were irradiated at 365 nm from 15 s to 60 min and subjected to SDS-PAGE and LC-MS analysis (Figure 23). This experiment also served to further examine, whether the +18 Da species (in the following denoted as Ub 48U**3**H) derived from AOAA **3** itself or from a protein modification unrelated to AOAA **3**. If Ub 48U**3**H originated from a protein modification unrelated to AOAA **3**, additionally to the expected mass of coumarin-deprotected Ub 48U**3** (Ub 48-ONH_2, 8566.7 Da), a mass of +18 Da respective to Ub 48-ONH_2 would be observed (8584.7 Da) upon coumarin removal.

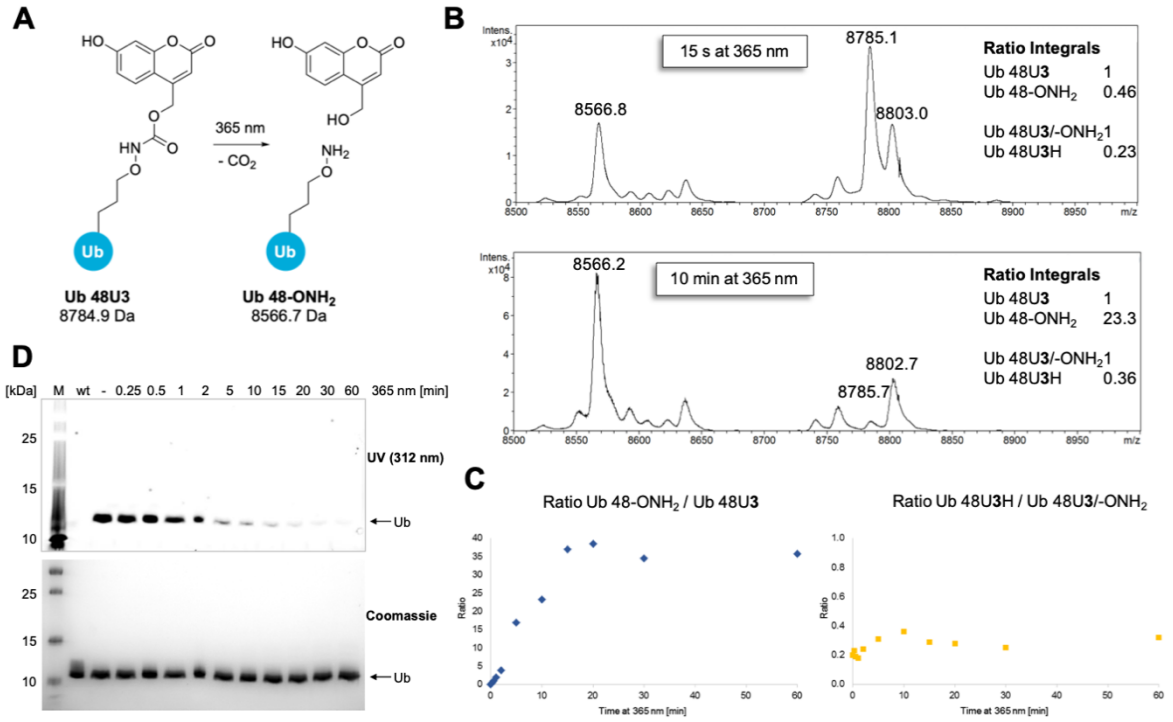

Figure 23: **A)** Expected mass values for deprotection of Ub 48U**3** upon irradiation at 365 nm. **B)** LC-MS analysis of Ub 48U**3** (90 µM) irradiated at 365 nm for 15 s and 10 min. A UV Lamp B-100AP, 365 nm, 100 W, 12 mW/cm^2 from UVP was used and protein samples were placed on a flat underground on ice. **C)** Ratio of mass signal integrals of Ub 48-ONH_2 to Ub 48U**3** (left) and Ub 48U**3**H to Ub48U**3**/-ONH_2 (right) vs time interval of irradiation. In both cases the nominator was set to 1. Deprotection as described in B) was performed for 15 s, 30 s, 1 min, 2 min, 5 min, 10 min, 15 min, 20 min, 30 min, and 60 min. **D)** SDS-PAGE analysis of irradiated Ub 48U**3** as described in B) and C). The fluorescence readout was performed by transilluminating the gel with 312 nm (Amersham Gel Reader Imager 600, EtBr filter).

SDS-PAGE analysis and subsequent fluorescence readout (Figure 23 D) showed that the longer Ub 48U**3** was irradiated at 365 nm the more the fluorescence signal decreased. That indicates the cleavage of the fluorescent coumarin group. Subsequent Coomassie staining confirmed the presence of protein in all samples. Mass analysis (Figure 23 B) corroborated these data. Upon irradiation at 365 nm the mass signal for Ub 48U**3** decreased and that for Ub48-ONH_2 emerged. After irradiation for 10 min the vast majority of the Ub 48U**3** mass

signal vanished and after 15 min irradiation the mass signal did not decrease anymore. Even after 60 min very small amounts (~5%) of Ub 48U**3** remained. That indicates the successful deprotection of Ub 48U**3** after irradiation for 10 min. Upon deprotection, no mass signal of 8584.7 Da was detected. That suggests that the +18 Da species did not derive from a random Ub 48U**3** modification but was likely to be linked to AOAA **3**. The mass signal of Ub 48U**3**H remained in a constant ratio to the sum of the signal of Ub 48U**3** and Ub 48-ONH_2 (Figure 23 C right) for all deprotection time periods. It can be concluded that Ub 48U**3**H was probably not generated during LC-MS measurements and is probably not in equilibrium with Ub 48U**3**. In these cases, the signal for Ub 48U**3**H would have vanished and the ratio between Ub 48U**3**H and Ub48U**3**/-ONH_2 would have drastically decreased upon deprotection.

These results led to the hypothesis that the lactone of the coumarin protection group of AOAA **3** was partially hydrolyzed (Figure 24). Hydrolysis would be in accordance with a mass shift of +18 Da and the spectral properties of the protection group could be altered in a way that the protection group could not be removed by irradiation at 365 nm anymore. This scenario would be disadvantageous for the application of AOAA **3**-equipped proteins in oxime ligation because aside from aminooxy-modified protein, there would always be unfunctionalized protein.

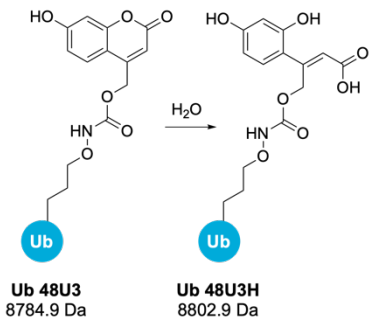

Figure 24: Hypothesis for the occurrence of the +18 Da species is hydrolysis of the coumarin lactone. The structure of Ub 48U**3**H therefore is hypothetical.

Keeping in mind all information gained until now, the potential lactone hydrolysis might have occurred upon incorporation of AOAA **3** into Ub or in the course of subsequent protein purification. To narrow down these possibilities, several changes to the expression and purification protocol were made (Table 2). Expression culture ranged from 50–500 mL in these experiments.

Table 2: Purification steps with corresponding conditions.

	Purification Protocol	
N°	**Purpose**	**Condition**
1	Resuspension/Sonication	20 mM Tris, 300 mM NaCl, 0.1% Triton x-100, pH 7.5
2	Immobilized metal ion chromatography	20 mM Tris, 300 mM NaCl, 0.1% Triton x-100, 5–500 mM imidazole, pH 7.5 cOmplete His-tag purification resin (Roche)
3	His-tag cleavage	UbCHL3, 0.1x PBS pH 7.2
4	Cation exchange	20 mM NaOAc, 0–1 M NaCl, pH 4.5
5	Dialysis	PBS, pH 7.2

First, His-tag cleavage by UbCHL3 (3) was omitted to ensure its hydrolase activity was not misdirected against the coumarin lactone (a). Furthermore, the use of Ni-coated beads for immobilized metal ion chromatography (2) was investigated since transition metals might catalyze hydrolytic cleavages. Therefore, either Ni-coated beads from Qiagen instead of Roche were used (c, step 3 left out too), or the immobilized metal ion chromatography step (2 and 3) was skipped (d). In another attempt, the cation exchange purification was not performed (b: step 3 and 4 skipped, c). Finally, after expression the cell pellet was only resuspended and sonicated, and the supernatant was directly applied to LC-MS analysis (e). In all cases the mass signal of Ub 48U**3**H was observed with a similar ratio of integrals towards the Ub 48U**3** mass signal as when the whole purification protocol was performed (Figure 25). This implies that the presumed lactone hydrolysis could not be traced back to one specific purification step. To exclude instability of AOAA **3** at 37 °C, expression of Ub 48U**3** was performed at rt, however, this did not lead to a different result (Figure 25).

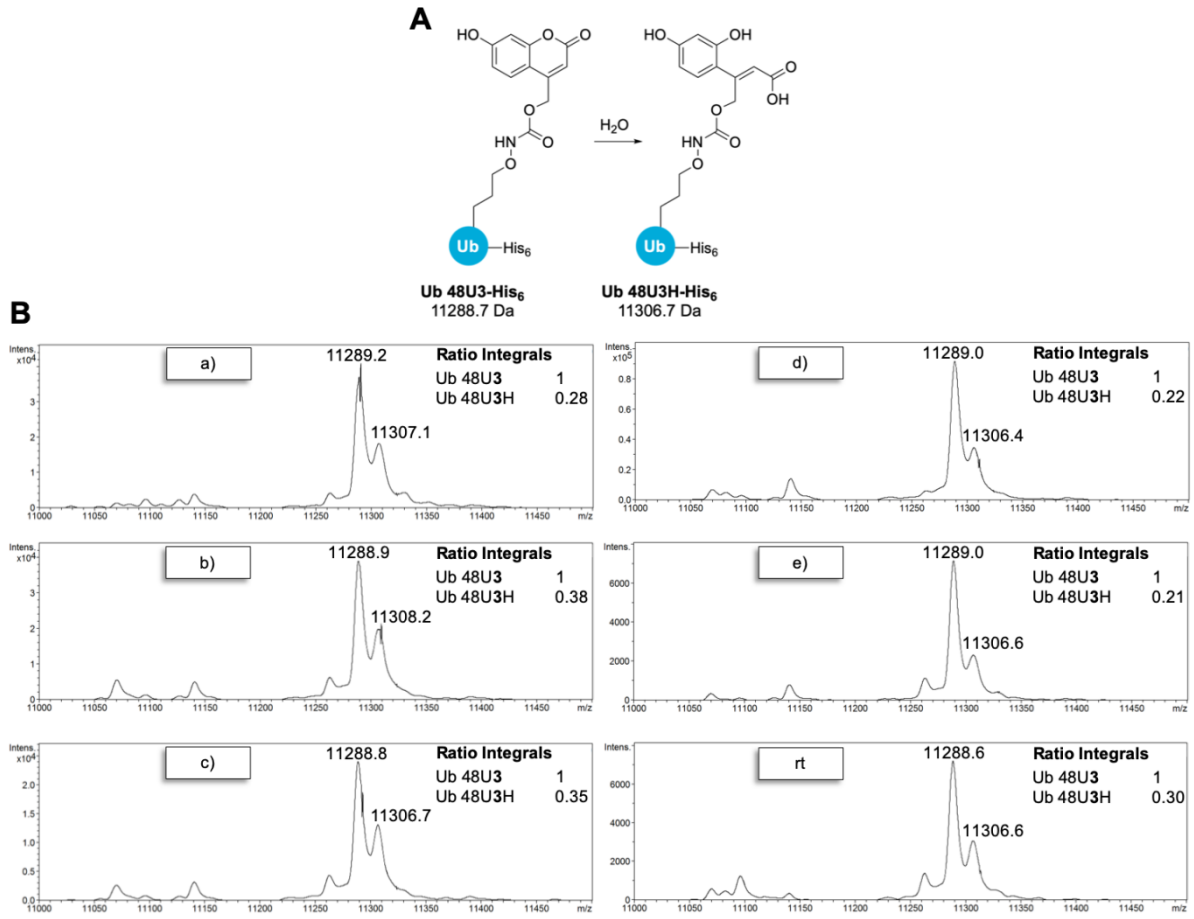

Figure 25: **A)** The hypothesis for the occurrence of the additional +18 Da mass upon incorporation of AOAA **3** into Ub 48TAG is the hydrolysis of the coumarin lactone. Schematic depiction of Ub 48U**3**-His_6 and Ub 48U**3**H-His_6 and respective calculated molecular weights. **B)** Mass spectra of Ub 48U**3**-His_6 purified by using modified protocols.

A more likely event might be potential lactone hydrolysis during protein expression (Figure 25 A). One possibility would be the existence of lactone-cleaving enzymes in *E. coli*. However, to the best of knowledge, there were only reports on *o*-coumaric acid as an intermediate in coumarin degradation in *Arthrobacter* or on lactone-cleaving enzymes in microorganisms different from *E. coli*.[208-210] In the event of an enzymatic lactone cleavage, protein expression in the presence of higher concentrations of coumarin/7-hydroxycoumarin or AOAA **3** might lead to less Ub 48U**3**H due to an increased number of binding events of a potentially involved enzyme. Therefore, Ub 48U**3** expression was performed with AOAA **3** (final concentration 1 mM) and coumarin (final concentration 2 mM) or 7-hydroxycoumarin (final concentration 1 mM). The coumarin/7-hydroxycoumarin concentrations applied here were the highest concentrations *E. coli* BL21 (DE3) cells could withstand without reduced cell growth compared to untreated cells (see attachments). Moreover, Ub 48U**3** was expressed in the presence of AOAA **3** at a final concentration of 5 mM instead of 1 mM. Mass data suggest that neither the presence of coumarin derivatives nor the use of more amino acid prevented the coumarin group of AOAA **3** from potential hydrolysis (Figure 26 A and B, respectively).

The result of this experiment must not be misinterpreted as proof against or for the presence of coumarin lactone-cleaving enzymes, it rather illustrates that AOAA **3** at 5 mM, coumarin at 1 mM, and 7-hydroxycoumarin at 2 mM concentration did not inhibit potentially involved enzymes. Since there were no profound information on such enzymes in *E. coli* cells, investigations in this direction were concluded.

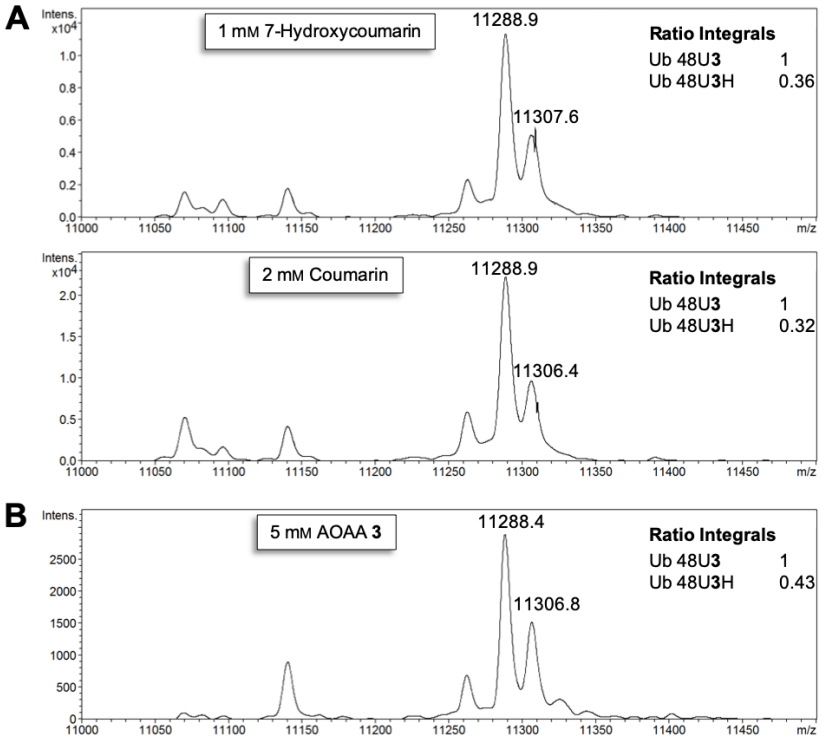

Figure 26: **A)** LC-MS analysis of Ub 48U**3**-His_6 expressed in the presence of coumarin or 7-hydroxycoumarin at final concentrations of 2 mM and 1 mM, respectively. **B)** LC-MS analysis of Ub 48U**3**-His_6 expressed in the presence of AOAA **3** at a final concentration of 5 mM.

Moreover, the cleavage of N_ε-amide bonds of UAAs by deacetylase CobB has been observed in *E. coli* cells.[188],[204],[211] This was circumvented by the knock-out of CobB in *E. coli* cells or the addition of deacetylase inhibitior nicotinamide during protein expression. Expression of Ub 48U**3** in the presence of nicotinamide at a final concentration of 10 mM did not prohibit the occurrence of Ub 48U**3**H in LC-MS (Figure 27). Hence, CobB is probably not responsible for the occurrence of Ub 48U**3**H. To definitely answer that question, expression in an *E. coli* CobB knockout strain would be necessary.

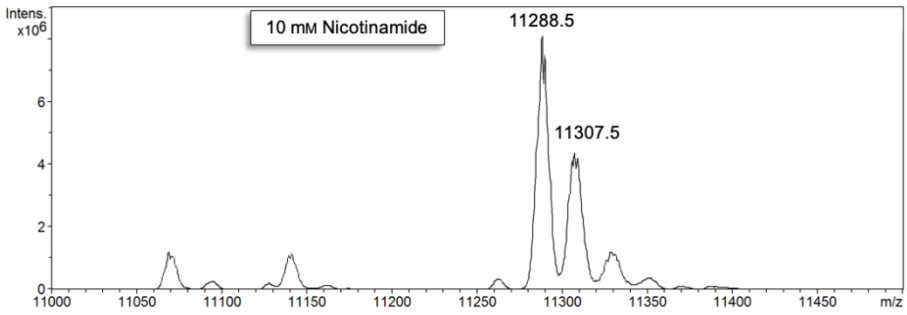

Figure 27: LC-MS analysis of Ub 48U**3**-His$_6$ expressed in the presence of nicotinamide (final concentration 10 mM). Nicotinamide concentration was chosen based on a similar procedure by Lang and coworkers.[204] The +18 Da species also occurred with this procedure. Similar results were obtained for incorporation of AOAA **3** with a Ub 48TAG construct lacking the C-terminal His-tag in the presence of nicotinamide (attachments).

Another possible explanation might be the change of the pK_a of the AOAA **3** side chain upon integration into a protein, which could favor hydrolysis. The question came up, if the potential hydrolysis was reversible, and if lactone formation could be induced by lowering the pH of the Ub 48U**3** sample. Therefore, samples of Ub 48U**3** were adjusted to pH 5, 4, 3, 2, and 1 with 1% aq. TFA in PBS. One half of these samples was directly applied to LC-MS analysis, the other half was irradiated at 365 nm for 10 min and subsequently subjected to mass analysis (attachments). The mass data did not reveal a dependence of the ratio of the integral for Ub 48U**3**H to Ub 48U**3** on the pH of the sample (Figure 28 right). Notably, an increased integral for Ub 48-ONH$_2$ compared to the integral for Ub 48U**3** can be observed the lower the pH upon irradiation at 365 nm for 10 min (Figure 28 left). On the one hand, this can occur because the absorption of the coumarin dye depends on the pH, on the other hand decarboxylation is the rate-limiting step for coumarin deprotection and can be enhanced under acidic conditions. Thus, potential lactone reformation could not be achieved by lowering the pH, but deprotection seems to be enhanced.

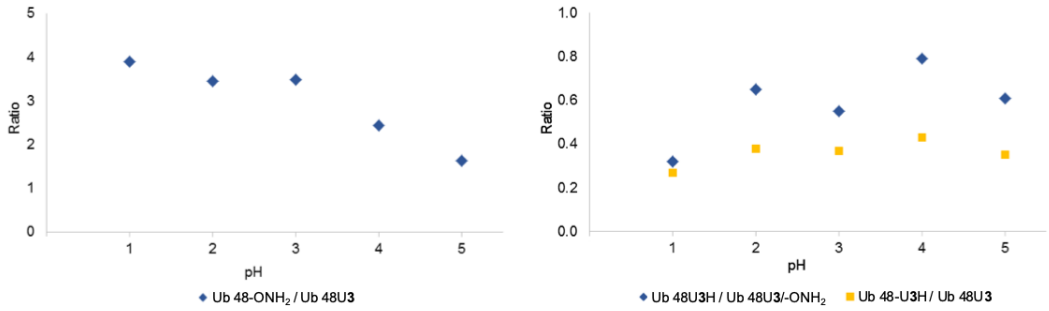

Figure 28: Ratio of mass signal integrals of Ub 48-ONH$_2$-His$_6$ to Ub 48U**3**-His$_6$ (left) after irradiation at 365 nm for 10 min, and Ub 48U**3**H-His$_6$ to Ub48U3-His$_6$/-ONH$_2$-His$_6$ (right, blue: samples irradiated for 10 min, yellow: no irradiation) vs pH of protein solution. In both cases the nominator was set to 1.

The respective Lys derivative of AOAA **3**, Coumarin-lysine (CouK), has been incorporated into eGFP and Renilla luciferase by PylRS Y271A L274M, however, no unexpected mass

results were reported.[186],[212] CouK was prepared as published[186], incorporated into Ub 48TAG and purified as described above (version b). LC-MS analysis was performed to investigate whether the formation of a +18 Da species is a general side-effect of coumarin-protected UAA incorporation into Ub 48TAG or is limited to the use of the respective AOAA. Mass analysis of the purified protein revealed a single mass signal that can be assigned to Ub 48CouK (Figure 29). These results indicate that the suggested lactone hydrolysis only takes place when the protection group is linked to an aminooxy-modified carbamate (AOAA **3**), but not when connected to an amine (CouK). Presumably, the aminooxy modification reduces the stability of the coumarin lactone.

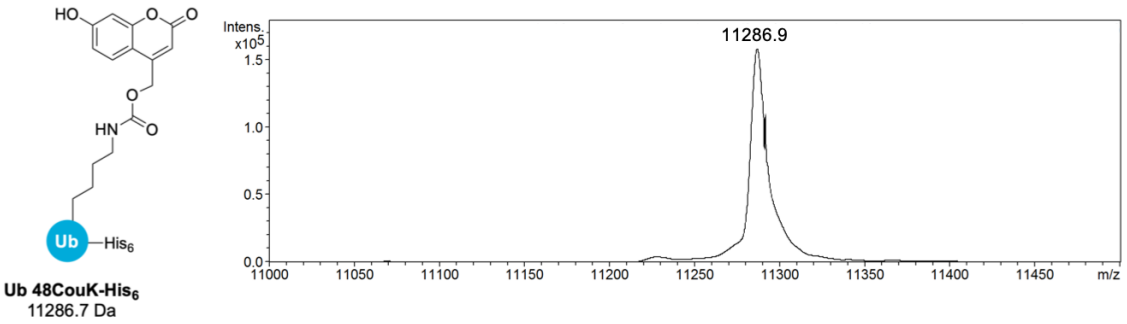

Figure 29: Schematic representation of Ub 48CouK-His_6 with calculated molecular weight and LC-MS analysis.

The protein environment surrounding Ub 48 could favor lactone hydrolysis. To investigate if potential lactone hydrolysis is a site-specific phenomenon, AOAA **3** was incorporated additionally into Ub 63TAG and Ub 6TAG. Mass analysis revealed the presence of Ub 6/63U**3** and the respective +18 Da mass signals with increased ratios of Ub 6/63U**3**H to Ub 6/63U**3** (Figure 30).

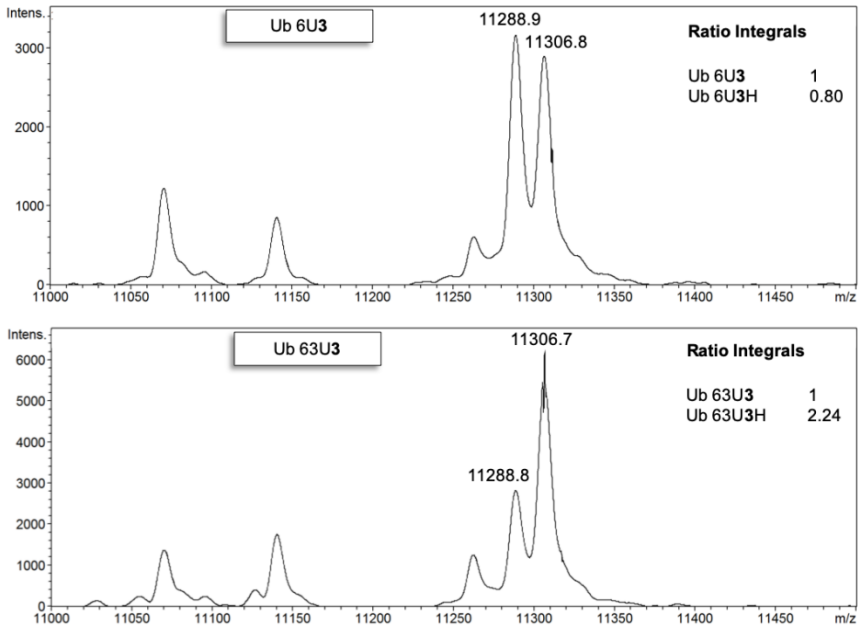

Figure 30: Mass spectrum of Ub 6U**3**-His_6 and Ub 63U**3**-His_6.

Therefore, the position of modification might have an impact on the generation of the Ub U**3**H derivatives. This could possibly be attributed to the presence of amino acid side chains that can catalyze acid/base reactions. One example is the imidazole of histidine, and the esterase activity of His residues, particularly of His-tags, has been described recently.[213] Thus, Ub 48U**3** was expressed as described in chapter 3.4.1.1 without tag, and purification was performed by heat-precipitation.

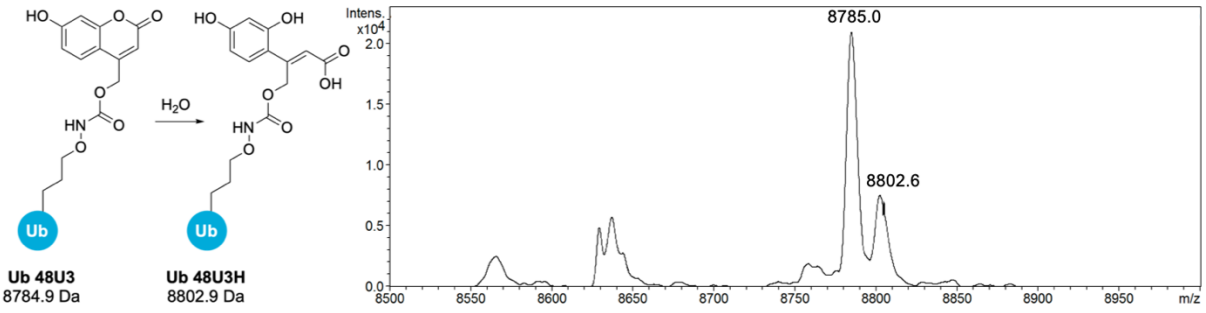

Figure 31: Schematic representation of Ub 48U**3** and hypothetical hydrolysis to Ub 48U**3**H, and LC-MS analysis of Ub 48U**3** that was expressed without any tag for purification.

The protein was subjected to LC-MS analysis and in the results both, a mass suiting to Ub 48U**3** and to Ub 48U**3**H can be observed (Figure 31). Hence, the presence of a His-tag is most likely not the cause for the hypothetical coumarin hydrolysis.

A related issue that could not be addressed in the course of this work is whether the assumed coumarin hydrolysis occurred on the free amino acid in cells or when embedded into Ub. This leads to the question, if PylRS Y271A L274M only accepts AOAA **3** or also its potentially hydrolyzed version, and if binding of AOAA **3** in the PylRS binding pocket is involved in the hypothetical hydrolysis. Since the aim of this project was the incorporation

and application of aminooxy-modified amino acids in protein–protein synthesis by oxime ligation, no expansive experiments were performed to investigate the kind and origin of these unexpected results.

3.4.2 Nitro-Aryl-Protected AOAA 4

3.4.2.1 Incorporation of Nitro-Aryl-Protected AOAA 4 in Ub 48TAG

Test incorporations of AOAA **4** by PylRS Y271M L274A C313A Y349F indicated the successful incorporation of AOAA **4** in response to an amber codon. There were some reports about the presence of nitroreductases in *E. coli* cells.[136],[203] The reduction of the nitro group of AOAA **4** to an amine would lead to the removal of the respective aryl and the release of the aminooxy group. To investigate this by mass analysis, Ub 48U**4** was expressed in the presence of AOAA **4** at a final concentration of 2 mM as described in chapter 3.4.1.1.

3.4.2.2 Mass Analysis of Ub 48U4

Ub 48U**4** was subjected to LC-MS analysis and in the mass spectrum predominantly the signal for full-length Ub 48U**4**-His_6 could be observed (Figure 32). Additional mass signals were present – the mass signal of 11070.2 Da could be assigned to Ub 48-ONH_2-His_6 or to misincorporation of Lys – however, these represent traces compared to Ub 48U**4**-His_6. A signal for Ub containing AOAA **4** with an amine instead of a nitro group was not observed (calc. 11274.7 Da).

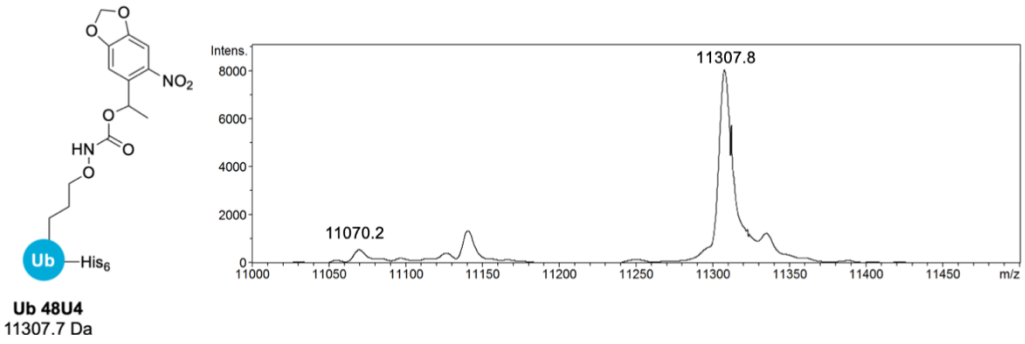

Figure 32: Schematic representation of Ub 48U**4** with calculated molecular weight and LC-MS analysis.

These results indicate that the nitro group of AOAA **4** was not reduced and not deprotected to a significant extent during protein expression in *E. coli* cells.
However, since a PylRS mutant for the incorporation of AOAA **4** had already been published[137], the synthesis of this amino acid resulted in low yields, and large amounts of amino acid (final concentration 2 mM) needed to be applied for an enhanced incorporation with the synthetase found in this work, the use of AOAA **4** in oxime ligation was not further investigated.

3.5. Protein-Ubiquitination by Oxime Ligation

3.5.1 DNA Pol β Ubiquitination

3.5.1.1 Previous Studies and General Considerations

In previous studies, Tatjana Schneider developed a method to site-specifically ubiquitinate DNA Pol β by means of CuAAC.[86],[130],[179-180],[214] DNA Pol β was modified with an alkyne by SCS with Plk and PylRS wt in position 41, 61, or 81 – positions, which are known to be ubiquitinated in nature. The C-terminus of Ub was equipped with an azide by SPI of azidohomoalanine (Aha) instead of Met in Met auxotrophic bacteria. The ligation of these proteins (turnover of ~95% for all DNA Pol β variants[86]) and the purification of DNA Pol β–Ub were successful. However, the purification proved to be very laborious (Heparin affinity chromatography, dialysis, cation exchange) due to the removal of the copper from the conjugate.[86] Hence, in this work, oxime ligation should be investigated as an alternative to CuAAC.

In order to study DNA Pol β ubiquitination by oxime ligation, DNA Pol β should be equipped with an aminooxy functionality by SCS with AOAAs **1** or **3** in position 41. The incorporation of KeK was neglected in this case, because incorporation efficiencies were very low (chapter 3.3.2.5). Also, the attachment of a modified linker to DNA Pol β by Cys nucleophilicity was considered to be disadvantageous, because DNA Pol β contains three native Cys residues. For a successful oxime ligation that is advantageous over CuAAC, the following conditions need to be met: Modified DNA Pol β needs to be completely converted because unmodified DNA Pol β cannot be easily separated from DNA Pol β–Ub. Reaction conditions for oxime ligation may not lead to precipitation of DNA Pol β and DNA Pol β–Ub.

3.5.1.2 Generation of Aminooxy-Modified DNA Pol β

In order to generate aminooxy-modified DNA Pol β, AOAA **1** or AOAA **3** were incorporated into position 41 by SCS. Amino acid concentrations and PylRS mutants for expression were chosen based on test incorporations in DNA Pol β performed in chapters 3.3.2.1 and 3.3.2.3. The expression and purification protocol were adapted from the procedure developed by Tatjana Schneider.[86],[130] Thus, DNA Pol β 41TAG and either PylRS Y349F and AOAA **1** (final concentration 1 mM) or PylRS Y271A L274M and AOAA **3** (final concentration 1 mM) were co-expressed (analogous to test incorporation in chapter 3.3.1). When AOAA **3** was incorporated, all steps were performed in the dark. After 16 h of expression, the cells were pelleted, resuspended, and sonicated. After centrifugation, the supernatant was purified by immobilized metal ion chromatography with cOmplete™ His-Tag Purification Resin. Pure fractions were identified by SDS-PAGE analysis (Figure 33), pooled, and dialyzed against PBS, 1 mM dithiothreitol (DTT, pH 7.2). In contrast to the procedure established by Tatjana Schneider, the protein was stored in PBS instead of Tris buffer to avoid the formation of imines between Tris and the carbonyl reaction partner in oxime ligation. The expression of DNA Pol β 41U**1** and DNA Pol β 41U**3** from 1 L culture yielded 6.4 mg and 3.9 mg protein, respectively. Glycerol was added to a final concentration of 50% and the proteins were stored at –20 °C.

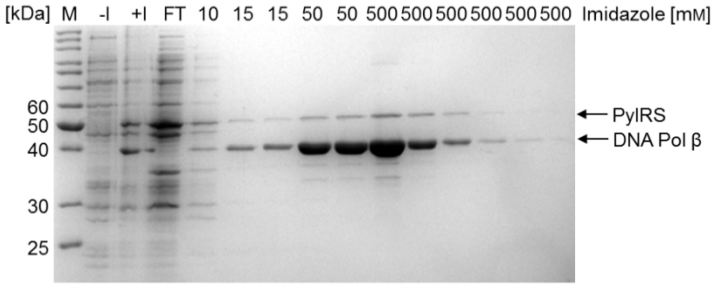

Figure 33: Purification of DNA Pol β 41U**3** by immobilized metal ion chromatography. M: Marker. -I/+I: Sample before induction of expression and after expression. FT: Flow-through.

Next, deprotection of DNA Pol β 41U**1**/U**3** was investigated. Therefore, DNA Pol β 41U**1** was treated with 67% TFA at rt for 2 h to remove the Boc protection group. However, all attempts to neutralize or dialyze the solution led to precipitation of the protein (data not shown). The same held true for deprotection attempts in less than 10% TFA. Hence, the focus was set on the aminooxy-modification of DNA Pol β 41U**3**. Upon cleavage of the coumarin group, the coumarin fluorescence and therefore the fluorescence signal of the protein sample is expected to decrease. Thus, DNA Pol β 41U**3** (55 µM) was irradiated at 365 nm (100 W) for 0–60 min on ice. The samples were analyzed by fluorescence readout and Coomassie staining after SDS-PAGE. In the fluorescence readout (Figure 34 A) it can be observed that

in comparison to non-irradiated protein, the fluorescence signal of DNA Pol β decreased when the sample was irradiated for 15 s. After irradiation for 5–10 min the signal almost vanished and did not further decrease. A slight fluorescence signal even remained after irradiation for 60 min. Coomassie staining confirmed the presence of same levels of DNA Pol β in all samples. To ensure that the reduced fluorescence signals resulted from coumarin deprotection and not from coumarin quenching, all irradiated samples were subjected to oxime ligation with TAMRA-Ketone (Figure 34 B). Upon coumarin removal, the aminooxy group is released, oxime ligation can occur, and fluorescence at λ_{ex} 532 nm is observed for the TAMRA-modified protein sample. After SDS-PAGE, TAMRA fluorescence can be observed for DNA Pol β that was irradiated for 15 s. After irradiation for 5 min this signal did not increase anymore. Slight fluorescence can be observed for a protein sample that was not treated with UV light. Possibly, traces of DNA Pol β 41U**3** were already deprotected or unspecific labeling occurred to minimal extent. These results suggest the removal of the coumarin group by irradiation at 365 nm and that the deprotection nearly reached completion after irradiation for 5 min for a 55 µM sample at pH 7.2. Note: The additional band at lower molecular weight than DNA Pol β is an impurity, which has already been observed after purification (Figure 33).

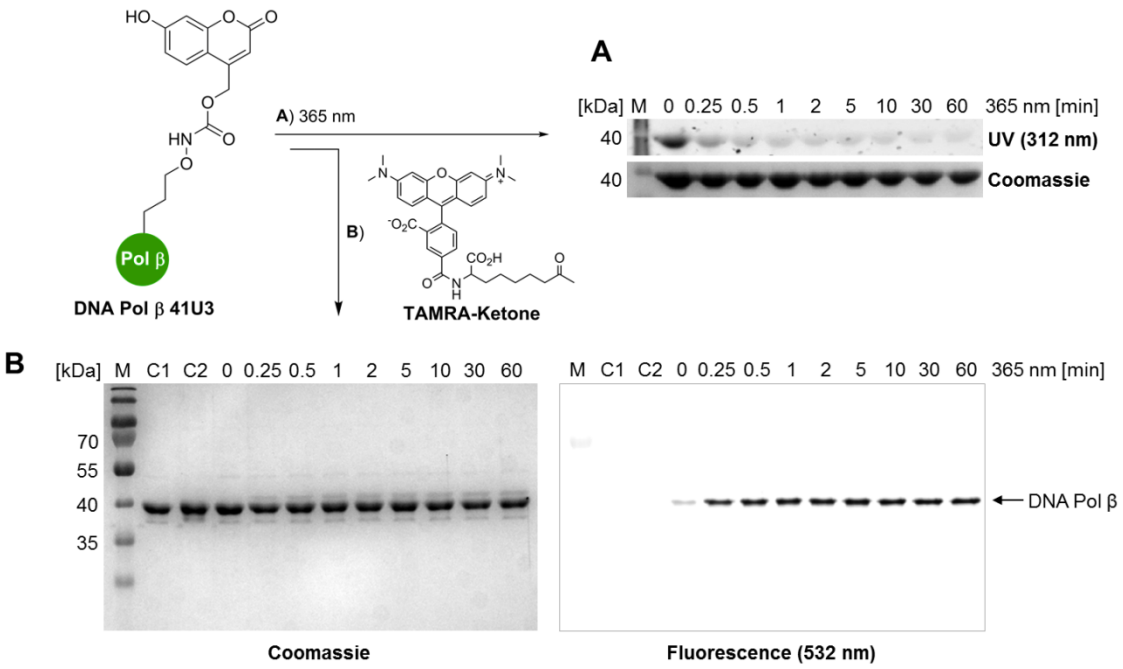

Figure 34: Schematic representation of DNA Pol β 41U**3** and SDS-PAGE analysis of **A)** irradiation of DNA Pol β 41U**3** (55 µM) at 365 nm for 0–60 min followed by **B)** oxime ligation with TAMRA-Ketone. The fluorescence readout in A) was performed by transilluminating the gel with 312 nm (Amersham Gel Reader Imager 600, EtBr filter). The fluorescence signal in B) was detected with Fluorescent Image Analyzer FLA-5000 (Fujifilm) (532 nm, LPG filter). M: Marker, C1: No TAMRA-Ketone, C2: Pol β K41U**1** – no deprotection. Ligation: PBS (pH 6.5), 3 h, 37 °C, 100 mM aniline, 1 mM SDS, 5 µM DNA Pol β; TAMRA-Ketone: 10 eq.

3.5.1.3 Generation of Ub-Aldehyde/Ketone

To ubiquitinate aminooxy-funtionalized DNA Pol β by oxime ligation, Ub should be modified with a ketone or an aldehyde. Hence, chloroacetone or chloroacetaldehyde should be site-specifically attached to Ub by nucleophilic substitution of the respective chloride residue by a Cys thiol of Ub.

This approach exploits the enhanced thiol nucleophilicity of Cys over the amine nucleophilicity of Lys at neutral pH in Ub and the fact that Ub does not contain any native Cys.[118-121] Hence, Cys can be mutated at any desired position for protein modification. Position 75 was chosen, because the oxime bond between carbonyl-modified Ub at 75C and an AOAA **1**/**3**-containing protein has the same atom count as an isopeptide bond (Figure 35). Oxime ligation should be investigated with Ub functionalized with a ketone as well as with an aldehyde in this work. Ketones are more stable and easier to store, however less reactive than their aldehyde counterparts. Aldehydes, on the other hand, might be more prone to imine formation with Lys side chains or the N-terminus of a protein.

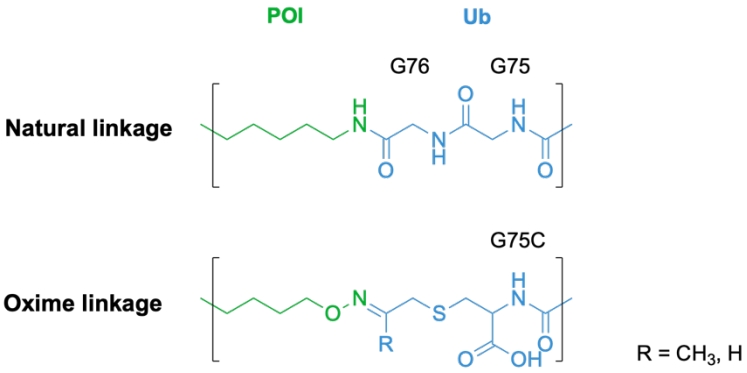

Figure 35: Schematic representation for the mimicry of protein ubiquitination by oxime ligation.

Ub 75C was expressed and purified as reported and Ub 75C functionalization was modified from Zhao *et al.* (LC-MS: Figure 36 A).[181] In short, Ub 75C in PBS pH 7.2 was treated with tris(2-carboxyethyl)phosphine (TCEP) to reduce disulfide bonds and the mixture was incubated with 1000 eq chloroacetone or chloroacetaldehyde. The reaction mixture was dialyzed several times and finally against 0.1 x PBS pH 7.2. LC-MS analysis of these modified Ub derivatives revealed the presence of species with mass values suiting to Ub 75C-Aldehyde (Ub-A), and Ub 75C-Ketone (Ub-K) (Figure 36 B and C, respectively). The additional +17 Da mass for Ub-A presumably corresponds to the respective hydrate that is in equilibrium with the aldehyde. Thus, Ub 75C was successfully modified with chloroacetone and chloroacetaldehyde.

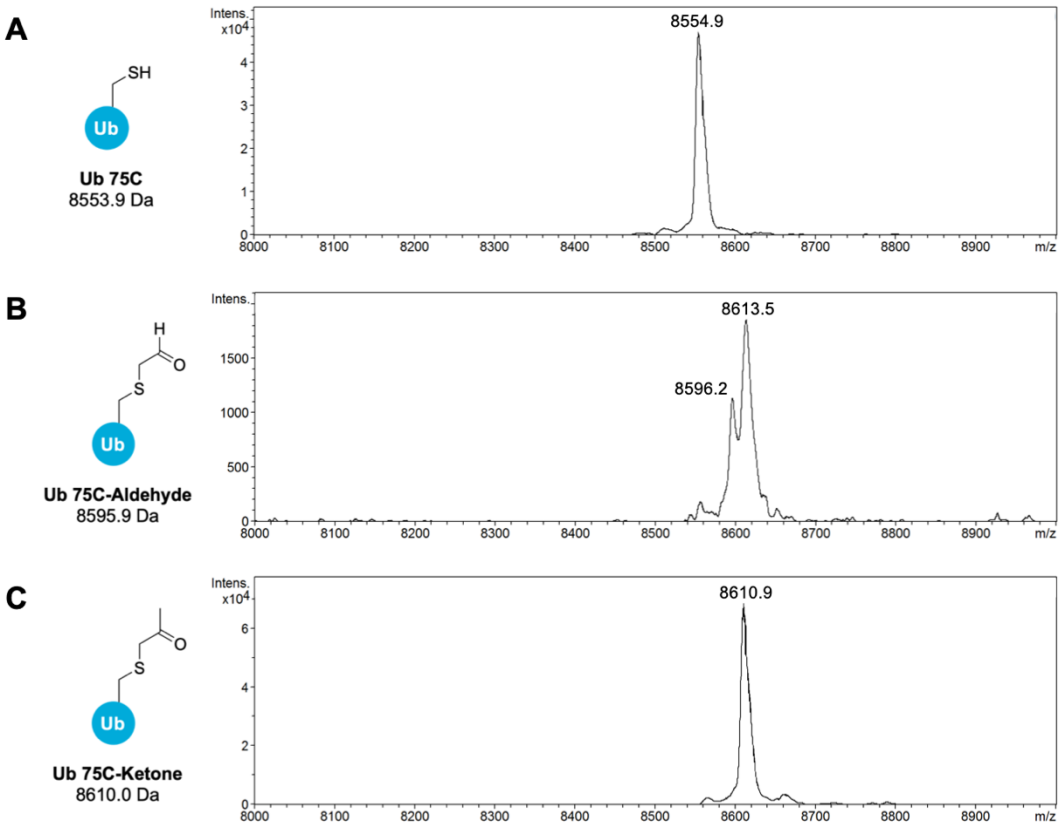

Figure 36: Schematic representation and calculated mass values (left) and LC-MS data (right) of **A)** Ub 75C, **B)** Ub75C-Aldehyde, and **C)** Ub 75C-Ketone.

3.5.1.4 Oxime Ligations

In order to generate DNA Pol β 41–Ub conjugates, DNA Pol β 41U**3** (55 µM) was irradiated at 365 nm for 10 min on ice (in the following denoted as DNA Pol β 41-ONH_2), and added to a reaction mixture that contained Ub-K or Ub-A, buffer, and optionally SDS or catalysts (Figure 37).

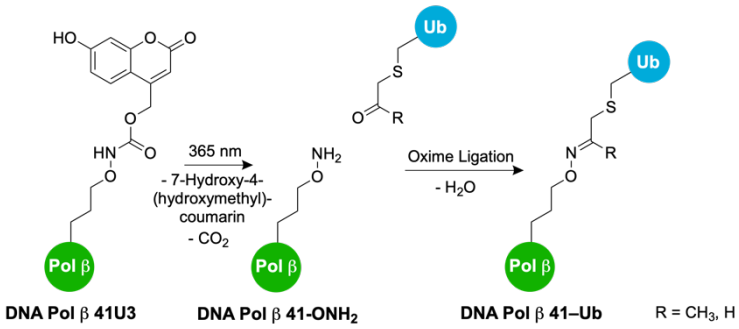

Figure 37: Schematic representation of DNA Pol β 41U**3** irradiation and oxime ligation with Ub-K/A.

After incubation, the reaction mixture was analyzed by SDS-PAGE. The shift of the band for DNA Pol β (~40 kDa) to higher molecular weights (~50 kDa) indicated successful ubiquitination with Ub-K/A. When precipitation of the protein in the course of the reaction was investigated, the mixture was centrifuged (10000 rpm, 10 min, 4 °C), the supernatant was removed, and the pellet was resuspended in water (same volume as reaction volume). Supernatant and pellet were analyzed separately by SDS-PAGE.

First, oxime ligation between DNA Pol β 41U**3** and Ub-K was investigated. The influence of SDS concentration and the effect of aniline on ligation turnover were studied. For increasing SDS and aniline concentrations bands at high molecular weights were observed. Probably, these occurred because of polymerization of modified Ub. Oxime ligation turnover was enhanced in the presence of SDS (final concentration 1 mM, Figure 38 A). The positive effect of SDS on DNA Pol β–Ub conjugation by CuAAC has already been described by Tatjana Schneider *et al.*[86],[180],[214] In that work, it was shown by primer extension reactions that DNA Pol β functionality was not reduced after treatment with SDS (final concentration 0.5 mM).[86] Additionally, it was shown by circular dichroism (CD) spectroscopy that the protein was not fully unfolded in the presence of up to 1 mM SDS, but the α-helical content increased.[86],[214] The same trend was observed for the CD spectrum of SDS-treated Ub. Hence, treatment of DNA Pol β with SDS was tolerated by the protein. It was hypothesized that the alkane part of SDS interacts with the protein by hydrophobic/van der Waals interactions, and that the negative charge of SDS leads to an increased Cu(I) concentration at the protein. That would lead to an enhanced CuAAC. This hypothesis was based on the finding by Whitesides *et al.* that when up to 11 eq SDS bind Ub the protein remains correctly folded and the number of negative charges increases.[215-217] They also reported that by binding of additional eq SDS,

Ub undergoes stepwise unfolding. The effect of SDS on oxime ligation might more likely be explained by altered interactions between Ub and DNA Pol β due to a change of the proteins' charge, and/or by a partial unfolding of the protein(s). That could make the reaction center more accessible for the reaction partner. Aniline slightly enhanced oxime ligation in PBS pH 6 (Figure 38 A/B). Ligation in PBS at pH 5 (not in buffer pH range anymore) or 6 proceeded superior to pH 7 and only small amounts of DNA Pol β precipitated (Figure 38 B).

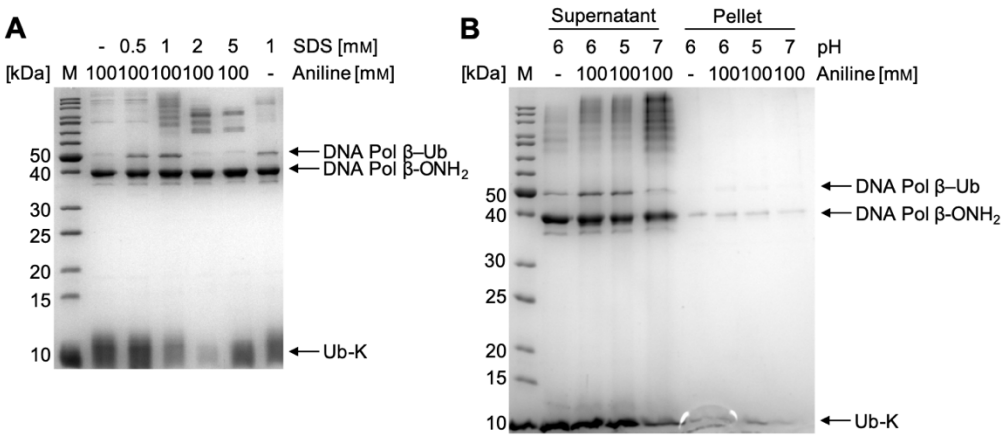

Figure 38: SDS-PAGE analysis of oxime ligation between Ub-K and DNA Pol β 41-ONH_2. **A)** SDS concentrations in the presence and absence of aniline were investigated. **B)** pH of PBS in the presence and absence of aniline was investigated. Reaction conditions (if not stated otherwise): 23 °C, o.n., 1 mM SDS, 5 eq Ub-K, 5 µM DNA Pol β 41-ONH_2, PBS pH 6. M: Marker.

Additionally to aniline, a series of reported oxime ligation catalysts[100-104] and aniline derivatives were tested for their ability to enhance DNA Pol β ubiquitination. A 10 mM catalyst concentration was chosen for testing. When *p*-phenylenediamine or *p*-anisidine were used, the band assigned to DNA Pol β–Ub increased and an additional weak band for higher molecular weights and a smear appeared (Figure 39 A). Moreover, when *p*-phenylenediamine was used, the band for Ub is shifted to higher molecular weight and additional bands appear that indicate Ub polymerization. The use of no other catalyst led to an increased conjugation turnover compared to the use of no catalyst or aniline. Protein precipitation was very similar for the use of most catalysts, but strongly increased when anthranilic acid, 4-aminobenzoic acid, or 4-(trifluoromethyl)aniline were present.

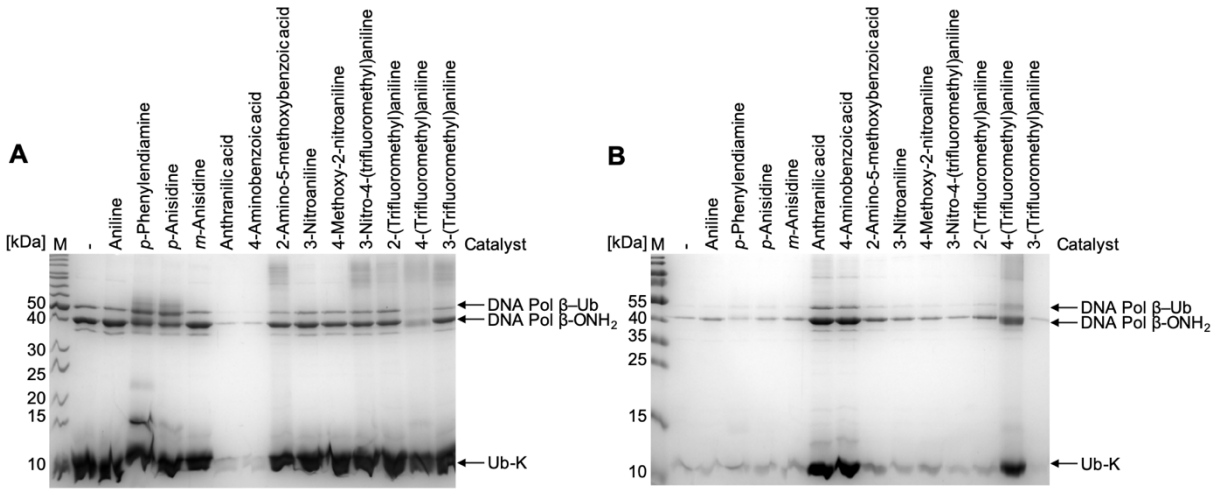

Figure 39: SDS-PAGE analysis of oxime ligation between Ub-K and DNA Pol β 41-ONH_2. Different catalysts (10 mM) were tested. **A)** Supernatant. **B)** Pellet. Reaction conditions: 23 °C, o.n., 1 mM SDS, 5 eq Ub-K, 5 µM DNA Pol β 41-ONH_2, PBS pH 6. M: Marker.

Catalysis with *p*-anisidine was further investigated and in Figure 40 A it can be seen that the band that had been assigned to DNA Pol β–Ub appeared to be a double band. Therefore, catalysis with *p*-anisidine was not further examined. Among the catalysts tested here, aniline seemed to enhance DNA Pol β–Ub conjugation to the greatest extent, however, not superior to the use of no catalyst. Hence, different concentrations of aniline during oxime ligation were applied. No catalyst or aniline (at 50–100 mM) were most beneficial for conjugation efficiency and to maintain a low level of protein precipitation (Figure 40 B).

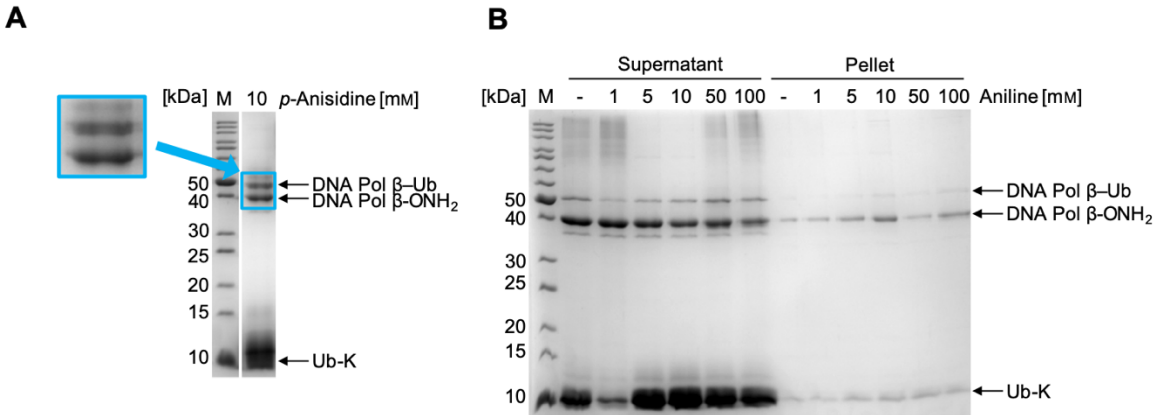

Figure 40: SDS-PAGE analysis of oxime ligation between Ub-K and DNA Pol β 41-ONH_2. **A)** Investigation of *p*-anisidine as catalyst. **B)** Different concentrations of aniline were tested. Reaction conditions: 23 °C, o.n., 1 mM SDS, 5 eq Ub-K, 5 µM DNA Pol β 41-ONH_2, PBS pH 6. M: Marker.

Subsequently, it was investigated, if the chemical equilibrium can be shifted to product formation by the use of additional equivalents of Ub-K and by varying the reaction temperature or applying freeze-thaw catalysis (3 cycles if not specified otherwise). The use of 10 eq Ub-K was most beneficial, the use of more equivalents led to protein precipitation (Figure 41 A). Freeze-thaw led to a diminished product formation compared to reactions

performed at 4, 16, and 23 °C, o.n., which proceeded very similar. Increasing the reaction temperature to 37 °C led to an increased ratio of DNA Pol β–Ub to DNA Pol β, however an additional, slight band at higher molecular weight was observed. Therefore, ligation at 4, 16, or 23 °C was considered to be more beneficial.

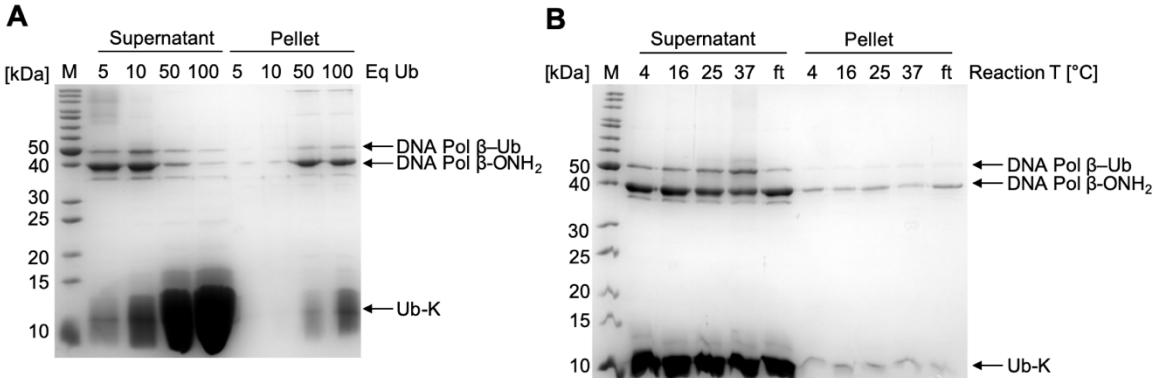

Figure 41: SDS-PAGE analysis of oxime ligation between Ub-K and DNA Pol β 41-ONH_2. **A)** Different eq of Ub-K were tested. **B)** Different reaction temperatures and freeze-thaw (ft) were tested. Reaction conditions (if not stated otherwise): 23 °C, o.n., 1 mM SDS, 50 mM aniline, 5 eq Ub-K, 5 µM DNA Pol β 41-ONH_2, PBS pH 6. M: Marker.

Because oxime ligation is known to proceed with slow reaction kinetics in low µM concentrations[96-97], ligation duration from 1–3 days was assessed. However, no striking differences in reaction turnover were observed (Figure 42 A). It has been reported that the presence of saline can accelerate oxime ligation.[109] Hence, DNA Pol β–Ub conjugation was performed in PBS (0.14 M NaCl) and increasing sodium chloride concentrations were applied. The higher the sodium chloride concentration, the less DNA Pol β–Ub is formed (Figure 42 B).

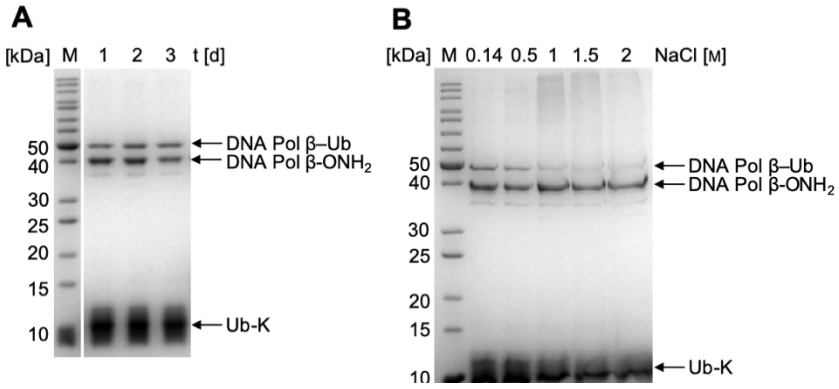

Figure 42: SDS-PAGE analysis of oxime ligation between Ub-K and DNA Pol β 41-ONH_2. **A)** Different reaction times were tested. **B)** Different NaCl concentrations were investigated. Reaction conditions (if not stated otherwise): 23 °C, o.n. (= 1 d), 1 mM SDS, 100 mM aniline, 10 eq Ub-K, 10 µM DNA Pol β 41-ONH_2, PBS pH 5. M: Marker.

Thus, oxime ligation conditions with highest turnover in the reaction between DNA Pol β 41-ONH_2 and Ub-K were: 4, 16, or 23 °C, o.n., 1 mM SDS, 50-100 mM aniline or no catalyst,

10 eq Ub-K, PBS pH 5 or 6. However, turnover could not be improved to more than ~20% by optimization of pH, kind and concentration of catalyst, freeze-thaw, reaction temperature and duration, SDS or sodium chloride concentration, and equivalents of Ub.

Subsequently, oxime ligation was assessed between DNA Pol β 41-ONH_2 and Ub-A, since aldehydes are known to be more reactive than their ketone counterparts. As starting point, optimized conditions for ligation with Ub-K were applied. Figure 43 reveals that oxime ligation in the presence of aniline (final concentration 100 mM) hardly resulted in product formation (A), whereas omission of aniline led to ubiquitination of approximately 40% DNA Pol β 41-ONH_2 (B). Hence, in the following the optimization of oxime ligation was performed in the absence of any catalyst. Additionally, bands at ~15 and ~22 kDa were observed, which might occur because of Ub-A polymerization due to imine formation. These bands were hardly present when Ub-K was applied in oxime ligation, which supports this hypothesis due to the higher reactivity of aldehydes towards imine formation.

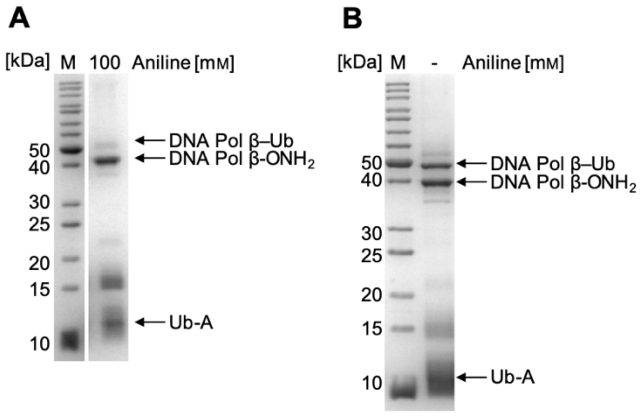

Figure 43: SDS-PAGE analysis of oxime ligation between Ub-A and DNA Pol β 41-ONH_2. Oxime ligation **A)** in the presence of aniline (final concentration 100 mM) **B)** in the absence of aniline. Reaction conditions: 23 °C, o.n., 1 mM SDS, 10 eq Ub-A, 5 µM DNA Pol β 41-ONH_2, PBS pH 5. M: Marker.

First, the choice of buffer and pH were examined (Figure 44 A and B). All buffers used at pH 6 led to a similar amount of DNA Pol β ubiquitination and protein precipitation. At pH 6, a band with higher molecular weight than expected for DNA Pol β–Ub appeared. At pH 7, that band and one more band with even higher molecular weight could be observed. The presence of all buffers at pH 4 and 5, except for PBS, resulted in protein precipitation to a great extent and in reduced turnover of DNA Pol β to DNA Pol β–Ub. In general, many bands that cannot be assigned to Ub-A, DNA Pol β, or DNA Pol β–Ub were present. These probably resulted from Ub-A polymerization by imine formation as described above. Following oxime ligations were performed in PBS pH 5 or 6, since these conditions were among the best tested here and DNA Pol β is stored in PBS.

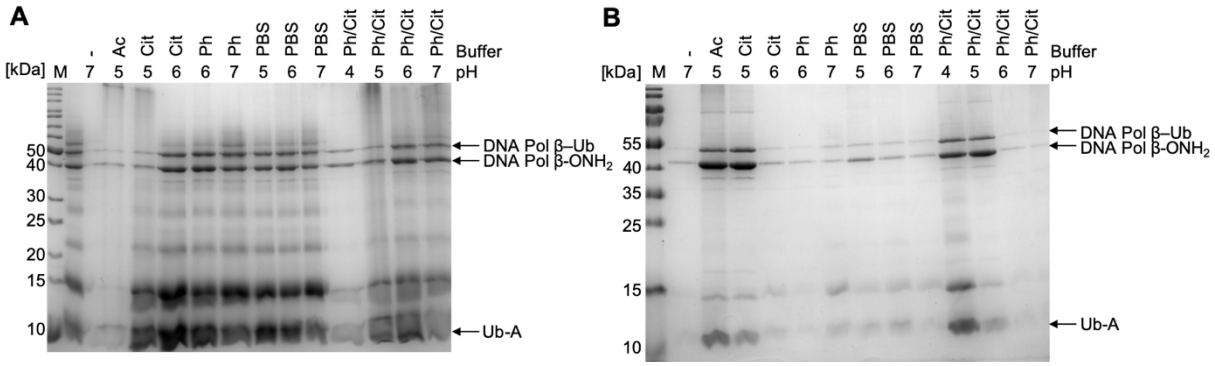

Figure 44: SDS-PAGE analysis of oxime ligation between Ub-A and DNA Pol β 41-ONH_2. Different buffers and pH were investigated. **A)** Supernatant. **B)** Pellet. Ac: 500 mM acetate, Cit: 100 mM citrate, Ph: 100 mM phosphate, Ph/Cit: 200 mM phosphate, 100 mM citrate. Reaction conditions: 23 °C, o.n., 1 mM SDS, 10 eq Ub-A, 5 µM DNA Pol β 41-ONH_2. M: Marker.

Next, the effect of equivalents of Ub-A and SDS concentration on oxime ligation turnover and protein precipitation were assessed. Oxime ligation proceeded very similarly for 5 and 10 eq Ub-A (Figure 45 A). When more equivalents were employed potential polymerization of Ub-A outweighed the amount of DNA Pol β/DNA Pol β–Ub. Similar to when Ub-K was used, when testing oxime ligations in the presence of 0–5 mM SDS a 1 mM final concentration led to the highest turnover and low protein precipitation (Figure 45 B). Hence, the most beneficial conditions for oxime ligation between DNA Pol β 41-ONH_2 and Ub-A were: 23 °C, o.n., 1 mM SDS, no catalyst, 5–10 eq Ub-A, PBS pH 5 or 6.

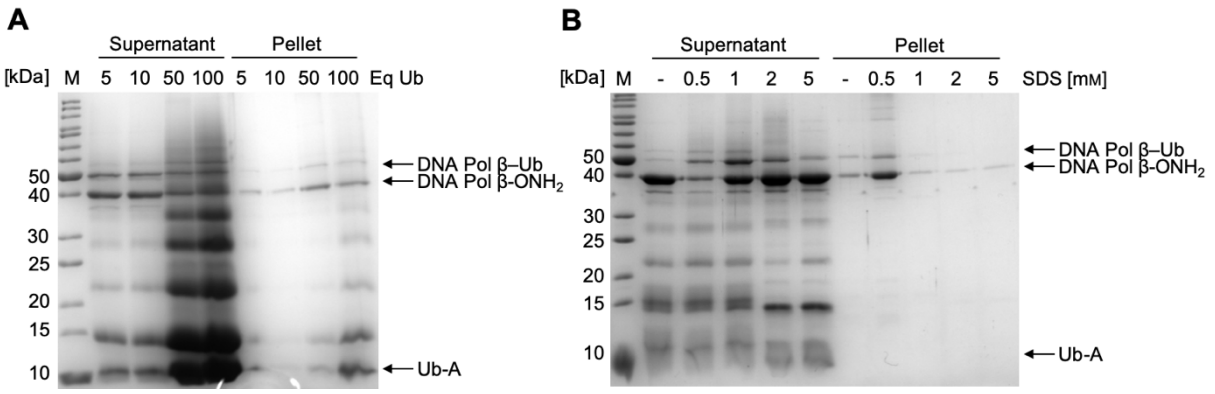

Figure 45: SDS-PAGE analysis of oxime ligation between Ub-A and DNA Pol β 41-ONH_2. **A)** Eq of Ub-A were investigated. **B)** Different SDS concentrations were tested. Reaction conditions (if not stated otherwise): 23 °C, o.n., 1 mM SDS, 5 eq Ub-A, 5 µM DNA Pol β 41-ONH_2, PBS pH 6. M: Marker.

Oxime ligation is a reversible reaction. In order to prevent oxime hydrolysis, the C-N double bond can be reduced to a single bond by $NaBH_3CN$, which results in a strongly reduced electrophilicity at the respective carbon atom. The removal of the oxime product from the chemical equilibrium of oxime ligation could result in a shift of the chemical equilibrium to product formation. Thus, oxime ligation between DNA Pol β 41-ONH_2 and Ub-K/A was performed, and half of the reaction was treated with $NaBH_3CN$, the other half was left

untreated. Treatment with $NaBH_3CN$ did not lead to a different result for oxime ligation with Ub-K (Figure 46). Oxime ligation with Ub-A followed by reductive treatment led to a slightly enhanced oxime ligation turnover (~50%). However, the presence of a band at higher molecular weights (hypothetically DNA Pol β–Ub_2) strongly increased compared to the untreated sample. Thus, treatment of the oxime ligation under reductive conditions did not lead to a more beneficial DNA Pol β 41 ubiquitination outcome.

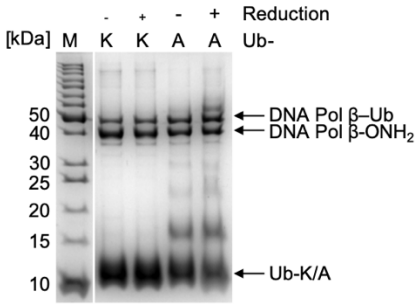

Figure 46: SDS-PAGE analysis of oxime ligation between Ub-A or Ub-K and DNA Pol β 41-ONH_2, optionally followed by treatment with $NaBH_3CN$. Reaction conditions: 23 °C, o.n., 1 mM SDS, 100 mM aniline for Ub-K, 5 eq Ub-A or 10 eq Ub-K, 5 µM DNA Pol β 41-ONH_2, PBS pH 5. Reduction: 500 µM $NaBH_3CN$ for 2 h, 23 °C. M: Marker.

Site-specific oxime ligation between DNA Pol β and Ub-K/A in contrast to imine formation with DNA Pol β Lys residues should be ensured. Hence, DNA Pol β 41U**3** irradiated at 365 nm and DNA Pol β 41U**1** that lacks a free aminooxy group were incubated with Ub-A and Ub-K under the same reaction conditions. Upon incubation of DNA Pol β 41U**1** with Ub-K and Ub-A very slight bands at 50 kDa appeared (Figure 47 A). That might indicate unspecific formation of DNA Pol β–Ub in traces. When DNA Pol β 41-ONH_2 was treated under the same conditions, this band became much more intense. These results suggest that site-specific oxime ligation between aminooxy-modified DNA Pol β and Ub-K/A can be performed while unspecific imine formation is negligible. Additionally, the presence of DTT during oxime ligation should be investigated since its presence has been shown to be important for storage of DNA Pol β.[86] Hence, DNA Pol β 41-ONH_2 was treated with Ub-K/A in the presence and absence of DTT. In Figure 47 B it can be seen that the presence of DTT (final concentration 1 mM) does not improve reaction turnover or protein precipitation and can therefore be omitted for oxime ligation optimization.

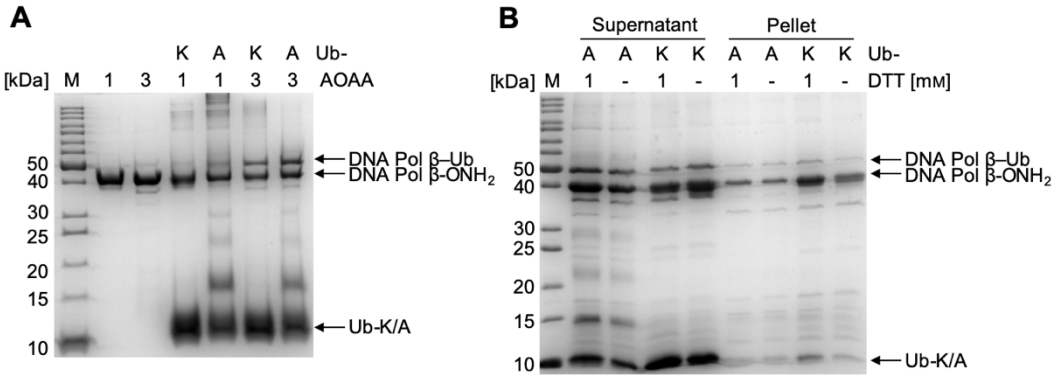

Figure 47: SDS-PAGE analysis of oxime ligation between **A)** DNA Pol β 41U**3** irradiated at 365 nm for 10 min or DNA Pol β 41U**1** as negative control, each treated without and with Ub-K/A. **B)** Oxime ligation of DNA Pol β 41-ONH_2 with Ub-K/A in the presence and absence of 1 mM DTT. Reaction conditions: 23 °C, o.n., 1 mM SDS, 100 mM aniline for Ub-K, 5 eq Ub-A or 10 eq Ub-K, 5 µM DNA Pol β 41U**3**/U**1**, PBS pH 5. M: Marker.

Thus, oxime ligation can be applied for protein-protein conjugation, however, only 40% DNA Pol β 41-ONH_2 could be ubiquitinated with Ub-A. This might be due to potential partial hydrolysis of AOAA **3** as described in chapter 3.4.1.2. Note: In LC-MS/MS experiments in chapter 3.3.2.3, Figure 15, no peptide that contained hydrolyzed AOAA **3** was found. If the coumarin of AOAA **3** was hydrolyzed, it could not be removed by irradiation at 365 nm and the respective amount of DNA Pol β could not react in oxime ligation anymore. Alternatively, the slow reaction kinetics of oxime ligation might be the reason for the low turnover (compared to CuAAC). To the best of knowledge, until now oxime ligation with Ub has been reported with quite small proteins and under denaturing conditions with guanidinium hydrochloride (Ub: 9 kDa, 60–85% turnover; SUMO: 12 kDa, turnover nearly complete; α-globulin: 15 kDa, turnover nearly complete; β-globulin: 16 kDa, double mono-ubiquitination, turnover nearly complete).[137],[184-185] The ligation with larger proteins might contribute to decreased reaction kinetics. Furthermore, no guanidinium hydrochloride was used for oxime ligations in this work to prevent complete protein denaturation. Hence, the accessibility of the reaction centers might be sterically hindered.

The generation of DNA Pol β–Ub by CuAAC could be optimized to turnover of 95%.[86] Purification after CuAAC has proven to be laborious, however, for the isolation of oxime-linked DNA Pol β–Ub the establishment of a new method would be necessary to remove unreacted DNA Pol β from the reaction mixture.

Nevertheless, oxime ligation between aminooxy-modified DNA Pol β and Ub-A/K yielded DNA Pol β–Ub.

3.5.2 H 1.2 Ubiquitination

3.5.2.1 Previous Studies and General Considerations

In previous studies, D. Rösner[18], C. Geßler[218], and E. Höllmüller[219] used CuAAC to site-specifically ubiquitinate H1.2. To do so, H1.2 was equipped with an alkyne by SCS of Plk and PylRS wt and the C-terminus of Ub was equipped with an azide by SPI of Aha in Met auxotrophic bacteria. The ligation (turnover of ~95%) and purification (ultrafiltration) of H1.2–Ub were successful, however, considerate amounts of H1.2 and H1.2–Ub, which varied from batch to batch, precipitated during these processes. This precipitation is not negligible since the expression of H1.2 combined with SCS has proven to be very low-yielding. Therefore, oxime ligation as an alternative to CuAAC should be investigated. In order to be advantageous over CuAAC, oxime ligation for the generation of H1.2–Ub needed to fulfill the following conditions: The turnover of H1.2 should be nearly complete and H1.2 and H1.2–Ub should not precipitate during ligation.

It has been known that H1.2 can withstand acidic treatment.[46],[220-222] Hence, H1.2 should be modified with an aminooxy group by genetic incorporation of acid-labile AOAA **1**. H1.2 position 114 was chosen as proof of principle, C-terminal position 206 as relevant ubiquitination site[51-54]. Ub 75C-A/K should be used as reaction partner.

3.5.2.2 Generation of Aminooxy-Modified H1.2

In order to modify histone H1.2 with an aminooxy functionality, the incorporation of AOAA **1** (final concentration 1–5 mM) in H1.2 E114TAG, which bears a C-terminal His_6-tag, was tested with PylRS Y349F and PylRS Y349W in 6 mL test expressions. The western blot against the His-tag of H1.2 shows that PylRS Y349F leads to an increased expression of H1.2 E114U**1** compared to the Y349W mutant, and that increasing concentrations of AOAA **1** do not lead to a proportionally enhanced incorporation (Figure 48 A). These results are in accordance with test incorporations in DNA Pol β (chapter 3.3.2.1).

Hence, AOAA **1** (final concentration 1 mM) was incorporated into H1.2 114TAG or H1.2 206TAG by PylRS Y349F. The expression and purification protocol of histone H1.2 were adapted from D. Rösner.[18] Hence, H1.2 114TAG/$tRNA_{CUA}$ or H1.2 206TAG/$tRNA_{CUA}$ and PylRS Y349F were co-expressed. At OD_{600} = 0.2–0.3 AOAA **1** (final concentration 1 mM) was added and expression was induced by addition of IPTG (final concentration 1 mM) when OD_{600} = 0.6–0.9 was reached. After expression at 37 °C for 20 h, the cells were pelleted and resuspended. After sonication, the mixture was centrifuged and washed several times. Inclusion bodies were solubilized by incubation with 50 mM Tris, 6 M urea, 1 M NaCl, β-mercaptoethanol (pH 7.0) at 4 °C overnight. After centrifugation, the supernatant was purified by immobilized metal ion chromatography with cOmplete™ His-Tag Purification Resin. Pure fractions identified by SDS-PAGE were pooled and dialyzed against water. Expression of 1 L culture of H1.2 114U**1** and H1.2 206U**1** yielded 0.75 mg and 0.49 mg, respectively.

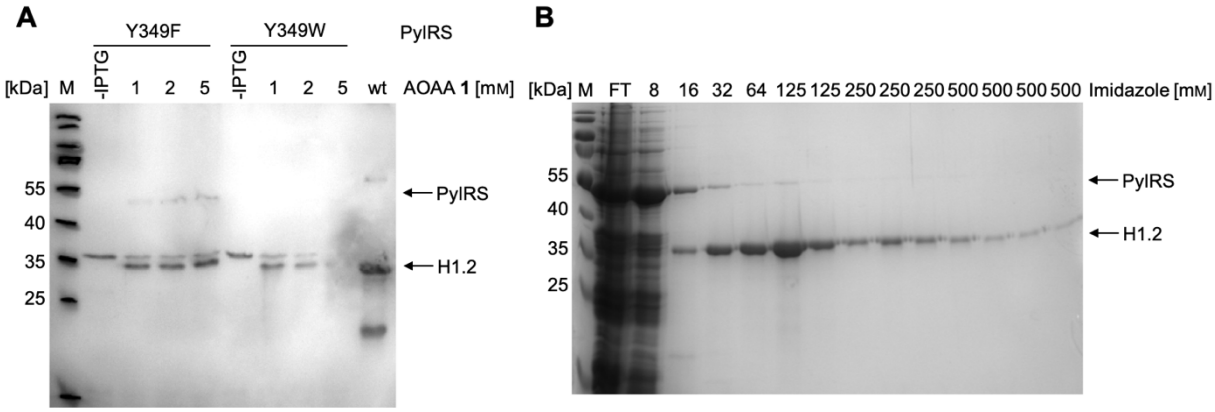

Figure 48: **A)** Test incorporation of AOAA **1** (1–5 mM) in H1.2 E114TAG with PylRS Y349F and PylRS Y349W. Protein expression was performed at 37 °C for 4 h. IPTG omission served as control. 1 mL samples were taken and OD_{600} was adjusted to 2.5. Incorporation efficiencies were visualized by western blot against the His-tag of H1.2. Note: The band with slightly higher molecular weight than H1.2 probably resulted from unspecific His-tag staining and was not present before induction of expression. The band at ~50 kDa probably resulted from PylRS. **B)** Purification of H1.2 114U**1** by immobilized metal ion chromatography. The SDS-PA gel was Coomassie-stained. M: Marker, FT: Flow-through.

LC-MS data (Figure 49 A) confirmed the presence of species with a mass of 22288.7 Da, which can be assigned to H1.2 114U**1** (calc.: 22289.7 Da). The species with a mass of 22160.7 Da can be assigned to H1.2 114U**1** lacking the initial Met (-Met1), (calc.: 22158.5 Da).

Subsequently, the deprotection of the Boc group of H1.2 114U**1** was investigated. First, H1.2 114U**1** was treated with up to 10% TFA for 5 h to overnight at rt or 4 °C and subsequently neutralized. The protein precipitated and could not be re-dissolved in water after centrifugation. Hence, treatment of H1.2 114U**1** with 67% TFA for 2 h at 4 °C or 23 °C was investigated. After incubation with TFA, the protein was precipitated in diethyl ether and centrifuged, followed by a washing step with diethyl ether and dissolution of the pellet in water. For deprotection at 23 °C, LC-MS data (Figure 49 B) revealed the presence of species with masses of 22188.3 Da/22060.8 Da, which can be assigned to H1.2 114-ONH_2/H1.2 114-ONH_2 -Met1, respectively (calc. 222189.6 Da, 22058.4 Da without Met1). Protected H1.2 114U**1** was still present when deprotection was performed at 4 °C (data not shown).

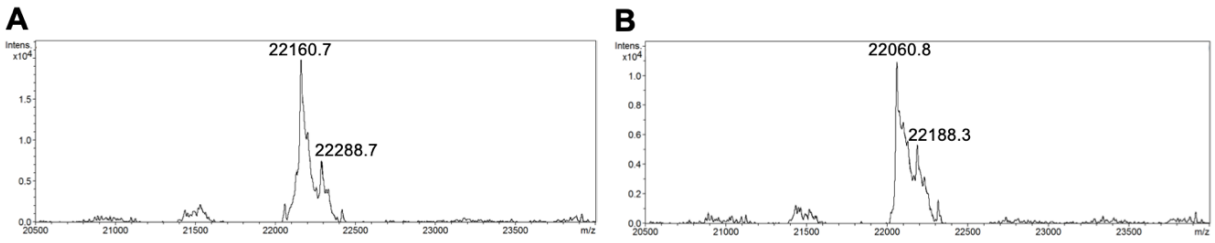

Figure 49: LC-MS data for **A)** H1.2 114U**1**-His_6 and **B)** H1.2 114-ONH_2-His_6.

However, it is difficult to determine, if there is still protected H1.2 left, since the resolution of the mass spectra is not very precise. Therefore, additionally to treatment with 67% TFA at 23 °C for 2 h, H1.2 114U**1** was incubated with 67% for 3 h, and with 88% for 2 h. In first test oxime ligations, all samples were incubated with Ub-K under the same oxime ligation conditions. The better the deprotection, the more H1.2-ONH_2 is present, and the more H1.2–Ub can be formed. Hence, the efficiency of deprotection conditions can be investigated by these test oxime ligations. The different deprotection conditions did not lead to a different ubiquitination turnover of H1.2 samples (Figure 50). Hence, deprotection was in the following performed for 2 h at 23 °C in 67% TFA. These conditions were transferred to the deprotection of H1.2 206U**1** (LC-MS data for H1.2 206U**1** in attachments).

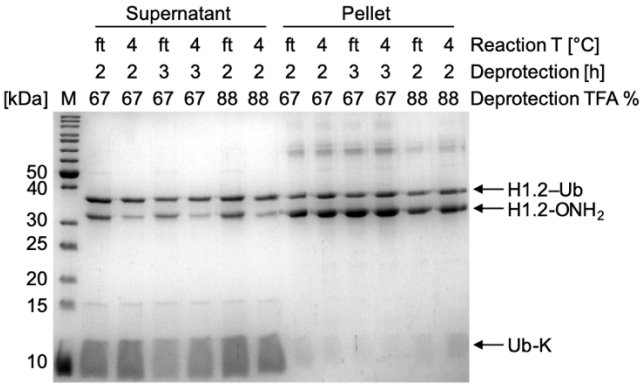

Figure 50: SDS-PAGE analysis of oxime ligation between Ub-K and H1.2 114U**1** treated with 67% or 88% TFA for 2 h or 3 h at 23 °C. Oxime ligation was performed at 4 °C o.n. or by the use of freeze-thaw catalysis (ft, 3 cycles). Reaction conditions: 2 mM SDS, 2 eq Ub-K, 5 µM H1.2 114U**1**, PBS pH 6. M: Marker.

3.5.2.3 Oxime Ligations

In order to generate H1.2–Ub conjugates, H1.2 114U**1** (77 µM) or H1.2 206U**1** (23 µM) were treated with 67% TFA at 23 °C for 2 h to generate H1.2 114-ONH_2 and H1.2 206-ONH_2, respectively. Note: Concentrations of H1.2 variants were used as obtained after expression and concentration. After precipitation in diethyl ether and dissolution in water, the respective protein was added to a reaction mixture that contained Ub-K or Ub-A, and optionally buffer, SDS, or catalysts (Figure 51). Ub-A and Ub-K were generated as described in chapter 3.5.1.3. Similarly, as described in 3.5.1.3, AOAA **1** modification of H1.2 in combination with Ub 75C-modification with chloroacetone and chloroacetaldehyde were chosen to maintain the atom count of an isopeptide bond for the oxime ligation product.

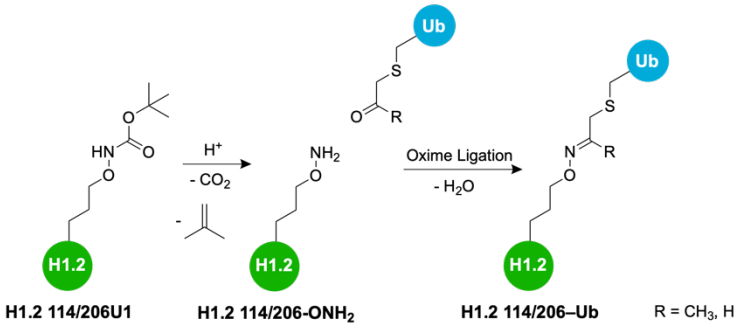

Figure 51: Schematic representation of H1.2 U**1** deprotection and oxime ligation with Ub-K/A.

Oxime ligation outcome was analyzed by SDS-PAGE. The shift of the H1.2 band (~32 kDa) to higher molecular weight (~38 kDa) indicated successful oxime ligation with Ub-K/A. Precipitation of the protein in the course of the reaction was assessed by centrifuging the mixture (10000 rpm, 10 min, 4 °C), removing the supernatant, and resuspending the pellet in water (same volume as reaction volume). Supernatant and pellet were analyzed separately.
First, oxime ligation between H1.2 114-ONH_2 and Ub-K was investigated. H1.2 114 was chosen to test oxime ligation as proof of principle. Ligation in the presence of PBS, acetate, or citrate buffer led to H1.2 ubiquitination but also to protein precipitation, while oxime ligation in water proceeded without significant protein precipitation (Figure 52). Thus, oxime ligation was further studied in water.

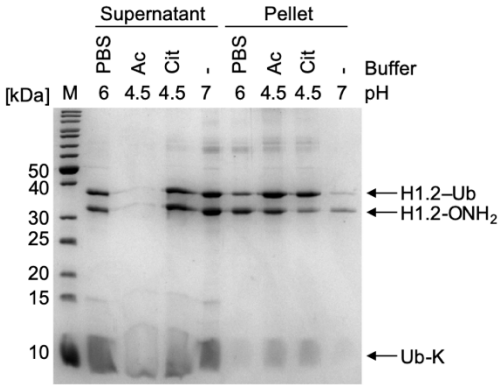

Figure 52: SDS-PAGE analysis of oxime ligation between Ub-K and H1.2 114-ONH_2. Different buffers and pH were tested. Ac: 500 mM acetate, Cit: 100 mM citrate. Reaction conditions: 4 °C, o.n., 2 mM SDS, 2 eq Ub-K, 5 µM H1.2 114-ONH_2. M: Marker.

Varying oxime ligation temperature and applying freeze-thaw catalysis (3 cycles if not specified otherwise) revealed that ubiquitination of H1.2 114-ONH_2 resulted in similar turnover and in similarly low amounts of precipitate (Figure 53 A and B). Increasing the freeze-thaw cycles for oxime ligation from 3 to 6, increasing the duration of oxime ligation, also combined with addition of fresh Ub-K, did not lead to significantly higher yields (Figure 53 C). Additionally, in Figure 53 A, the results for oxime ligation with freeze-thaw in the presence and absence of 1 mM aniline suggest, that oxime ligation proceeded in higher yield without any aniline. In the following, freeze-thaw was continued in the absence of any catalyst.

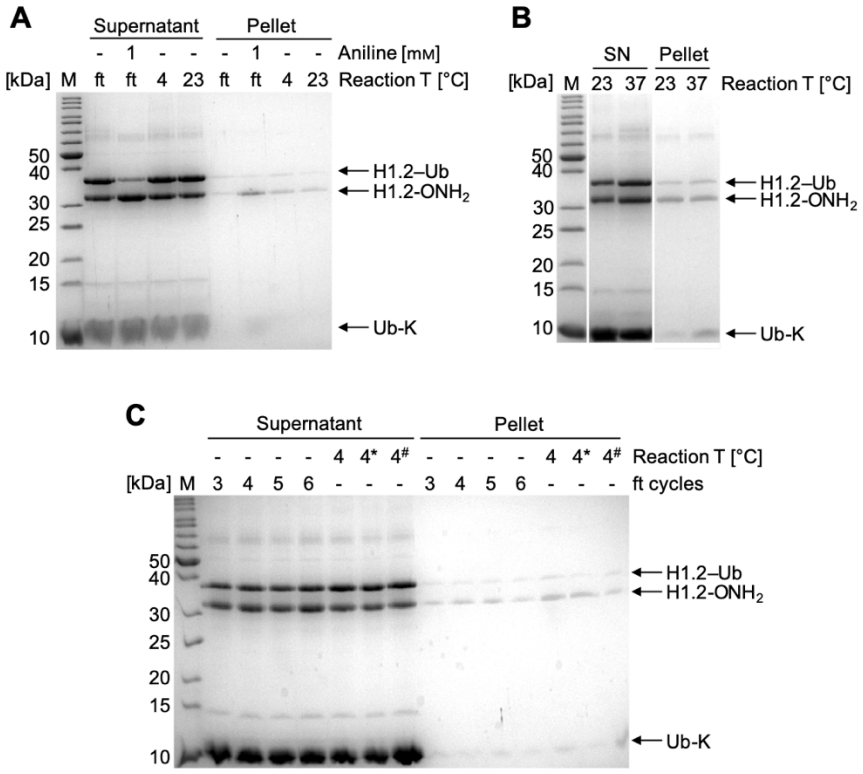

Figure 53: SDS-PAGE analysis of oxime ligation between Ub-K and H1.2 114-ONH_2. **A)** Different reaction temperatures (o.n.) and freeze-thaw were tested (2 mM SDS, 2 eq Ub-K, 5 µM H1.2 114-ONH_2, water pH 7). **B)** Investigation of 37 °C (2 mM SDS, 5 eq Ub-K, 5 µM H1.2 114-ONH_2, water pH 7). **C)** Investigation of freeze-thaw cycles and ligation at 4 °C for 1 d, 2 d (*), and for 2 d with addition of fresh Ub-K after 1 d ($^{\#}$) (2 mM SDS, 5 eq Ub-K, 10 µM H1.2 114-ONH_2, water pH 7). M: Marker.

Similarly to DNA Pol β ubiquitination (chapter 3.5.1.4), SDS was found to increase CuAAC between alkyne-modified H1.2 and azide-modified Ub.[18] Since the use of SDS increased the oxime ligation turnover of DNA Pol β ubiquitination, it was also investigated for H1.2 ubiquitination. Titration of SDS concentration revealed that SDS at a final concentration of 2 mM led to the largest amount of H1.2 ubiquitination and least protein precipitation in oxime ligation reactions (Figure 54).

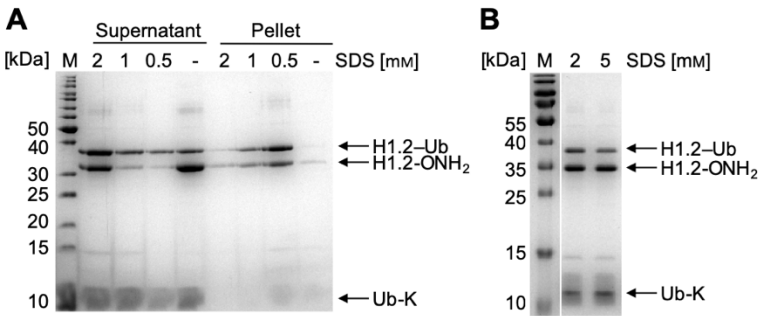

Figure 54: SDS-PAGE analysis of oxime ligation between Ub-K and H1.2 114-ONH_2. **A)** Examination of SDS concentrations for ligation turnover and precipitation of protein during the reaction (freeze-thaw, 2 eq Ub-K, 5 µM H1.2 114-ONH_2, water pH 7). **B)** Comparison of 2 mM and 5 mM SDS (freeze-thaw, 2 eq Ub-K, 5 µM H1.2 114-ONH_2, PBS pH 6). M: Marker.

Next, the use of different eq of Ub-K was studied. Increasing Ub-K from 2 eq to 5 eq and increasing the H1.2 concentration from 5 µM to 10 µM led to an enhanced ligation turnover (Figure 55). The presence of 10 eq instead of 5 eq did not lead to a significantly enhanced reaction outcome. Precipitation was not influenced by the choice of Ub equivalents or H1.2 concentration.

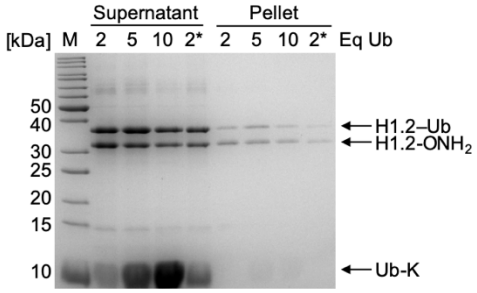

Figure 55: SDS-PAGE analysis of oxime ligation between Ub-K and H1.2 114-ONH_2. Different eq of Ub-K (freeze-thaw, 2 mM SDS, 5 µM and 10 (*) µM H1.2 114-ONH_2, water pH 7). M: Marker.

These optimized reaction conditions (water, freeze-thaw or 4 or 23 °C o.n., 2 mM SDS, 5 eq Ub, 10 µM H1.2) were applied for the conjugation of H1.2 114-ONH_2 with Ub-A. Aldehyde-modified Ub-A was used, because aldehydes are known to be more reactive than their reactive ketone counterparts and a higher oxime ligation turnover was anticipated. However, ligation proceeded with significantly diminished turnover (~20%, Figure 56 A). To assure, that the band at 38 kDa, which is assigned to H1.2–Ub, occurred because of oxime ligation between H1.2 114-ONH_2 and Ub-K (or Ub-A) in contrast to imine formation, H1.2 114U**1** containing a Boc-protected aminooxy group was incubated under the same conditions. Figure 56 A and B reveals that the band for H1.2–Ub only occured when H1.2 has previously been treated with TFA and thus contained a free aminooxy group. Therefore, oxime ligation was successfully performed between H1.2 114-ONH_2 and Ub-K/A, particularly with a turnover of up to 20% when Ub-A was used and 80% when Ub-K was employed (Figure 56).

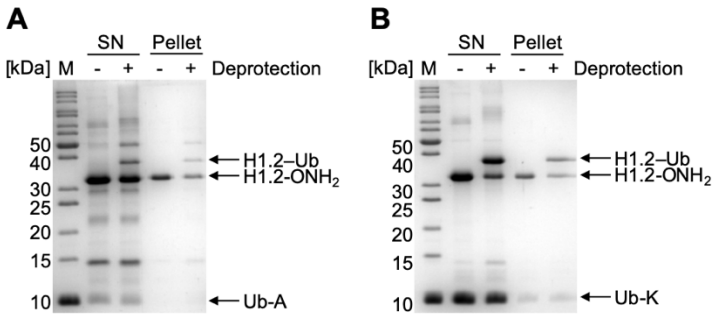

Figure 56: SDS-PAGE analysis of oxime ligation between **A)** Ub-A or **B)** Ub-K and untreated H1.2 114U**1** and H1.2 114U**1** treated with 67% TFA for 2 h at 23 °C. Reaction conditions: freeze-thaw, 2 mM SDS, 5 eq Ub-A/K 10 µM H1.2 114U**1**, water pH 7. M: Marker.

With these promising results in hand, ubiquitination of H1.2 should be performed at position 206 – a position that is known to be ubiquitinated in nature. As starting point, conditions optimized for conjugation with H1.2 114-ONH_2 were applied. However, ligation under these conditions led to a low amount of ubiquitinated H1.2 (Figure 57 A, ~10% in comparison to ~80% for H1.2 114-ONH_2). Hence, in the following, the effect of SDS concentration, buffer or catalyst, reaction temperature, and the number of equivalents in oxime ligation with Ub-K/A were investigated. Compared to the use of Ub-K, when Ub-A is used, several additional bands appear. These might result from Ub polymerization due to imine formation, which is possibly increased for Ub-A because aldehydes are generally more reactive than their respective ketone counterparts. A similar observation was made in chapter 3.5.1.4.

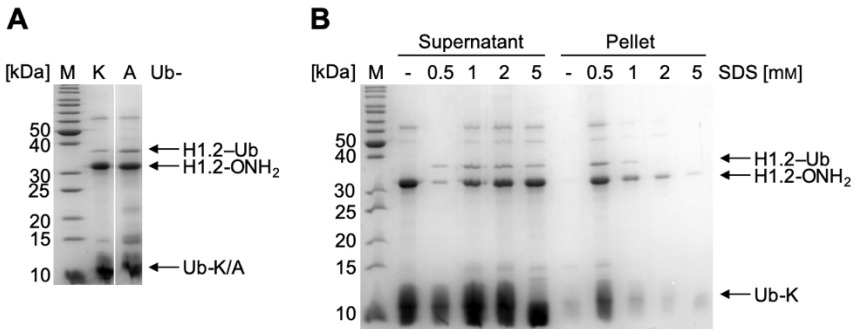

Figure 57: SDS-PAGE analysis of oxime ligation between **A)** Ub-K or Ub-A and H1.2 206-ONH_2. Reaction conditions: freeze-thaw, 2 mM SDS, 5 eq Ub-K, 10 µM H1.2 206-ONH_2, water pH 7. **B)** Investigation of SDS concentration during oxime ligation with Ub-K (freeze-thaw, 5 eq Ub-K, 10 µM H1.2 206-ONH_2, water pH 7). M: Marker.

Furthermore, it was investigated if the use of different SDS concentrations (Figure 57 B), buffers (Figure 58 A/B), or of nucleophilic catalysts (Figure 59 A/B) leads to an enhanced oxime ligation turnover for H1.2 206-ONH_2 with Ub-K. Figure 57 B, Figure 58 A/B, and Figure 59 A/B reveal that similarly for H1.2 114-ONH_2, for ubiquitination of H1.2 206-ONH_2 with Ub-K the use of SDS at a final concentration of 1–2 mM and the absence of any buffer and catalyst are most beneficial for ligation turnover and to minimize protein precipitation.

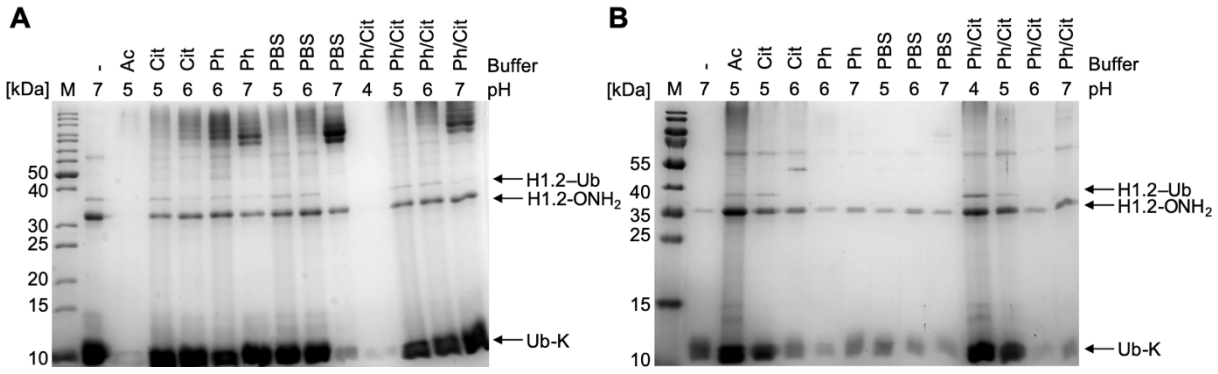

Figure 58: SDS-PAGE analysis of oxime ligation between Ub-K and H1.2 206-ONH_2. **A)** Supernatant. **B)** Pellet. Different buffers and pH were tested. Ac: 500 mM acetate, Cit: 100 mM citrate, Ph: 100 mM phosphate, Ph/Cit: 200 mM phosphate, 100 mM citrate. Reaction conditions: freeze-thaw, 2 mM SDS, 5 eq Ub-K, 10 µM H1.2 206-ONH_2. M: Marker.

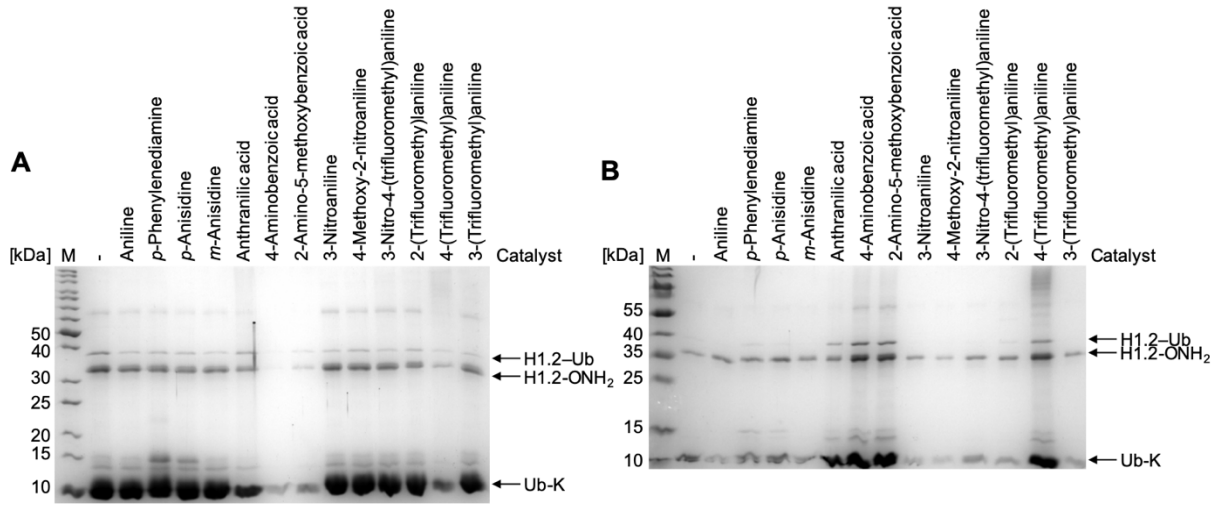

Figure 59: SDS-PAGE analysis of oxime ligation between Ub-K and H1.2 206-ONH_2. **A)** Supernatant. **B)** Pellet. Different catalysts (100 mM) were tested. Reaction conditions: freeze-thaw, 2 mM SDS, 5 eq Ub-K, 10 µM H1.2 206-ONH_2, water pH 7. M: Marker.

Next, the reaction temperature and freeze-thaw catalysis were assessed for ligation between H1.2 206-ONH_2 with Ub-K and Ub-A. Variation of reaction temperature and the use of freeze-thaw revealed no striking differences, except for slightly increased H1.2 and H1.2–Ub precipitation at 37 °C. (Figure 60 A/B).

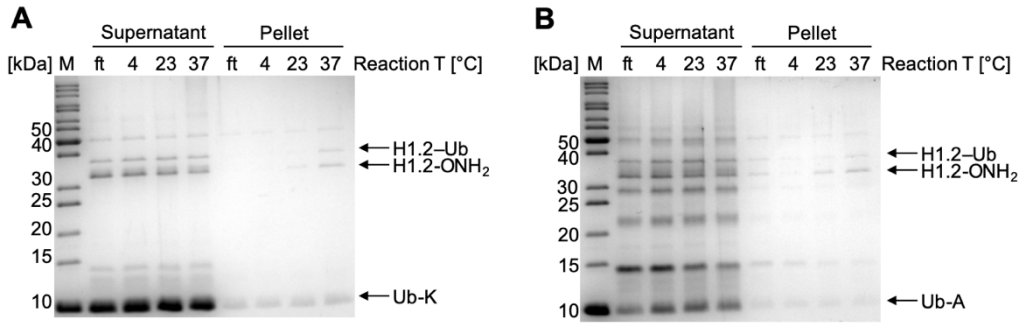

Figure 60: SDS-PAGE analysis of oxime ligation between **A)** Ub-K or **B)** Ub-A and H1.2 206-ONH_2. Different reaction temperatures and freeze-thaw (ft) were tested. Reaction conditions: o.n., 2 mM SDS, 5 eq Ub-K/A, 10 µM H1.2 206-ONH_2, water pH 7. M: Marker.

Increasing the equivalents of Ub-K from 2 to 5 strongly increased ubiquitination, whereas for Ub-A no significant difference could be observed (Figure 61). The use of 10 eq Ub did not increase oxime ligation turnover, but for Ub-A the amount of potentially polymerized Ub outweighed H1.2–Ub. Thus, most efficient oxime ligation conditions were: water, freeze-thaw or 4 or 23 °C o.n., 2 mM SDS, 5 eq Ub-K, 10 µM H1.2. However, the reaction turnover could not be increased to more than ~30%.

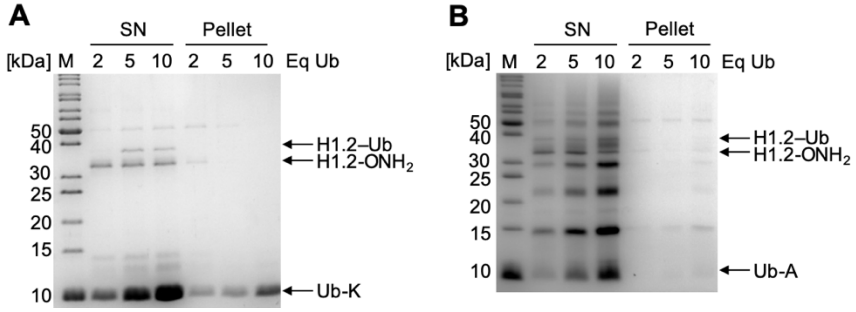

Figure 61: SDS-PAGE analysis of oxime ligation between **A)** Ub-K or **B)** Ub-A and H1.2 206-ONH_2. Different equivalents of Ub-K or Ub-A were tested. Reaction conditions: freeze-thaw 2 mM SDS, 10 µM H1.2 206-ONH_2, water pH 7. M: Marker.

In order to verify that oxime ligation proceeded between H1.2 206-ONH_2 and Ub-K or Ub-A and no unspecific imine formation with H1.2 Lys residues, untreated H1.2 206U**1** and H1.2 206-ONH_2 were incubated under the same conditions. The band assigned to H1.2–Ub only occured, when H1.2 was treated with TFA and therefore contained a free aminooxy group (Figure 62). Thus, the reaction observed most likely resulted from site-specific oxime ligation.

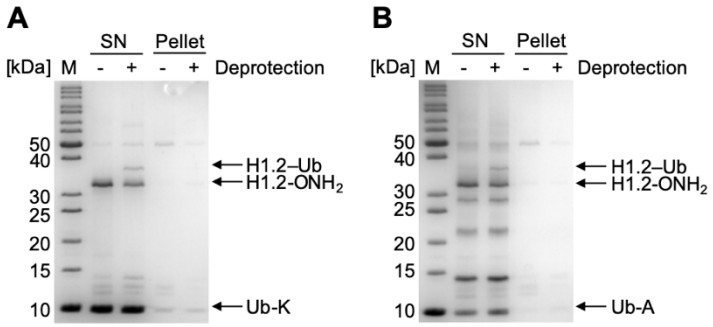

Figure 62: SDS-PAGE analysis of oxime ligation between **A)** Ub-K or **B)** Ub-A and untreated H1.2 206U**1** and H1.2 206U**1** treated with 67% TFA for 2 h at 23 °C. Reaction conditions: freeze-thaw, 2 mM SDS, 5 eq Ub-A/K 10 µM H1.2 206U**1**, water pH 7. M: Marker.

Hence, oxime ligation between H1.2 114-ONH_2 and H1.2 206-ONH_2 was successfully performed with Ub-K. The presence of 2 mM SDS in water (no buffer), without any catalyst present was crucial for oxime ligation turnover and to minimize protein precipitation with all H1.2 and Ub variants investigated here. Ubiquitination of H1.2 modified in position 114 served as proof of principle and proceeded with a yield of up to ~80% with Ub-K. The use of Ub-A under the same conditions proceeded in significantly reduced yield. While the reaction conditions optimized for H1.2 114-ONH_2 turned out to be the most beneficial conditions for oxime ligation with H1.2 206-ONH_2, the oxime ligation turnover was generally much lower (~30%). Also, the use of Ub-K or Ub-A did not strongly influence the level of H1.2 ubiquitination at position 206. However, when Ub-A was used a high background of potentially polymerized Ub was observed. Therefore, oxime ligation with site-specifically aminooxy-modified H1.2 and Ub-K/A seems to be very site-dependent.

During CuAAC considerate amounts of protein precipitated, however, ligation turnover could be tuned to ~95% for the generation of ubiquitinated H1.2 in known positions for ubiquitination[18], among them position 206[218-219]. That facilitates the isolation of H1.2–Ub. For the use of oxime ligation, very low amounts of protein precipitated. However, the establishment of a new purification protocol for the removal of unreacted H1.2 (and potential Ub polymers when Ub-A is employed) would be necessary, since ligation turnover for H1.2 206-ONH_2 and Ub-A/K did not exceed ~30%.

Nevertheless, oxime ligation between H1.2 and Ub-K/A yielded H1.2-Ub, and for the use of H1.2 114-ONH_2 and Ub-K ligation turnover could be optimized to 80%.

3.5.3 p53 Ubiquitination

3.5.3.1 General Considerations

This project was performed in collaboration with Alexandra Julier (Scheffner group, Universität Konstanz). In previous studies, Alexandra Julier attempted to generate p53–Ub conjugates by CuAAC. It was found that the addition of SDS increased ligation turnover, however, p53–Ub and p53 were not functional after treatment with copper anymore. Particularly, they were not ubiquitinated by E6/E6AP or HDM2 anymore and DNA binding was hampered by treatment of p53 with Cu(I) (unpublished data, to be published in dissertation of Alexandra Julier). p53 contains a zink finger motif that modulates DNA binding and is therefore pivotal for p53 functionality. Hypothetically, there might have been a Zn-Cu exchange, which would interfere with the functionality of the zink finger.[223-224] Hence, the effect of site-specific p53 ubiquitination on p53's functions cannot be assessed with p53–Ub conjugates generated by CuAAC. Therefore, instead of CuAAC oxime ligation should be used for the site-specific ubiquitination of p53 as a milder ligation strategy and without the necessity of transition metal catalysis. In this work, it should be investigated, if the treatment of p53 under oxime ligation conditions furnishes functional p53 variants. This should be performed by enzymatic ubiquitination of the respective p53 variants by E6/E6AP. In particular, p53 ubiquitination of position 120 should be investigated. Position 120 is known to participate in p53–DNA interaction and is post-translationally modified by ubiquitination, acetylation, and methylation.[53],[68-69] Hence, it should be assessed, if the ubiquitination of p53 120 by oxime ligation has an effect on its ubiquitination by E6/E6AP or HDM2. Moreover, the stability and DNA binding ability of oxime-linked p53–Ub should binvestigated.

p53 is structurally not stable under acidic conditions[225] and contains Cys residues that are crucial for the functionality of p53, e.g. in p53's zink finger in the DNA-binding domain.[57] Hence, the incorporation of AOAA **1** and the attachment of a modified linker by Cys nucleophilicity were neglected for the modification of p53. The use of AOAA **3** was not considered to be advantageous over KeK incorporation because a significant amount of AOAA **3** seems to be modified upon embedment into a protein environment (see chapter 3.4.1.2). Therefore, p53 should be equipped with KeK by the use of SCS and the C-terminus of Ub should be aminooxy-modified with AOAA **1**. The bond formed upon oxime ligation with these functionalized p53 and Ub variants is depicted in Figure 63.

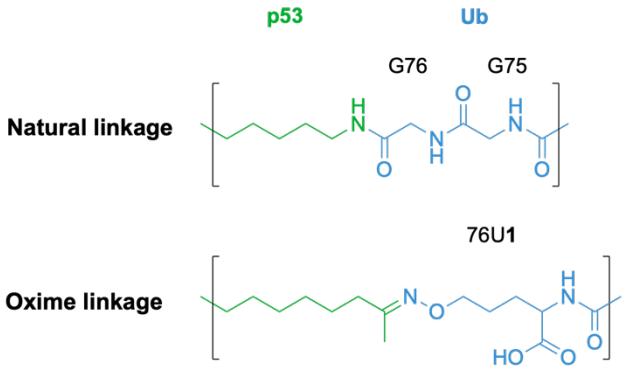

Figure 63: Schematic representation of naturally and oxime-linked p53–Ub.

3.5.3.2 Generation of Keto-Modified p53

In order to modify p53 with a ketone functionality, the incorporation of KeK (final concentration 5–15 mM) into His_6-lipoyl tagged p53 120TAG was tested with AcKRS in 6 mL test expressions. AcKRS was identified to be the most suiting PylRS mutant for the incorporation of KeK by test expressions into DNA Pol β (chapter 3.3.2.5 and 3.3.3). SDS-PAGE analysis revealed, that increasing the concentration of KeK during expression leads to an approximately proportionally enhanced expression of His_6-lipoyl tagged p53 120KeK (Figure 64). Omission of KeK led to a slight band for p53. For large-scale expression a final concentration of 10 mM KeK was used to ensure incorporation of KeK, but the amount of KeK per expression volume was kept as low as possible since KeK is synthesized in 5 steps (chapter 3.2.5) and its availability is therefore limited.

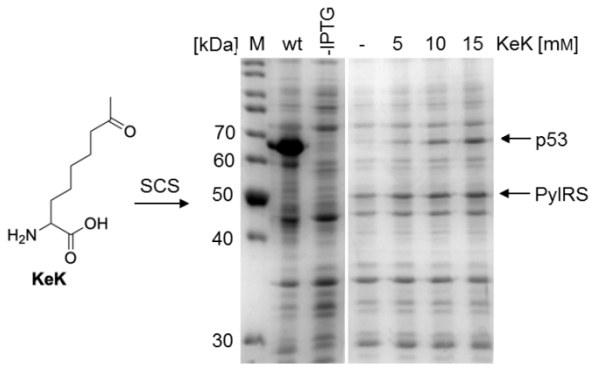

Figure 64: Test incorporation of KeK (final concentrations 5–15 mM) in p53 120TAG with AcKRS. Protein expression was performed at 25 °C for 19 h. IPTG and KeK omission served as negative control. wt: Positive control – incorporation of 1 mM BocK by PylRS wt. 1 mL samples were taken and OD_{600} was adjusted to 2.5. Incorporation efficiencies were visualized by SDS-PAGE and Coomassie staining. M: Marker.

The expression and purification protocol of p53 were adapted as reported[226] and modified by Alexandra Julier. Here, p53 was expressed fused to an N-terminal His_6-lipoyl domain tag, His_6-lipoyl domain StrepII-tag or to a StrepII-tag (Sp53). p53 120TAG/$tRNA_{CUA}$ and AcKRS were co-expressed in the presence of 10 mM KeK for 19 h at 25 °C in LB medium. The cells were pelleted and resuspended in lysis buffer. The suspension was sonicated and centrifuged. The supernatant was purified by HisTrap fast protein liquid chromatography (FPLC) by applying an increasing gradient of imidazole. Pure fractions were identified by SDS-PAGE, pooled, and dialyzed against 50 mM phosphate, 100 mM NaCl, 2 mM DTT, 0.01% NP-40 (pH 7.2). At this step, thrombin was added when the respective tag should be cleaved. The mixture was purified by HiTrap Heparin FPLC by applying an increasing gradient of NaCl (150 mM–1000 mM NaCl over 25 CV). After SDS-PAGE, pure fractions were pooled and dialyzed against 50 mM phosphate buffer, 150 mM NaCl, 2 mM DTT, 0.01% NP-

40, and 10% glycerol. Expression of 1 L yielded 0.25 mg modified p53. The protein was shock-frosted in liquid nitrogen and stored at –80 °C.

To verify the correct incorporation of KeK into p53 120TAG the protein was digested with trypsin and analyzed by LC-MS/MS (Proteomics Center, Universität Konstanz). The p53 peptide fragment containing KeK in position 120TAG was identified (Table 3). Additionally, a peptide fragment containing acetyl lysine (AcK) in position 120TAG was found, which indicates the misincorporation of AcK by AcKRS. This is in accordance with the fact, that AcK is a substrate of AcKRS[188] and might explain that a slight band for p53 was observed in the SDS-PAGE analysis of test incorporations lacking KeK (Figure 65). Presumably, considerable amounts of AcK might be present in LB medium or *E. coli* cells. Thus, the expression of p53 120KeK was performed in new minimal medium (NMM) analogous the description above. Additionally, test expressions with PylRS wt were performed in LB and NMM medium and yielded 0.02 mg for 1 L expression culture (LB). These experiments were performed in the absence and presence of KeK. Thus, when no KeK was applied but a band for full-length p53 was detected, this indicated misincorporation of AcK into p53 120TAG.

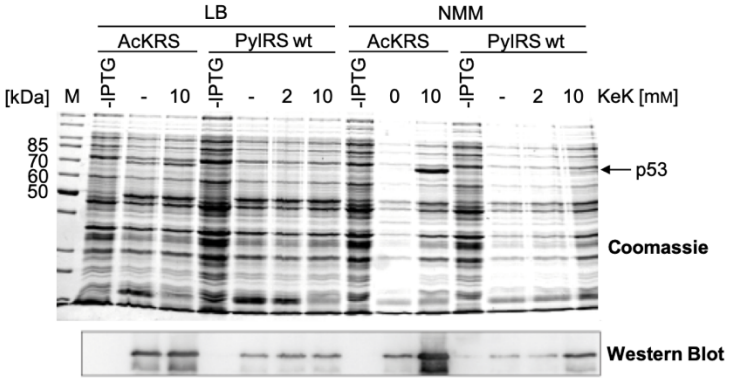

Figure 65: SDS-PAGE analysis and western blot (antibody DO-I against p53) of test incorporations of KeK into p53 120TAG by AcKRS and PylRS wt in LB or NMM medium. M: Marker.

SDS gel and western blot analysis suggested AcK misincorporation into p53 120TAG for all conditions, however, in a reduced ratio towards KeK incorporation when NMM instead of LB medium and PylRS was used. p53 120KeK expression with PylRS did not result in detectable misincorporation of AcK by LC-MS/MS (Table 4), but p53 expression was very poor in comparison to expression with AcKRS. LC-MS/MS analysis of tryptically digested protein expressed in NMM revealed the presence of the peptide fragment containing 120KeK and 120AcK (data not shown). Hence, LB medium with AcKRS was used for SCS of p53 120TAG with KeK in following experiments. Despite the misincorporation of AcK, KeK was successfully incorporated into p53 by AcKRS in LB medium.

Table 3: Refined mass analysis of tryptically digested p53 120KeK, which was generated with AcKRS in LB. The identified peptides contain Lys, KeK, and AcK at position 120. Protein coverage: 81.7%. PSM: peptide spectrum matches. ΔM: Mass measurement error. CAM: Carbamidomethyl.

Peptide sequence	#PSMs	Ion score	ΔM [ppm]	Modification
LGFLHSGTAkSVTcTYSPALNK	12	96	0.63	K10(Lys->Keto); C14(CAM)
LGFLHSGTAkSVTcTYSPALNK	45	135	0.78	K10(Acetyl); C14(CAM)
LGFLHSGTAK	4	47	-0.25	
LGFLHSGTAkSVTcTYSPALNKmFcQLAK		21	-1.79	K10(Acetyl); C14(CAM; M23(Ox); C25(CAM)
LGFLHSGTAkSVTcTYSPALNKmFcQLAK	1	26	4.10	K10(Acetyl); C14(CAM); C25(CAM)

Table 4: Refined mass analysis of tryptically digested 120 KeK, which was generated with PylRS in LB. The identified peptide contains KeK at position 120. Protein coverage: 58.8%. PSM: peptide spectrum matches. ΔM: Mass measurement error. CAM: Carbamidomethyl.

Peptide sequence	#PSMs	Ion score	ΔM [ppm]	Modification
LGFLHSGTAkSVTcTYSPALNK	2	40	-0.39	K10(Lys->Keto); C14(CAM)

3.5.3.3 Generation of Ub-Hydroxylamine

In order to mimic p53 ubiquitination by oxime ligation with KeK-modified p53, the C-terminus of Ub needed to be equipped with an aminooxy group. Therefore, AOAA **1** was incorporated into Ub 76TAG. To do so, Ub 76TAG/tRNA$_{CUA}$ and PylRS Y349F were co-expressed. Protein expression in the presence of 1 mM AOAA **1** was performed as described in chapter 3.4.1.1 and Ub 76U**1** was purified by size exclusion chromatography (SEC, HiLoad 26/600 Superdex). This approach yielded 14.3 mg protein for 1 L expression medium. LC-MS analysis revealed the presence of Ub 76U**1** and Ub termination fragment (Ub 75, Figure 66). Since Ub 75 and Ub 76U**1** differ in only one amino acid, AOAA **1**, these variants cannot be separated from each other with standard chromatographic methods. The incorporation was additionally performed in presence of 3 mM AOAA **1** in order to enhance incorporation efficiency and therefore increase the ratio of the integrals of Ub 76U**1** to Ub 75. However, mass analysis revealed that this ratio could probably not be increased. Since it can only be assumed that Ub 76U**1** and Ub 75 show similar properties in ESI-ToF, the integrals of mass signals do not represent exact ratios of the amount of the respective compounds. They rather represent a trend of these. AOAA **1** can be successfully incorporated at the C-terminus of Ub.

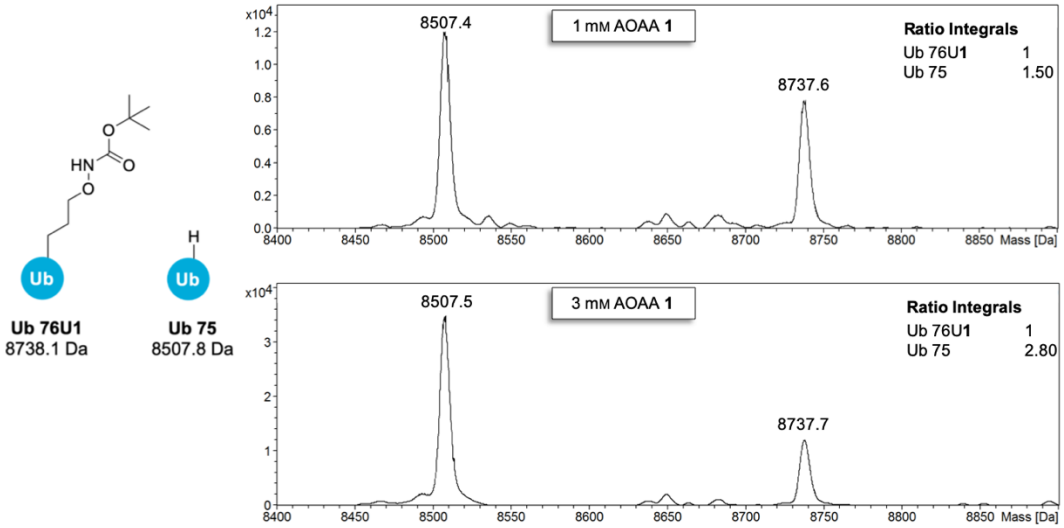

Figure 66: Schematic representation of Ub 76U**1** and Ub 75 with calculated masses (left) and LC-MS results of Ub 76U**1** expressed in the presence of 1 mM and 3 mM AOAA **1** (left).

Next, the deprotection of the Boc group of Ub 76U**1** was investigated. Hence, Ub was treated with 60% TFA for 2 h at 37 °C and the protein was precipitated in diethyl ether. The pellet was washed with diethyl ether, dissolved in water, and lyophilized. The residue was dissolved in water. Compared to the LC-MS data of untreated Ub 76U**1**, the mass signal of Ub 76U**1** vanished and a signal for Ub 76-ONH$_2$ emerged upon treatment with TFA (Figure

67). The low intensity of the mass signal for the deprotected Ub variant compared to Ub 76U**1** may be attributed to different properties in ESI-ToF. Hence, the deprotection of Ub 76U**1** by treatment with 67% TFA was successful. Note: For the following oxime ligations, the amount of Ub 76-ONH_2 is related to the sum of Ub75 and Ub76-ONH_2.

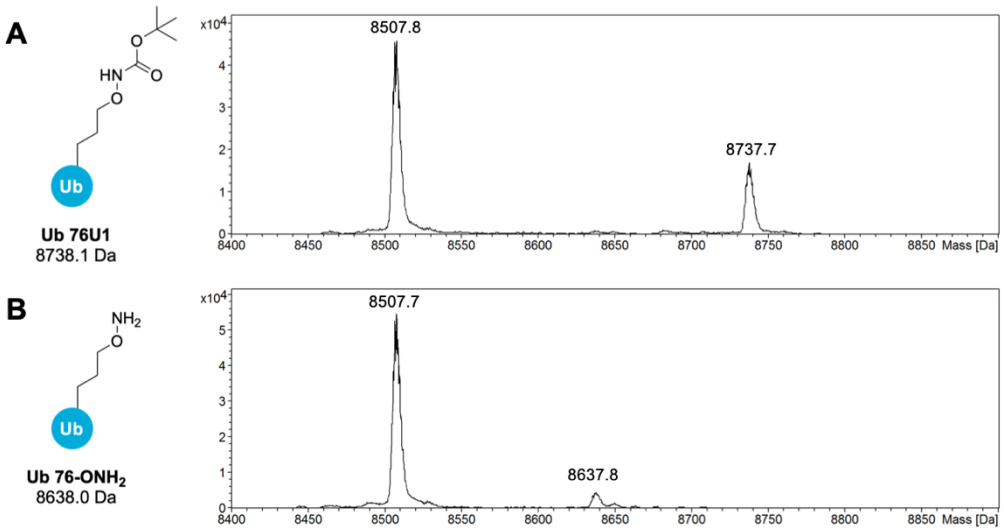

Figure 67: Schematic representation of and calculated masses of Ub 76U**1** and Ub 76-ONH_2 (left) and LC-MS results of Ub 76U**1** **A)** before and **B)** after treatment with TFA (right).

3.5.3.4 Oxime Ligation

For the generation of a site-specifically ubiquitinated p53 conjugate, p53 120KeK and Ub 76-ONH_2 were generated as described in 3.5.3.2 and 3.5.3.3, respectively, and used for oxime ligation (Figure 68).

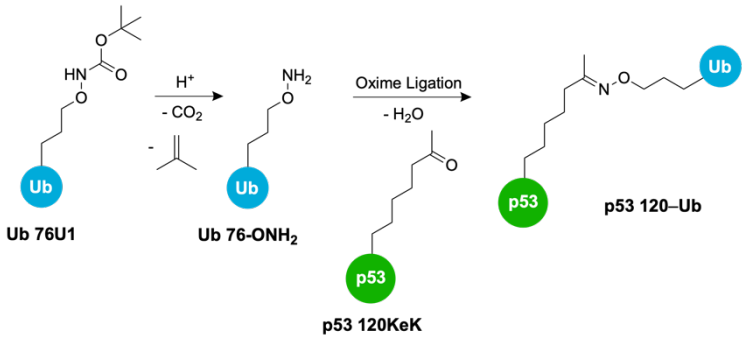

Figure 68: Schematic representation of Ub 76U**1** deprotection and p53 120KeK ligation Ub 76-ONH_2.

The reaction turnover was analyzed by SDS-PAGE. The shift of the p53 band (~55 kDa) to higher molecular weight (~65 kDa) indicated successful oxime ligation. Precipitation of the protein in the course of the reaction was assessed by centrifuging the mixture (10000 rpm, 10 min, 4 °C), removing the supernatant, and resuspending the pellet in PBS (same volume as reaction volume). Supernatant and pellet were analyzed separately by SDS-PAGE.

Oxime ligation can be enhanced by acidic, arylamine, or freeze-thaw[108] catalysis.[96-97] For oxime ligations with p53, acidic conditions are not beneficial since p53 has shown to be structurally altered after acidic treatment.[225]

First, oxime ligation was performed at 25 °C for 20 h in PBS in the absence and presence of subdenaturing concentrations of SDS (Figure 69). As observed for CuAAC (unpublished data, to be published in dissertation of Alexandra Julier), in the presence of SDS oxime ligation turnover was enhanced. In the absence of SDS no oxime ligation occured, and the highest turnover and least precipitation were observed when a final concentration of 0.5–1 mM SDS was used.

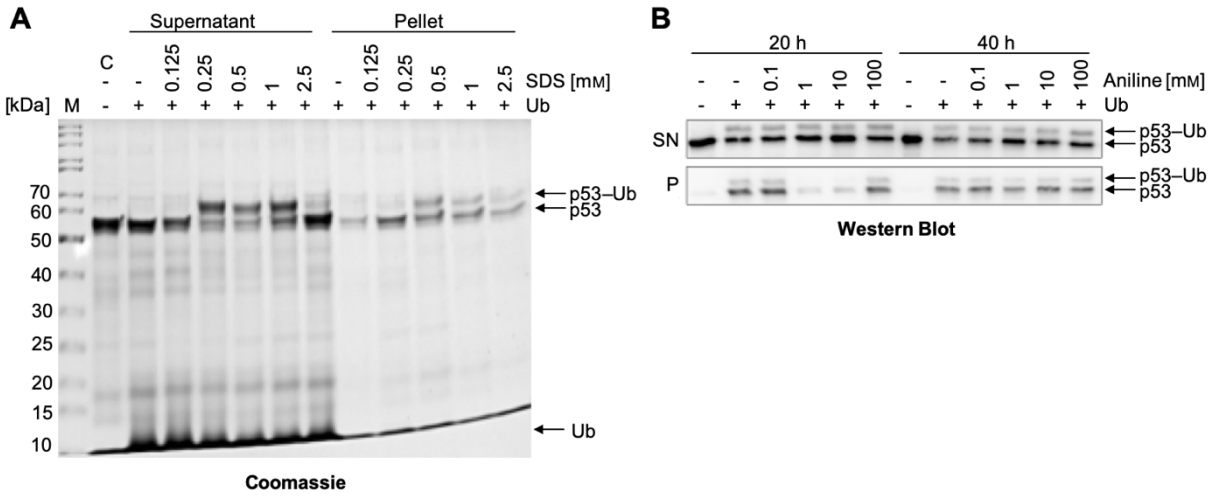

Figure 69: SDS-PAGE analysis and western blot (antibody DO-I against p53) of oxime ligation between p53 120KeK and Ub 76-ONH_2 **A)** in the presence of increasing concentrations of SDS and **B)** for 20 h and 40 h in the presence of different concentrations of aniline. If not stated otherwise, oxime ligation conditions were: 4 µM p53, 25 eq Ub, 120KeK, 0.5 mM SDS, PBS pH 7, 25 °C, 20 h. M. Marker, C: without Ub.

Moreover, the reaction time and presence of aniline on the ligation turnover was investigated (Figure 69). When the reaction time was increased from 20 h to 40 h, oxime ligation was similarly efficient, but protein precipitation increased. Moreover, the addition of aniline did not result in a higher ligation turnover (max. 30%). Different published oxime ligation catalysts (*p*-methoxyaniline, anthranilic acid)[104] were assessed, however, none of them led to an increased p53–Ub formation (data not shown).

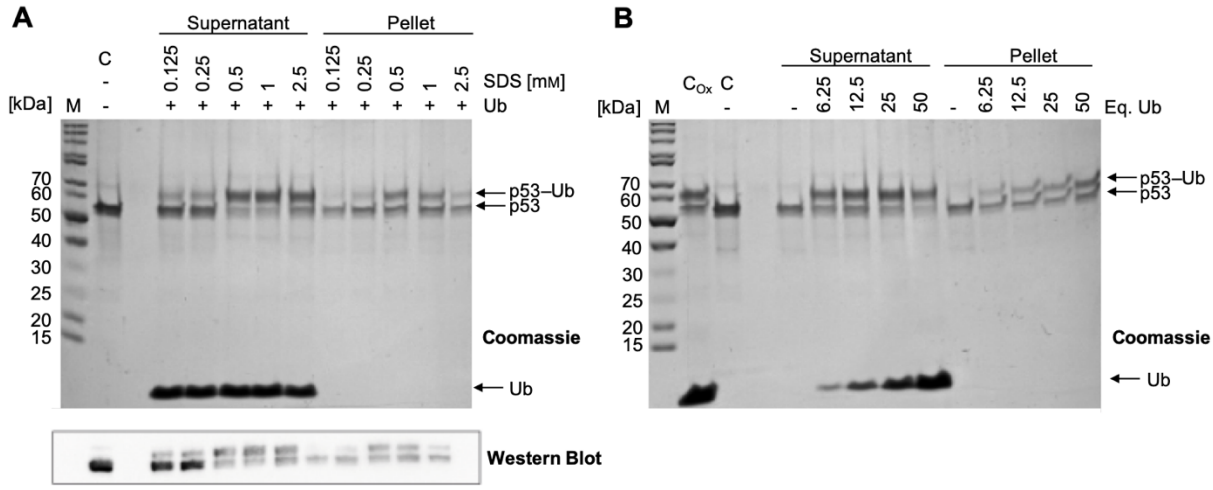

Figure 70: SDS-PAGE analysis and western blot (antibody DO-I against p53) of oxime ligation by freeze-thaw catalysis between Sp53 120KeK and Ub 76-ONH_2 **A)** in the presence of different concentrations of SDS and **B)** in the presence of differerent equivalents of Ub 76-ONH_2. If not stated otherwise, oxime ligation conditions were: 4 µM p53 120KeK, 25 eq Ub, 0.5 mM SDS, PBS pH 7, 2 x freeze-thaw. M. Marker, C: without Ub. C_{OX}: Oxime ligation at 25 °C.

Freeze-thaw (2 cycles) in the presence of SDS showed similar results as ligation at 25 °C for 20 h, however, slightly more precipitation was observed (Figure 70). Increasing the amount

of Ub76-ONH_2 revealed best turnover conditions the more Ub 76-ONH_2 was used. Since freeze-thaw proceeded much faster than ligations at rt and showed similar results, this condition was used for future experiments in the presence of 100 eq Ub 76-ONH_2 and a final concentration of 0.5 mM SDS. Note: For each batch Ub 76U**1**, the eq with respect to p53 120KeK needed to be optimized seperatley.

In order to verify oxime ligation between p53 120KeK and Ub76-ONH_2, the respective oxime ligation product was in-solution digested and analyzed by LC-MS/MS (Table 5, Figure 71). Peptides matching to the keto-, and oxime-modification, and to Lys and AcK in p53 120 were identified. As described before, AcK in position 120 probably derives from AcK misincorporation by AcKRS (chapter 3.5.3.2). p53 120Lys might derive from misincorporation of Lys or from deacetylation of p53 120AcK. Nevertheless, the oxime linkage upon ligation of p53 120KeK and Ub76-ONH_2 was successfully verified by LC-MS/MS.

Table 5: Refined mass analysis of oxime ligated p53 120 after tryptic digest in solution. Incorporation of Lys, KeK, and AcK into position 120 are observed and the formation of oxime linked p53 120–Ub is confirmed. Protein coverage is 71.33%. PSM: peptide spectrum matches. ΔM: Mass measurement error. Carbamidomethyl: CAM.

Peptide sequence	#PSMs	Ion score	ΔM [ppm]	Modification
LGFLHSGTAK	1	37	-0.29	
LGFLHSGTAkSVTcTYSPALNK	40	109	0.73	K10(Lys->Keto); C14(CAM)
LGFLHSGTAkSVTcTYSPALNK	30	89	-4.93	K10(Acetyl); C14(CAM)
LGFLHSGTAkSVTcTYSPALNK	5	48	-0.22	K10(Lys->Oxime); C14(CAM)
TYQGSYGFRLGFLHSGTAkSVTcTYSPALNK	4	26	-0.35	K10(Lys->Keto); C14(CAM)
TYQGSYGFRLGFLHSGTAkSVTcTYSPALNK	2	21	-0.38	K10(Acetyl); C14(CAM)

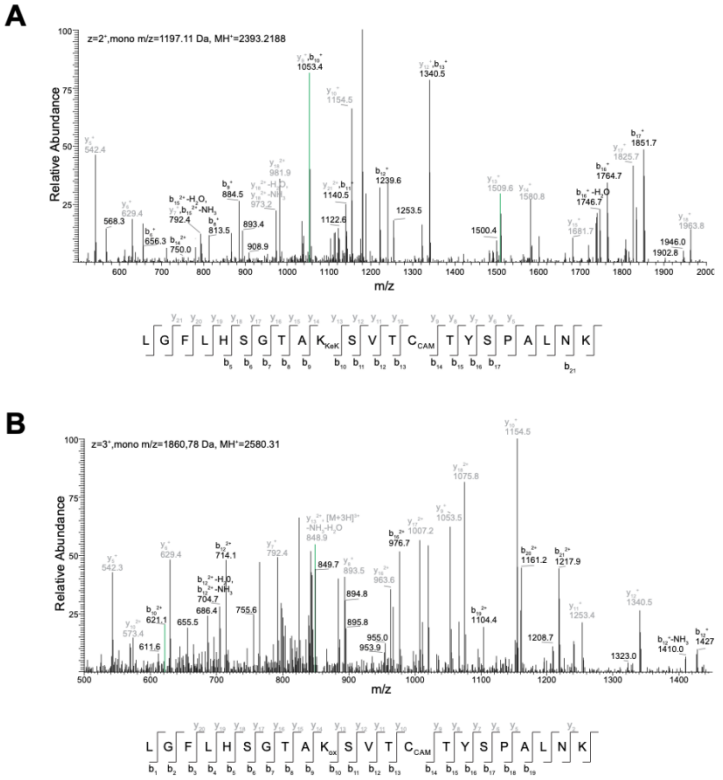

Figure 71: LC-MS/MS analysis of tryptically digested p53 120KeK and p53 120–Ub. **A)** LC-MS/MS spectrum of p53 120KeK peptide (amino acid positions 111–132). **B)** LC-MS/MS spectrum of oxime linked p53 120–Ub peptide (p53 amino acid positions 111–132). CAM: Carbamidomethyl. Ox: oxime-linked.

With optimized oxime ligation conditions, large-scale reactions (5 mL) were performed in order to purify the Sp53–Ub conjugate (4 nmol p53 120KeK, 100 eq. Ub76-ONH_2, 0.5 mM SDS, 2 x freeze-thaw). As control, Sp53 120KeK was incubated under the same conditions, however, without Ub. The reaction mixtures were first subjected to a 0.2 mL Heparin column (Repligen) with a NaCl gradient of 5 CV 15% B, 5 CV 15–35% B, 2 CV 35%, 5 CV 35–100% B (gradient delay 2 mL) (Figure 72). As predicted from previous p53 purifications, p53 120KeK was mainly eluted at 300–400 mM NaCl. However, for p53–Ub only about 50% of the protein (107 µg) eluted at that NaCl concentration and were found in the flow-through after enrichment by a Q Sepharose gravity column (elution with 200, 400, and 1000 mM NaCl, 200 µL per elution fraction, Figure 72). Sp53–Ub eluted at 400 mM (56.9 µg, 80% conjugation) and 1000 mM NaCl (10.4 µg, 90% conjugation). This could be explained by the fact that Sp53 position 120 is known to participate in DNA binding, and upon ubiquitination that function might be altered. Hence, binding of p53 120–Ub to Heparin might be reduced compared to non-ubiquitinated Sp53 120, since Heraprin, like DNA, is polyanionic. Hence, ubiquitination of p32 in position 120 was successfully achieved by oxime ligation and Sp53–Ub could be enriched by Heparin and Q Sepharose purification.

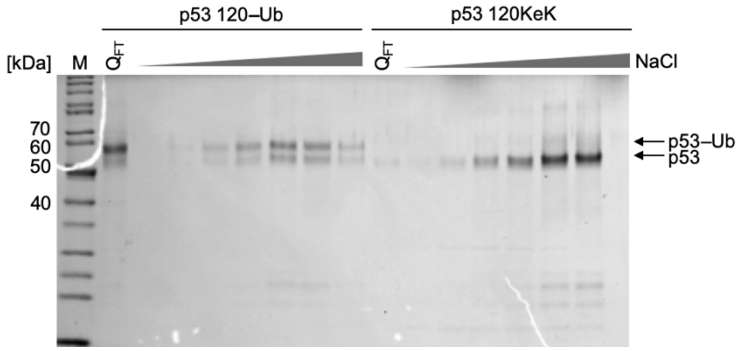

Figure 72: SDS-PAGE analysis of Sp53 120–Ub purification of by 0.2 mL Heparin column and comparison with Sp53 120KeK that was treated under mock conditions without Ub. Flow-through was enriched by Q Sepharose beads (Q_{FT}). M: Marker.

3.5.3.5 Functional Studies

3.5.3.5.1 Effect on p53 Ubiquitination

It should be investigated, if the treatment of p53 under oxime ligation conditions leads to an alteration of the functionality of p53. p53 can be ubiquitinated by E6/E6AP or HDM2, and E6 only recognizes correctly folded p53.[227] Hence, ubiquitination of a p53 variant by E6/E6AP is a hint for the correct functionality of the p53 variant. Moreover, the site-specific ubiquitination of p53 could have an impact on its ability to serve as ubiquitination target. That should also be investigated by E6/E6AP- and HDM2-mediated ubiquitination.

Enzamtic ubiquitination was performed by incubating the respective p53 sample with E1, E2 (UbcH5b), Ub, ATP, and E6/E6AP or HDM2 for (up to) 60 min at 30 °C. The samples were then analyzed by SDS-PAGE and visualized by western blot. First, it was assessed if the conditions used for oxime ligation lead to an alteration of p53's functionality. To do so, E6/E6AP-mediated ubiquitination of p53 wt and of p53 wt that had been treated under oxime ligation mock conditions was assessed, since E6 only recognizes correctly folded p53.[227] Mock-treated p53 wt was equally ubiquitinated as untreated p53 wt (data not shown). This indicated, that oxime ligation conditions did not alter p53's functionality.

Next, ubiquitination of oxime-linked p53 120–Ub by E6/E6AP was investigated. The p53 120–Ub sample also contained unreacted p53, which presumably consisted of p53 120KeK and p53 120AcK (due to misincorporation of AcK, see chapter 3.5.3.2). Hence, p53 120KeK and p53 120AcK (generated by Alexandra Julier) served as control to ensure that possibly observed effects did not result from p53 120AcK or p53 120KeK impurities in the p53 120–Ub sample. Untreated p53 wt served as positive control.

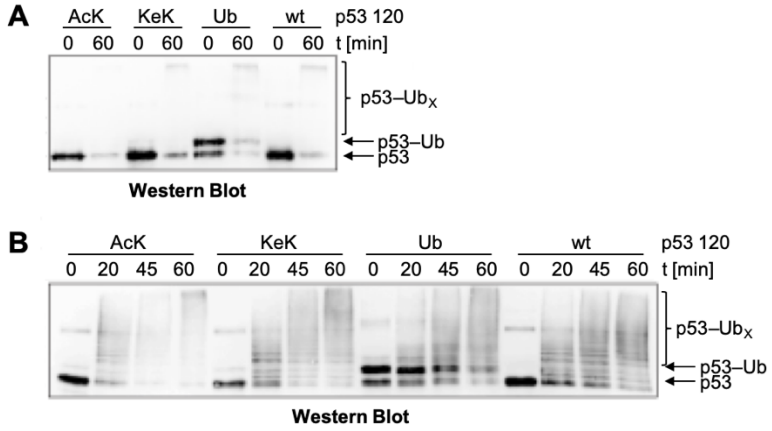

Figure 73: SDS-PAGE analysis followed by western-blot (antibody DO-I against p53) of enzymatic ubiquitination of p53 120AcK/KeK/–Ub, and p53 wt (untreated). **A)** Endpoint assay for ubiquitination of p53 variants by E6/E6AP. **B)** Time course for ubiquitination of p53 variants by HDM2.

Upon treatment of the p53 variants for as described above, a reduced band intensity with respect to untreated sample (0 min) and/or a shift to higher molecular weights can be

observed (Figure 73 A), which indicated equal ubiquitination of all p53 variants after 60 min. Ubiquitination of these p53 variants by HDM2 showed the same results (Figure 73 B). Hence, ubiquitination of p53 at position 120 had no observable effect on enzymatic ubiquitination. Equal ubiquitination of all samples by E6/E6AP furthermore suggests that the oxime ligation conditions applied for the generation of p53 120–Ub did not lead to an altered functionality of p53. For further characterization of oxime-linked p53 120–Ub, p53 was StrepII-tagged. For all respective p53 variants slightly less efficient ubiquitination by HDM2 was observed by the use of the StrepII-tag (data not shown).

Hence, oxime ligated p53 120–Ub was recognized by interaction partners and ubiquitinated, which indicates that the oxime ligation conditions applied here did not hamper with p53's structure/functionality. Moreover, ubiquitination of p53 in position 120 did not result in a significantly altered enzymatic ubiquitination.

3.5.3.5.2 Stability of p53 Conjugates

To investigate if p53 120–Ub conjugates generated as described in chapter 3.5.3.4 are suited to study ubiquitination of p53 at position 120, the stability of the conjugate should be assessed. Since oxime ligation is reversible, the hydrolytic stability of the oxime linked p53 120–Ub conjugate should be examined. Moreover, enzymatically ubiquitinated p53 can be deubiquitinated by DUBs. Hence, the stability of p53 120–Ub against DUBs should be investigated. (Note: No DUB for the specific cleavage of p53 120–Ub was known to us at the time of the experiment.)

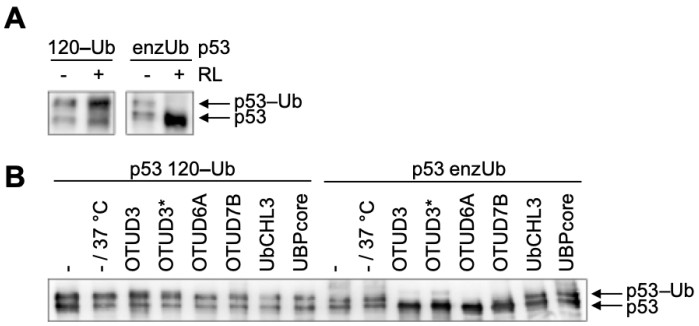

Figure 74: SDS-PAGE analysis followed by western blot (antibody DO-I against p53) of hydrolytic stability of oxime-linked p53 120Ub. **A)** Incubation of p53 120**–**Ub in rabbit reticulocyte lysate (RL) for 30 min at 37 °C. **B)** Incubation of p53 120**–**Ub with different DUBs for 30 min at 37 °C. For sample "-" no DUB was added and incubation was performed at 4 °C. ODUT3*: Mutation ΔK635 with respect to OTUD3. UbCHL3 and UBPcore do not cleave isopeptide bonds but peptide bonds after the C-terminal Gly of Ub.

Hence, the conjugate was incubated at 4 °C and 37 °C and in the presence of different DUBs (Figure 74 B). Enzymatically generated, isopeptide-linked p53–Ub served as control. SDS-PAGE revealed that oxime-linked p53 120–Ub was stable at 37 °C and upon incubation with all DUBs tested, whereas the natively ubiquitinated p53–Ub was degraded in the presence of DUBs OTUD3, OTUD3*, OTUD6A, and OTUD7B. The stability of oxime-linked and enzymatically generated p53–Ub against UbCHL3 and UBPcore indicated that these enzymes were not functional against mono-ubiquitinated p53. This is in accordance with the fact that these enzymes do not cleave isopeptide bonds, but peptide bonds after the C-terminal Gly of Ub.

Furthermore, the stability of oxime-linked p53 120–Ub in rabbit reticulocyte lysate (RL) and U2OS cell lysate (data not shown) was investigated. In Figure 74 A it can be seen that oxime-linked p53–Ub was stable whereas the natively ubiquitinated p53 was deubiquitinated. Hence, the oxime-linked p53 120–Ub conjugate is stable and suitable for experiments in cell lysates.

3.5.3.5.3 Effect on p53 DNA Binding Ability

The experiments described in this chapter were performed by Alexandra Julier. p53 Lys position 120 is located in the DNA-binding domain and is known to be post-translationally modified by ubiquitination.[53],[68-69] However, the effect of mono-ubiquitination at position 120 on DNA binding has not been elucidated yet.

Therefore, an electromobility shift assay (EMSA) was performed to assess the binding of p53 variants to *p21* recognition element, which is a known target of p53.[228-229] In addition to p53 120–Ub, p53 120AcK and p53 120KeK were investigated by EMSA. These controls were chosen since small impurities of these variants were probably present in the p53 120–Ub sample (Figure 75 B, see chapter 5.3.5.2) and it should be ensured that possibly observed effects did not predominantly resulted from these impurities. To do so, fluorescently-labeled *p21* response element was incubated with increasing amounts of p53 120AcK/KeK/–Ub, and p53 wt. The samples were analyzed by PAGE followed by detection of the *p21* fluorescence signal. Upon binding of a p53 variant to *p21*, the amount of free p21 is reduced. Therefore, less fluorescence of free *p21* should be detected and a smear at higher molecular weights should appear. PAGE-analysis and subsequent readout indicate a reduced binding of p53 120–Ub to *p21* compared to that of p53 wt and p53 120KeK (Figure 75). The binding of p53 120KeK to *p21* seems to be decreased too, however, slightly less than that of p53 120–Ub. p53 ubiquitination has been suggested to influence p53's DNA binding ability, especially when ubiquitination occurs at the DNA-binding domain.[71] The results of that experiment might be a hint in this direction. This experiment was only performed in two biological replicates and further experiments are necessary to draw a general conclusion about a possibly altered DNA binding ability of mono-ubiquitinated p53 at position 120. To perform these experiments, larger amounts of p53 120–Ub were necessary than available at the time when the experiments were performed.

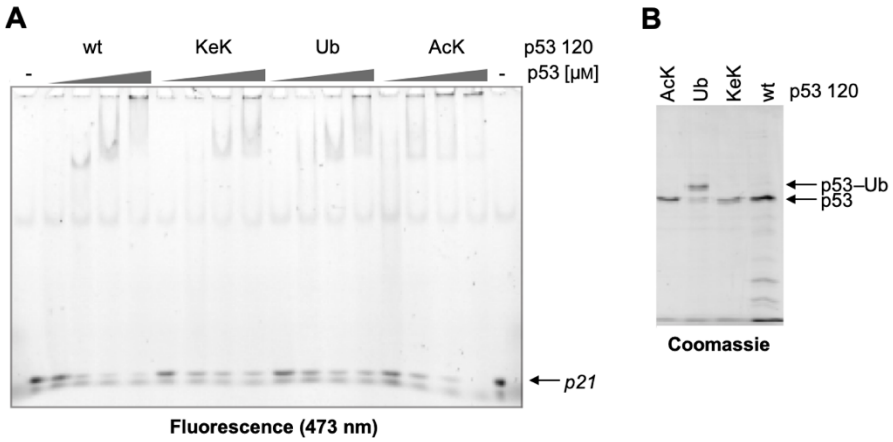

Figure 75: EMSA with p53 120AcK/KeK/–Ub, and p53 wt. **A)** Different concentrations of p53 variants were incubated with fluorescein-labelled *p21* recognition element and analyzed by PAGE. Subsequently the signal (473 nm, LPB filter) was detected with Fluorescent Image Analyzer FLA-5000 (Fujifilm). (-): no p53 was added. **B)** SDS-PAGE analysis of p53 variants used in A).

3.5.4 Overall Discussion on Oxime Ligations

Oxime ligations were performed in order to generate DNA Pol β 41–Ub, H1.2 114–Ub, H1.2 206–Ub, and p53 120–Ub. Reaction turnover was optimized to ~40% for ligation between DNA Pol β 41-ONH_2 and Ub-Aldehyde, ~80% for H1.2 114-ONH_2 with Ub-Ketone, ~30% for H1.2 206-ONH_2 with Ub-Ketone, and ~85% for p53 120KeK with Ub 76-ONH_2.

It is striking that for all POIs investigated in this study, SDS has a positive effect on oxime ligation. Whitesides *et al.* reported that when Ub binds up to 11 eq SDS (< 2 mM SDS), Ub remains correctly folded and the number of its negative charges increases.[215-217] Upon binding of additional eq SDS, Ub undergoes stepwise unfolding. The effect of SDS on oxime ligation might be explained by altered interactions between Ub and the POI due to a change of the proteins' charge, and/or by partial unfolding of the proteins. That could bring Ub and the POI in close proximity to each other and/or make the reaction centers of the protein(s) more accessible. Moreover, the use of Ub-Aldehyde must be fine-tuned to achieve a high ligation turnover but to diminish side reactions, which probably occurred because of imine formation. For all POIs, the addition of arylamine catalyst did not significantly increase the ligation turnover, but rather decreased oxime formation and led to protein precipitation. Except for DNA Pol β ubiquitination, freeze-thaw catalysis was successful, but turnover did no exceed reactions at 4, 16, or 23 °C, o.n.

For ligation with DNA Pol β 41-ONH_2, the use of Ub-A resulted in significantly better turnover than the use of Ub-Ketone. It was surprising that the use of Ub-Aldehyde was not superior to Ub-Ketone for ligations with H1.2 114-ONH_2 and H1.2 206-ONH_2 although aldehydes are usually more reactive in oxime ligations than the respective ketones. Moreover, oxime ligation turnover of H1.2 strongly depended on the site of the modification.

These results illustrate, that the presence of SDS and absence of arylamines has a positive impact on the turnover and protein solubility regarding protein ubiquitination by oxime ligation investigated in this work. No further general statement about beneficial ligation conditions can be made, since these were strongly dependent on the POI and the position of ubiquitination.

In general, in this work (and in the work of Alexandra Julier, to be published), chemical protein ubiquitination was performed for the first time with proteins exceeding 16 kDa (note: 16 kDa β-globulin was double mono-ubiquitinated[185]). To the best of knowledge, until now oxime ligation with Ub has been reported with quite small proteins (Ub: 9 kDa, 60–85% turnover; SUMO: 12 kDa, turnover nearly complete; α-globulin: 15 kDa, turnover nearly complete; β-globulin: 16 kDa, double mono-ubiquitination, turnover nearly complete).[137],[184-185] In these previous studies, oxime ligation was usually performed under denaturing conditions (guanidinium hydrochloride).[137],[185] Such harsh treatment was prevented in this

work. Moreover, it was shown, that oxime-linked p53 120–Ub is stable towards proteolysis by DUBs and in cell lysates. Hence, oxime ligation can be a poweful tool to study site-specific mono-ubiquitination of proteins.

4. Summary and Outlook

The aim of this thesis was the synthesis and the genetic incorporation of AOAAs into proteins, and the investigation of oxime ligation as tool for protein ubiquitination.

Hence, the respective proteins needed to be modified with an aminooxy group or a carbonyl functionality. Keto-modified KeK was site-specifically incorporated into proteins by SCS with a published PylRS mutant (AcKRS)[189], but KeK incorporation by AcKRS proved to be inefficient. For example, high amounts of KeK (final concentration 10 mM) were necessary to obtain reasonable amounts of p53 120KeK. Attempts to further enhance the activity of AcKRS for KeK incorporation with published methods[140],[205] were not successful. The question came up, if KeK is an inhibitor of Lys deacetylase CobB, and if the availability of KeK during expression is therefore reduced and leads to inefficient $tRNA_{CUA}$ aminoacylation. In the presence of CobB inhibitor nicotinamide, incorporation efficiency was not increased. To finally answer that question SCS with KeK should be performed in an *E. coli* CobB knockout strain.[204] Nevertheless, KeK was successfully incorporated into p53 120TAG. Alternatively, an aldehyde or keto-modified alkyl chloride was site-specifically attached to a Cys residue in Ub 75C in a nucleophilic substitution to yield Ub 75C-Aldehyde/Ketone.

To site-specifically equip the POI with an aminooxy group, SCS should be applied. Therefore, AOAAs **1**–**4** bearing carbamate-based protection groups were synthesized and PylRS Y349F, PylRS Y271A L274M, and PylRS Y271M L274A C313A Y349F were identified for the incorporation of AOAAs **1**, **3**, and **4**, respectively. The incorporation of AOAA **1** by PylRS Y349F was very efficient. For AOAA **2**, no suiting PylRS mutant could be identified. The embedment of photolabilly-protected AOAAs **3** and **4** into Ub 48TAG as model protein was analyzed by LC-MS. Analysis of Ub 48U**3** revealed presence of a species of + 18 Da in addition to the expected mass. This species was also observed upon incorporation of AOAA **3** in Ub positions 6 and 63, upon expression with and without His-tag, when conditions for purification were varied, and in presence of CobB inhibitor nicotinamide. When the respective Lys variant of AOAA **3**, CouK, was incorporated into Ub 48TAG, only the expected mass for Ub 48CouK was observed. It was hypothesized that the +18 Da species occurred upon hydrolysis of the coumarin lactone. That might be favored by the presence of the aminooxy group at the carbamate, which might alter the electronic properties in the coumarin ring. Irradiation of Ub 48U**3** at 365 nm and subsequent ligation with TAMRA-Ketone as well as LC-MS analysis confirmed the removal of the coumarin protection group. The +18 Da species remained upon irradiation. To finally answer the question, if the additional mass derived from CobB, incorporation of AOAA **3** could be performed in an *E. coli* CobB knockout strain.[204] To understand how that 18 Da species was generated would help for the design of new AOAAs with photolabile protection groups.

Despite several reports about *E. coli* reductases[136],[203] that might reduce the nitro group of the AOAA **4** protection group and therefore lead to the deprotection of **4** during protein expression, there was no hint for that process for AOAA **4**. Since a different behavior was observed for the incorporation of coumarin-protected AOAA **3** and CouK by LC-MS analysis, it would be interesting to investigate, if the nitro group of the respective Lys variant of AOAA **4**, Nitro-lysine, is affected by nitroreductases. Hence, Nitro-lysine could be synthesized, incorporated into Ub 48TAG and analyzed by LC-MS. That would give more insight into the possibly altered behavior of AOAAs compared to the respective Lys variant. For the incorporation of AOAA **4** into proteins by PylRS Y271M L274A C313A Y349F a final concentration of 2 mM AOAA **4** was identified to lead to efficient SCS. Since during AOAA **4** synthesis, the acidic removal of the Boc and *t*Bu ester protection groups proceeded in low yield, the synthesis of AOAA **4** might be optimized. That could be done by using an alternative protection group strategy.

To enable or further increase the incorporation efficiency of AOAAs **2**, **3**, **4**, and of KeK, a screening of PylRS mutants as described in chapter 3.3.2.1 could be performed. The PylRS libraries should be based on PylRS wt and randomized positions could include residues 271, 274, 313, and 349. These positions have frequently been identified to direct the acceptance of side-chain modified amino acids by PylRS by several researchers and in this thesis.[91],[135],[186],[188-189] Additional residues for randomization could be determined by modeling of the respective amino acid into the PylRS amino acid binding pocket.

W. Liu *et al.* reported that the introduction of R19H H29R T122S (related to *M. mazei* PylRS) generally enhanced amino acid incorporation, e.g., AcK incorporation was enhanced 4.4-fold.[141] These mutations could be introduced into AcKRS to investigate if these mutations also enhance aminoacylation of $tRNA_{CUA}$ with KeK.

Next, the feasibility of oxime ligation for the mimicry of protein ubiquitination was assessed. DNA Pol β 41TAG was modified with AOAA **1** or **3**. Acidic treatment for deprotection of DNA Pol β 41U**1** resulted in precipitation of the protein. LC-MS/MS analysis of tryptically digested DNA Pol β 41U**3** confirmed the correct incorporation of AOAA **3**. Deprotection of DNA Pol β 41U**3** was performed by irradiation at 365 nm and followed by labeling with TAMRA-Ketone. For DNA Pol β ubiquitination, the best oxime ligation turnover of ~40% was achieved by ligation with Ub-Aldehyde in 1 mM SDS, 5–10 eq Ub-A, PBS pH 5 or 6 at 4, 16, or 23 °C, o.n. AOAA **1** was incorporated into H1.2 114TAG as proof of principle and into H1.2 206TAG since K206 is a known ubiquitination site. Deprotection of the Boc group was performed in 67% TFA for 2 h at rt and followed by LC-MS. Oxime ligation with Ub 75C-Aldehyde/Ketone revealed significantly higher turnover for H1.2 114U**1** than for H1.2 206U**1** and with Ub 75C-Ketone. Best turnover of ~80% was obtained in water in the presence of 2 mM SDS with 5 eq

Ub-Ketone at 4, 23 °C, o.n. or freeze-thaw. Thus, for H1.2 oxime ligation efficiency seemed to depend on the ligation site at the substrate.
Compared to CuAAC the generation of DNA Pol β–Ub and H1.2 206–Ub by oxime ligation was moderately efficient. That might be due to incomplete deprotection of AOAA **3** in DNA Pol β (due to potential hydrolysis) or because of the slow reaction kinetics of oxime ligation in submillimolar concentrations. Moreover, the large size of the substrates might contribute to decreased kinetics. Nevertheless, DNA Pol β and H1.2 were site-specifically ubiquitinated by oxime ligation.

The site-specific ubiquitination of p53 was studied in cooperation with Alexandra Julier (Scheffner group). KeK was incorporated into p53 120TAG and AOAA **1** into Ub 76TAG. Expression of Ub 76U**1** yielded considerate amounts of truncated protein that could not be separated from Ub 76U**1** because these Ub variants differ in only one amino acid (AOAA **1**). Deprotection of Ub 76U**1** was performed in ~60% TFA for 2 h at 37 °C and was confirmed by LC-MS analysis. Upon expression of p53 120KeK, AcK was partially misincorporated into p53 120TAG. It was assumed that AcK is present in LB medium and *E. coli* cells, and it is known that AcKRS that was used for KeK incorporation, accepts AcK well[188]. Oxime ligation was performed in PBS pH 7, 0.5 mM SDS by means of freeze-thaw catalysis with 100 eq Ub 76U**1**. The conjugate was isolated, and it could be shown, that oxime-linked p53 is stable against DUBs and is recognized by interaction partners. Furthermore, first EMSAs indicate a reduced binding affinity of p53 to DNA upon mono-ubiquitination.
Hence, oxime ligation is a powerful tool for the site-specific mimicry of protein ubiquitination and is especially suited for substrates that require mild ligation conditions. Interestingly, the presence of SDS ehanced the ligation efficiency for the ubiquitination of all proteins tested in this thesis, presumably due to altered interactions between Ub and the POI due to a change of the proteins' charge, and/or by partial unfolding of the proteins. Moreover, oxime ligation enabled the synthesis of functional site-specifically ubiquitinated p53, which was performed for the first time in the course of this project. The turnover of p53 ubiquitination was satisfying (~85%), yet might be further enhanced by increasing the efficiency and selectivity of PylRS for KeK incorporation over AcK incorporation. Additionally, the presence of unfunctionalized Ub besides Ub 76U**1** might reduce reaction kinetics. Hence, the development of methods for the traceless incorporation of amino acids at a protein C-terminus should be considered. To do so, protein expression could be performed with a C-terminal tag or fusion protein to enable the separation of the termination fragment from full-length protein. This would be followed by the enzymatic cleavage of that tag/fusion protein at the C-terminal site of the unnatural amino acid, since the environment of the isopeptide mimic should be as native as possible. This step would most likely be very challenging, since that enzyme should tolerate

the UAA in close proximity to its recognition site. Probably, the directed evolution of such an enzyme would be necessary. The development of a method based on that concept would not only find application for protein ubiquitination, but also for the mimicry of other PTMs at a protein C-terminus by means of SCS.

The synthesis and characterization of p53-Ub conjugates should also be performed for different ubiquitination sites of p53 to examine, if the site of ubiquitination has an impact on the proteins fate, and if yes, what that fate is. Particularly, the investigation of ubiquitination sites located in different p53 domains would be of high interest.
Moreover, to study the interplay of different POI PTMs, oxime ligation could be combined with other ligation chemistries or the genetic incorporation of amino acids that mimic PTMs themselves (e.g. phospho-Ser or AcK mimics). In this context, investigating the sortase-mediated protein ubiquitination published by Lang *et al.*[167] would be of high interest.

5. Experimental Part

5.1 Material

General Information

Chemicals for molecular biology were of p.a. or molecular biology grade. Chemicals for synthesis and molecular biology were ordered from ABCR, Merck/Sigma Aldrich, Roth, Bachem, TCI, Roth, Acros Organics, Fluka, Riedel de Häen, or Iris Bioctech GmbH. Solvents for MPLC were ordered from VWR and were of HPLC grade. Milli-Q water (MQ H_2O) was obtained from a Milli-Q system from Millipore Corporation. NMR solvents were obtained by Deutero or Eurisotop.

MPLC was performed on a PrepChrom C-700 (Büchi) or Sepacore® Flash System X (Büchi). RP-columns were prepacked (25-40 microns, Götec).

NMR spectra were recorded at ambient temperature with Bruker Avance III 400 instrument. Samples were prepared in deuterated solvents. The chemical shift δ was measured in parts per million (ppm) and calibrated to residual ^{1}H or ^{13}C solvent signal. Multiplicity was assigned as singlet (s), doublet (d), triplet (t), quadruplet (q), pentuplet (p), or multiplet (m).
LC-MS high-resolution mass spectra (HRMS) were obtained on a Bruker Daltonics microTOF II instrument. LC-MS/MS spectra were recorded by the Proteomics Center, Universität Konstanz.

All culture media and objects for work with bacterial culture were sterilized prior to use (120 °C, 20 min, 1 bar). Buffer containing heat sensitive substances were filtered with a filter with a pore size of 0.2 µm. Culture medium was warmed to 37 °C before inoculation with bacteria. Bacteria were grown under aerobic conditions at 37 °C, 160 rpm if not stated otherwise.

Laboratory Equipment

Device	Supplier
Agarose Gel Electrophoresis	BioRad
Agarose Gel Racks	Fisher Scientific
Äkta™ Pure FPLC System	GE Lifescience
Electroporator Gene PulserXcell	BioRad

Filtration System Solvac	Pall
Freeze Dryer Beta 2-8 LDplus	Christ
Freeze Dryer Lyovac GT 2	Leybold-Heraeus
Gel Reader Chemidoc XRS	BioRad
Gel Reader Imager 600	Amersham
Heating Cabinet	Memmert
Incubation Shaker	New Brunswick Scientific
Incubator HeraTherm	Thermo Scientific
LC-MS Amazon SL	Bruker
LC-MS Micro-ToF (High Resolution)	Bruker
Magnetic Stirrer/Heating Plate	Heidolph
NanoDrop 1000	PeqLab
Overhead Shaker	Heidolph Reax2
pH meter 766 Calimatic	Knick
Photometer	Eppendorf
Pipettes	Eppendorf
Pipet-Boy	Eppendorf
Power Supply for Electrophoresis Power Pac 3000	BioRad
PrepChrom C700 (MPLC/HPLC)	Büchi
Refrigerated Centrifuge 5810	Eppendorf
Refrigerated Centrifuge Biofuge primoR	Heraeus
Refrigerated Centrifuge Multifuge 4 KR	Heraeus
Refrigerated Centrifuge Sorvall LYNX 4000	Thermo Scientific
Rotation Evaporator	Büchi
Sepacore® Flash System X (MPLC)	Büchi
Sterile Bench	HERA safe
Sonicator Sonoplus	Bandelin
Table Top Centrifuges	Eppendorf 5417C, 5804R
Thermocycler	Biometra
Thermomixer Comfort	Eppendorf
Fluorescent Image Analyzer FLA-5000	Fujifilm
UV Lamp B-100AP, 365 nm, 100 W, 12 mW/cm^2	UVP
96-well plate Reader Infinite M200	Tecan

Disposables

Disposable	Supplier
Amicon® Ultra Cetrifugal Filters	Merck
Cuvettes	Roth
Electroporation Cuvettes Gene Pulser	BioRad
Frits, 20 µm	Isolute® Spe Accessories
Microcentrifuge Tubes, Extended Capacity, Siliconized	Sigma Aldrich
Petri Dishes	Roth
Pipette Tips	Starlab
PVDF membrane Immobilion-P, 0.45 µl pore size	Millipore
Reaction Tubes	Sarstedt
Snake Skin Tubes for Dialysis	Roth
Sterile Filtration Filter	Nalgene
Syringe Filters	Quali Lab
Syringes and Canula	B. Braun
Tips, C18, 10 µL bed volume	Thermo Fisher
TLC silica gel 60 F_{254}, Aluminium	Merck
Vivaspin® Ultrafiltration Unit	Sartorius
Whatman Paper	Merck
96-well plates, transparent	Greiner

Software

NMR spectra were edited with MestreNova from Mestrelab Research. Molecule structures were created with ChemDraw from Perkin Elmer. DNA sequence translations and calculation of proteins masses were performed with the Bioinformatics Resource Portal ExPASy. Mass data were analyzed with Compass Data Analysis program from Bruker. Gel pictures were edited with Image Lab 5.2 from BioRad. Pictures were generated and edited with Microsoft Power Point 2010 and Adobe Illustrator CS4. DNA primers were designed with SnapGene Viewer 3.0.3 and DNA sequences were aligned with Clustal Omega.

Bacterial Strains

Strain	Genotype	Source
E. coli XL10-Gold	*endA1 glnV44 recA1 thi-1 gyrA96 relA1 lac Hte Δ(mcrA)183 Δ(mcrCB-hsdSMR-mrr)173 tet^R* F' [*proAB lacI^{q}ZΔM15 Tn10(Tet^R Amy Cm^R)*]	Stratagene
E. coli BL21 (DE3)	*F$^-$ompT gal dcm lon hsdSB(r_B^- m_B^-) λ(DE3 [lacI lacUV5-T7 gene 1 ind1 sam7 nin5])*	Stratagene

Constructs

Construct (Vector)	Description
Ub 75C (pET-3a)	No tag, kindly provided by Xiaohui Zhao
DNA Pol β/tRNA$_{CUA}$ (pET11a)	N-terminal His$_5$-tag, kindly provided by Tatjana Schneider
Ub 76TAG/tRNA$_{CUA}$ (pET11a)	No tag, kindly provided by Daniel Schneider
Ub 48TAG, Ub 6TAG, Ub 63TAG/tRNA$_{CUA}$ (pGEX2TK)	C-terminal His$_6$-tag, kindly provided by Simon Kienle
Ub 48TAG	No tag, generated from Ub 48TAG with His$_6$-tag by SDM
Ub wt (pGEX2TK)	C-terminal His$_6$-tag, kindly provided by Kathrin Stuber
Histone H1.2 wt (pET11a)	C-terminal His$_6$-tag, kindly provided by Daniel Rösner
Histone H1.2 E114TAG/tRNA$_{CUA}$ (pET11a)	C-terminal His$_6$-tag, kindly provided by Simon Geigges
Histone H1.2 K206TAG/tRNA$_{CUA}$ (pET11a)	C-terminal His$_6$-tag, kindly provided by

	Simon Geigges
PylRS wt (pRSFDuet-1)	Origin: *Methanosarcina barkeri*, kindly provided by Marina Rubini
p53 120TAG/ $tRNA_{CUA}$ (pGEX2TK)	C-terminal His_6-tag, kindly provided by Alexandra Julier
p53 120TAG/$tRNA_{CUA}$ (pET11a)	C-terminal His_6-lipoyl domain, kindly provided by Alexandra Julier
p53 120TAG (pGEX2TK)	C-terminal His_6-lipoyl domain, kindly provided by Alexandra Julier
p53 120TAG (pGEX2TK)	C-terminal His_6-lipoyl domain and StrepII-tag, kindly provided by Alexandra Julier

Service Providers

Oder	**Provider**
DNA sequencing	GATC
Oligonucleotides	Metabion and biomers
gBlocks	Integrated DNA Technologies

Enzymes

Enzyme	**Supplier**
Acl I	New England Biolabs
CIP (Alkaline Phosphatase, Calf Intestinal)	New England Biolabs
DpnI	New England Biolabs
Phusion HF DNA polymerase, HF and GC buffer	New England Biolabs
SacI-HF	New England Biolabs
Thrombin	Sigma Aldrich
Trypsin	Promega
T4 DNA Ligase	New England Biolabs

UbCHL3	Kindly provided by Kathrin Stuber

Antibodies

Antibody	**Supplier**
HRP α-mouse (goat)	Dianova
DO-I (p53)	Calbiochem

Kits and Standards

Kit/Standard	**Supplier**
BSA Standard	Thermo Scientific
CloneJET PCR Cloning Kit	Thermo Scientific
DNA loading dye (6x)	New England Biolabs
dNTP set, 10 mM	Fermentas
His Detector™ Nickel-AP	KPL
Histone Standard	Calbiochem
MinElute® Reaction Clean Up Kit	Qiagen
Page Ruler™ Unstained Protein Ladder	Thermo Scientific
Page Ruler™ Prestained Protein Ladder	Thermo Scientific
Pierce™ BCA Protein Assay Kit	Thermo Scientific
Pierce™ Bovine Serum Albumine Standard	Thermo Scientific
Pierce ECL Western Blotting Substrate	Thermo Scientific
QIAprep® Spin Miniprep Kit	Qiagen
QIAquick® Gel Extraction Kit	Qiagen
Roti® Quant Bradford Protein Assay	Roth
Ubiquitin Standard	Sigma Aldrich
1kb DNA Ladder	New England Biolabs
1-Step™ NBT/BCIP	Thermo Scientific

Resins

Resin	Supplier
cOmplete™ His-Tag Purification Resin	Roche
Ni-NTA Agarose	Qiagen
Q Sepharose® Fast Flow	GE Healthcare
Sephadex™ G-25 Superfine	GE Healthcare
SP Sepharose® Fast Flow	GE Healthcare

FPLC, HPLC and MPLC Columns

Column	Supplier
HiTrap™ SPHP 1 mL, 5 mL	GE Healthcare
HiTrap™ Heparin HP 1mL	GE Healthcare
HisTrap™ 1 mL	GE Healthcare
RP 18, SVP D40 25–40 5 µm (10, 30 or 80 g)	Götec Labortechnik
Superdex™ 75 Increase 10/300 GL	GE Healthcare
Superdex™ HiLoad 26/600	GE Healthcare

Media

Medium	Component	Concentration
Bacterial Cell Culture		
LB	LB-medium	20% (w/v)
LB Carb	LB-medium	
	Carbenicillin	100 µg/mL
LB Kan	LB-medium	
	Kanamycin	34 µg/mL
SOB Medium pH 7.0	Tryptone	20 g/L
	Yeast ectract	5 g/L

	NaCl	0.01 M
	$MgCl_2$	0.01 M
	$MgSO_4$	0.01 M
SOC Medium pH 7	SOB medium	
	Glucose	0.02 M
TSS Buffer	LB medium	85% (v/v)
	PEG6000	10% (w/v)
	$MgCl_2$	50 mM
	DMSO	5% (v/v)

SDS-PAGE

Loading Dye (6x)	Tris-HCl, pH 6.8	225 mM
	SDS	5% (w/v)
	Glycerol	50% (v/v)
	β-Mercaptoethanol	1.25% (v/v)
	Bromphenol Blue	0.05% (w/v)
Resolving Gel (12.5%)	Trizma base, pH 8.8 (1.5 M)	1.25 mL
	10 % SDS	50 µL
	H_2O	1.65 ml
	30 % Bis-Acrylamide	2.15 mL
	APS	50 µL
	TEMED	5 µL
Stacking Gel (4%)	Trizma base, pH 6.8 (0.5 M)	1.25 mL
	10% SDS	20 µL
	H_2O	3.1 mL
	30% Bis-Acrylamide	0.65 mL
	10% APS	35 µL
	TEMED	10 µL
Electrophoresis Buffer	Trizma base	250 mM
pH 8.9	Glycin	2 M
	SDS	1%

Coomassie Staining	Coomassie Brilliant Blue R-250	0.2% (w/v)
	Methanol	50% (v/v)
	Acetic acid glacial	10% (v/v)
Coomassie Destaining	Methanol	50% (v/v)
	Acetic acid glacial	10% (v/v)

Agarose Gel Electrophoresis

TAE buffer (50x)	Trizma base	2 M
pH 8.5	0.5 M EDTA, pH 8	10% (v/v)
	Acetic acid glacial	5.7% (v/v)
Agarose Gel	TAE buffer	
	Agarose	0.8% (w/v)
	Ethidium bromide	0.05% (v/v)

Western Blot

Transfer Buffer	MeOH	20% (v/v)
	SDS electrophoresis buffer (1x)	20% (v/v)
PBS-T	PBS	
	Tween 20	0.05%
AP Buffer	Trizma base	100 mM
pH 9.5	NaCl	100 mM
	$MgCl_2$	100 mM
TNE-T	TNE	
	Tween 20	0.1%

Histone Purification

$IB^{+/-}$	Trizma base	50 mM

pH 8.5	NaCl	100 mM
	EDTA	1 mM
	Triton X-100	1% / -
Buffer S	Trizma base	50 mM
pH 7.0	Urea	6 M
	NaCl	1 M
	β-Mercaptoethanol	10 mM
Buffer A	Trizma base	50 mM
pH 6.4	Urea	6 M
	NaCl	1 M
Buffer B	Buffer A	
pH 6.4	Imidazole	500 mM

Pol β Purification

Lysis Buffer	Tris-HCl	20 mM
pH 7.9	NaCl	500 mM
	Phenylmethylsulfonyl chloride	1 mM
	Imidazole	5 mM
Buffer A	Tris-HCl	20 mM
pH 7.9	NaCl	500 mM
Dialysis Buffer	PBS	
pH 7.2	DTT	1 mM
Buffer B	Buffer A	
pH 7.9	Imidazole	500 mM

p53 Purification

Lysis Buffer	Sodium phosphate	50 mM
pH 8	NaCl	300 mM
	DTT	10 mM

	NP-40	0.01% (v/v)
	Pefa	100 µM
	Aprotinin/Leupeptin	1 µg/µL
Buffer AI	Sodium phosphate	50 mM
pH 7.2	NaCl	150 mM
	DTT	2 mM
	NP-40	0.01% (v/v)
Buffer BI	Buffer A	
	Imidazole	1 M
Dialysis Buffer 1	Sodium phosphate	50 mM
pH 7.2	NaCl	100 mM
	DTT	2 mM
	NP-40	0.01% (v/v)
Buffer AS	Sodium phosphate	50 mM
pH 7.2	DTT	2 mM
	NP-40	0.01% (v/v)
Buffer BS	Buffer AS	
	NaCl	1 M
Dialysis Buffer 2	Sodium phosphate	50 mM
pH 7.2	NaCl	150 mM
	DTT	2 mM
	NP-40	0.01% (v/v)
	Glycerol	10% (v/v)
pH 4.5		
Buffer BS	Buffer AS	
	NaCl	1 M
Lysis Buffer 2	Tris-HCl	20 mM
pH 7.5	NaCl	300 mM
	Triton x-100	0.1% (v/v)

Buffer AI	Tris-HCl	20 mM
pH 7.5	NaCl	300 mM
Buffer BI	Buffer A	
pH 7.5	Imidazole	500 mM
NMM	$(NH_4)_2SO_4$	7.5 mM
	NaCl	8.5 mM
	KH_2PO_4	55 mM
	K_2HPO_4	100 mM
	$MgSO_4$	10 mM
	$CaCl_2$	1mg/L
	$FeCl_2$	1mg/L
	$CuCl_2$	1µg/L
	$MnCl_2$	1µg/L
	$ZnCl_2$	1 µg/L
	Na_2Mo0_4	1 µg/L
	Glucose	20 mM
	Amino acids mix (-Met)	50 mg/L
	L-Biotin	10 mg/L
	Thiamin	10 mg/L
	Carbenicillin	100 mg/L

Oxime Ligations

PBS 1 x	Disodiumhydrogen phosphate	10 mM
7.2	Pottassiumdihydrogen phosphate	1.8 mM
	NaCl	140 mM
	KCl	2.7 mM
Acetate 2 x	Sodium acetate/acetic acid	1 M
Citrate 2 x	Sodium citrate/citric acid	200 mM
Phosphate 2 x (200 mM)	Disodiumhydrogen phosphate/ sodiumdihydrogen phosphate	200 mM

Phosphate/Citrate 2 x	Disodiumhydrogen phosphate	400 mM
	Citric acid	200 mM

EMSA

10 x TBE buffer	TRIS	500 mM
	Boric acid	500 mM
	EDTA	10 mM
Running buffer	TBE buffer	0.5 x
	NP-40	0.01 %(v/v)
Binding buffer	Sodium phosphate buffer (pH 7.2)	25 mM
pH 7.2	NaCl	75 mM
	Glycerine	10%
	BSA	0.2 mg/mL
	DTT	2 mM
	p21 RE	10 nM

5.2 Standard Procedures in Molecular Biology

5.2.1 Preparation of electrocompetent *E. coli* BL21 (DE3) cells

LB medium (500 mL) was inoculated with an overnight culture (2 mL) of *E. coli* BL21 (DE3) cells and grown to an OD_{600} of 0.5−0.6. Cells were chilled on ice (15 min) and centrifuged (4000 g, 30 min, 4 °C). The following steps were performed on ice with sterile and ice-cold media. The supernatant was discarded, and the cell pellet was resuspended in water (500 mL). The cells were pelleted (4000 g, 30 min, 4 °C) and resuspended in water (500 mL). After an additional centrifugation step (4000 g, 30 min, 4 °C), the pellet was washed with 10% glycerol (25 mL) and centrifuged (4000 g, 10 min, 4 °C). The cells were resuspended in 10% glycerol (6 mL), aliquoted (100 µL) and shock-frosted with liquid nitrogen. Electrocompetent *E. coli* BL21 cells were stored at −80 °C.

5.2.2 Transformation of electrocompetent *E. coli* BL21 (DE3) cells

An aliquot of electrocompetent *E. coli* BL21 (DE3) cells was thawed on ice, mixed with DNA (100 ng), and transferred into a Gene Pulser electroporation microcuvette (0.1 cm electrode gap). After incubation on ice for 5 min, electroporation was performed with Gene Pulser Xcell (1.8 kV, 200 Ω, 5 ms). The cells were suspended in preheated SOC (1 mL) and incubated (37 °C, 45 min, 450 rpm). A 50 µL sample was plated on Agar plates that contained a suitable antibiotic. The plates were incubated at 37 °C overnight.

5.2.3 Preparation of chemically competent XL10-Gold *E. coli* cells

LB medium (500 mL) was inoculated with an overnight culture (5 mL) of *E. coli* XL10-Gold cells and grown to an OD_{600} of 0.6−0.8 at 37 °C. Cells were centrifuged (4400 rpm, 20 min, 4 °C) and the supernatant was removed. The following steps were performed on ice with sterile and ice-cold media. The pellet was resuspended in water and pelleted (4400 rpm, 20 min, 4 °C). The cell pellet was resuspended in TSS buffer, aliquoted (100 µL) and shock-frosted in liquid nitrogen. Chemically competent *E. coli* XL10-Gold cells were stored at −80 °C.

5.2.4 Transformation of chemically competent XL10-Gold *E. coli* cells

An aliquot of chemically competent XL10-Gold cells was thawed on ice and incubated with DNA (100 ng) for 7 min. Heat-shock was performed (45 s, 42 °C) and cells were chilled on

ice for additional 7 min. The sample was added to preheated SOC medium (1 mL), incubated (37 °C, 30 min, 450 rpm) and 50 µL were plated on Agar plates that contained a suitable antibiotic. The plates were incubated at 37 °C overnight.

5.2.5 Cryopreservation

To store bacteria hosting DNA of interest, an overnight culture of bacteria (0.5 mL) in LB medium that contained the suiting antibiotic was mixed with 50% glycerol (0.5 mL). That glycerol stock was shock-frosted with liquid nitrogen and stored at −80 °C.

5.2.6 Preparation of Plasmid DNA and Concentration Determination

An overnight culture (10 mL) of *E. coli* XL10-Gold cells containing the desired plasmid was centrifuged (4000 rpm, 10 min, 4 °C). The plasmid was isolated by following the instruction of the QIAprep® Spin Miniprep Kit. The DNA was eluted with 20 µL MQ H_2O and DNA concentration was determined by measuring the absorption at 260 nm with a NanoDrop spectrophotometer (OD_{260} = 1 ≙ 50 µg/mL double-stranded DNA). The plasmid was stored at −20 °C until futher use.

5.2.7 Site-Directed Mutagenesis

To generate PylRS mutants, site-directed mutagenesis was performed. Therefore, a PCR reaction with primers that contain the desired base change was performed. Complementary primers were used, if not stated otherwise.

	Stock Concentration	Volume [µL]
Template	100 ng/µL	1
HF/GC Buffer	5x	20
dNTPs	10 mM	2
Primer f	10 µM	4
Primer r	10 µM	4
Phusion		1
H_2O		68

Step	Temperature [°C]	Time	
1	98	60 s	
2	98	10 s	
3	55–75	30 s	
4	72	3 min	18 x back to 2
5	72	10 min	
6	4	Pause	

After the PCR, the reaction was incubated with DpnI (1 h, 37 °C, 0.5 µL) to digest parental, methylated DNA. For analysis of PCR success and purification, agarose gel electrophoresis was performed, and the plasmid was purified by gel extraction and transformed into *E. coli* XL10 cells. The plasmids from single colonies were isolated and sent for sequencing (GATC).
When back-to-back primers were used, one of them was 5′ phosphorylated and PCR product was ligated with T4 DNA polymerase prior to transformation into *E. coli* XL10 cells.

5.2.8 Agarose Gel Electrophoresis

DNA samples were mixed with DNA loading buffer and loaded on an agarose gel that contained 0.05% ethidium bromide. Electrophoresis was performed (1 h, 120 V). After electrophoresis, the DNA was visualized by UV exposure with the Gel Reader Chemidoc XRS from BioRad. For plasmid isolation, gel extraction was performed.

5.2.9 Gel Extraction

Gel Extraction of plasmids from agarose gels was performed following the instructions of the QIAquick® Gel Extraction Kit.

5.2.10 Cloning of gBlock AcKRS Liu into pRSF Duet-1

gBlock ordered from Integrated DNA Technologies was cloned into pJET 1.2 blunt with CloneJET PCR Cloning Kit from Thermo Scientific. The ligation product was transformed into chemically competent *E. coli* XL10-Gold cells and the plasmid was isolated. pJet containing the gBlock and pRSF-Duet-1 vector containing PylRS wt were digested with SacI-HF and Acl I for 17 h at 37 °C.

	Stock Concentration	**Volume [µL]**
Plasmid	100 ng/µL	15
Cut Smart	10x	2
Acl I		1.5
SacI-HF		0.375
H_2O		1.125

After digestion 1 µL CIP was added to the gBlock sample and incubated at 37 °C for 50 min. All plasmids were subjected to agarose gel electrophoresis followed by gel extraction. The DNA fragments were ligated and transformed into chemically competent *E. coli* XL10-Gold cells. The plasmid was isolated and sent for sequencing (GATC).

5.2.11 SDS-PAGE

Protein samples were mixed with SDS loading dye, heated (5 min, 95 °C), and loaded on an SDS gel. Electrophoresis was performed (30 min, 35 mA). The protein bands were stained by shaking the gel in staining solution (30 min, 50 rpm) and washing the stained gel with destaining solution.
When the fluorescence signal was detected, prior to Coomassie staining the gel was washed with water and the signal was detected with the Fluorescent Image Analyzer FLA-5000 (Fujifilm) for fluorescein (473 nm, LPB filter) and TAMRA (532 nm, LPG filter) visualization and the Gel Reader Imager 600 (Amersham) for coumarin (312 nm, EtBr filter) vasualization.

5.2.12 Western Blot

To identify proteins with specific antibodies western blot was performed. SDS gel electrophoresis was performed and the proteins were transferred to a PTVD membrane by electrophoresis in transfer buffer (90 min, 60 V).
For the detection of p53, the membrane was blocked with 5% milk powder, washed with TNE-T (3 x 10 mL) and incubated with DO-I antibody (0.5 mL in 10 mL TNE-T, 1 h, rt). After

washing with TNE-T, incubation with HRP α-mouse (1 h, rt) and an additional washing step, the signal was detected with Pierce ECL Western Blotting Substrate from Thermo Scientific and the Amersham Gel Imager 600.
For the detection of His-tagged proteins, HisDetector™ Nickel-AP kit from KPL was used.

5.3 Gene Expression, Protein Purification, and Modification

5.3.1 DNA Pol β

5.3.1.1 Expression of DNA Pol β

The expression and purification of DNA Pol β variants was adapted from Tatjana Schenider.[86] LB Carb (1 L) was inoculated with an *E. Coli* BL21 (DE3) overnight culture (10 mL) of DNA Pol β and grown (37 °C, 160 rpm) to OD_{600} = 0.6–0.9. Expression was induced by the addition of IPTG (1 mL, 1 M) and cells were grown for 16 h (37 °C, 160 rpm). The expression culture was pelleted (4400 rpm, 15 min, 4 °C) and the pellet was stored at −20 °C.

5.3.1.2 Expression of DNA Pol β 41TAG

LB Carb/Kan (1 L) was inoculated with an *E. Coli* BL21 (DE3) overnight culture (10 mL) of DNA Pol β 41TAG/$tRNA_{CUA}$ and PylRS mutant and grown (37 °C, 160 rpm) to OD_{600} = 0.2–0.3. Unnatural amino acid was added, and cells were grown to OD_{600} = 0.6–0.9. Expression was induced by the addition of IPTG (1 mL, 1 M) and cells were harvested after 16 h at 37 °C (4400 rpm, 15 min, 4 °C). The cell pellet was stored at −20 °C.

5.3.1.3 Purification of DNA Pol β Variants

The cell pellet obtained as described in 5.3.1.2 or 5.3.1.1 was thawed on ice and resuspended in lysis buffer (20 mL). Cell lysis was achieved by sonication (3 x 1 min, 8 cycles, 20% power) and the suspension was centrifuged (20000 rpm, 20 min, 4 °C). The supernatant was incubated with cOmplete™ His-Tag Purification Resin (2 h, 4 °C, 1 mL). The supernatant was collected, and the beads were washed with increasing concentrations of imidazole (10, 15, 50 mM, 10 mL each, for 1 L expression). The protein was eluted with buffer B (4 x 5 mL) and pure fractions were identified by SDS-PAGE. Alternatively, DNA Pol β was purified by HisTrap FPLC. Fractions containing pure protein were dialyzed against PBS pH 7.2, 1 mM DTT and concentrated wtih Amicon® Ultra Cetrifugal Filters (10 kDa

cutoff). The protein was diluted with glycerol to a final concentration of 50% and stored at −20 °C.
DNA Pol β 41U**3** was in gel digested and analyzed by LC-MS/MS by the Proteomics Center, Universität Konstanz.

5.3.1.4 DNA Pol β Concentration Determination

Concentration of expressed DNA Pol β was determined by Bradford assay with Roti® Quant Bradford Protein Assay. The protein (20 µL) was mixed with Bradford working solution (980 µL) and incubated (10 min, rt). OD_{595} was measured and a standard curve of commercially available BSA (25 µg/mL−1500 µg/mL) was measured for comparison with unknown DNA Pol β sample concentrations.

5.3.2 H1.2

5.3.2.1 Expression of H1.2 wt

Expression and purification of H1.2 variants was adapted from Daniel Rösner.[18] LB Carb (1 L) was inoculated with an *E. Coli* BL21 (DE3) overnight culture (10 mL) of H1.2 wt and grown (37 °C, 160 rpm) to OD_{600} = 0.6. Expression was induced by the addition of IPTG (1 mL, 1 M) and cells were harvested after 4 h (4400 rpm, 15 min, 4 °C). The cell pellet was stored at −20 °C.

5.3.2.2 Expression of H1.2 114U1 or H1.2 206U1

LB Carb/Kan was inoculated with an *E. Coli* BL21 (DE3) overnight culture (10 mL) of H1.2 114TAG/$tRNA_{CUA}$ or 206TAG/$tRNA_{CUA}$ and pRFS PylRS Y349F. Cells were grown (37 °C, 160 rpm) to OD_{600} = 0.2−0.3. and AOAA **1** (1 mM final concentration) was added. Expression was induced at OD_{600} = 0.6. by addition of IPTG (1 mL, 1 M). After 20 h, cells were harvested (4400 rpm, 15 min, 4 °C) and the cell pellet was stored at −20 °C.

5.3.2.3 Purification of H1.2 wt and H1.2 114U1 and H1.2 206U1

The cell pellet obtained as described in 5.3.2.1 or 5.3.2.2 was thawed on ice and the following purification steps were performed on ice. The pellet was resuspended in IB^+ (20 mL) buffer supplemented with phenylmethylsolfonyl chloride (2 mM) and the suspension

was sonicated (3 x 1 min, 8 cycles, 20% power). After centrifugation (17000 g, 20 min, 4 °C) the supernatant was discarded and the pellet was resuspended in IB^+ (20 mL) and centrifuged again (17000 g, 10 min, 4 °C). The pellet was washed twice with IB^- (20 mL) and centrifuged each time. Inclusion bodies were solubilized by resuspension and incubation with Buffer S (15 mL, 4 °C, overnight) on a roller. After centrifugation (21000 g, 20 min, 4 °C) the supernatant is incubated with 5 mM imidazole and cOmplete His-Tag Purification Resin slurry (2 h, 4 °C, 1 mL for wt, 0.5 mL for SCS) on an overhead shaker. The supernatant was removed, and the beads were washed with buffer A (10 mL). The protein was eluted with 32, 64, 125, 250, and finally 500 mM imidazole (buffer A/B). The fractions were analyzed by SDS-PAGE and desired protein fractions were pooled and dialyzed against water. The protein was concentrated with VivaSpin (10 kDa cutoff, 4000 rpm, 4 °C) and stored in aliquots at −20 °C.

5.3.2.4 H1.2 Concentration Determination

Concentration of expressed H1.2 was determined with Pierce™ BCA Protein Kit (Thermo Fisher) according to the manufacturer's protocol. H1.2 samples (10 µL) were incubated with BCA working reagent (30 min, 37 °C, 200 µL) and OD_{562} was detected. A standard curve of commercially available H1.2 (25 µg/mL−1500 µg/mL) was measured for comparison with unknown H1.2 sample concentrations.

5.3.3 p53

5.3.3.1 Expression of p53 120KeK

A single colony of *E. Coli* BL21 (DE3) hosting p53 120TAG/$tRNA_{CUA}$ and AcKRS was inoculated with LB Carb/Kan (100 mL) and cells were grown to OD_{600} = 1 (37 °C, 160 rpm). This pre-culture (50 mL) was added to fresh LB Carb/Kan (450 mL) and the cells were grown to OD_{600} = 0.2–0.3. Unnatural amino acid was added and expression was induced at OD_{600} = 0.6 by addition of IPTG (0.5 mL, 1 M). Cells were grown o.n. (25 °C, 160 rpm) and harvested by centrifugation (4400 rpm, 15 min, 4 °C). The pellet was stored at –20 °C.

5.3.3.2 p53 120KeK Purification

The cell pellet obtained as described in 5.3.3.1 was thawed on ice, resuspended in lysis buffer (10 mL), and sonicated (3 x 30 s, 8 cycles, 20% power). Purification was performed as

described.[226] The suspension was centrifuged (15000 rpm, 20 min, 4 °C) and the supernatant was purified by HisTrap FPLC (buffer AI and BI, 5–100% in 25 column volumes). Desired fractions were identified by SDS-PAGE and thrombin (1 u per mg protein) cleavage was performed during dialysis against dialysis buffer 1 (4 °C, o.n.). The mixture was purified by HiTrap Heparin FPLC (buffer AS/BS, 0–100% in 25 column volumes). Pure fractions were detected by SDS-PAGE, pooled, and dialyzed against dialysis buffer 2. The protein was shock-frosted in liquid nitrogen and stored at –80 °C.
p53 120KeK was in solution digested and analyzed by LC-MS/MS by the Proteomics Center, Universität Konstanz.

5.3.3.3 p53 Concentration Determination

p53 concentration was determined by comparing intensities of Comassie-stained p53 samples with BSA standards after SDS-PAGE and Coomassie staining.

5.3.4 Ubiquitin

5.3.4.1 Expression of Ub wt

A single colony of *E. Coli* BL21 (DE3) hosting Ub wt was inoculated with LB Carb (200 mL) and cells were grown to OD_{600} = 1 (37 °C, 160 rpm). This pre-culture (100 mL) was added to fresh LB Carb (900 mL) and the cells were grown to OD_{600} = 0.6–0.9 (37 °C, 160 rpm). Expression was induced by addition of IPTG (0.5 mL, 1 M) and cells were harvested by centrifugation (4400 rpm, 15 min, 4 °C) after 4 h. The pellet was stored at –20 °C.

5.3.4.2 Expression of Ub 48U3/U4

A single colony of *E. Coli* BL21 (DE3) hosting Ub 48TAG/PylRS mutant was inoculated with LB Carb/Kan (200 mL) and cells were grown to OD_{600} = 1 (37 °C, 160 rpm). This pre-culture (100 mL) was added to fresh LB Carb/Kan (900 mL) and unnatural amino acid (final concentration 1 mM) was added at OD_{600} = 0.2–0.3 (37 °C, 160 rpm). Expression was induced at OD_{600} = 0.6 and cells were grown for 16 h (37 °C, 160 rpm). The expression culture was centrifuged (4400 rpm, 15 min, 4 °C) and the pellet was stored at –20 °C.

5.3.4.3 Expression of Ub 75C

Expression was adapted from Zhao *et al.*[181] An overnight culture (10 mL) of *E. Coli* BL21 (DE3) cells of Ub 75C was added to fresh LB Carb (1 L). The cells were grown to OD_{600} = 0.6–0.9 (37 °C, 160 rpm) and expression was induced by addition of IPTG (1 mL, 1 M). Cells were harvested after 4 h by centrifugation (4400 rpm, 15 min, 4 °C). The cell pellet was stored at –20 °C.

5.3.4.4 Expression of Ub 76U1

An overnight culture (10 mL) of *E. Coli* BL21 (DE3) cells of Ub 76 TAG/$tRNA_{CUA}$ and PylRS Y349F was added to fresh LB Carb (1 L). The cells were grown to OD_{600} = 0.2–0.3 (37 °C, 160 rpm) and unnatural amino acid was added (final concentration 1 mM). Expression was induced by addition of IPTG (1 mL, 1 M) OD_{600} = 0.6–0.9. Cells were harvested after 16 h by centrifugation (4400 rpm, 15 min, 4 °C). The cell pellet was stored at –20 °C.

5.3.4.5 Purification of Ub wt and Ub 48U3

The pellet obtained as described in 5.3.4.1 and 5.3.4.2 was thawed on ice and resuspended in lysis buffer 2 (10 mL). Cell lysis was achieved by sonication (3 x 30 s, 8 cycles, 20% power) and the suspension was centrifuged (15 min, 20 000 rpm, 4 °C). Buffer BI was added to the supernatant to a final concentration of 5 mM imidazole and the mixture was incubated with cOmplete™ His-Tag Purification Resin (2 h, 4 °C, 1 mL). The supernatant was collected, and the beads were washed with increasing concentrations of imidazole (5, 20 mM, 10 mL, buffer AI/BI). The protein was eluted with increasing concentration of imidazole (100, 250 500 mM, 10 mL, buffer AI/BI) and pure fractions identified by SDS-PAGE were pooled.
For His tag cleavage, UbCHL3 (2.28 g/L, 1 mL per 50 mL Ub) was added during dialysis against 0.1 x PBS pH 7.2, followed by dialysis against buffer AS. The protein was applied to SP Sepharose® Fast Flow resin (400 µL). The resin was washed with buffer AS (5 mL) and the protein was eluted with a gradient from 50 mM to 1 M NaCl in 50 mM steps (buffer AS/BS, 1–2 mL each). Pure fractions were identified by SDS-PAGE and dialyzed against PBS pH 7.2.
When the His tag was not cleaved, pure Ub was dialyzed against PBS pH 7.2 or dialyzed against buffer AS and purified by SP Sepharose® Fast Flow as described above.
The pure protein was concentrated with Amicon® Ultra Cetrifugal Filters (3.5 kDa cutoff) and stored at –20 °C.

5.3.4.6 Purification of Ub 75C

Purification was adapted from Zhao *et al.*[181] The cell pellet obtained as described in 5.3.4.3 was resuspended in lysis buffer (10 mL) and sonicated (3 x 30 s, 8 cycles, 20% power). The mixture was centrifuged (20 000 rpm, 15 min, 4 °C) and the supernatant was heated (65 °C for 30 min). After centrifugation (20 000 rpm, 30 min, 4 °C), the supernatant was adjusted to pH 4.5 and was purified by HiTrap™ SPHP FPLC (buffer AS/BS). Pure fractions were identified by SDS-PAGE and dialyzed against PBS pH 7.2. The protein was concentrated by Amicon® Ultra Cetrifugal Filters (3.5 kDa cutoff) and stored at –20 °C.

5.3.4.7 Purification of Ub 76U1

Lysis, sonication, and subsequent centrifugation of the cell pellet obtained as described in chapter 5.3.4.4 was performed as described in 5.3.4.6. The supernatant was heated for 10 min at 60 °C and purified by SEC in PBS by a HiLoad 26/600 Superdex column. Pure fractions were identified by SDS-PAGE and pooled.

5.3.4.8 Ub Concentration Determination

Concentration of expressed Ub was determined with Pierce™ BCA Protein Kit (Thermo Fisher) according to the manufacturer's protocol. Ub samples (10 µL) were incubated with BCA working reagent (30 min, 37 °C, 200 µL) and OD_{562} was detected. A standard curve of commercially available Ub (25 µg/mL−1500 µg/mL) was measured for comparison with unknown Ub sample concentrations.

5.3.5 Test Incorporations in DNA Pol β 41TAG

To test the incorporation efficiency of an amino acid by a PylRS mutants, test incorporations into DNA Pol β 41TAG were performed. The level of DNA polymerase β in the lysate after expression is a measure of amino acid incorporation.
An overnight culture (60 µL) of *E. Coli* BL21 (DE3) hosting DNA Pol β 41TAG/$tRNA_{CUA}$ and PylRS mutant was added to LB Carb/Kan (6 mL). At OD_{600} = 0.2–0.3 unnatural amino acid was added and cells were grown to OD_{600} = 0.6–0.9 (37 °C, 160 rpm). A sample before induction (1 mL) was taken and expression was induced by addition of IPTG (5 µL, 1 M). After 16 h OD_{600} was measured and a sample (1 mL) was taken. The OD_{600} of the samples

was adjusted to 2.5 by centrifugation (4000 rpm, 10 min) and resuspension of the pellet in suiting amounts of water. As a positive control, Boc lysine is incorporated into DNA Pol β by wt PylRS. The samples were analyzed by SDS-PAGE and the level of DNA polymerase β is compared to the positive control after Coomassie staining.
Before unnatural amino acids were added to expression media, they were freshly dissolved in minimum amount of solvents.

Amino Acid	**Solvent**
AOAA **1**	H_2O
AOAA **2**	200 mM NaOH
AOAA **3**	DMSO/H_2O
AOAA **4**	DMSO
Keto-lysine **5**	H_2O
Boc lysine	H_2O
Propargyl-lysine	DMSO
Coumarin-lysine	DMSO

5.4 Protein Modification

5.4.1 Modification of Ub 75C with Chloroaceton or Chloroacetaldehyde

This procedure was modified from Zhao *et al.*[181] A solution of Ub 75C (100 µM) in PBS pH 7.2 was treated with TCEP (37 °C, 30 min, 10 eq.). The solution was diluted 5-fold with PBS pH 7.2 containing chloroaceton or chloroacetaldehyde (1000 eq.) and incubated (25 °C, 250 rpm, 90 min). A sample (20 µL) was incubated with 25 eq. fluorescein maleimide in the dark (10 min, rt) and analyzed by SDS-PAGE. As a control, TCEP-treated Ub75C of same concentration and volume was reacted with fluorescein maleimide. The gel was read out by FLA Imager at 473 nm and was stained by Coomassie. Upon completion of the reaction, the reaction mixture was dialyzed (3.5 kDa cutoff) against PBS pH 7.2/25% MeOH, PBS pH 7.2/2.5% MeOH and subsequently against 0.1 x PBS pH 7.2. The protein was concentrated with Amicon® Ultra Cetrifugal Filters (3.5 kDa cutoff) and stored at –20 °C.

5.4.2 Deprotection of Ub 76U1

The deprotection was performed in a flask or in siliconized multicentrifuge tubes. Ub 76U**1** was mixed with TFA to a final concentration of 60% and incubated (2 h, 37 °C, 250 rpm). The protein was precipitated in diethyl ether and centrifuged (4000 rpm, 45 min, 4 °C). The pellet was washed with diethyl ether, centrifuged (4000 rpm, 30 min, 4 °C), and dissolved in MQ

H_2O. The protein was lyophilized, dissolved in MQ H_2O and concentration was determined as described in chapter 5.3.4.8. A similar procedure was described by Virdee *et al.*[137]

5.4.3 Deprotection of H1.2 114U1/206U1

The deprotection was performed in siliconized multicentrifuge tubes. H1.2 114**U1**/206**U1** was mixed with TFA to a final concentration of 67% and incubated (2 h, 23 °C, 250 rpm). The protein was precipitated in diethyl ether and centrifuged (10000 rpm, 20 min, 4 °C). The pellet was washed with diethyl ether followed by centrifugation (10000 rpm, 20 min, 4 °C) and dissolved in MQ H_2O.

5.4.4 Deprotection of Proteins Containing Photolabile Amino Acids

In general, protein samples were placed on a flat underground on ice and irradiated at 365 nm (UV Lamp B-100AP from UVP, 100 W, 12 mW/cm^2) for different time periods.

5.4.5 Oxime Ligations

Test oxime ligations were performed in 10 µL scale. Concentration of the POI was always maintained, if not stated otherwise. All components were added in liquid form to the reaction mixture. The aminooxy compound was added last.

When arylamines were used, the compounds were usually dissolved in 2:1 (aniline) or 1:2 PBS pH 5.5/DMSO and incubated for 10 min at rt with the reaction mixture that lacks the aminooxy compound. Freeze-thaw was performed by freezing the sample at –20 °C for usually 2 or 3 cycles.

To analyze supernatant and pellet separately, the reaction mixture was centrifuged (10000 rpm, 10 min, 4 °C), the supernatant was removed, and the pellet was resuspended in PBS (same volume as reaction volume).

Oxime ligations with TAMRA–Ketone were subjected to SDS-PAGE and analyzed by FLA-500 reader. This was followed by Coomassie staining.

5.4.6 p53 Oxime Ligation

p53 120KeK, Ub 76-ONH_2 (amount depends on reactivity), and SDS (final concentration 0.5 mM) were incubated at 4–25 °C for 20–40 h. Alternatively, the mixture was frozen twice at

–20 °C. The reactions were analyzed by SDS-PAGE followed by western blot or Coomassie staining.

5.5 p53 Functional Assays

5.5.1 General Information

Expression and purification of p53 wt, ubiquitinating enzymes, and DUBs, as well as generation of enzymatically ubiquitinated p53 and the annealing and purification of double-stranded, fluorescein-labeled *p21*, were performed by Alexandra Julier (unpublished, procedures, to be published in dissertation by Alexandra Julier, AG Scheffner, Universität Konstanz).

5.5.2 Ubiquitination Assay

The respective p53 variant (20-50 ng) was mixed with 150 ng E1, 150 ng UbcH5b, 5 µg Ub and 200 ng HDM2 or 200 ng bacterially-expressed E6AP in the absence or presence of 200 ng GST-16 E6 in 25 mM Tris·HCl pH 7.5, 1 mM DTT, 2 mM ATP, and 4 mM $MgCl_2$ (reaction volume 30 µL). The mixture was incubated at 30 °C for up to 60 min and the reaction was stopped by addition of SDS loading buffer (final concentration 1 x) and subsequent boiling at 95 °C for 5 min. The mixtures were analyzed by SDS-PAGE (8–10% v/v SDS) and western blot.

5.5.3 Stability of the Oxime Bond

This experiment was performed by Alexandra Julier. p53 120–Ub (750 ng) or enzymatically generated p53–Ub were incubated with 1 mg/mL of the respsective DUB or 5 µL reticulo lysate in 20 µL for 30 min at 37 °C or 4 °C. The reactions were stopped by addition of SDS loading buffer buffer. Subsequently, 5 µL of the mixtures were ananlyzed by SDS-PAGE and western blot.

5.5.4 Electromobility Shift Assay

This experiment was performed by Alexandra Julier. p53 variants were incubated with 400 fmol double-stranded, fluorescein-labelled *p21* RE at 25 °C for 30 min. The mixture was analyzed by a 4% native gel (90 min, 200 V, 4 °C). The gel was equilibrated before in

running buffer by loading dye and electrophoresis (30 min at 200 V (4 °C). The fluorescence signal was detected with a FLA reader 5000.

5.6 Chemical Syntheses

5.6.1 AOAA 1

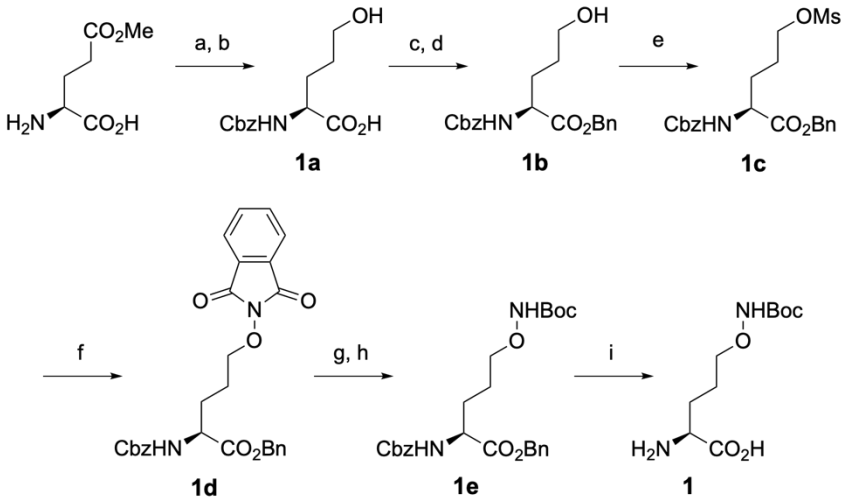

Supplementary Scheme 1: a) $NaBH_4$, THF b) Benzyl chloroformate, sat. $NaHCO_3$ c) aq. NaOH, EtOH d) Benzyl bromide, DMF e) MsCl, NEt_3, DCM f) *N*-hydroxyphthalimide, DBU, DMF g) Methylhydrazine DCM h) Boc_2O, NEt_3, THF i) H_2, Pd/C, THF/MeOH.

Compounds **1a**−**1e** were synthesized according to literature.[190],[191]

1

Compound **1e** (3.20 g, 6.78 mmol) was placed unter inert atmosphere and dissolved in MeOH/THF. 10 wt.% Pd/C (144 mg, 1.36 mmol) was added to the solution and H_2 was introduced into the flask. The heterogeneous mixture was stirred overnight. The solvent was removed, the solid was dissolved in water, and Pd/C was removed by filtration with a syringe filter. Compound **1** (1.66 g, 6.71 mmol) was obtained in 99% yield.

^{1}H NMR (400 MHz, Deuterium Oxide) δ = 3.95 (t, *J* = 6.1 Hz, 2H, δ-C**H**$_2$), 3.82 (t, *J* = 6.1 Hz, 1H, α-C**H**), 2.09–1.94 (m, 2H, β-C**H**$_2$), 1.87–1.70 (m, 2H, γ-C**H**$_2$), 1.53 (s, 9H, C(C**H**$_3$)$_3$) ppm.

^{13}C NMR (400 MHz, Deuterium Oxide) δ = 175.86 (**C**O$_2$H), 159.83 (NH**C**O), 84.89 (**C**(CH$_3$)$_3$), 77.29 (δ-**C**), 55.97 (α-**C**), 28.95 (C(**C**H$_3$)$_3$), 28.61 (β-**C**), 24.67 (γ-**C**) ppm.

HRMS [M+H$^+$] (m/z): observed: 249.1441, calculated: 249.1445, deviation: 1.6 ppm

5.6.2 AOAA 2

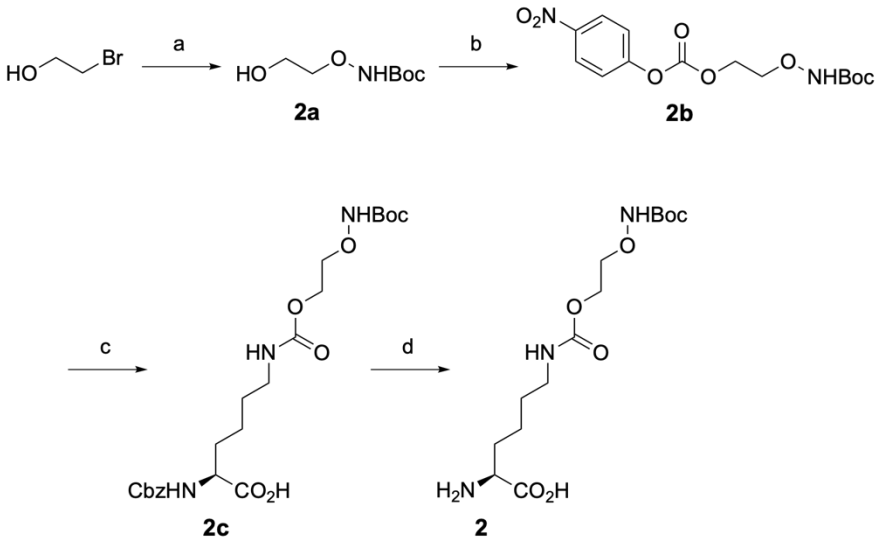

Supplementary Scheme 2: a) *N*-Boc hydroxylamine, DBU, DCM b) *p*-Nitrophenyl chloroformate, pyridine, DCM c) N_{α}-Cbz-L-Lys, $NaHCO_3$, DMF/H_2O/DME d) H_2, Pd/C, THF/MeOH.

Compound **2a** was synthesized according to literature.[193]

2b

Compound **2a** (3.70 g, 20.79 mmol) was dissolved in dry DCM (100 mL) and the solution was cooled to 0 °C. Dry pyridine (3.40 mL, 42.12 mmol) was added and the mixture was stirred for 30 min. *p*-Nitrophenyl chloroformate (4.72 g, 24.95 mmol) was added and the reaction mixture was stirred for 5 h. DCM (30 mL) was added and the organic phase was washed with H2O, brine, and 0.1M HCl (50 mL each). The organic phase was dried over Na_2SO_4, filtered, and the solvent was evaporated. The residue was purified by column chromatography (3:1 → 2:1 hexane/ethyl acetate). **2b** (6.58 g, 19.23 mmol) was obtained in 93% yield.

R_f: 0.25 in EtOAc/Hexane 1:3

^{1}H NMR (400 MHz, Chloroform-*d*) δ = 8.28 (d, *J* = 2.2 Hz, 1H, C**H**-$2_{a/b}$), 7.40 (d, *J* = 2.1 Hz, 1H, C**H**-$3_{a/b}$), 7.34 (s, 1H, ON**H**), 4.54–4.52 (m, 2H, C$\mathbf{H}_2$-6), 4.16–4.14 (m, 2H, C$\mathbf{H}_2$-7), 1.48 (s, 9H, (C$\mathbf{H}_3$)$_3$) ppm.

^{13}C NMR (400 MHz, Chloroform-*d*) δ = 157.00 (**C**-8), 155.60 (**C**-4), 152.94 (**C**-5), 145.62 (**C**-1), 125.45 (**C**-$2_{a/b}$), 121.97 (**C**-$3_{a/b}$), 82.39 (**C**$(CH_3)_3$), 73.78 (**C**-7), 66.30 (**C**-6), 28.31 ($C(\mathbf{C}H_3)_3$) ppm.

2c

Compound **2b** (6.1 g, 17.84 mmol) was dissolved in 2:1:1 DME/DMF/H_2O and Cbz-Lys-OH (5 g, 17.84 mmol) and $NaHCO_3$ (1.6 g, 19.05 mmol) were added. The suspension was stirred overnight. H_2O (500 mL) was added to the yellow solution and the aqueous phase was washed with diethyl ether. The aqueous phase was acidified with 10% citric acid to pH = 3.8 and extracted with EtOAc (4 x 500 mL). The organic phase was washed with brine (3 x 250 mL) and dried over Na_2SO_4, filtered, and the solvent was evaporated. The residue was purified by MPLC and **2c** (5.98 g, 12.37 mmol) was obtained in 70% yield.

^{1}H NMR (400 MHz, Aceton-d_6) δ = 8.90 (s, 1H, ON**H**), 7.39–7.28 (m, 5H, Aryl-**H**), 6.52 (d, *J* = 8.0 Hz, 1H, ε-N**H**), 6.27 (s, 1H, α-N**H**), 5.09 (s, 2H, Aryl-C$\mathbf{H}_2$), 4.25–4.18 (m, 1H, α-C**H**), 4.19 (t, *J* = 4.4 Hz, 2H, C$\mathbf{H}_2$-2), 3.93 (t, *J* = 4.4 Hz, 2H, C$\mathbf{H}_2$-3), 3.14 (dt appear. q, *J* = 6.2 Hz, 2H, ε-C$\mathbf{H}_2$), 1.93–1.85 (m, 1H, β-C**H**), 1.81–1.73 (m, 1H, β-C**H**), 1.60 - 1.47 (m, 4H, δ-C$\mathbf{H}_2$, γ-C$\mathbf{H}_2$), 1.44 (s, 9H, $C(C\mathbf{H}_3)_3$) ppm.

^{13}C NMR (400 MHz, Chloroform-*d*) δ = 175.43 (**C**O_2H), 157.31 (NH**C**O), 157.01 (NH**C**O), 156.32 (NH**C**O), 136.33 (Aryl-**C**), 128.65 (Aryl-**C**), 128.32 (Aryl-**C**), 128.25 (Aryl-**C**), 82.22 (**C**$(CH_3)_3$), 74.76 (**C**-23), 67.20 (Aryl-**C**H_2), 62.10 (**C**-2), 53.67 (α-**C**), 40.49 (ε-**C**), 31.79 (β-**C**), 29.26 (δ-**C**), 28.35 ($C(\mathbf{C}H_3)_3$), 22.04 (γ-**C**) ppm.

HRMS [$M+H^+$] (m/z): observed: 484.2279, calculated: 484.2290, deviation: 2.3 ppm

2

Compound **2c** (5.69 g, 11.78 mmol) was placed under inert atmosphere and dissolved in MeOH (120 mL). 10 wt.% Pd/C (122 mg, 1.18 mmol) was added to the solution and H_2 was introduced into the flask. The heterogeneous mixture was stirred overnight. Water (120 mL) was added and Pd/C was removed by filtration with a syringe filter. The solvent was evaporated and **2** (3.91 g, 11.19 mmol) was obtained in 95% yield.

^{1}H NMR (400 MHz, Methanol-d_4) δ = 4.20 (t, J = 4.5 Hz, 2H, C**H**$_2$-2), 3.94 (t, J = 4.5 Hz, 2H, C**H**$_2$-3), 3.59 (dd, $^{3}J_{HH}$ = 6.9, $^{3}J_{HH}$ = 5.4 Hz, 1H, α-C**H**), 3.12 (t, J = 6.7 Hz, 2H, ε-C**H**$_2$), 1.94–1.79 (m, 2H, β-C**H**$_2$), 1.56–1.51 (m, 2H, δ-C**H**$_2$), 1.47 (s, 9H, C(C**H**$_3$)$_3$), 1.45–1.39 (m, 2H, γ-C**H**$_2$) ppm.

^{13}C NMR (400 MHz, Deuterium Oxide) δ = 176.17 (**C**O$_2$H), 159.79 (**C**=O), 159.75 (**C**=O), 84.97 (**C**(CH$_3$)$_3$), 75.92 (**C**-2/3), 64.11 (**C**-2/3), 56.19 (α-**C**), 41.48 (ε-**C**), 31.55 (β-**C**), 29.99 (δ-**C**), 28.93 (C(**C**H$_3$)$_3$), 23.11 (γ-**C**) ppm.

HRMS [M+H$^+$] (m/z): observed: 350.1918, calculated: 350.1922, deviation: 1.0 ppm

5.6.3 AOAA 3

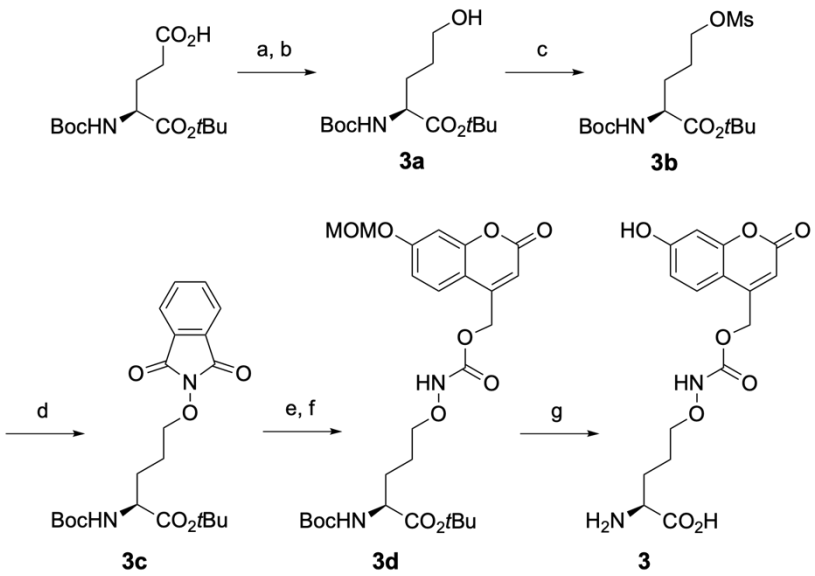

Supplementary Scheme 3: a) Ethyl chloroformate, NEt_3, THF, b) $NaBH_4$, THF c) MsCl, NEt_3, DCM d) *N*-hydroxyphthalimide, DBU, DMF e) Methylhydrazine, DCM f) **6**, NEt_3, THF g) TFA/DCM triethyl silane.

Compounds **3a**−**b** were synthesized according to literature.[194-195] Compound **3** was synthesized modified from literature.[186]

3c

N-Hydroxyphthalimide (443 mg, 2.62 mmol) was dissolved in DMF (3 mL) and cooled to 0 °C. DBU (406 uL, 2.62 mmol) was added and the solution was stirred for 30 min at 0 °C. Compound **4b** (500 mg, 1.31 mmol) was dissolved in DMF (2 mL) and added to the red reaction mixture. The mixture was stirred for 1 h at 0 °C and the at rt overnight. EtOAc (50 mL) was added and the organic phase was washed with water, brine and sat. $NaHCO_3$. The organic phase was dried over Na_2SO_4, filtered and the solvent was removed by evaporation. Compound **4c** (539 mmol, 1.24 mmol) was obtained in 95% yield.

R_f: 0.28 in EtOAc/Hexane 1:3

^{1}H NMR (400 MHz, Chloroform-d_3) δ = 7.84–7.71 (m, 4H, C**H**-3/$4_{a/b}$), 5.11 (d, *J* = 7.5 Hz, 1H, α-N**H**), 4.23–4.17 (m, 3H, α-C**H**, δ-C$\mathbf{H}_2$), 2.06–1.99 (m, 1H, β-C**H**), 1.88–1.78 (m, 3H, β-C**H**, γ-C$\mathbf{H}_2$), 1.46 (s, 9H, C(C$\mathbf{H}_3$)$_3$), 1.42 (s, 9H, C(C$\mathbf{H}_3$)$_3$) ppm.

^{13}C NMR (400 MHz, Chloroform-d_3) δ = 171.76 (**C**O_2*t*Bu), 163.69 (**C**-$1_{a/b}$), 155.55 (NH**C**O), 134.49 (**C**-$4_{a/b}$), 129.07 (**C**-$2_{a/b}$), 123.62 (**C**-$3_{a/b}$), 82.09 **C**$(CH_3)_3$, 79.72 **C**$(CH_3)_3$, 77.90 (δ-**C**), 77.36, 53.78 (α-**C**), 29.34 (β-**C**), 28.44 (C(**C**$H_3)_3$), 28.13 (C(**C**$H_3)_3$, 24.49 (γ-**C**) ppm.

HRMS [M+H^+] (m/z): observed: 435.2108, calculated: 435.2126, deviation: 4.1 ppm

3d

Compound **3c** (3 g, 6.91 mmol) was dissolved in DCM (30 mL) and cooled to 0 °C. Methylhydrazine (543 µL, 10.37 mmol) was added and the solution was stirred at 0 °C for 1.5 h. The precipitate was filtered, and the filtrate was concentrated by evaporation. The residue was dissolved in DMF (60 mL) and DIPEA (2.35 mL, 13.82 mmol) and **6** (4.15 g, 10.37 mmol) were added. The reaction mixture was stirred overnight in the dark. DCM (150 mL) was added and the organic phase was washed with water, sat. $NaHCO_3$ and brine. The organic phase was dried over Na_2SO_4, filtered and the solvent was evaporated. The residue was purified by column chromatography (3:2 → 2:3 hexane/ethyl acetate) and **3d** (2.52 g, 4.46 mmol) was obtained in 65% yield.

R_f: 0.4 in EtOAc/Hexane 1:1

^{1}H NMR (400 MHz, Acetone-d_6) δ = 9.70 (s, 1H, ON**H**), 7.68 (d, *J* = 8.8 Hz, 1H, C**H**-10), 7.04 (dd, $^3J_{HH}$ = 8.8 Hz, $^4J_{HH}$ = 2.1 Hz, 1H, C**H**-9), 7.00 (d, $^4J_{HH}$ = 2.1 Hz, 1H, C**H**-7), 6.28 (s, 1H, C**H**-4), 6.07 (d, *J* = 8.0 Hz, 1H, α-N**H**), 5.40 (s, 2H, CH_2-2), 5.33 (s, 2H, CH_2-11), 4.06–4.01 (m, 1H, α-C**H**), 3.92 (t, *J* = 5.8 Hz, 2H, δ-CH_2), 3.47 (s, 3H, CH_2-13), 1.95–1.86 (m, 1H, β-C**H**), 1.81–1.70 (m, 3H, β-C**H**, γ-CH_2), 1.44 (s, 9H, C(C$H_3)_3$), 1.40 (s, 9H, C(C$H_3)_3$) ppm.

^{13}C NMR (400 MHz, Acetone-d_6) = 172.67 (**C**O_2*t*Bu), 161.41 (**C**-8), 160.69 (**C**-5), 157.23 (**C**-3), 156.60 (NH**C**O), 156.26 (NH**C**O), 151.23 (**C**-6), 126.39 (**C**-10), 114.33 (**C**-9), 112.40 (**C**-11), 110.80 (**C**-4), 104.46 (**C**-7), 95.30 (**C**-12), 81.50 (**C**$(CH_3)_3$), 79.26 (**C**$(CH_3)_3$), 76.70 (δ-**C**), 62.66 (**C**-2), 56.58 (**C**-13), 55.25 (α-**C**), 29.35 (β-**C**), 28.70 (C(**C**$H_3)_3$), 28.30 (C(**C**$H_3)_3$), 25.33 (γ-**C**) ppm.

HRMS [M+H^+] (m/z): observed: 567.2527, calculated: 567.2548, deviation: 3.7 ppm

3

Compound **3d** (2.15 g, 6.91 mmol) was placed under N_2 and DCM/TFA 1:1 (20 mL) and triethylsilane (1.21 mL, 7.60 mmol) were added. The solution was stirred at rt for 3 h before the liquid was removed. The residue was dissolved in a small amount of MeOH and evaporated under reduced pressure. This process was repeated until the residue was dry. The solid was dissolved in a small amount of MeOH and precipitated in Et_2O. Filtration yielded compound **3** (1.46 g, 3.05 mmol) in 80% yield as TFA salt.

^{1}H NMR (400 MHz, Dimethyl sulfoxide-d_6) δ = 10.88 (s, 1H, ON**H**), 7.53 (d, J = 8.6 Hz, 1H, C**H**-10), 6.84 (dd, $^3J_{HH}$ = 8.7 Hz, $^4J_{HH}$ = 2.2 Hz, 1H, C**H**-9), 6.79 (d, $^4J_{HH}$ = 2.2 Hz, 1 C**H**-7) 6.10 (s, 1H, C**H**-4), 5.32 (s, 2H, C**H**$_2$-2), 3.77 (t, J = 5.6 Hz, 2H, δ-C**H**$_2$), 3.34 (t, J = 5.6 Hz, 1H, α-C**H**), 1.87–1.79 (m, 1H, β-C**H**), 1.75–1.62 (m, 3H β-C**H**, γ-C**H**$_2$) ppm.

^{13}C NMR (400 MHz, Dimethyl sulfoxide-d_6) δ =171.18 (**C**O_2H), 162.78 (**C**-8), 160.70 (**C**-5), 156.27 (**C**-3), 155.53 (**C**-1), 151.74 (**C**-6), 126.05 (**C**-10), 113.79 (**C**-9), 109.02 (**C**-11), 107.57 (**C**-4), 103.19 (**C**-7), 75.84 (δ-**C**), 61.89 (**C**-2), 54.26 (α-**C**), 28.08 (β-**C**), 24.23 (γ-**C**) ppm.

HRMS [M+H$^+$] (m/z): observed: 367.1136, calculated: 367.1136, deviation: 0 ppm

Compound **6** was synthesized as described in literature.[196],[186]

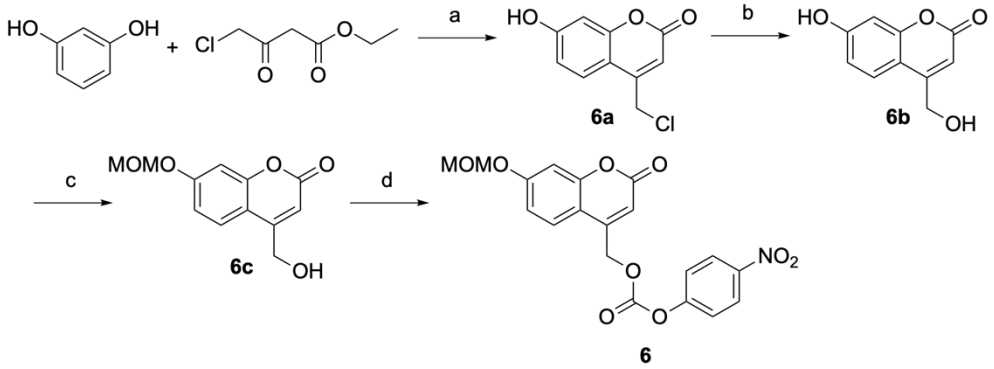

Supplementary Scheme 4: a) *p*-TsOH, toluene b) H_2O c) MOMCl, DIPEA, DCM d) *p*-nitrophenyl chloroformate, DIPEA, DCM.

5.6.4 AOAA 4

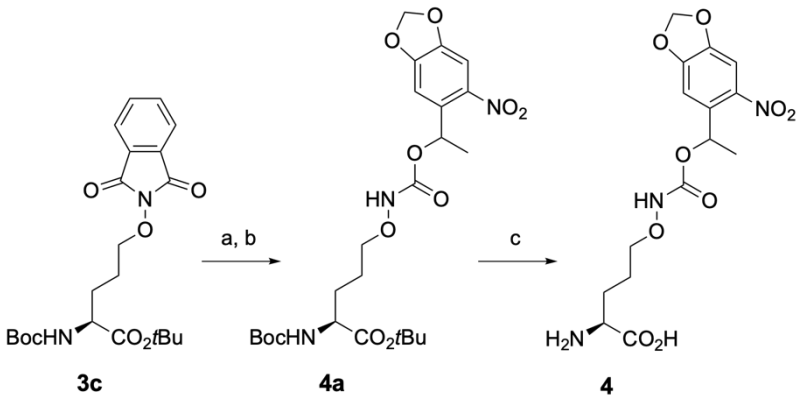

Supplementary Scheme 5: a) Methylhydrazine, DCM b) **7**, NEt_3, THF c) TFA/DCM triethyl silane.

Compounds **3a**−**b** were synthesized according to literature.[194-195] Compound **3c** was synthesized as described above. A synthesis of compound **4** was also described by Virdee *et al*.[137]

4a

Compound **3c** (0.30 g, 0.68 mmol) was dissolved in DCM (5 mL) and cooled to 0 °C. Methylhydrazine (55 µL, 1.05 mmol) was added and the solution was stirred at 0 °C for 1.5 h. The precipitate was filtered, and the filtrate was concentrated by evaporation. The residue was dissolved in THF (8 mL) and triethylamine (140 µL, 1.36 mmol) and **6** (383 mg, 1.05 mmol) were added. The reaction mixture was stirred overnight in the dark. EtOAc (50 mL) was added and the organic phase was washed with water, brine, and sat. $NaHCO_3$ (50 mL). The organic phase was dried over Na_2SO_4, filtered and the solvent was evaporated. The residue was purified by column chromatography (3:1 → 2:1 hexane/ethyl acetate) and **4a** (272 mg, 0.50 mmol) was obtained in 74% yield.

R_f: 0.33 in EtOAc/Hexane 1:2

^{1}H NMR (400 MHz, Chloroform-*d*) δ = 7.80 (s, 1H, ON**H**), 7.48 (s, 1H, C**H**-6), 7.00 (s, 1H, C**H**-10), 6.35 (q, *J* = 6.4 Hz, 1H, C**H**-2), 6.10 (s, 2H, C**H**$_2$-8), 5.11 (d, *J* = 6.5 Hz, 1H, α-N**H**), 4.17–4.21 (m, 1H, α-C**H**), 3.88 (t, *J* = 5.3 Hz, 2H, δ-C**H**$_2$), 1.89–1.82 (m, 1H, β-C**H**), 1.72–1.67 (m, 3H, β-C**H,** γ-C**H**$_2$), 1.62 (dd, $^3J_{HH}$ = 6.4 Hz, $^3J_{HH}$ = 1.3 Hz, 3H, C**H**$_3$-3), 1.46 (s, 9H, C(C**H**$_3$)$_3$), 1.42 (d, *J* = 1.8 Hz, 9H, C(C**H**$_3$)$_3$) ppm.

^{13}C NMR (400 MHz, Chloroform-*d*) δ = 171.28 (**C**O_2*t*Bu), 156.44 (**C**-1), 155.70 (NH**C**O), 152.54 (**C**-9), 147.34 (**C**-7), 141.56 (**C**-5), 135.60 (**C**-4), (126.21), 105.82 (**C**-10), 105.42 (**C**-6), 103.17 (**C**-8), 82.16 (**C**$(CH_3)_3$), 79.69 (**C**$(CH_3)_3$), 76.70 (δ-**C**) 70.10 (**C**-2), 53.76 (α-**C**), 29.98 (β-**C**), 28.45 (C(**C**$H_3)_3$), 28.12 (C(**C**$H_3)_3$), 23.82 (γ-**C**), 22.31, 22.29 (**C**-3) ppm.

HRMS [M+H^+] (m/z): observed: 542.2343, calculated: 542.2344, deviation: 0.2 ppm

4

Compound **4a** (100 mg, 0.18 mmol) was placed under N_2 and DCM/TFA 1:1 (5 mL) and triethylsilane (0.032 mL, 0.20 mmol) were added. The solution was stirred at rt for 3 h before the liquid was removed until 0.5 mL were left. The residue was precipitated in Et_2O. Filtration yielded compound **4** (25 mg, 0.05 mmol) in 28% yield as TFA salt.

^{1}H NMR (400 MHz, Acetonitrile-d_3 / Deuterium Oxide 1:1) δ = 7.43 (s, 1H, C**H**-6), 7.05 (s, 1H, C**H**-10), 6.14 (q, *J* = 6.4 Hz, 1H, C**H**-2), 6.09 (s, 2H, C$\mathbf{H}_2$-8), 3.75 (t, *J* = 6.1 Hz, 2H, δ-C$\mathbf{H}_2$), 3.61–3.58 (m, 1H, α-C**H**), 1.91–1.74 (m, 2H, β-C$\mathbf{H}_2$), 1.67–1.58 (m, 2H, γ-C$\mathbf{H}_2$), 1.51 (d, *J* = 6.4 Hz, 3H, C**H**-3) ppm.

^{13}C NMR (400 MHz, Acetonitrile-d_3 / Deuterium Oxide 1:1) δ = 173.25 (**C**O_2H), 156.79 (**C**-1), 152.58 (**C**-9), 147.23 (**C**-7), 140.99 (**C**-5), 134.71 (**C**-4), 105.55 (**C**-10), 104.55 (**C**-6), 103.57 (**C**-8), 75.69 (δ-**C**), 69.34 (**C**-2), 54.21 (α-**C**), 26.92 (β-**C**), 23.17 (γ-**C**), 20.92 (**C**-3) ppm.

HRMS [M+H^+] (m/z): observed: 368.1180, calculated: 368.1194, deviation: 3.8 ppm

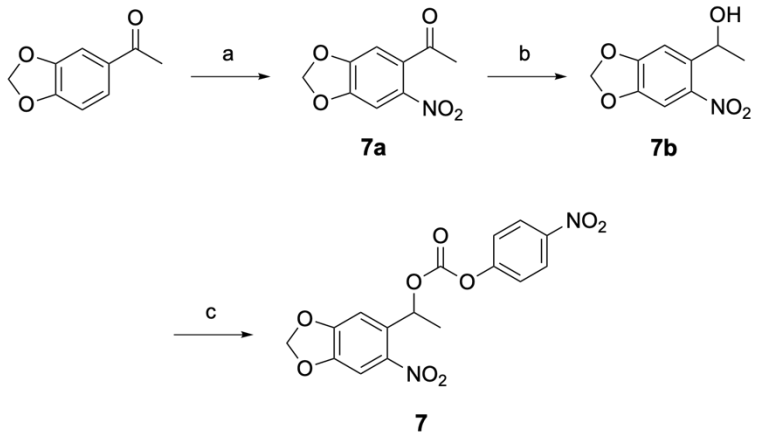

Supplementary Scheme 6: a) TFA, $NaNO_2$ b) $NaBH_4$, THF/EtOH c) *p*-nitrophenyl chloroformate, DCM, pyridine.

Compounds **7a** and **7b** were synthesized as described in literature.[230]

7

Compound **7b** (6.80 g, 32.23 mmol) was dissolved in dry DCM (150 mL) and dry pyridine (5.10 mL, 64.46 mmol) was added. The solution was cooled to 0 °C and *p*-nitrophenyl chloroformate (7.75 g, 64.46 mmol) was added. The reaction mixture was stirred at 0 °C for 1 h and at rt overnight. DCM (200 mL) was added and the organic phase was washed with water, brine, and 0.1M HCl (50 mL). The organic phase was dried over Na_2SO4, filtered and the solvent was reduced by evaporation until the compound is dissolved in minimum amount of DCM. The residue was precipitated in hexane/diethyl ether 1:1. Compound **7** (11.33 g, 20.13 mmol) was obtained in 93% yield.

R_f: 0.38 in EtOAc/Hexane 1:3

^{1}H NMR (400 MHz, Chloroform-*d*) δ = 8.30–8.20 (m, 2H, C**H**-$2_{a/b}$), 7.52 (s, 1H, C**H**-10), 7.39–7.31 (m, 2H, C**H**-$3_{a/b}$), 7.13 (s, 1H, C**H**-14), 6.42 (q, *J* = 6.4 Hz, 1H, C**H**-6), 6.15 (s, 2H, C$\mathbf{H}_2$-12), 1.75 (d, *J* = 6.4 Hz, 3H, C**H**-7) ppm.

^{13}C NMR (400 MHz, Chloroform-*d*) δ = 155.45 (**C**-4), 152.76 (**C**-13), 151.57 (**C**-5), 147.84 (**C**-11), 145.59 (**C**-1), 141.92 (**C**-9), 133.83 (**C**-8), 125.43 (**C**-$2_{a/b}$), 121.79 (**C**-$3_{a/b}$), 106.78 (**C**-14), 106.58 (**C**-10), 103.41 (**C**-12), 73.90 (**C**-6), 22.12 (**C**-7) ppm.

5.6.5 Keto-Lysine

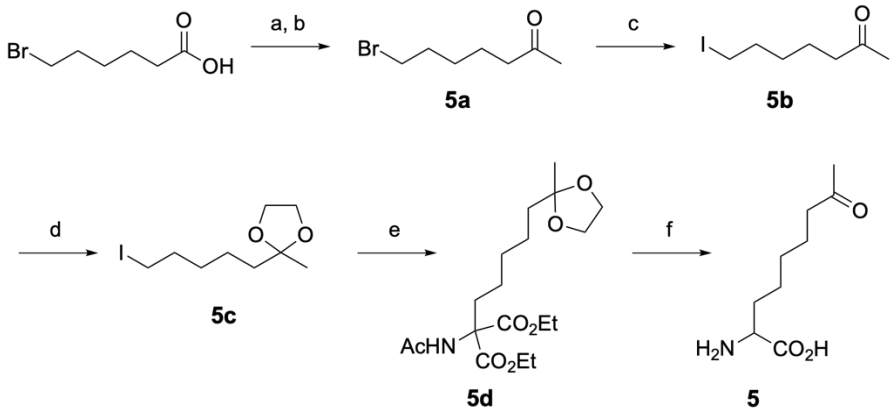

Supplementary Scheme 7: a) EDC, *N*,*O*-dimethylhydroxylamine, DMAP, DCM b) MeMgBr, THF c) NaI, acetone d) Ethylene glycol, *p*-TsOH, toluene e) diethyl acetamidomalonate, NaH, DMF f) HCl.

Keto-lysine was synthesized as described in literature[189] with minor changes in the final step. Here, the product was purified by MPLC. Note: The synthesis of **5a** proceeds in higher yields when step a) is performed for at least 40 h.

^{1}H NMR (400 MHz, Deuterium Oxide) δ = 4.06 (t, *J* = 6.2 Hz, 2H, α-C**H**), 2.62 (t, *J* = 7.3 Hz, 2H, ζ-C**H**$_2$), 2.25 (s, 3H, θ-C**H**$_3$), 2.02–1.93 (m, 2H, β-C**H**$_2$), 1.61 (p, 2H, *J* = 7.4 Hz, ε-C**H**$_2$), 1.58–1.37 (m, 4H, γ-C**H**$_2$, δ-C**H**$_2$) ppm.

^{13}C NMR (400 MHz, Deuterium Oxide) δ = 217.44 (η-**C**O), 172.80 (**C**O$_2$H), 53.27 (α-**C**), 43.06 (ζ-**C**), 29.67 (β-**C**), 29.32 (θ-**C**), 27.70 (δ-**C**), 23.90 (γ-**C**), 22.87 (ε-**C**) ppm.

5.6.6 Coumarin-Lysine

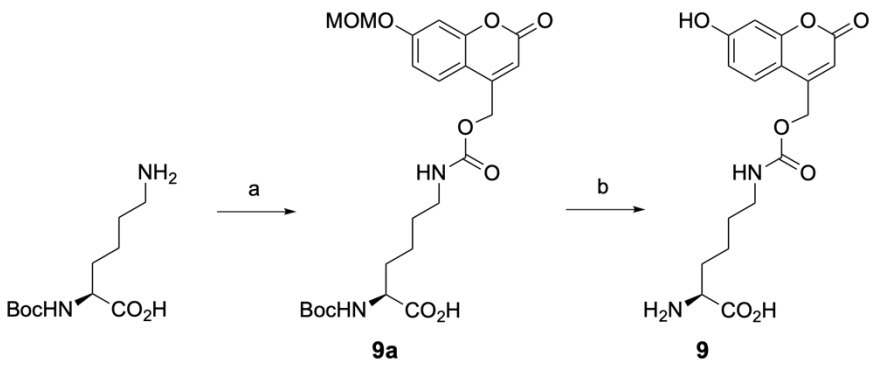

Supplementary Scheme 8: a) **6**, DMF b) TFA/DCM triethyl silane.

Coumarin-lysine **9** was synthesized as described in literature.[186]

^{1}H NMR (400 MHz, Dimethyl sulfoxide-d_6) δ = 7.55–7.49 (m, 2H, C**H**-10, ε-N**H**), 6.85–6.80 (m, 2H, C**H**-9, C**H**-7), 6.11 (s, 1H, C**H**-4), 5.22 (s, 2H, C**H**$_2$-2), 3.28 (t, *J* = 5.8 Hz, 1H, α-C**H**), 3.05–2.99 (m, 2H, ε-C**H**$_2$), 1.78–1.73 (m, 1H, β-C**H**), 1.69–1.64 (m, 1H β-C**H**), 1.41–1.34 (m, 4H, δ-C**H**$_2$, γ-C**H**$_2$) ppm.

^{13}C NMR (400 MHz, Dimethyl sulfoxide-d_6) δ =170.81 (**C**O$_2$H), 162.18 (**C**-8), 160.33 (**C**-5), 155.34 (**C**-3), 155.05 (**C**-1), 152.03 (**C**-6), 125.54 (**C**-10), 113.40 (**C**-9), 108.72 (**C**-11), 106.96 (**C**-4), 102.58 (**C**-7), 61.89 (**C**-2), 53.88 (α-**C**), 40.27 (ε-**C**), 30.61 (β-**C**), 29.06 (δ-**C**), 22.28 (γ-**C**) ppm.

HRMS [M+H$^+$] (m/z): observed: 365.1340, calculated: 365.1343, deviation: 0.8 ppm

5.6.7 TAMRA-Ketone

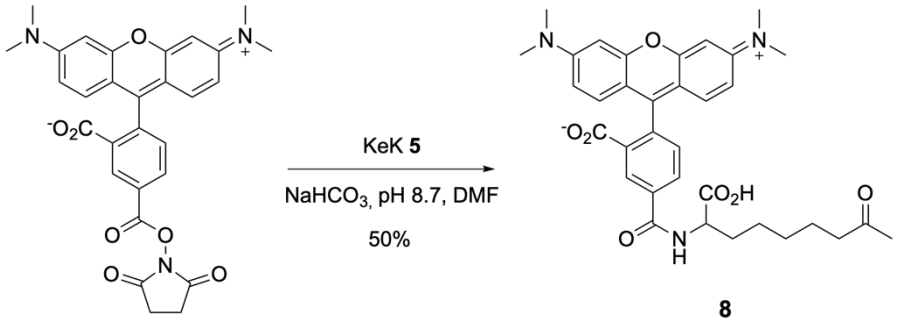

Supporting Scheme 9: a) KeK **5**, $NaHCO_3$, DMF, pH 8.7.

Reaction conditions for the synthesis of TAMRA-Ketone were adapted from Buntz *et al*.[200] Keto-lysine **5** (9 mg, 0.04 mmol) was dissolved in 100 mM $NaHCO_3$ pH = 8.7 (3 mL) and TAMRA-NHS (25 mg, 0.06 mmol) in DMF (1 mL) was added. The pH was adjusted to 8.7. The solution was stirred overnight and purified by RP-MPLC. TAMRA-Ketone **8** (12 mg, 0.02 mmol) was obtained in 50% yield.
TAMRA-NHS was kindly provided by Maike Lehner and synthesized as described.[198-199]

^{1}H NMR (400 MHz, Deuterium Oxide) δ = 8.35 (s, 1H, C**H**-3), 8.17 (d, = 7.9 Hz, 1H, C**H**-7), 7.64 (d, *J* = 7.9 Hz, 1H, C**H**-6), 7.25 (d, *J* = 9.5 Hz, 2H, C**H**-$10_{a/b}$), 6.87 (dd, *J* = 9.4 Hz, 1H, C**H**-$11_{a/b}$), 6.36 (s, 2H, C**H**-$13_{a/b}$), 4.53 (dd, $^3J_{HH}$ = 8.8 Hz, $^3J_{HH}$ = 4.8 Hz, 1H, α-C**H**), 3.04 (s, 12H, N(C**H**$_3$)$_2$) 2.63 (t, *J* = 7.3 Hz, 2H, ζ-C**H**$_2$), 2.26 (s, 3H, θ-C**H**$_3$), 2.09–1.99 (m, 1H, β-C**H**), 1.97–1.88 (m, 1H, β-C**H**), 1.65 (p, *J* = 7.1, 2H, ε-C**H**$_2$), 1.54 (p, *J* = 7.3, 2H, γ-C**H$_2$**), 1.47–1.41 (m, 2H, δ-C**H$_2$**) ppm.

^{13}C NMR (600 MHz, Deuterium Oxide) δ = 217.37 (η-**C**O), 179.05 (α-**C**O_2H), 173.25 (4-**C**O_2H), 170.81 (**C**-$14_{a/b}$), 168.84 (**C**-1), 157.76 (**C**-8), 156.66 (**C**-12), 140.34 (**C**-2/4), 135.23 (**C**-2/4), 134.02 (**C**-5), 130.77 (**C**-$10_{a/b}$), 130.15 (**C**-6), 128.17 (**C**-7), 127.34 (**C**-3), 113.73 (**C**-$9_{a/b}$), 112.67 (**C**-$11_{a/b}$), 96.00 (**C**-$13_{a/b}$), (81.65), 55.86 (α-**C**), 43.11 (ζ-**C**), 39.88 (N(**C**H$_3$)$_2$), 31.35 (β-**C**), 29.17 (θ-**C**), 27.82 (δ-**C**), 25.16 (γ-**C**), 23.16 (ε-**C**) ppm.

HRMS [M+H$^+$] (m/z): observed: 600.2693, calculated: 600.2704, deviation: 1.8 ppm

6. List of References

[1] M. Li, C. L. Brooks, F. Wu-Baer, D. Chen, R. Baer, W. Gu, *Science* **2003**, *302*, 1972–1975.
[2] M. A. E. Lohrum, D. B. Woods, R. L. Ludwig, É. Bálint, K. H. Vousden, *Mol. Cell Biol.* **2001**, *21*, 8521–8532.
[3] R. K. McGinty, J. Kim, C. Chatterjee, R. G. Roeder, T. W. Muir, *Nature* **2008**, *453*, 812–816.
[4] S. Eger, B. Castrec, U. Hübscher, M. Scheffner, M. Rubini, A. Marx, *ChemBioChem* **2011**, *12*, 2807–2812.
[5] S. Eger, M. Scheffner, A. Marx, M. Rubini, *J. Am. Chem. Soc.* **2010**, *132*, 16337–16339.
[6] N. D. Weikart, H. D. Mootz, *ChemBioChem* **2010**, *11*, 774–777.
[7] S. Li, H. Cai, J. He, H. Chen, S. Lam, T. Cai, Z. Zhu, S. J. Bark, C. Cai, *Bioconjugate Chem.* **2016**, *27*, 2315–2322.
[8] *Eur. J. Biochem.* **1984**, *138*, 9–37.
[9] M. H. Glickman, A. Ciechanover, *Physiol. Rev.* **2002**, *82*, 373–428.
[10] D. Komander, M. J. Clague, S. Urbé, *Nat. Rev. Mol. Cell Biol.* **2009**, *10*, 550–563.
[11] M. Hochstrasser, *Curr. Opin. Chem. Biol.* **1995**, *7*, 215–223.
[12] S. M. B. Nijman, M. P. A. Luna-Vargas, A. Velds, T. R. Brummelkamp, A. M. G. Dirac, T. K. Sixma, R. Bernards, *Cell* **2005**, *123*, 773–786.
[13] A. Ciechanover, H. Heller, R. Katz-Etzion, A. Hershko, *Proc. Natl. Acad. Sci. USA* **1981**, *78*, 761–765.
[14] A. Ciechanover, S. Elias, H. Heller, A. Hershko, *J. Biol. Chem.* **1982**, *257*, 2537–2542.
[15] A. Hershko, H. Heller, S. Elias, A. Ciechanover, *J. Biol. Chem.* **1983**, *258*, 8206–8214.
[16] M. Scheffner, U. Nuber, J. M. Huibregtse, *Nature* **1995**, *373*, 81–83.
[17] K. K. Dove, R. E. Klevit, *J. Mol. Biol.* **2017**, *429*, 3363–3375.
[18] D. Rösner, Chemical ubiquitylation of linker histone H1.2 by combining unnatural amino acids with click chemistry, Universität Konstanz **2016**.
[19] M. Koegl, T. Hoppe, S. Schlenker, H. D. Ulrich, T. U. Mayer, S. Jentsch, *Cell* **1999**, *96*, 635–644.
[20] W. Li, Y. Ye, *Cell. Mol. Life Sci.* **2008**, *65*, 2397–2406.
[21] J. S. Thrower, L. Hoffman, M. Rechsteiner, C. M. Pickart, *EMBO J.* **2000**, *19*, 94–102.
[22] The Nobel Prize in Chemistry 2004. NobelPrize.org. Nobel Media AB 2019. Mon. 17 Jun 2019. https://www.nobelprize.org/prizes/chemistry/2004/summary/.
[23] J. Terrell, S. Shih, R. Dunn, L. Hicke, *Mol. Cell* **1998**, *1*, 193–202.
[24] A.-D. Pham, F. Sauer, *Science* **2000**, *289*, 2357–2360.
[25] Timothy M. Thomson, M. Guerra-Rebollo, *Biochem. Soc. Trans.* **2010**, *38*, 116–131.
[26] T. T. Huang, A. D. D'Andrea, *Nat. Rev. Mol. Cell Biol.* **2006**, *7*, 323–334.
[27] G. L. Dianov, C. Meisenberg, J. L. Parsons, *Biochemistry (Moscow)* **2011**, *76*, 69–79.
[28] J. L. Parsons, P. S. Tait, D. Finch, I. I. Dianova, M. J. Edelmann, S. V. Khoronenkova, B. M. Kessler, R. A. Sharma, W. G. McKenna, G. L. Dianov, *EMBO J.* **2009**, *28*, 3207–3215.
[29] L. Hicke, R. Dunn, *Annu. Rev. Cell Dev. Biol.* **2003**, *19*, 141–172.
[30] G. L. Dianov, U. Hübscher, *Nucleic Acids Res.* **2013**, *41*, 3483–3490.
[31] S. S. David, V. L. O'Shea, S. Kundu, *Nature* **2007**, *447*, 941–950.
[32] S. L. Allinson, I. I. Dianova, G. L. Dianov, *EMBO J.* **2001**, *20*, 6919–6926.
[33] W. A. Beard, R. Prasad, S. H. Wilson, in *Methods Enzymol., Vol. 408*, Academic Press, **2006**, pp. 91–107.
[34] D. O. Zharkov, *Cell. Mol. Life Sci.* **2008**, *65*, 1544–1565.
[35] A. Kumar, S. G. Widen, K. R. Williams, P. Kedar, R. L. Karpel, S. H. Wilson, *J. Biol. Chem.* **1990**, *265*, 2124–2131.
[36] D. Liu, E. F. DeRose, R. Prasad, S. H. Wilson, G. P. Mullen, *Biochemistry* **1994**, *33*, 9537–9545.
[37] H. Pelletier, M. R. Sawaya, A. Kumar, S. H. Wilson, J. Kraut, *Science* **1994**, *264*, 1891–1903.
[38] Y. Canitrot, M. Fréchet, L. Servant, C. Cazaux, J.-S. Hoffmann, *FASEB J.* **1999**, *13*, 1107–1111.
[39] D. C. Cabelof, Z. Guo, J. J. Raffoul, R. W. Sobol, S. H. Wilson, A. Richardson, A. R. Heydari, *Cancer Res.* **2003**, *63*, 5799–5807.
[40] R. T. Simpson, *Biochemistry* **1978**, *17*, 5524–5531.
[41] F. Thoma, T. Koller, A. Klug, *J. Cell Biol.* **1979**, *83*, 403–427.
[42] K. Luger, A. W. Mäder, R. K. Richmond, D. F. Sargent, T. J. Richmond, *Nature* **1997**, *389*, 251–260.

[43] A. Roque, I. Ponte, P. Suau, *Biochim. Biophys. Acta, Gene Regul. Mech.* **2016**, *1859*, 444–454.
[44] K. Kim, J. Choi, K. Heo, H. Kim, D. Levens, K. Kohno, E. M. Johnson, H. W. Brock, W. An, *J. Biol. Chem.* **2008**, *283*, 9113–9126.
[45] N. Yan, Y. Shi, *Nat. Struct. Mol. Biol.* **2003**, *10*, 983–985.
[46] A. Konishi, S. Shimizu, J. Hirota, T. Takao, Y. Fan, Y. Matsuoka, L. Zhang, Y. Yoneda, Y. Fujii, A. I. Skoultchi, Y. Tsujimoto, *Cell* **2003**, *114*, 673–688.
[47] S. B. Rothbart, B. D. Strahl, *Biochim. Biophys. Acta Gene Regul. Mech.* **2014**, *1839*, 627–643.
[48] B. D. Strahl, C. D. Allis, *Nature* **2000**, *403*, 41–45.
[49] C. Liu, D. Wang, J. Wu, J. Keller, T. Ma, X. Yu, *J. Cell Sci.* **2013**, *126*, 2042–2051.
[50] T. Thorslund, A. Ripplinger, S. Hoffmann, T. Wild, M. Uckelmann, B. Villumsen, T. Narita, T. K. Sixma, C. Choudhary, S. Bekker-Jensen, N. Mailand, *Nature* **2015**, *527*, 389–393.
[51] N. J. Denis, J. Vasilescu, J.-P. Lambert, J. C. Smith, D. Figeys, *Proteomics* **2007**, *7*, 868–874.
[52] J. M. R. Danielsen, K. B. Sylvestersen, S. Bekker-Jensen, D. Szklarczyk, J. W. Poulsen, H. Horn, L. J. Jensen, N. Mailand, M. L. Nielsen, *Mol. Cell. Proteomics* **2011**, *10*, M110.003590.
[53] W. Kim, Eric J. Bennett, Edward L. Huttlin, A. Guo, J. Li, A. Possemato, Mathew E. Sowa, R. Rad, J. Rush, Michael J. Comb, J. W. Harper, Steven P. Gygi, *Mol. Cell* **2011**, *44*, 325–340.
[54] S. A. Wagner, P. Beli, B. T. Weinert, M. L. Nielsen, J. Cox, M. Mann, C. Choudhary, *Mol. Cell. Proteomics* **2011**, *10*, M111.013284.
[55] D. P. Lane, *Nature* **1992**, *358*, 15–16.
[56] K. H. Vousden, C. Prives, *Cell* **2009**, *137*, 413–431.
[57] A. C. Joerger, A. R. Fersht, *Cold Spring Harbor Perspect. Biol.* **2010**, *2*, a000919.
[58] J.-P. Kruse, W. Gu, *Cell* **2009**, *137*, 609–622.
[59] R. L. Weinberg, D. B. Veprintsev, A. R. Fersht, *J. Mol. Biol.* **2004**, *341*, 1145–1159.
[60] N. L. Lill, S. R. Grossman, D. Ginsberg, J. DeCaprio, D. M. Livingston, *Nature* **1997**, *387*, 823–827.
[61] C. J. Thut, J. L. Chen, R. Klemm, R. Tjian, *Science* **1995**, *267*, 100–104.
[62] J. C. Marine, S. Francoz, M. Maetens, G. Wahl, F. Toledo, G. Lozano, *Cell Death Differ.* **2006**, *13*, 927–934.
[63] F. Toledo, G. M. Wahl, *Nat. Rev. Cancer* **2006**, *6*, 909–923.
[64] M. Wade, Y.-C. Li, G. M. Wahl, *Nat. Rev. Cancer* **2013**, *13*, 83–96.
[65] T. Crook, K. H. Vousden, J. A. Tidy, *Cell* **1991**, *67*, 547–556.
[66] J. M. Huibregtse, M. Scheffner, P. M. Howley, *EMBO J.* **1991**, *10*, 4129–4135.
[67] J. M. Huibregtse, M. Scheffner, S. Beaudenon, P. M. Howley, *Proc. Natl. Acad. Sci. USA* **1995**, *92*, 2563–2567.
[68] S. Boeing, L. Williamson, V. Encheva, I. Gori, R. E. Saunders, R. Instrell, O. Aygün, M. Rodriguez-Martinez, J. C. Weems, G. P. Kelly, J. W. Conaway, R. C. Conaway, A. Stewart, M. Howell, A. P. Snijders, J. Q. Svejstrup, *Cell Rep.* **2016**, *15*, 1597–1610.
[69] L. Nie, M. Sasaki, C. G. Maki, *J. Biol. Chem.* **2007**, *282*, 14616–14625.
[70] N. D. Marchenko, S. Wolff, S. Erster, K. Becker, U. M. Moll, *EMBO J.* **2007**, *26*, 923–934.
[71] V. Landré, B. Revi, M. G. Mir, C. Verma, T. R. Hupp, N. Gilbert, K. L. Ball, *Cell Death Differ.* **2017**, *24*, 903–916.
[72] H. C. Kolb, M. G. Finn, K. B. Sharpless, *Angew. Chem. Int. Ed.* **2001**, *40*, 2004–2021.
[73] T. Wieland, E. Bokelmann, L. Bauer, H. U. Lang, H. Lau, *Justus Liebigs Ann. Chem.* **1953**, *583*, 129–149.
[74] P. E. Dawson, T. W. Muir, I. Clark-Lewis, S. B. Kent, *Science* **1994**, *266*, 776–779.
[75] C. P. R. Hackenberger, D. Schwarzer, *Angew. Chem. Int. Ed.* **2008**, *47*, 10030–10074.
[76] R. Yang, K. K. Pasunooti, F. Li, X.-W. Liu, C.-F. Liu, *Chem. Commun.* **2010**, *46*, 7199–7201.
[77] K. S. Ajish Kumar, M. Haj-Yahya, D. Olschewski, H. A. Lashuel, A. Brik, *Angew. Chem.* **2009**, *121*, 8234–8238.
[78] M. Haj-Yahya, K. S. Ajish Kumar, L. A. Erlich, A. Brik, *Biopolymers* **2010**, *94*, 504–510.
[79] E. Saxon, J. I. Armstrong, C. R. Bertozzi, *Org. Lett.* **2000**, *2*, 2141–2143.
[80] B. L. Nilsson, L. L. Kiessling, R. T. Raines, *Org. Lett.* **2000**, *2*, 1939–1941.
[81] L. Liang, D. Astruc, *Coord. Chem. Rev.* **2011**, *255*, 2933–2945.
[82] V. V. Rostovtsev, L. G. Green, V. V. Fokin, K. B. Sharpless, *Angew. Chem. Int. Ed.* **2002**, *41*, 2596–2599.
[83] C. W. Tornøe, C. Christensen, M. Meldal, *J. Org. Chem.* **2002**, *67*, 3057–3064.
[84] W. S. Horne, M. K. Yadav, C. D. Stout, M. R. Ghadiri, *J. Am. Chem. Soc.* **2004**, *126*, 15366–15367.
[85] A. Brik, J. Alexandratos, Y.-C. Lin, J. H. Elder, A. J. Olson, A. Wlodawer, D. S. Goodsell, C.-H. Wong, *ChemBioChem* **2005**, *6*, 1167–1169.

[86] T. Schneider, A chemical biological toolbox to study protein ubiquitylation, Universität Konstanz **2015**.
[87] J. M. Baskin, C. R. Bertozzi, *QSAR Comb. Sci.* **2007**, *26*, 1211–1219.
[88] N. J. Agard, J. A. Prescher, C. R. Bertozzi, *J. Am. Chem. Soc.* **2004**, *126*, 15046–15047.
[89] C. S. McKay, M. G. Finn, *Chem. Biol.* **2014**, *21*, 1075–1101.
[90] B. L. Oliveira, Z. Guo, G. J. L. Bernardes, *Chem. Soc. Rev.* **2017**, *46*, 4895–4950.
[91] K. Lang, J. W. Chin, *Chem. Rev.* **2014**, *114*, 4764–4806.
[92] V. Meyer, A. Janny, *Ber. Dtsch. Chem. Ges.* **1882**, *15*, 1525–1529.
[93] A. Janny, *Ber. Dtsch. Chem. Ges.* **1883**, *16*, 170–177.
[94] V. Meyer, A. Janny, *Ber. Dtsch. Chem. Ges.* **1882**, *15*, 1324–1326.
[95] V. Meyer, A. Janny, *Ber. Dtsch. Chem. Ges.* **1882**, *15*, 1164–1167.
[96] D. K. Kölmel, E. T. Kool, *Chem. Rev.* **2017**, *117*, 10358–10376.
[97] S. Ulrich, D. Boturyn, A. Marra, O. Renaudet, P. Dumy, *Chem. Eur. J.* **2014**, *20*, 34–41.
[98] W. P. Jencks, *Prog. Phys. Org. Chem.* **1964**, *2*, 63–128.
[99] E. H. Cordes, W. P. Jencks, *J. Am. Chem. Soc.* **1962**, *84*, 4319–4328.
[100] E. H. Cordes, W. P. Jencks, *J. Am. Chem. Soc.* **1962**, *84*, 826–831.
[101] A. Dirksen, T. M. Hackeng, P. E. Dawson, *Angew. Chem. Int. Ed.* **2006**, *45*, 7581–7584.
[102] P. Crisalli, E. T. Kool, *Org. Lett.* **2013**, *15*, 1646–1649.
[103] P. Crisalli, E. T. Kool, *J. Org. Chem.* **2013**, *78*, 1184–1189.
[104] M. Wendeler, L. Grinberg, X. Wang, P. E. Dawson, M. Baca, *Bioconjugate Chem.* **2014**, *25*, 93–101.
[105] M. B. Thygesen, H. Munch, J. Sauer, E. Cló, M. R. Jørgensen, O. Hindsgaul, K. J. Jensen, *J. Org. Chem.* **2010**, *75*, 1752–1755.
[106] M. Rashidian, M. M. Mahmoodi, R. Shah, J. K. Dozier, C. R. Wagner, M. D. Distefano, *Bioconjugate Chem.* **2013**, *24*, 333–342.
[107] D. Larsen, M. Pittelkow, S. Karmakar, E. T. Kool, *Org. Lett.* **2015**, *17*, 274–277.
[108] S. M. Agten, D. P. L. Suylen, T. M. Hackeng, *Bioconjugate Chem.* **2016**, *27*, 42–46.
[109] S. Wang, G. N. Nawale, S. Kadekar, O. P. Oommen, N. K. Jena, S. Chakraborty, J. Hilborn, O. P. Varghese, *Sci. Rep.* **2018**, *8*, 2193.
[110] V. A. Polyakov, M. I. Nelen, N. Nazarpack-Kandlousy, A. D. Ryabov, A. V. Eliseev, *J. Phys. Org. Chem.* **1999**, *12*, 357–363.
[111] J. Kalia, R. T. Raines, *Angew. Chem. Int. Ed.* **2008**, *47*, 7523–7526.
[112] R. Vanderesse, L. Thevenet, M. Marraud, N. Boggetto, M. Reboud, C. Corbier, *J. Pept. Sci.* **2003**, *9*, 282–299.
[113] W. P. Jencks, *J. Am. Chem. Soc.* **1959**, *81*, 475–481.
[114] R. B. Merrifield, *J. Am. Chem. Soc.* **1963**, *85*, 2149–2154.
[115] T. W. Muir, D. Sondhi, P. A. Cole, *Proc. Natl. Acad. Sci. USA* **1998**, *95*, 6705–6710.
[116] T. C. Evans, J. Benner, M.-Q. Xu, *J. Biol. Chem.* **1999**, *274*, 3923–3926.
[117] J. N. deGruyter, L. R. Malins, P. S. Baran, *Biochemistry* **2017**, *56*, 3863–3873.
[118] K. A. Andersen, L. J. Martin, J. M. Prince, R. T. Raines, *Protein Sci.* **2015**, *24*, 182–189.
[119] L. Yin, B. Krantz, N. S. Russell, S. Deshpande, K. D. Wilkinson, *Biochemistry* **2000**, *39*, 10001–10010.
[120] J. E. Jung, H.-P. Wollscheid, A. Marquardt, M. Manea, M. Scheffner, M. Przybylski, *Bioconjugate Chem.* **2009**, *20*, 1152–1162.
[121] X. Zhao, J. Lutz, E. Höllmüller, M. Scheffner, A. Marx, F. Stengel, *Angew. Chem. Int. Ed.* **2017**, *56*, 15764–15768.
[122] P. Lengyel, *J. Gen. Physiol.* **1966**, *49*, 305–330.
[123] B. Wiltschi, N. Budisa, *Appl. Microbiol. Biotechnol.* **2007**, *74*, 739–759.
[124] K. L. Kiick, E. Saxon, D. A. Tirrell, C. R. Bertozzi, *Proc. Natl. Acad. Sci. USA* **2002**, *99*, 19–24.
[125] A. Ambrogelly, S. Palioura, D. Söll, *Nat. Chem. Biol.* **2007**, *3*, 29–35.
[126] T. Mukai, A. Hayashi, F. Iraha, A. Sato, K. Ohtake, S. Yokoyama, K. Sakamoto, *Nucleic Acids Res.* **2010**, *38*, 8188–8195.
[127] D. B. Johnson, J. Xu, Z. Shen, J. K. Takimoto, M. D. Schultz, R. J. Schmitz, Z. Xiang, J. R. Ecker, S. P. Briggs, L. Wang, *Nat. Chem. Biol.* **2011**, *7*, 779–786.
[128] H. Neumann, K. Wang, L. Davis, M. Garcia-Alai, J. W. Chin, *Nature* **2010**, *464*, 441–444.
[129] J. W. Chin, *Annu. Rev. Biochem.* **2014**, *83*, 379–408.
[130] D. Rösner, T. Schneider, D. Schneider, M. Scheffner, A. Marx, *Nat. Protoc.* **2015**, *10*, 1594–1611.
[131] S. Herring, A. Ambrogelly, S. Gundllapalli, P. O'Donoghue, C. R. Polycarpo, D. Söll, *FEBS Lett.* **2007**, *581*, 3197–3203.
[132] J. M. Kavran, S. Gundllapalli, P. Donoghue, M. Englert, D. Söll, T. A. Steitz, *Proc. Natl. Acad. Sci. USA* **2007**, *104*, 11268–11273.

[133] W. Wan, J. M. Tharp, W. R. Liu, *Biochim. Biophys. Acta* **2014**, *1844*, 1059–1070.
[134] C. C. Liu, P. G. Schultz, *Annu. Rev. Biochem.* **2010**, *79*, 413–444.
[135] T. Yanagisawa, R. Ishii, R. Fukunaga, T. Kobayashi, K. Sakamoto, S. Yokoyama, *Chem. Biol.* **2008**, *15*, 1187–1197.
[136] C. Moreno-Vivián, E. Pérez-Reinado, F. Castillo, M. D. Roldán, *FEMS Microbiol. Rev.* **2008**, *32*, 474–500.
[137] M. Stanley, S. Virdee, *ChemBioChem* **2016**, *17*, 1472–1480.
[138] E. Scolnick, R. Tompkins, T. Caskey, M. Nirenberg, *Proc. Natl. Acad. Sci. USA* **1968**, *61*, 768–774.
[139] M. Pott, M. J. Schmidt, D. Summerer, *ACS Chem. Biol.* **2014**, *9*, 2815–2822.
[140] D. I. Bryson, C. Fan, L.-T. Guo, C. Miller, D. Söll, D. R. Liu, *Nat. Chem. Biol.* **2017**, *13*, 1253–1260.
[141] V. Sharma, Y. Zeng, W. W. Wang, Y. Qiao, Y. Kurra, W. R. Liu, *ChemBioChem* **2018**, *19*, 26–30.
[142] S. Faggiano, C. Alfano, A. Pastore, *Anal. Biochem.* **2016**, *492*, 82–90.
[143] V. H. Trang, E. M. Valkevich, S. Minami, Y.-C. Chen, Y. Ge, E. R. Strieter, *Angew. Chem. Int. Ed.* **2012**, *51*, 13085–13088.
[144] E. M. Valkevich, R. G. Guenette, N. A. Sanchez, Y. Chen, Y. Ge, E. R. Strieter, *J. Am. Chem. Soc.* **2012**, *134*, 6916–6919.
[145] V. H. Trang, M. L. Rodgers, K. J. Boyle, A. A. Hoskins, E. R. Strieter, *ChemBioChem* **2014**, *15*, 1563–1568.
[146] R. Layfield, K. Franklin, M. Landon, G. Walker, P. Wang, R. Ramage, A. Brown, S. Love, K. Urquhart, T. Muir, R. Baker, R. J. Mayer, *Anal. Biochem.* **1999**, *274*, 40–49.
[147] C. Marinzi, J. Offer, R. Longhi, P. E. Dawson, *Bioorg. Med. Chem.* **2004**, *12*, 2749–2757.
[148] C. Chatterjee, R. K. McGinty, J.-P. Pellois, T. W. Muir, *Angew. Chem.* **2007**, *119*, 2872–2876.
[149] L. Z. Yan, P. E. Dawson, *J. Am. Chem. Soc.* **2001**, *123*, 526–533.
[150] K. S. A. Kumar, L. Spasser, L. A. Erlich, S. N. Bavikar, A. Brik, *Angew. Chem. Int. Ed.* **2010**, *49*, 9126–9131.
[151] S. N. Bavikar, L. Spasser, M. Haj-Yahya, S. V. Karthikeyan, T. Moyal, K. S. Ajish Kumar, A. Brik, *Angew. Chem. Int. Ed.* **2012**, *51*, 758–763.
[152] K. S. A. Kumar, S. N. Bavikar, L. Spasser, T. Moyal, S. Ohayon, A. Brik, *Angew. Chem. Int. Ed.* **2011**, *50*, 6137–6141.
[153] X. Li, T. Fekner, J. J. Ottesen, M. K. Chan, *Angew. Chem. Int. Ed.* **2009**, *48*, 9184–9187.
[154] L. A. Erlich, K. S. A. Kumar, M. Haj-Yahya, P. E. Dawson, A. Brik, *Org. Biomol. Chem.* **2010**, *8*, 2392–2396.
[155] A. C. Conibear, E. E. Watson, R. J. Payne, C. F. W. Becker, *Chem. Soc. Rev.* **2018**, *47*, 9046–9068.
[156] S. Virdee, P. B. Kapadnis, T. Elliott, K. Lang, J. Madrzak, D. P. Nguyen, L. Riechmann, J. W. Chin, *J. Am. Chem. Soc.* **2011**, *133*, 10708–10711.
[157] M. Haj-Yahya, B. Fauvet, Y. Herman-Bachinsky, M. Hejjaoui, S. N. Bavikar, S. V. Karthikeyan, A. Ciechanover, H. A. Lashuel, A. Brik, *Proc. Natl. Acad. Sci. USA* **2013**, *110*, 17726–17731.
[158] M. Pan, S. Gao, Y. Zheng, X. Tan, H. Lan, X. Tan, D. Sun, L. Lu, T. Wang, Q. Zheng, Y. Huang, J. Wang, L. Liu, *J. Am. Chem. Soc.* **2016**, *138*, 7429–7435.
[159] J. Li, Q. He, Y. Liu, S. Liu, S. Tang, C. Li, D. Sun, X. Li, M. Zhou, P. Zhu, G. Bi, Z. Zhou, J.-S. Zheng, C. Tian, *ChemBioChem* **2017**, *18*, 176–180.
[160] C. E. Weller, A. Dhall, F. Ding, E. Linares, S. D. Whedon, N. A. Senger, E. L. Tyson, J. D. Bagert, X. Li, O. Augusto, C. Chatterjee, *Nat. Commun.* **2016**, *7*, 12979.
[161] B. Fierz, S. Kilic, A. R. Hieb, K. Luger, T. W. Muir, *J. Am. Chem. Soc.* **2012**, *134*, 19548–19551.
[162] H. P. Hemantha, S. N. Bavikar, Y. Herman-Bachinsky, N. Haj-Yahya, S. Bondalapati, A. Ciechanover, A. Brik, *J. Am. Chem. Soc.* **2014**, *136*, 2665–2673.
[163] X. Bi, K. K. Pasunooti, A. H. Tareq, J. Takyi-Williams, C.-F. Liu, *Org. Biomol. Chem.* **2016**, *14*, 5282–5285.
[164] S. Virdee, Y. Ye, D. P. Nguyen, D. Komander, J. W. Chin, *Nat. Chem. Biol.* **2010**, *6*, 750–757.
[165] C. Castañeda, J. Liu, A. Chaturvedi, U. Nowicka, T. A. Cropp, D. Fushman, *J. Am. Chem. Soc.* **2011**, *133*, 17855–17868.
[166] R. Yang, X. Bi, F. Li, Y. Cao, C.-F. Liu, *Chem. Commun.* **2014**, *50*, 7971–7974.
[167] M. Fottner, A.-D. Brunner, V. Bittl, D. Horn-Ghetko, A. Jussupow, V. R. I. Kaila, A. Bremm, K. Lang, *Nat. Chem. Biol.* **2019**, *15*, 276–284.
[168] X. Zhao, An Approach for the Generation of Ubiquitin Chains of Various Topologies Based on Bioorthogonal Chemistry, Universität Konstanz **2017**.
[169] N. S. Russell, K. D. Wilkinson, *Biochemistry* **2004**, *43*, 4844–4854.

[170] R. E. Morgan, V. Chudasama, P. Moody, M. E. B. Smith, S. Caddick, *Org. Biomol. Chem.* **2015**, *13*, 4165–4168.
[171] L. Long, M. Furgason, T. Yao, *Methods* **2014**, *70*, 134–138.
[172] C. Chatterjee, R. K. McGinty, B. Fierz, T. W. Muir, *Nat. Chem. Biol.* **2010**, *6*, 267–269.
[173] B. Fierz, C. Chatterjee, R. K. McGinty, M. Bar-Dagan, D. P. Raleigh, T. W. Muir, *Nat. Chem. Biol.* **2011**, *7*, 113–119.
[174] J. Chen, Y. Ai, J. Wang, L. Haracska, Z. Zhuang, *Nat. Chem. Biol.* **2010**, *6*, 270–272.
[175] F. Meier, T. Abeywardana, A. Dhall, N. P. Marotta, J. Varkey, R. Langen, C. Chatterjee, M. R. Pratt, *J. AM. Chem. Soc.* **2012**, *134*, 5468–5471.
[176] T. Abeywardana, Yu H. Lin, R. Rott, S. Engelender, Matthew R. Pratt, *Chem. Biol.* **2013**, *20*, 1207–1213.
[177] S. Sommer, N. D. Weikart, A. Brockmeyer, P. Janning, H. D. Mootz, *Angew. Chem.* **2011**, *123*, 10062–10066.
[178] N. D. Weikart, S. Sommer, H. D. Mootz, *Chem. Commun.* **2012**, *48*, 296–298.
[179] T. Schneider, D. Schneider, D. Rösner, S. Malhotra, F. Mortensen, T. U. Mayer, M. Scheffner, A. Marx, *Angew. Chem. Int. Ed.* **2014**, *53*, 12925–12929.
[180] D. Schneider, T. Schneider, D. Rösner, M. Scheffner, A. Marx, *Bioorg. Med. Chem.* **2013**, *21*, 3430–3435.
[181] X. Zhao, M. Mißun, T. Schneider, F. Müller, J. Lutz, M. Scheffner, A. Marx, M. Kovermann, *ChemBioChem* **2019**, *20*, 1772–1777.
[182] D. Flierman, Gerbrand J. van der Heden van Noort, R. Ekkebus, Paul P. Geurink, Tycho E. T. Mevissen, Manuela K. Hospenthal, D. Komander, H. Ovaa, *Cell Chem. Biol.* **2016**, *23*, 472–482.
[183] X. Zhang, A. H. Smits, G. B. A. van Tilburg, P. W. T. C. Jansen, M. M. Makowski, H. Ovaa, M. Vermeulen, *Mol. Cell* **2017**, *65*, 941–955.
[184] A. Shanmugham, A. Fish, M. P. A. Luna-Vargas, A. C. Faesen, F. E. Oualid, T. K. Sixma, H. Ovaa, *J. Am. Chem. Soc.* **2010**, *132*, 8834–8835.
[185] S. K. Singh, I. Sahu, S. M. Mali, H. P. Hemantha, O. Kleifeld, M. H. Glickman, A. Brik, *J. Am. Chem. Soc.* **2016**, *138*, 16004–16015.
[186] J. Luo, R. Uprety, Y. Naro, C. Chou, D. P. Nguyen, J. W. Chin, A. Deiters, *J. Am. Chem. Soc.* **2014**, *136*, 15551–15558.
[187] A. Gautier, D. P. Nguyen, H. Lusic, W. An, A. Deiters, J. W. Chin, *J. Am. Chem. Soc.* **2010**, *132*, 4086–4088.
[188] H. Neumann, S. Y. Peak-Chew, J. W. Chin, *Nat. Chem. Biol.* **2008**, *4*, 232–234.
[189] Y. Huang, W. Wan, W. K. Russell, P.-J. Pai, Z. Wang, D. H. Russell, W. Liu, *Bioorg. Med. Chem. Lett.* **2010**, *20*, 878–880.
[190] G. A. Rosenthal, D. L. Dahlman, P. A. Crooks, S. N. Phuket, L. S. Trifonov, *J. Agric. Food Chem.* **1995**, *43*, 2728–2734.
[191] F. Liu, J. Thomas, T. R. Burke, Jr., *Synthesis* **2008**, *15*, 2432–2438.
[192] S. Jiang, P. Li, C. C. Lai, J. A. Kelley, P. P. Roller, *J. Org. Chem.* **2006**, *71*, 7307–7314.
[193] G. N. Grover, J. Lee, N. M. Matsumoto, H. D. Maynard, *Macromolecules* **2012**, *45*, 4958–4965.
[194] Y. Itoh, K. Aihara, P. Mellini, T. Tojo, Y. Ota, H. Tsumoto, V. R. Solomon, P. Zhan, M. Suzuki, D. Ogasawara, A. Shigenaga, T. Inokuma, H. Nakagawa, N. Miyata, T. Mizukami, A. Otaka, T. Suzuki, *J. Med. Chem.* **2016**, *59*, 1531–1544.
[195] S. Han, R. A. Moore, R. E. Viola, *Bioorg. Chem.* **2002**, *30*, 81–94.
[196] E. A. Chamsaz, S. Mankoci, H. A. Barton, A. Joy, *ACS Appl. Mater. Interfaces* **2017**, *9*, 6704–6711.
[197] T. Terai, E. Maki, S. Sugiyama, Y. Takahashi, H. Matsumura, Y. Mori, T. Nagano, *Chem. Biol.* **2011**, *18*, 1261–1272.
[198] M. Yokoyama, S. Yoshida, T. Imamoto, *Synthesis* **1982**, 591–592.
[199] S. M. Menchen, S. Fung, d, 5- And 6-succinimidylcarboxylate isomers of rhodamine dyes, 0272007, **1988**.
[200] A. Buntz, S. Wallrodt, E. Gwosch, M. Schmalz, S. Beneke, E. Ferrando-May, A. Marx, A. Zumbusch, *Angew. Chem. Int. Ed.* **2016**, *55*, 11256–11260.
[201] M. Schmidt, Expanding the Genetic Code to Study the Structure and Interactions of Proteins, Universität Konstant **2015**.
[202] D. P. Nguyen, H. Lusic, H. Neumann, P. B. Kapadnis, A. Deiters, J. W. Chin, *J. Am. Chem. Soc.* **2009**, *131*, 8720–8721.
[203] P. R. Chen, D. Groff, J. Guo, W. Ou, S. Cellitti, B. H. Geierstanger, P. G. Schultz, *Angew. Chem.* **2009**, *121*, 4112–4115.

[204] M. Cigler, T. G. Müller, D. Horn-Ghetko, M.-K. von Wrisberg, M. Fottner, R. S. Goody, A. Itzen, M. P. Müller, K. Lang, *Angew. Chem. Int. Ed.* **2017**, *56*, 15737–15741.
[205] T. Umehara, J. Kim, S. Lee, L.-T. Guo, D. Söll, H.-S. Park, *FEBS Lett.* **2012**, *586*, 729–733.
[206] W. Schumann, L. C. S. Ferreira, *Genet. Mol. Biol.* **2004**, *27*, 442–453.
[207] K. H. Götz, M. Mex, K. Stuber, F. Offensperger, M. Scheffner, A. Marx, *Cell Chem. Biol.* **2019**, *26*, 1535–1543.
[208] C. C. Levy, *Nature* **1964**, *204*, 1059–1061.
[209] M. Kobayashi, M. Shinohara, C. Sakoh, M. Kataoka, S. Shimizu, *Proc. Natl. Acad. Sci. USA* **1998**, *95*, 12787–12792.
[210] S. Shimizu, M. Kataoka, K. Honda, K. Sakamoto, *J. Biotechnol.* **2001**, *92*, 187–194.
[211] B. J. Wilkins, L. E. Hahn, S. Heitmüller, H. Frauendorf, O. Valerius, G. H. Braus, H. Neumann, *ACS Chem. Biol.* **2015**, *10*, 939–944.
[212] J. Liu, J. Hemphill, S. Samanta, M. Tsang, A. Deiters, *J. Am. Chem. Soc.* **2017**, *139*, 9100–9103.
[213] L. Schoonen, K. S. van Esterik, C. Zhang, R. V. Ulijn, R. J. M. Nolte, J. C. M. v. Hest, *Scientific Reports* **2017**, *7*, 14772.
[214] D. Schneider, T. Schneider, J. Aschenbrenner, F. Mortensen, M. Scheffner, A. Marx, *Bioorg. Med. Chem.* **2016**, *24*, 995–1001.
[215] G. F. Schneider, B. F. Shaw, A. Lee, E. Carillho, G. M. Whitesides, *J. Am. Chem. Soc.* **2008**, *130*, 17384–17393.
[216] B. F. Shaw, G. F. Schneider, H. Arthanari, M. Narovlyansky, D. Moustakas, A. Durazo, G. Wagner, G. M. Whitesides, *J. Am. Chem. Soc.* **2011**, *133*, 17681–17695.
[217] B. F. Shaw, G. F. Schneider, G. M. Whitesides, *J. Am. Chem. Soc.* **2012**, *134*, 18739–18745.
[218] C. Geßler, In vitro Ubiquitinierung von Histonen durch Klick-Chemie, Universität Konstanz **2015**.
[219] E. Höllmuller, Universität Konstanz, unpublished data.
[220] M. Kratzmeier, W. Albig, T. Meergans, D. Doenecke, *Biochem. J.* **1999**, *337*, 319–327.
[221] H. Hashimoto, Y. Takami, E. Sonoda, T. Iwasaki, H. Iwano, M. Tachibana, S. Takeda, T. Nakayama, H. Kimura, Y. Shinkai, *Nucleic Acids Res.* **2010**, *38*, 3533–3545.
[222] Y. Li, P. Trojer, C.-F. Xu, P. Cheung, A. Kuo, W. J. Drury, 3rd, Q. Qiao, T. A. Neubert, R.-M. Xu, O. Gozani, D. Reinberg, *J. Biol. Chem.* **2009**, *284*, 34283–34295.
[223] J. Duan, L. Nilsson, *Biochemistry* **2006**, *45*, 7483–7492.
[224] Y. Kim, S. H. Kim, D. Ferracane, J. A. Katzenellenbogen, C. M. Schroeder, *Bioconjugate Chem.* **2012**, *23*, 1891–1901.
[225] S. Bell, S. Hansen, J. Buchner, *Biophys. Chem.* **2002**, *96*, 243–257.
[226] A. N. Bullock, J. Henckel, B. S. DeDecker, C. M. Johnson, P. V. Nikolova, M. R. Proctor, D. P. Lane, A. R. Fersht, *Proc. Natl. Acad. Sci. USA* **1997**, *94*, 14338–14342.
[227] E. A. Medcalf, J. Milner, *Oncogene* **1993**, *8*, 2847–2851.
[228] W. S. El-Deiry, T. Tokino, V. E. Velculescu, D. B. Levy, R. Parsons, J. M. Trent, D. Lin, W. E. Mercer, K. W. Kinzler, B. Vogelstein, *Cell* **1993**, *75*, 817–825.
[229] W. S. El-Deiry, J. W. Harper, P. M. Connor, V. E. Velculescu, C. E. Canman, J. Jackman, J. A. Pietenpol, M. Burrell, D. E. Hill, Y. Wang, K. G. Wiman, W. E. Mercer, M. B. Kastan, K. W. Kohn, S. J. Elledge, K. W. Kinzler, B. Vogelstein, *Cancer Res.* **1994**, *54*, 1169–1174.
[230] M. C. Pirrung, C.-Y. Huang, *Bioconjugate Chem.* **1996**, *7*, 317–321.

7. Attachments

Oligonucleotides

PylRS Mutation	Sequence
Y349F	f 5′-CCTGTATGGTCTTTGGGGATACCCT-3′
	r 5′-AGGGTATCCCCAAAGACCATACAGG-3′
L274A	f 5′-CTTTACAACTATGCGCGAAAACTCGAT-3′
	r 5′-ATCGAGTTTTCGCGCATAGTTGTAAAG-3′
M315A	f 5′-AACTTCTGTCAGGCGGGTTCGGGATGT-3′
	r 5′-ACATCCCGAACCCGCCTGACAGAAGTT-3′
I378A	f 5′-CCATGGTTTGTCCGCGCCCCATTCCCT-3′
	r 5′-AGGGAATGGGGCGCGGACAAACCATGG-3′
Y271A	f 5′-CTTGCCCCGACTCTTGCGAACTATCTGCGAAAACTC-3′
	r 5′-GAGTTTTCGCAGATAGTTCGCAAGAGTCGGGGCAAG-3′
C313A	f 5′-GCGCAGATGGGTTCGGGATGTACTC-3′
	r 5′-Phosphate-GAAGTTCACCATGGTAAATTCTTCCAGG-3′
W382A	f 5′-GCGATAGGTGCAGGTTTTGGGC-3′
	r 5′-Phosphate-TGGTTTGTCAATGCCCCATTCCC-3′
Y271A, L274A	Y271A was used as template
	f 5′-CTTGCCCCGACTCTTGCGAACTATCTGCGAAAACTC-3′
	r 5′-GAGTTTTCGCAGATAGTTCGCAAGAGTCGGGGCAAG-3′
Y349W	5′-ATTCCTGTATGGTCTGGGGGGATACCCTT-3′
	5′-AAGGGTATCCCCCCAGACCATACAGGAAT-3′
Y271A, L274M	Y271A was used as template
	f 5′-ATCGAGTTTTCGCATATAGTTCGCAAG-3′
	r 5′-ATCGAGTTTTCGCATATAGTTCGCAAG-3′
Y271M	f 5′-CTTGCCCCGACTCTTATGAACTATCTGCGAAAACTC-3′
	r 5′-GAGTTTTCGCAGATAGTTCATAAGAGTCGGGGCAAG-3′

IPYE

V31I	f 5′-CAAACACTATGAGATTTCAAGAAGTAAAATATAC-3′
	r 5′-GTATATTTTACTTCTTGAAATCTCATAGTGTTTG-3′
T56P	f 5′-CTAGGAGTTGTAGACCGGCCAGAGCATTC-3′

	r 5′-GAATGCTCTGGCCGGTCTACAACTCCTAG-3′
H62Y	f 5′-CCAGAGCATTCAGATATCATAAGTAC-3′
	r 5′-GTACTTATGATATCTGAATGCTCTGG-3′
A100E	f 5′-GGTAGTTTCTGAACCAAAGGTCA-3′
	r 5′-TGACCTTTGGTTCAGAAACTACC-3′

AcKRS

D76G	f 5′-TGTAGGGTTTCGGGCGAGGATATCAAT-3′
	r 5′-ATTGATATCCTCGCCCGAAACCCTACA-3′
L266V	f 5′-CTTAAGGCCAATGGTTGCCCCGACTC-3′
	r 5′-GAGTCGGGGCAACCATTGGCCTTAAG-3′
L274A	f 5′-CTTTACAACTATGCGCGAAAACTCGATAGG-3′
	r 5′-CCTATCGAGTTTTCGCGCATAGTTGTAAAG-3′
L266V, L270I, Y271F, L274A	f 5′-GCCCCGACTATTTTCAACTATGCGCGAAAACTCGATAGGATT-3′
	r 5′-ATAGTTGAAAATAGTCGGGGCAACCATTGGCCTTAAGCAG-3′
C313F	f 5′-CCATGGTGAACTTCTTTCAGATGGGTTCGG-3′
	r 5′-CCGAACCCATCTGAAAGAAGTTCACCATGG-3′

DNA Polymerase β

K41TAG	f 5′-CGCGTATCGTAAAGCGGCGAGCGTG-3′
	r5′-CACGCTCGCCGCTTTACGATACGCG-3′

Ubiquitin

STOP before His-tag	f 5′-GCGTGGTGGTTAATAACGTGATCCGAG-3′
	r 5′-AGACGCAGAACCAGATGC-3′

EMSA (IDT)

p21 RE 5′ (5’- Fluorescein)	5′- ATCAGGAACATGTCCCAACATGTTGAGCTC- 3′
p21 RE 3′	5′- GAGCTCAACATGTTGGGACATGTTCCTGAT- 3′

Sequencing Primers

Ub-His 5′ (pGEX)	5′-CCGACATCATAACGGTTCTG-3′
PylRS 5′ (pRSF Duet)	5′-GGATCTCGACGCTCTCCCT-3′
PylRS 3′ (pRSF Duet)	5′-GATTATGCGGCCGTGTACAA-3′
T7	5′-TAATACGACTCACTATAGGG-3′
T7 term	5′-GCTAGTTATTGCTCAGCGG-3′

Protein Sequences

DNA Polymerase β wt / 41TAG

ATG AGA GGA TCT *TAC CAT CAC CAT CAC CAT* ACG GAT CCG ATG AGC AAA CGT AAA GCG CCG CAG GAA ACC CTG AAC GGC GGC ATT ACC GAT ATG CTG ACC GAA CTG GCC AAC TTT GAA AAA AAC GTG AGC CAG GCG ATC CAT AAA TAT AAC GCG TAT CGT **AAA** GCG GCG AGC GTG ATT GCG AAA TAT CCG CAC AAA ATT AAA AGC GGT GCG GAA GCG AAA AAA CTG CCG GGC GTG GGC ACC AAA ATT GCG GAA AAA ATC GAT GAA TTT CTG GCC ACC GGC AAA CTG CGT AAA CTG GAA AAA ATT CGC CAG GAT GAT ACC AGC AGC AGC ATT AAC TTT CTG ACC CGT GTG AGC GGC ATT GGT CCG AGC GCG GCG CGT AAA TTT GTG GAT GAA GGC ATC AAA ACC CTG GAG GAT CTG CGT AAA AAC GAA GAT AAA CTG AAC CAT CAT CAG CGT ATT GGC CTG AAA TAT TTT GGC GAT TTC GAA AAA CGT ATT CCG CGT GAA GAA ATG CTG CAG ATG CAG GAT ATT GTG CTG AAC GAA GTG AAA AAA GTG GAT AGC GAA TAT ATT GCG ACC GTG TGC GGC AGC TTT CGT CGT GGC GCG GAA AGC AGC GGC GAT ATG GAT GTG CTG CTG ACC CAT CCG AGC TTT ACC AGC GAA AGC ACC AAA CAG CCG AAA CTG CTG CAT CAG GTG GTG GAA CAG CTG CAG AAA GTG CAT TTT ATT ACC GAT ACC CTG AGC AAA GGC GAA ACC AAA TTT ATG GGC GTG TGC CAG CTG CCG AGC AAA AAC GAT GAA AAA GAA TAT CCG CAT CGC CGT ATT GAT ATT CGT CTG ATC CCG AAA GAT CAG TAT TAT TGC GGC GTG CTG TAT TTT ACC GGC AGC GAT ATC TTC AAC AAA AAC ATG CGT GCG CAT GCG CTG GAA AAA GGC TTT ACC ATC AAC GAA TAC ACC ATT CGT CCG CTG GGC GTG ACC GGT GTT GCG GGT GAA CCG CTG CCG GTG GAT AGC GAA AAA GAT ATC TTC GAT TAC ATC CAG TGG AAA TAT CGT GAA CCG AAA GAT CGT AGC GAA TAA

MRGSYHHHHHTDPMSKRKAPQETLNGGITDMLTELANFEKNVSQAIHKYNAYR**K**AASVIAK
YPHKIKSGAEAKKLPGVGTKIAEKIDEFLATGKLRKLEKIRQDDTSSSINFLTRVSGIGPSAAR

KFVDEGIKTLEDLRKNEDKLNHHQRIGLKYFGDFEKRIPREEMLQMQDIVLNEVKKVDSEYIA
TVCGSFRRGAESSGDMDVLLTHPSFTSESTKQPKLLHQVVEQLQKVHFITDTLSKGETKFM
GVCQLPSKNDEKEYPHRRIDIRLIPKDQYYCGVLYFTGSDIFNKNMRAHALEKGFTINEYTIR
PLGVTGVAGEPLPVDSEKDIFDYIQWKYREPKDRSE

Underlined: Start DNA Polymerase β

Ub 75C

ATG CAG ATT TTT GTT AAA ACC CTG ACC GGT AAA ACC ATT ACC CTG GAA GTT GAA CCG AGC GAT ACC ATT GAA AAT GTG AAA GCC AAA ATT CAG GAT AAA GAA GGT ATT CCG CCG GAT CAG CAG CGT CTG ATT TTT GCA GGT AAA CAG CTG GAA GAT GGT CGT ACC CTG AGC GAT TAT AAT ATT CAG AAG GAA AGC ACC CTG CAT CTG GTT CTG CGT CTG CGT **TGC** TAA TAA

MQIFVKTLTGKTITLEVEPSDTIENVKAKIQDKEGIPPDQQRLIFAGKQLEDGRTLSDYNIQKE
STLHLVLRLR**C**

Ub76TAG

ATG CAA ATC TTC GTC AAA ACT CTT ACG GGA AAA ACT ATC ACC TTG GAA GTT GAG CCT TCC GAC ACT ATC GAG AAT GTC AAA GCA AAG ATT CAA GAC AAG GAA GGT ATT CCT CCT GAC CAA CAA CGC TTA ATC TTC GCG GGT AAG CAA TTA GAA GAC GGA CGC ACA CTG TCT GAC TAC AAC ATT CAG AAA GAA AGT ACG CTT CAC TTG GTC TTG CGC CTG CGT GGT TAG

MQIFVKTLTGKTITLEVEPSDTIENVKAKIQDKEGIPPDQQRLIFAGKQLEDGRTLSDYNIQKE
STLHLVLRLRG

Ub-His wt

ATG CAA ATC TTC GTC AAA ACT CTT ACG GGA AAA ACT ATC ACC TTG GAA GTT GAG CCT TCC GAC ACT ATC GAG AAT GTC AAA GCA AAG ATT CAA GAC AAG GAA GGT ATT CCT CCT GAC CAA CAA CGC TTA ATC TTC GCG GGT AAG CAA TTA GAA GAC GGA CGC ACA CTG TCT GAC TAC AAC ATT CAG AAA GAA AGT ACG CTT CAC

TTG GTC TTG CGC CTG CGT GGT GGT GTA CAA CGG GAT CCG AGC TCC GTC GAC AAG CTT GCG GCC GCA CTC GAG *CAC CAT CAT CAT CAC CAC* TAA

MQIFVKTLTGKTITLEVEPSDTIENVKAKIQDKEGIPPDQQRLIFAGKQLEDGRTLSDYNIQKE STLHLVLRLRGGVQRDPSSVDKLAAALEHHHHHH

Ub 48TAG-His / <u>Ub 48TAG</u>

ATG CAG ATC TTT GTT AAA ACC CTG ACC GGT AAA ACC ATT ACA CTG GAA GTT GAA CCG AGC GAT ACC ATT GAA AAT GTG AAA GCC AAA ATC CAG GAC AAA GAA GGT ATT CCG CCT GAT CAG CAG CGT CTG ATT TTT GCA GGT **TAG** CAG CTG GAA GAT GGT CGT ACC CTG AGC GAT TAT AAC ATT CAG AAA GAA AGC ACC CTG CAT CTG GTT CTG CGT CTG CGT GGT GGT <u>GTT CAG</u> CGT GAT CCG AGC AGC GTT GAT AAA CTG GCA GCA GCA CTG GAA *CAT CAT CAC CAT CAT CAT* TAA

MQIFVKTLTGKTITLEVEPSDTIENVKAKIQDKEGIPPDQQRLIFAG**K**QLEDGRTLSDYNIQKE STLHLVLRLRGG<u>VQ</u>RDPSSVDKLAAALE*HHHHHH*

Ub 48TAG: Underlined codons are mutated to TAA

Ub wt

ATG CAA ATC TTC GTC AAA ACT CTT ACG GGA AAA ACT ATC ACC TTG GAA GTT GAG CCT TCC GAC ACT ATC GAG AAT GTC AAA GCA AAG ATT CAA GAC AAG GAA GGT ATT CCT CCT GAC CAA CAA CGC TTA ATC TTC GCG GGT **AAG** CAA TTA GAA GAC GGA CGC ACA CTG TCT GAC TAC AAC ATT CAG AAA GAA AGT ACG CTT CAC TTG GTC TTG CGC CTG CGT GGT GGT TAA TAA

MQIFVKTLTGKTITLEVEPSDTIENVKAKIQDKEGIPPDQQRLIFAG**K**QLEDGRTLSDYNIQKE STLHLVLRLRGG

H1.2 wt / 114TAG / 206TAG

ATG AGC GAA ACC GCA CCG GCA GCA CCT GCT GCA GCA CCT CCG GCA GAA AAA GCA CCG GTT AAA AAA AAA GCA GCC AAA AAA GCC GGT GGT ACC CCG CGT AAA GCA AGC GGT CCT CCG GTT AGC GAA CTG ATT ACC AAA GCA GTT GCA GCA AGC AAA GAA CGT AGC GGT GTT AGC CTG GCA GCA CTG AAA AAA GCA CTG GCA GCA GCA GGT TAT GAT GTG GAA AAA AAT AAT AGC CGC ATT AAA CTG GGC CTG AAA AGC CTG GTT AGC AAA GGC ACC CTG GTT CAG ACC AAA GGC ACC GGT GCA AGC GGT TCA TTT AAA CTG AAT AAA AAA GCC GCA AGC GGT **GAA** GCA AAA CCG AAA GTT AAA AAA GCG GGT GGC ACC AAA CCG AAA AAA CCG GTT GGT GCA GCA AAA AAA CCG AAA AAA GCA GCC GGT GGT GCA ACC CCG AAA AAA AGC GCA AAA AAA ACG CCG AAA AAA GCC AAA AAA CCG GCA GCA GCA ACC GTT ACC AAA AAA GTT GCA AAA TCT CCG AAA AAA GCG AAA GTT GCG AAA CCG AAA AAG GCC GCA AAA AGC GCA GCA AAA GCA GTT AAA CCG AAA GCC GCT AAA CCG AAA GTG GTT AAA CCG AAG **AAA** GCG GCA CCG AAA AAA AAA *CAT CAT CAC CAT CAC CAC* TAA TAA

MSETAPAAPAAAPPAEKAPVKKKAAKKAGGTPRKASGPPVSELITKAVAASKERSGVSLAAL KKALAAAGYDVEKNNSRIKLGLKSLVSKGTLVQTKGTGASGSFKLNKKAASG**E**AKPKVKKA GGTKPKKPVGAAKKPKKAAGGATPKKSAKKTPKKAKKPAAATVTKKVAKSPKKAKVAKPKK AAKSAAKAVKPKAAKPKVVKPK**K**AAPKKK*HHHHHH*

p53 wt / p53 120TAG

ATG TCG *CAC CAT CAC CAT CAT CAT CAC CAT CAC* GGA TCG GCT TTT GAA TTT AAA TTG CCA GAC ATT GGC GAA GGT ATC CAT GAG GGG GAA ATT GTT AAG TGG TTT GTC AAG CCA GGG GAC GAA GTA AAT GAA GAC GAC GTT TTA TGT GAA GTT CAA AAC GAT AAG GCG GTG TGG GTC GAA ATT CCC TCA CCA GTC AAA GGC AAG GTT CTT GAA ATC CTG GTA CCG GAA GGA ACA GTC GCT ACG GTC GGA CAA ACT TTA ATT ACC CTG GAT GCA CCT GGG TAC GAG AAT ATG ACA TTC TTG GTC CCA CGC GGC AGC CGT CGT GCC TCG GTT GGA TCC ATG GAA GAA CCG CAG AGC GAT CCG AGC GTT GAA CCG CCT CTG AGC CAA GAA ACC TTT AGC GAT CTG TGG AAA CTG CTG CCG GAA AAT AAT GTT CTG AGT CCG CTG CCG AGC CAG GCA ATG GAT GAT CTG ATG CTG AGT CCG GAT GAT ATT GAA CAG TGG TTT ACC GAA GAT CCG GGT CCT GAT GAA GCA CCG CGT ATG CCG GAA GCA GCA CCG CCT GTT GCA CCG GCA CCG GCA GCA CCT ACA CCA GCA GCT CCA GCT CCG GCA CCG AGC TGG CCT CTG AGT AGC AGC GTT CCG AGC CAG AAA ACC TAT CAG GGT AGC TAT GGT TTT

CGT CTG GGT TTT CTG CAT AGC GGC ACC GCA **AAA** AGC GTT ACC TGT ACC TAT AGT CCG GCA CTG AAT AAA ATG TTT TGT CAG CTG GCC AAA ACC TGT CCG GTT CAG CTG TGG GTT GAT AGC ACC CCT CCG CCT GGC ACC CGT GTT CGT GCA ATG GCA ATC TAT AAA CAG AGC CAG CAC ATG ACC GAA GTT GTT CGT CGT TGT CCG CAT CAT GAA CGT TGT AGC GAT AGT GAT GGT CTG GCA CCG CCT CAG CAT CTG ATT CGT GTT GAA GGT AAT CTG CGT GTT GAA TAT CTG GAT GAT CGT AAT ACC TTT CGT CAT AGC GTT GTT GTT CCG TAT GAA CCT CCG GAA GTT GGT AGC GAT TGT ACC ACC ATT CAT TAT AAC TAT ATG TGC AAC AGC AGC TGC ATG GGT GGT ATG AAT CGT CGT CCG ATT CTG ACC ATT ATT ACC CTG GAA GAT AGC AGC GGC AAT CTG CTG GGT CGT AAT AGC TTT GAA GTT CGT GTT TGT GCA TGT CCG GGT CGT GA TCG TCG TAC CGA AGA AGA AAA TCT GCG TAA AAA AGG TGA ACC GCA TCA CGA ACT GCC TCC GGG TAG CAC CAA ACG TGC ACT GCC GAA TAA TAC CAG CAG CAG TCC GCA GCC GAA AAA AAA ACC GCT GGA TGG TGA ATA TTT CAC CCT GCA AAT TCG TGG TCGT GAA CGC TTT GAA ATG TTT CGT GAA CTG AAT GAA GCA CTG GAA CTG AAA GAT GCA CAG GCA GGT AAA GAA CCG GGT GGT AGC CGT GCA CAT AGC AGC CAT CTG AAA AGC AAA AAA GGT CAG AGC ACC AGC CGT CAT AAA AAA CTG ATG TTT AAA ACC GAA GGT CCG GAT AGC GAT TAA

MS*HHHHHHHHHH*GSAFEFKLPDIGEGIHEGEIVKWFVKPGDEVNEDDVLCEVQNDKAVWVEI PSPVKGKVLEILVPEGTVATVGQTLITLDAPGYENMTFLVPRGSRRASVGSMEEPQSDPSVE PPLSQETFSDLWKLLPENNVLSPLPSQAMDDLMLSPDDIEQWFTEDPGPDEAPRMPEAAPP VAPAPAAPTPAAPAPAPSWPLSSSVPSQKTYQGSYGFRLGFLHSGTA**K**SVTCTYSPALNKM FCQLAKTCPVQLWVDSTPPPGTRVRAMAIYKQSQHMTEVVRRCPHHERCSDSDGLAPPQ HLIRVEGNLRVEYLDDRNTFRHSVVVPYEPPEVGSDCTTIHYNYMCNSSCMGGMNRRPILTI ITLEDSSGNLLGRNSFEVRVCACPGRDRRTEEENLRKKGEPHHELPPGSTKRALPNNTSSS PQPKKKPLDGEYFTLQIRGRERFEMFRELNEALELKDAQAGKEPGGSRAHSSHLKSKKGQS TSRHKKLMFKTEGPDSD

Underlined: p53 start

PylRS wt

ATG GAT AAA AAA CCA TTA GAT GTT TTA ATA TCT GCG ACC GGG CTC TGG ATG TCC AGG ACT GGC ACG CTC CAC AAA ATC AAA CAC TAT GAG GTC TCA AGA AGT AAA ATA TAC ATT GAA ATG GCG TGT GGA GAC CAT CTT GTT GTG AAT AAT TCT AGG AGT TGT AGA ACA GCC AGA GCA TTC AGA CAT CAT AAG TAC AGA AAA ACC

TGC AAA CGA TGT AGG GTT TCG GAC GAG GAT ATC AAT AAT TTC CTC ACA AGA TCA ACT GAA GGC AAA ACC AGT GTG AAA GTT AAG GTA GTT TCT GCT CCA AAG GTC AAA AAA GCT ATG CCG AAA TCA GTT TCG AGG GCT CCA AAG CCT CTG GAA AAT CCT GTG TCT GCA AAG GCA TCA ACG GAC ACA TCC AGA TCT GTA CCT TCG CCT GCA AAA TCA ACT CCA AAT TCG CCT GTT CCC ACA TCG GCT CCT GCT CCT TCA CTT ACA AGA AGC CAG CTC GAT AGG GTT GAG GCT CTC TTA AGT CCA GAG GAT AAA ATT TCT CTG AAT ATT GCA AAG CCT TTC AGG GAA CTT GAG TCC GAA CTT GTG ACA AGA AGA AAA AAC GAT TTT CAG CGG CTC TAT ACC AAT GAT AGA GAA GAC TAC CTT GGT AAA CTC GAA CGG GAC ATT ACG AAA TTT TTC GTA GAC CGG GAT TTT CTG GAG ATA AAG TCT CCT ATC CTT ATT CCG GCA GAA TAC GTG GAG AGA ATG GGT ATT AAC AAT GAT ACT GAA CTT TCA AAA CAG ATC TTC AGG GTG GAT AAA AAT CTC TGC TTA AGG CCA ATG CTT GCC CCG ACT CTT TAC AAC TAT CTG CGA AAA CTC GAT AGG ATT TTA CCA GAT CCT ATA AAG ATT TTC GAA GTC GGG CCC TGT TAC CGG AAA GAG TCT GAC GGC AAA GAG CAC CTG GAA GAA TTT ACC ATG GTG AAC TTC TGT CAG ATG GGT TCG GGA TGT ACT CGG GAA AAT CTT GAA TCC CTC ATC AAA GAG TTT CTG GAC TAT CTG GAA ATC GAC TTC GAA ATC GTA GGA GAT TCC TGT ATG GTC TAT GGG GAT ACC CTT GAT ATA ATG CAC GGG GAC CTG GAG CTT TCT TCG GCA GTC GTC GGG CCA GTT CCT CTT GAT AGG GAA TGG GGC ATT GAC AAA CCA TGG ATA GGT GCA GGT TTT GGG CTT GAA CGC TTG CTC AAG GTT ATG CAT GGC TTT AAA AAC ATT AAG AGA GCA TCA AGG TCC GAA TCT TAC TAT AAT GGG ATT TCA ACC AAT CTA TGA

MDKKPLDVLISATGLWMSRTGTLHKIKHYEVSRSKIYIEMACGDHLVVNNSRSCRTARAFRH HKYRKTCKRCRVSDEDINNFLTRSTEGKTSVKVKVVSAPKVKKAMPKSVSRAPKPLENPVS AKASTDTSRSVPSPAKSTPNSPVPTSAPAPSLTRSQLDRVEALLSPEDKISLNIAKPFRELES ELVTRRKNDFQRLYTNDREDYLGKLERDITKFFVDRDFLEIKSPILIPAEYVERMGINNDTELS KQIFRVDKNLCLRPMLAPTLYNYLRKLDRILPDPIKIFEVGPCYRKESDGKEHLEEFTMVNFC QMGSGCTRENLESLIKEFLDYLEIDFEIVGDSCMVYGDTLDIMHGDLELSSAVVGPVPLDRE WGIDKPWIGAGFGLERLLKVMHGFKNIKRASRSESYYNGISTNL

PylRS AcKRS Liu (as published)

ATG TCA GAT AAA AAA CCA TTA GAT GTT TTA ATA TCT GCG ACC GGG CTC TGG ATG TCC AGG ACT GGC ACG CTC CAC AAA ATC AAG CAC CAT GAG GTC TCA AGA AGT AAA ATA TAC ATT GAA ATG GCG TGT GGA GAC CAT CTT GTT GTG AAT AAT TCC AGG AGT TGT AGA ACA GCC AGA GCA TTC AGA CAT CAT AAG TAC AGA AAA

ACC TGC AAA CGA TGT AGG GTT TCG GGC GAG GAT ATC AAT AAT TTT CTC ACA AGA TCA ACC GAA AGC AAA AAC AGT GTG AAA GTT AGG GTA GTT TCT GCT CCA AAG GTC AAA AAA GCT ATG CCG AAA TCA GTT TCA AGG GCT CCG AAG CCT CTG GAA AAT TCT GTT TCT GCA AAG GCA TCA ACG AAC ACA TCC AGA TCT GTA CCT TCG CCT GCA AAA TCA ACT CCA AAT TCG TCT GTT CCC GCA TCG GCT CCT GCT CCT TCA CTT ACA AGA AGC CAG CTT GAT AGG GTT GAG GCT CTC TTA AGT CCA GAG GAT AAA ATT TCT CTG AAT ATG GCA AAG CCT TTC AGG GAA CTT GAG CCT GAA CTT GTG ACA AGA AGA AAA AAC GAT TTT CAG CGG CTC TAT ACC AAT GAT AGA GAA GAC TAC CTC GGT AAA CTC GAA CGT GAT ATT ACG AAA TTT TTC GTA GAC CGG GGT TTT CTG GAG ATA AAG TCT CCT ATC CTT ATT CCG GCG GAA TAC GTG GAG AGA ATG GGT ATT AAT AAT GAT ACT GAA CTT TCA AAA CAG ATC TTC CGG GTG GAT AAA AAT CTC TGC TTG AGG CCA ATG GTT GCC CCG ACT ATT TTC AAC TAT GCG CGA AAA CTC GAT AGG ATT TTA CCA GGC CCA ATA AAA ATT TTC GAA GTC GGA CCT TGT TAC CGG AAA GAG TCT GAC GGC AAA GAG CAC CTG GAA GAA TTT ACT ATG GTG AAC TTC TTT CAG ATG GGT TCG GGA TGT ACT CGG GAA AAT CTT GAA GCT CTC ATC AAA GAG TTT CTG GAC TAT CTG GAA ATC GAC TTC GAA ATC GTA GGA GAT TCC TGT ATG GTC TAT GGG GAT ACT CTT GAT ATA ATG CAC GGG GAC CTG GAG CTT TCT TCG GCA GTC GTC GGG CCA GTT TCT CTT GAT AGA GAA TGG GGT ATT GAC AAA CCA TGG ATA GGT GCA GGT TTT GGT CTT GAA CGC TTG CTC AAG GTT ATG CAC GGC TTT AAA AAC ATT AAG AGG GCA TCA AGG TCC GAA TCT TAC TAT AAT GGG ATT TCA ACC AAT CTG TAA

MSDKKPLDVLISATGLWMSRTGTLHKIKHHEVSRSKIYIEMACGDHLVVNNSRSCRTARAFR
HHKYRKTCKRCRVSGEDINNFLTRSTESKNSVKVRVVSAPKVKKAMPKSVSRAPKPLENSV
SAKASTNTSRSVPSPAKSTPNSSVPASAPAPSLTRSQLDRVEALLSPEDKISLNMAKPFREL
EPELVTRRKNDFQRLYTNDREDYLGKLERDITKFFVDRGFLEIKSPILIPAEYVERMGINNDTE
LSKQIFRVDKNLCLRPMVAPTIFNYARKLDRILPGPIKIFEVGPCYRKESDGKEHLEEFTMVNF
FQMGSGCTRENLEALIKEFLDYLEIDFEIVGDSCMVYGDTLDIMHGDLELSSAVVGPVSLDR
EWGIDKPWIGAGFGLERLLKVMHGFKNIKRASRSESYYNGISTNL

gBlock for cloning PylRS AcK Liu into pRSF Duet-1 (ordered from Integrated DNA Technologies)

AA CGT TAC TGG TTT CAC ATT CAC CAC CCT GAA TTG ACT CTC TTC CGG GCG CTA TCA TGC CAT ACC GCG AAA GGT TTT GCG CCA TTC GAT GGT GTC CGG GAT CTC GAC GCT CTC CCT TAT GCG ACT CCT GCA TTA GGA AAT TAA TAC GAC TCA CTA

TAG GGG AAT TGT GAG CGG ATA ACA ATT CCC CTG TAG AAA TAA TTT TGT TTA ACT TTA ATA AGG AGA TAT ACC ATG TCA GAT AAA AAA CCA TTA GAT GTT TTA ATA TCT GCG ACC GGG CTC TGG ATG TCC AGG ACT GGC ACG CTC CAC AAA ATC AAG CAC CAT GAG GTC TCA AGA AGT AAA ATA TAC ATT GAA ATG GCG TGT GGA GAC CAT CTT GTT GTG AAT AAT TCC AGG AGT TGT AGA ACA GCC AGA GCA TTC AGA CAT CAT AAG TAC AGA AAA ACC TGC AAA CGA TGT AGG GTT TCG GGC GAG GAT ATC AAT AAT TTT CTC ACA AGA TCA ACC GAA AGC AAA AAC AGT GTG AAA GTT AGG GTA GTT TCT GCT CCA AAG GTC AAA AAA GCT ATG CCG AAA TCA GTT TCA AGG GCT CCG AAG CCT CTG GAA AAT TCT GTT TCT GCA AAG GCA TCA ACG AAC ACA TCC AGA TCT GTA CCT TCG CCT GCA AAA TCA ACT CCA AAT TCG TCT GTT CCC GCA TCG GCT CCT GCT CCT TCA CTT ACA AGA AGC CAG CTT GAT AGG GTT GAG GCT CTC TTA AGT CCA GAG GAT AAA ATT TCT CTG AAT ATG GCA AAG CCT TTC AGG GAA CTT GAG CCT GAA CTT GTG ACA AGA AGA AAA AAC GAT TTT CAG CGG CTC TAT ACC AAT GAT AGA GAA GAC TAC CTC GGT AAA CTC GAA CGT GAT ATT ACG AAA TTT TTC GTA GAC CGG GGT TTT CTG GAG ATA AAG TCT CCT ATC CTT ATT CCG GCG GAA TAC GTG GAG AGA ATG GGT ATT AAT AAT GAT ACT GAA CTT TCA AAA CAG ATC TTC CGG GTG GAT AAA AAT CTC TGC TTG AGG CCA ATG GTT GCC CCG ACT ATT TTC AAC TAT GCG CGA AAA CTC GAT AGG ATT TTA CCA GGC CCA ATA AAA ATT TTC GAA GTC GGA CCT TGT TAC CGG AAA GAG TCT GAC GGC AAA GAG CAC CTG GAA GAA TTT ACT ATG GTG AAC TTC TTT CAG ATG GGT TCG GGA TGT ACT CGG GAA AAT CTT GAA GCT CTC ATC AAA GAG TTT CTG GAC TAT CTG GAA ATC GAC TTC GAA ATC GTA GGA GAT TCC TGT ATG GTC TAT GGG GAT ACT CTT GAT ATA ATG CAC GGG GAC CTG GAG CTT TCT TCG GCA GTC GTC GGG CCA GTT TCT CTT GAT AGA GAA TGG GGT ATT GAC AAA CCA TGG ATA GGT GCA GGT TTT GGT CTT GAA CGC TTG CTC AAG GTT ATG CAC GGC TTT AAA AAC ATT AAG AGG GCA TCA AGG TCC GAA TCT TAC TAT AAT GGG ATT TCA ACC AAT CTG TGA GCT C

AcKRS Liu pE (provided by by W. Liu group, AM Texas University)

MDKKPLNTLISATGLWMSRTGTIHKIKHHEVSRSKIYIEMACGDHLVVNNSRSSRTARALRH
HKYRKTCKRCRVSDEDLNKFLTKANEDQTSVKVKVVSAPTRTKKAMPKSVARAPKPLENTE
AAQAQPSGSKFSPAIPVSTQESVSVPASVSTSISSISTGATASALVKGNTNPITSMSAPVQAS
APALTKSQTDRLEVLLNPKDEISLNSGKPFRELESELLSRRKKDLQQIYAEERENYLGKLERE
ITRFFVDRGFLEIKSPILIPLEYIERMGIDNDTELSKQIFRVDKNFCLRPMMAPNLLNLARKLDR
ALPDPIKIFEIGPCYRKESDGKEHLEEFTMLNFFQMGSGCTRENLESIITDFLNHLGIDFKIVG

DSCMVYGDTLDVMHGDLELSSAVVGPIPLDREWGIDKPWIGAGFGLERLLKVKHDFKNIKR
AARSESYYNGISTNL

ATG GAT AAG AAA CCG CTG AAT ACT CTG ATT TCT GCA ACT GGT CTG TGG ATG
AGC CGT ACC GGC ACC ATC CAC AAG ATC AAA CAC CAC GAG GTT TCC CGT AGC
AAA ATC TAC ATC GAA ATG GCG TGC GGT GAC CAC CTG GTG GTA AAC AAC TCC
CGT TCT TCT CGT ACT GCA CGT GCT CTG CGC CAC CAC AAG TAC CGT AAG ACC
TGC AAG CGC TGT CGC GTG TCT GAT GAA GAC CTG AAC AAA TTC CTG ACT AAA
GCG AAC GAA GAT CAG ACT TCT GTG AAG GTG AAA GTT GTT TCT GCC CCA ACC
CGC ACC AAG AAA GCG ATG CCG AAG TCC GTT GCA CGC GCT CCG AAA CCG CTG
GAG AAC ACC GAA GCC GCA CAG GCC CAG CCG TCT GGT TCT AAG TTT TCT CCG
GCA ATC CCG GTT TCT ACT CAG GAG TCT GTG TCT GTG CCA GCT TCT GTT AGC
ACT TCT ATT TCC TCT ATC AGC ACT GGT GCG ACT GCG TCC GCT CTG GTA AAA
GGT AAC ACT AAC CCG ATC ACC AGC ATG TCT GCT CCG GTT CAG GCT TCT GCA
CCG GCA CTG ACT AAA AGC CAG ACT GAC CGT CTG GAG GTT CTG CTG AAC CCG
AAA GAT GAA ATC AGC CTG AAC TCT GGC AAA CCG TTC CGT GAA CTG GAA TCC
GAA CTG CTG TCT CGT CGT AAG AAA GAC CTG CAA CAA ATC TAT GCT GAA GAG
CGT GAA AAC TAC CTG GGT AAA CTG GAA CGT GAA ATC ACC CGT TTC TTT GTG
GAC CGT GGT TTC CTG GAA ATC AAG TCT CCG ATC CTG ATC CCG CTG GAA TAC
ATC GAG CGC ATG GGT ATT GAT AAC GAC ACC GAA CTG TCC AAG CAG ATT TTC
CGT GTG GAC AAG AAC TTC TGC CTG CGT CCG ATG ATG GCA CCG AAC CTG CTG
AAT CTG GCG CGT AAA CTG GAT CGT GCA CTG CCG GAC CCG ATC AAA ATC TTT
GAA ATC GGT CCA TGC TAT CGT AAG GAG AGC GAC GGT AAA GAA CAC CTG GAA
GAG TTC ACT ATG CTG AAC TTT TTT CAG ATG GGT TCT GGC TGC ACC CGT GAA
AAT CTG GAA TCT ATC ATC ACC GAC TTC CTG AAC CAC CTG GGC ATT GAC TTC
AAA ATC GTT GGT GAT TCC TGC ATG GTT TAC GGT GAC ACT CTG GAC GTT ATG
CAT GGT GAT CTG GAA CTG AGC AGC GCT GTT GTG GGT CCG ATT CCG CTG GAT
CGT GAA TGG GGT ATC GAT AAA CCG TGG ATT GGT GCT GGC TTC GGT CTG GAA
CGT CTG CTG AAA GTT AAG CAC GAC TTT AAG AAC ATC AAA CGT GCT GCG CGT
TCC GAG TCC TAT TAC AAC GGC ATT AGC ACT AAC CTG

NMR Spectra

Compound 1

^{1}H NMR

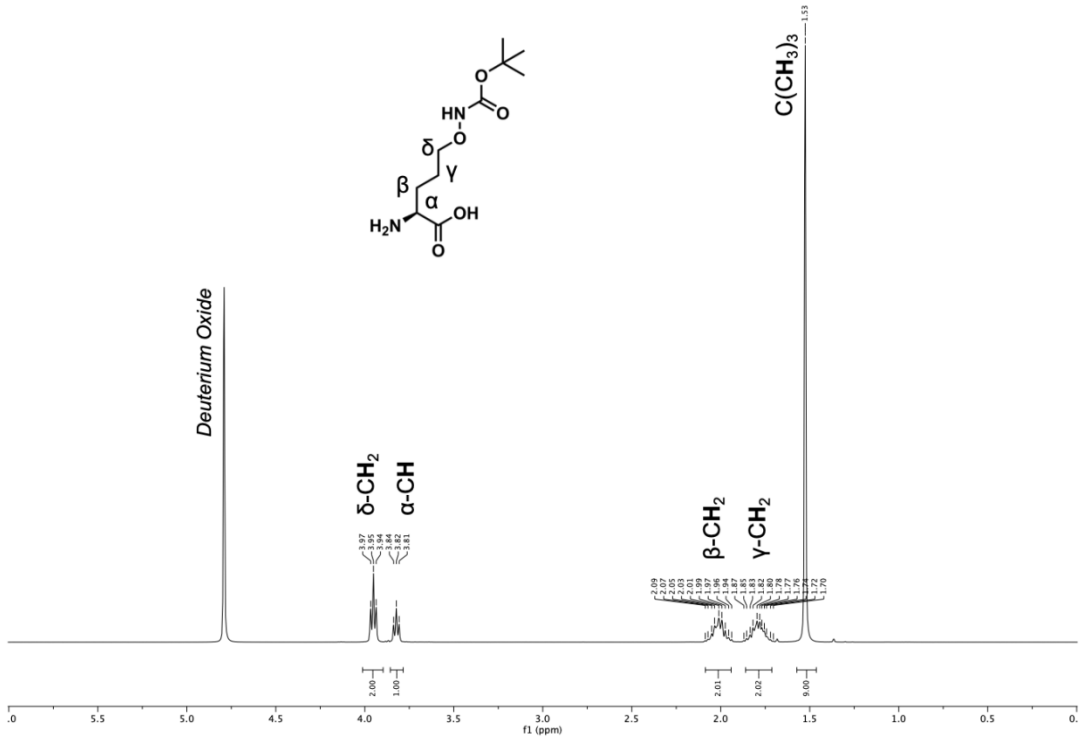

^{13}C NMR

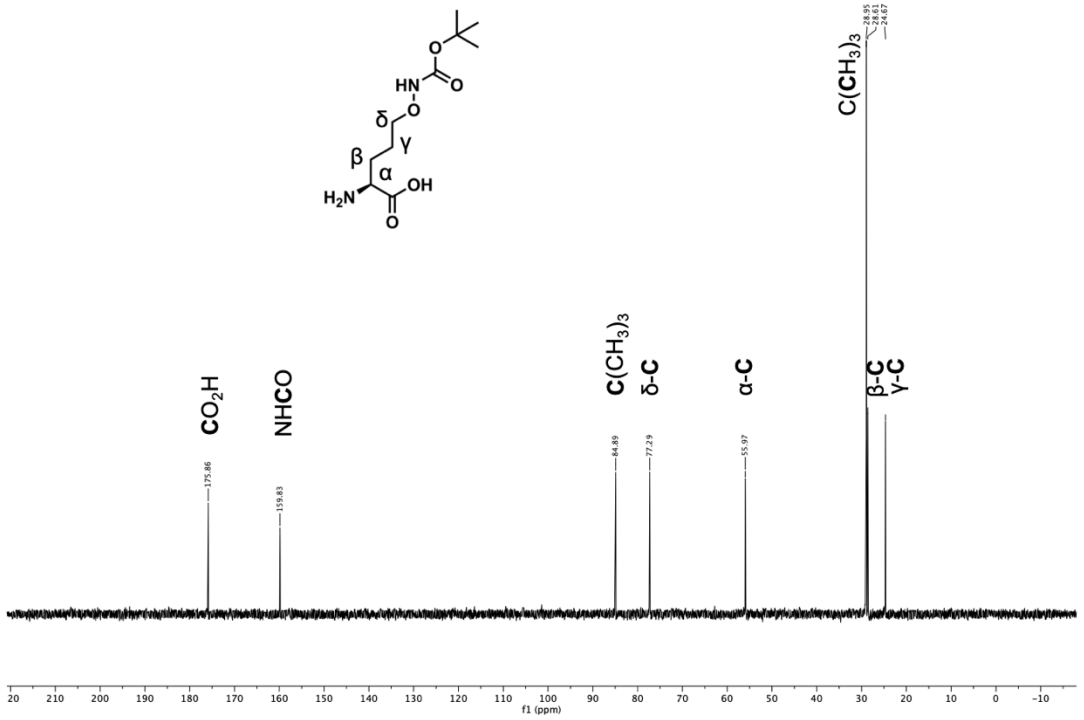

Compound 2b

^{1}H NMR

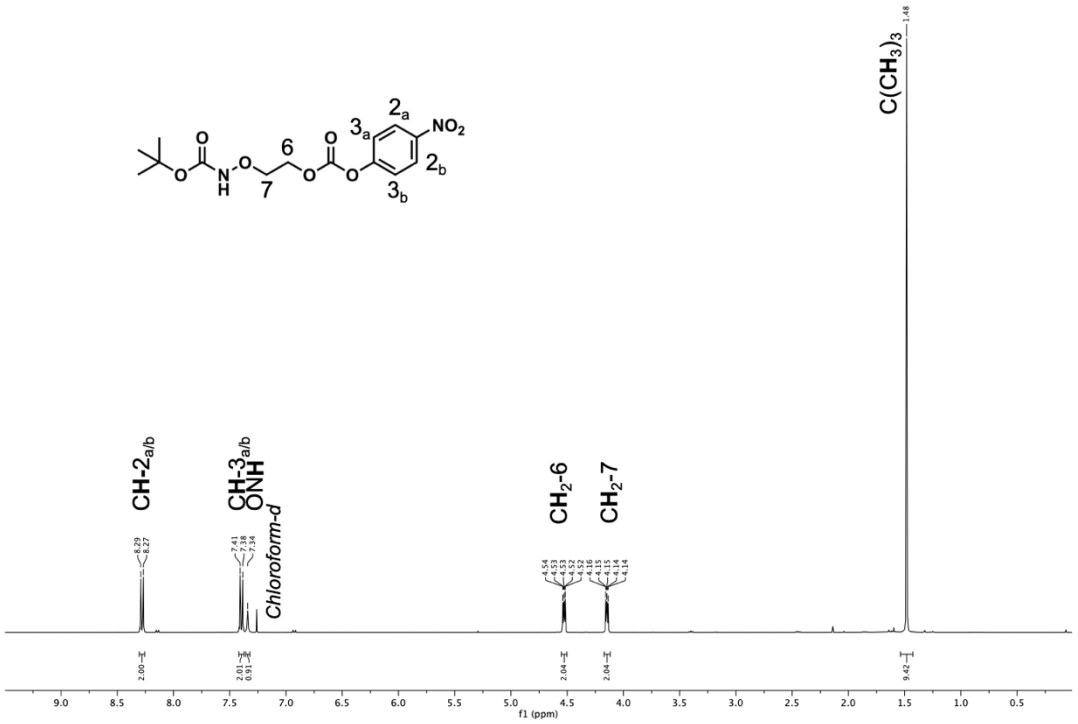

^{13}C NMR

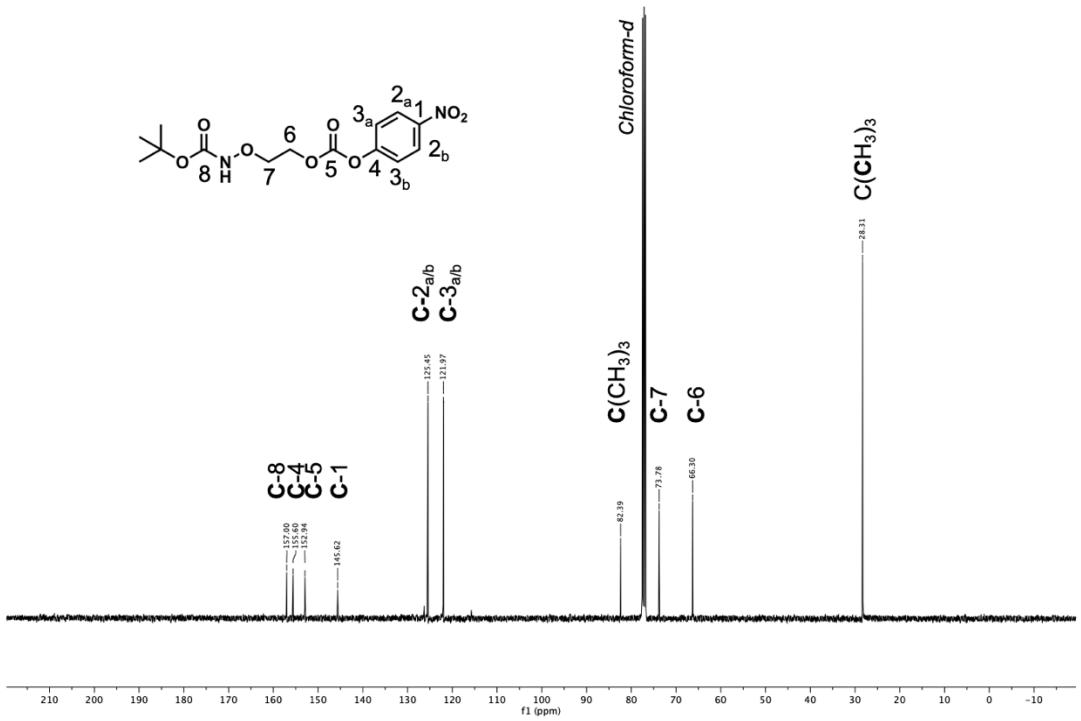

Compound 2c

^{1}H NMR

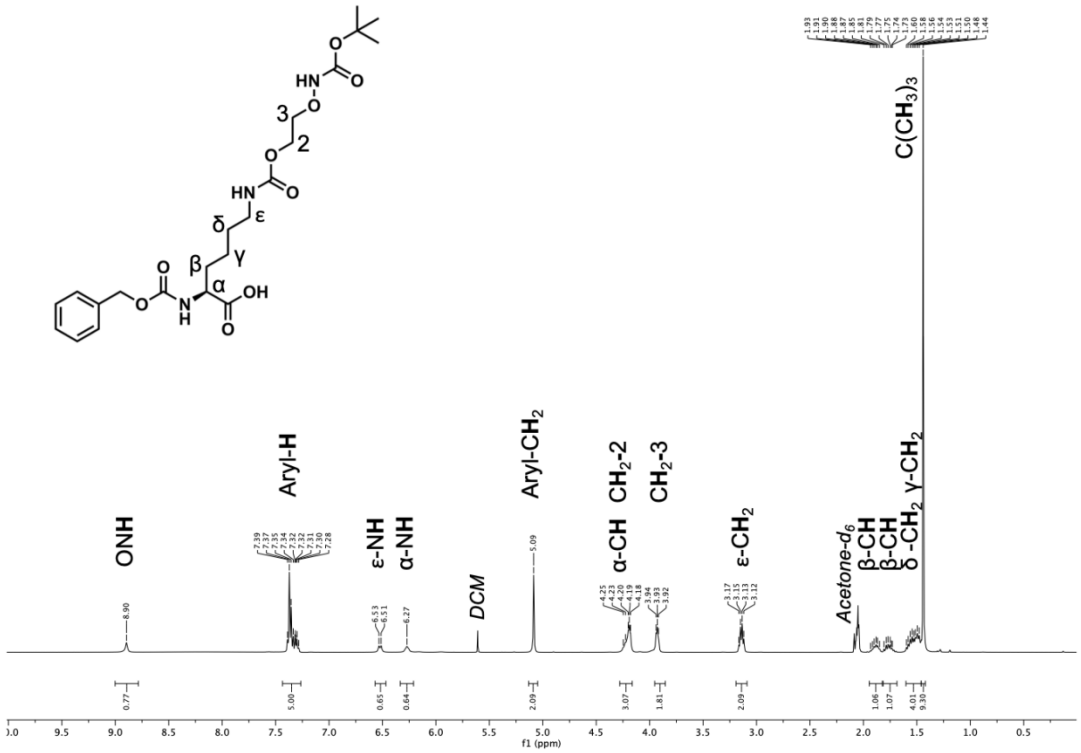

^{13}C NMR

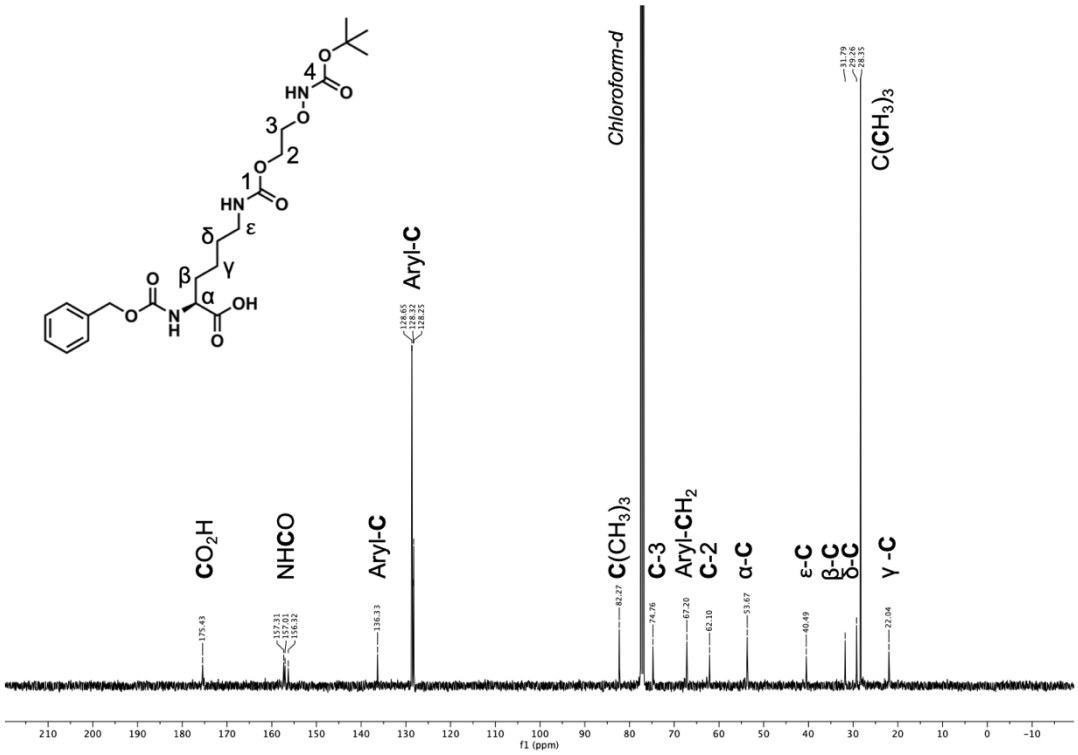

Compound 2

^{1}H NMR

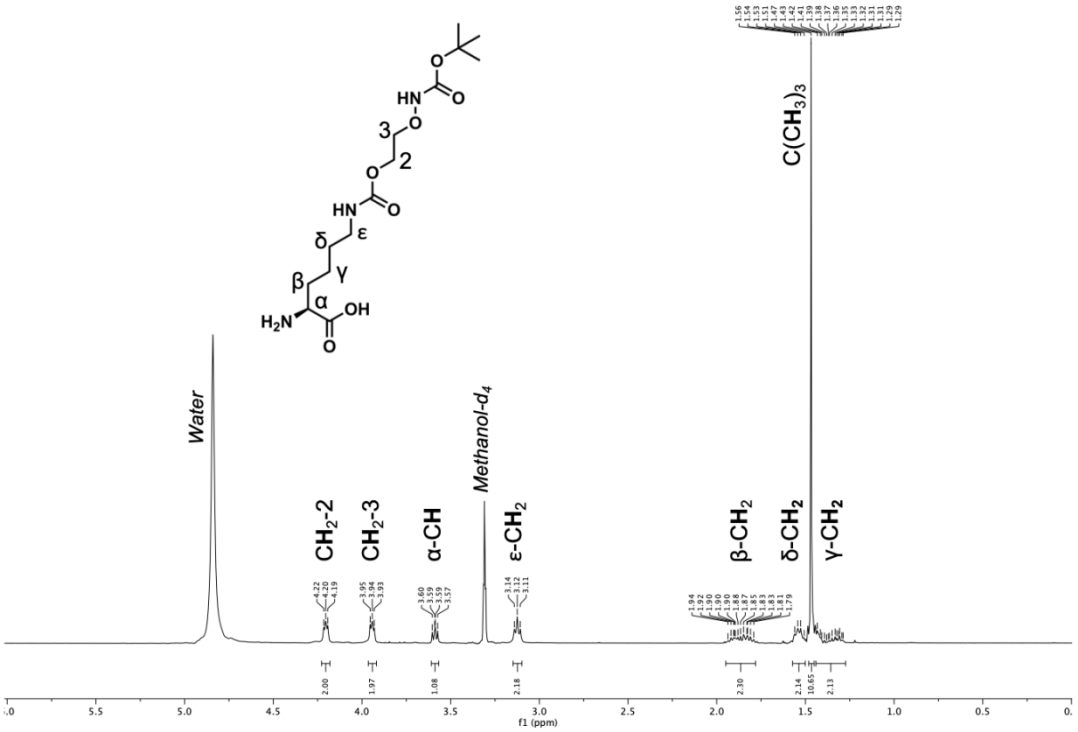

^{13}C NMR

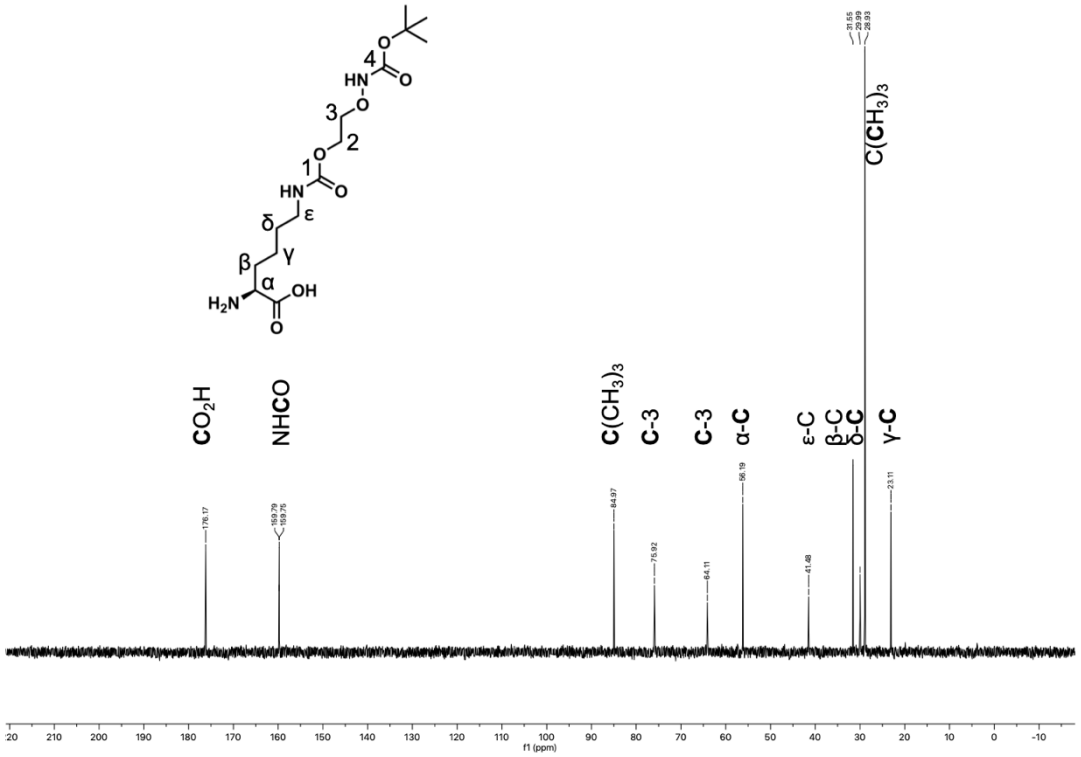

Compound 3c

^{1}H NMR

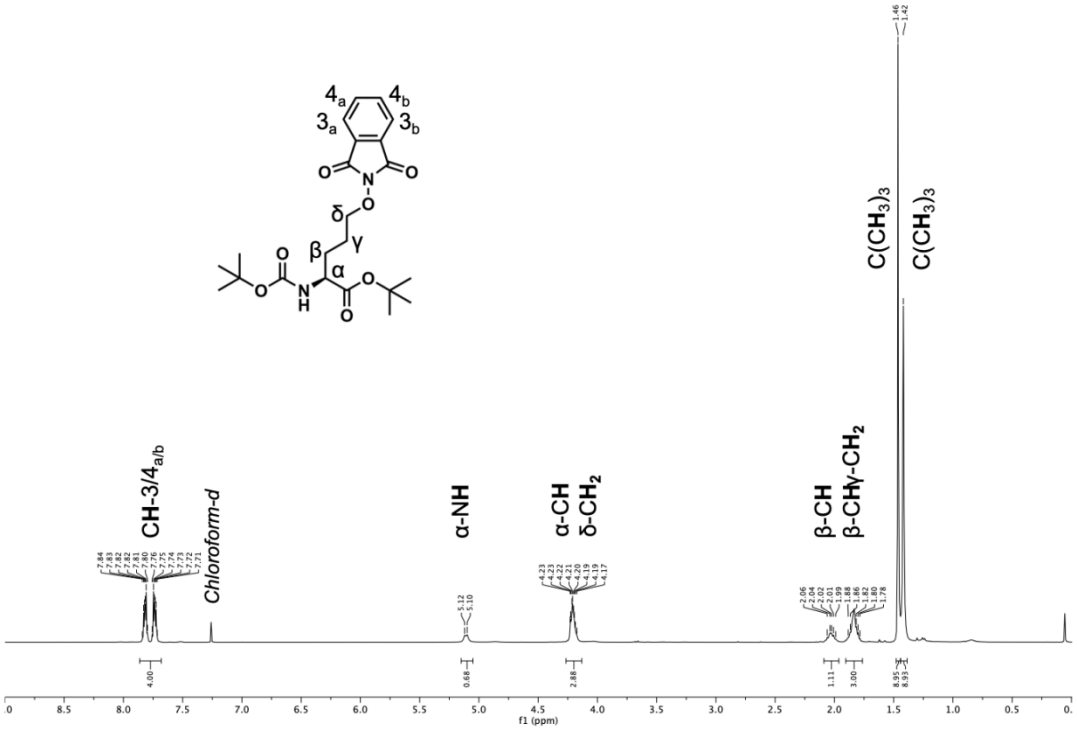

^{13}C NMR

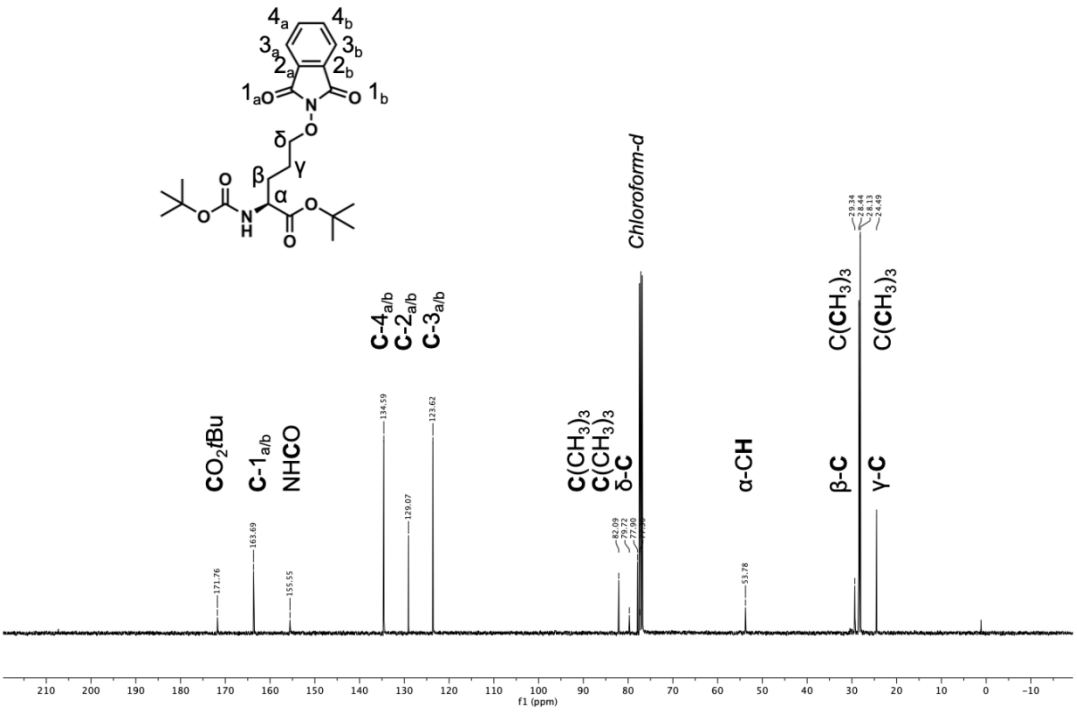

Compound 3d

^{1}H NMR

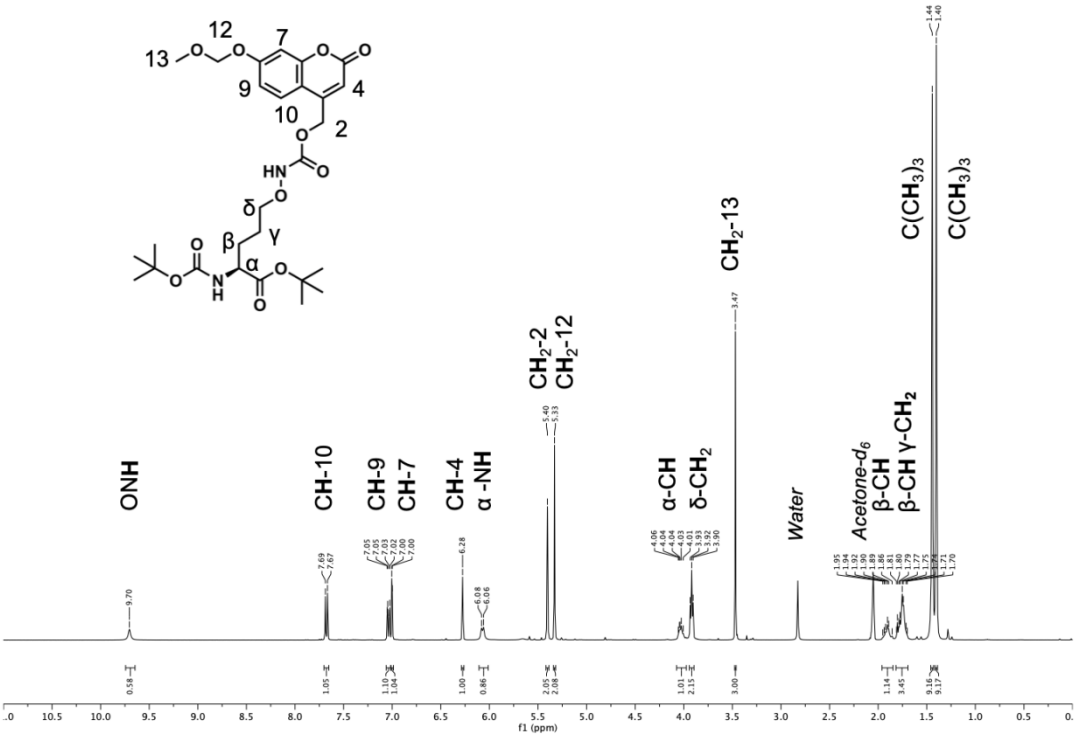

^{13}C NMR

Compound 3

^{1}H NMR

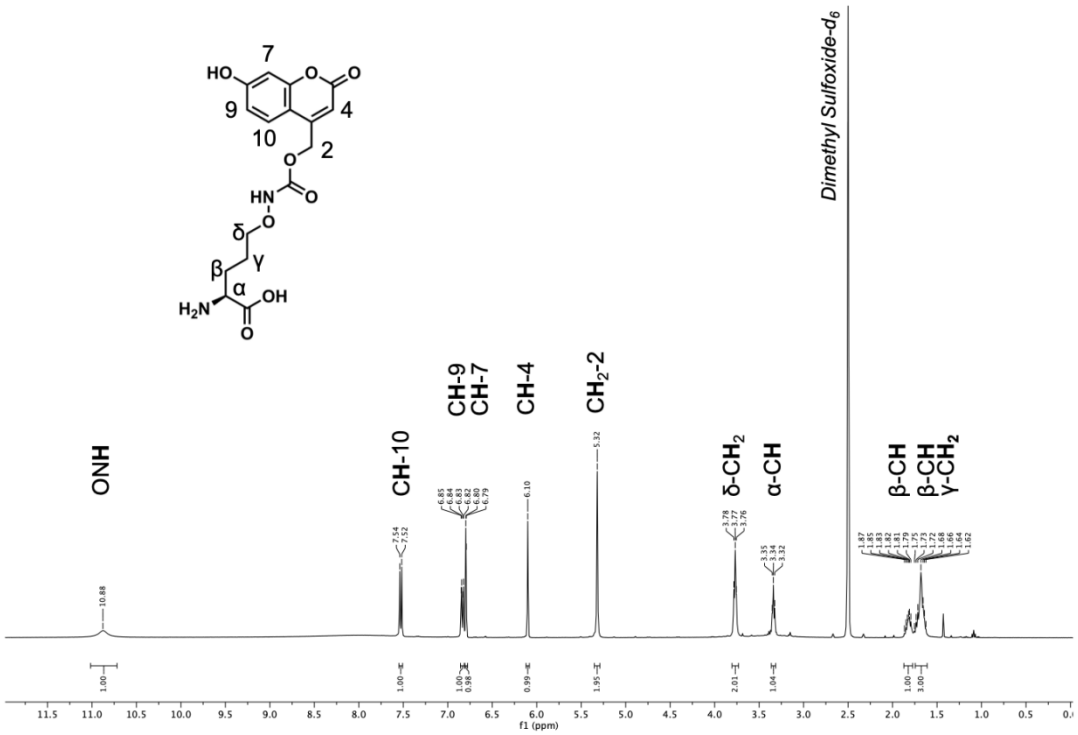

^{13}C NMR

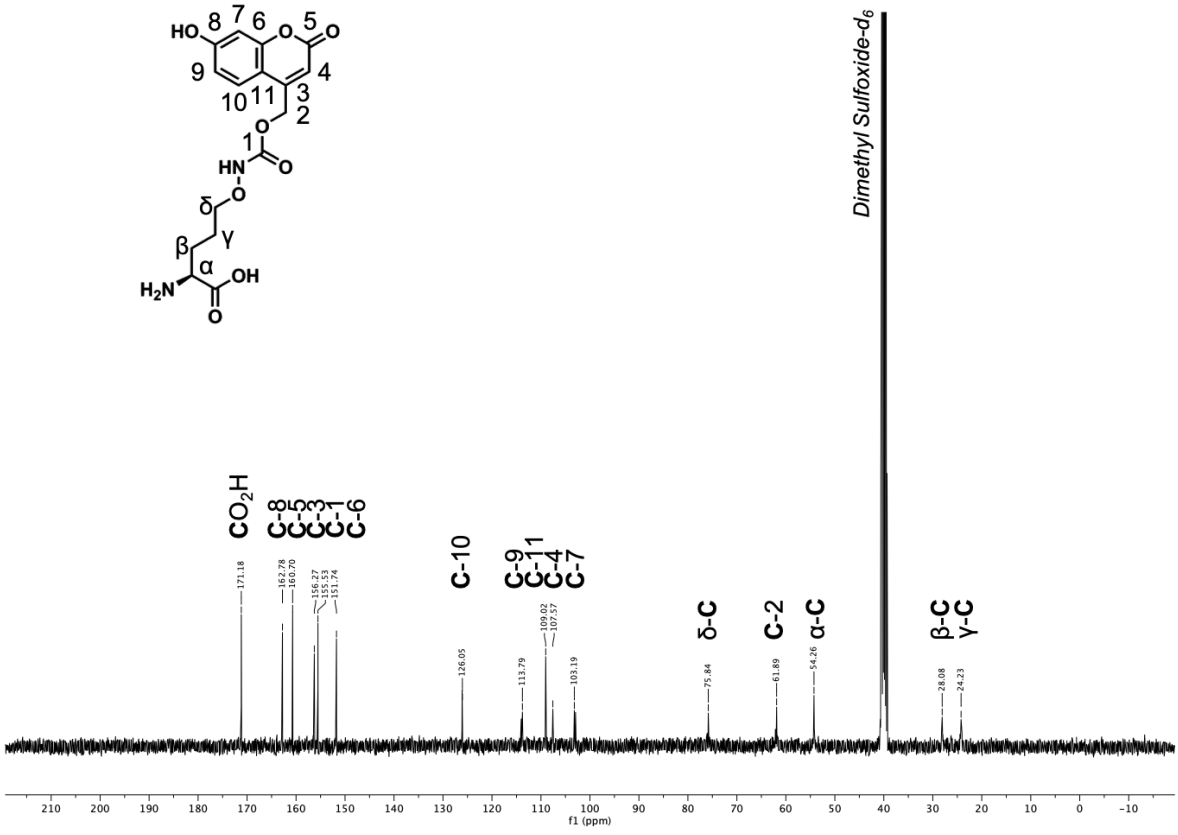

Compound 4

^{1}H NMR

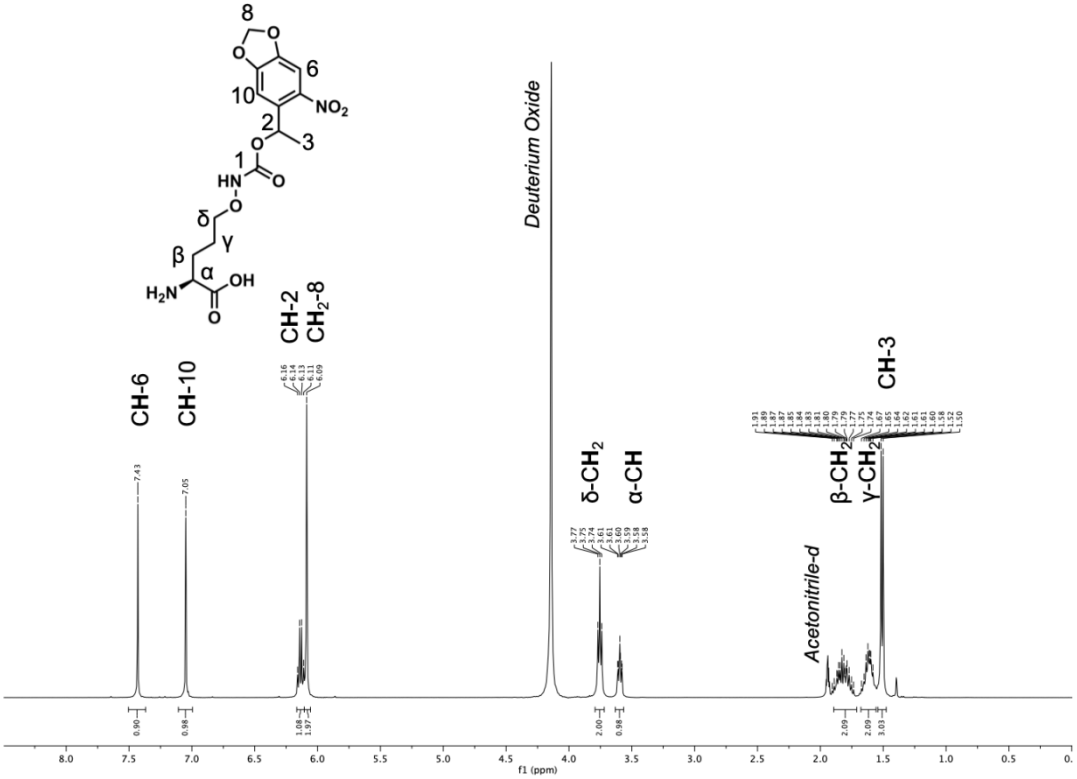

^{13}C NMR

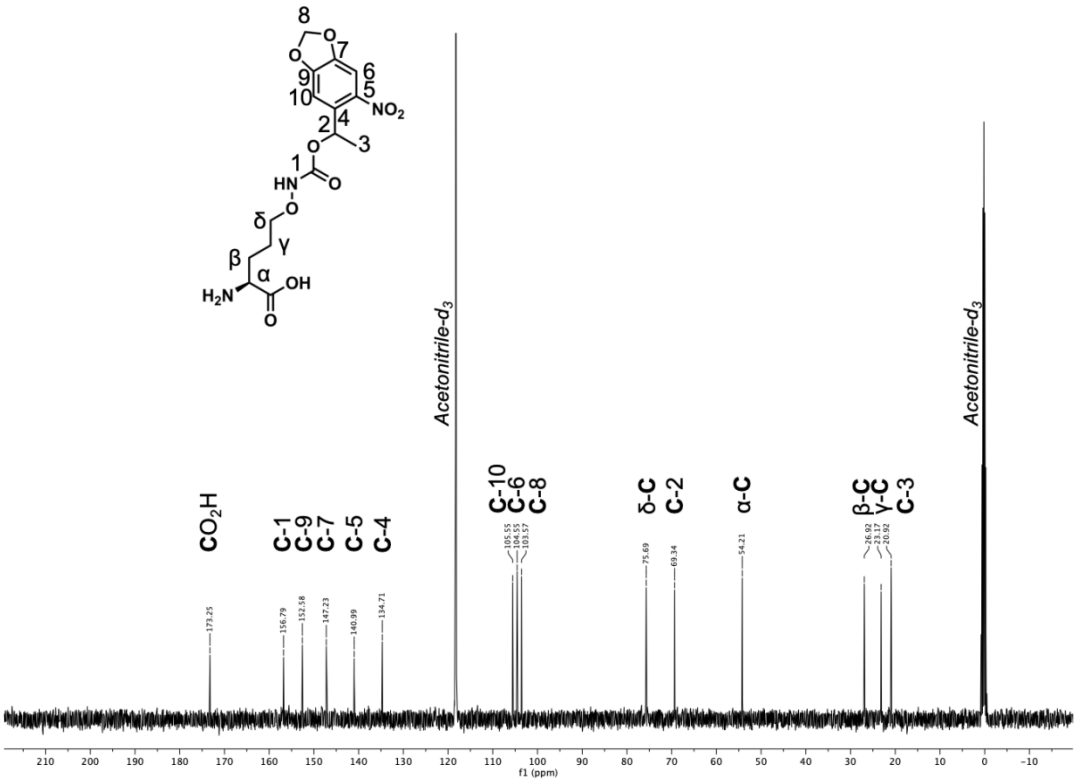

Compound 7

^{1}H NMR

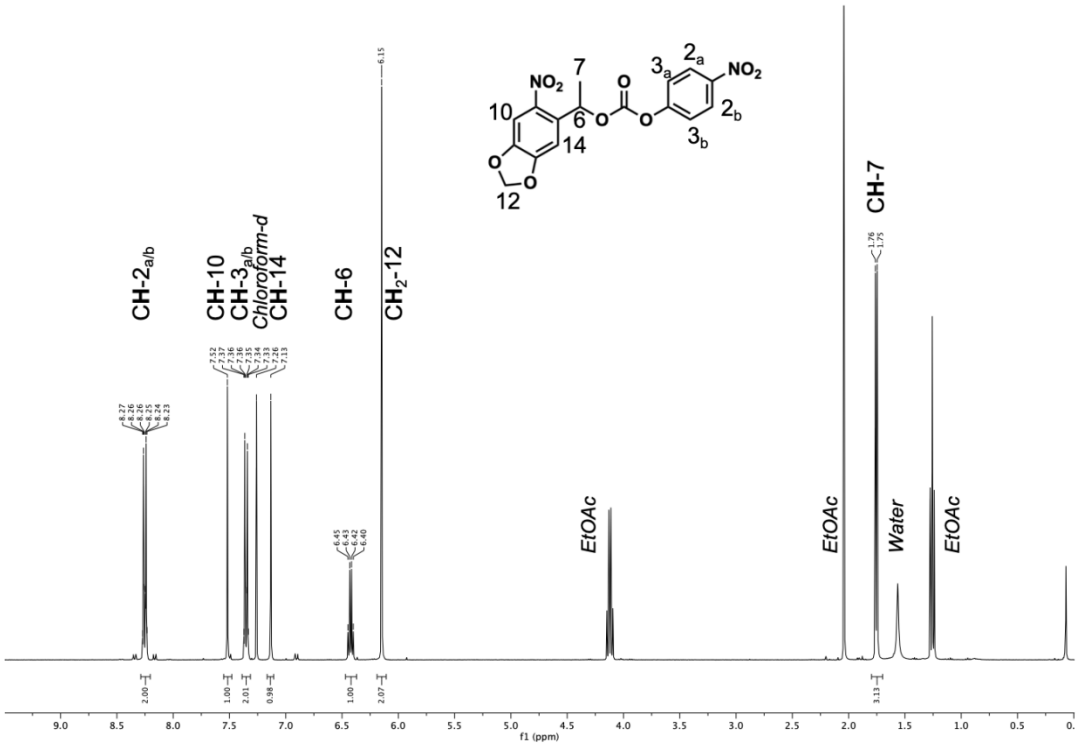

^{13}C NMR

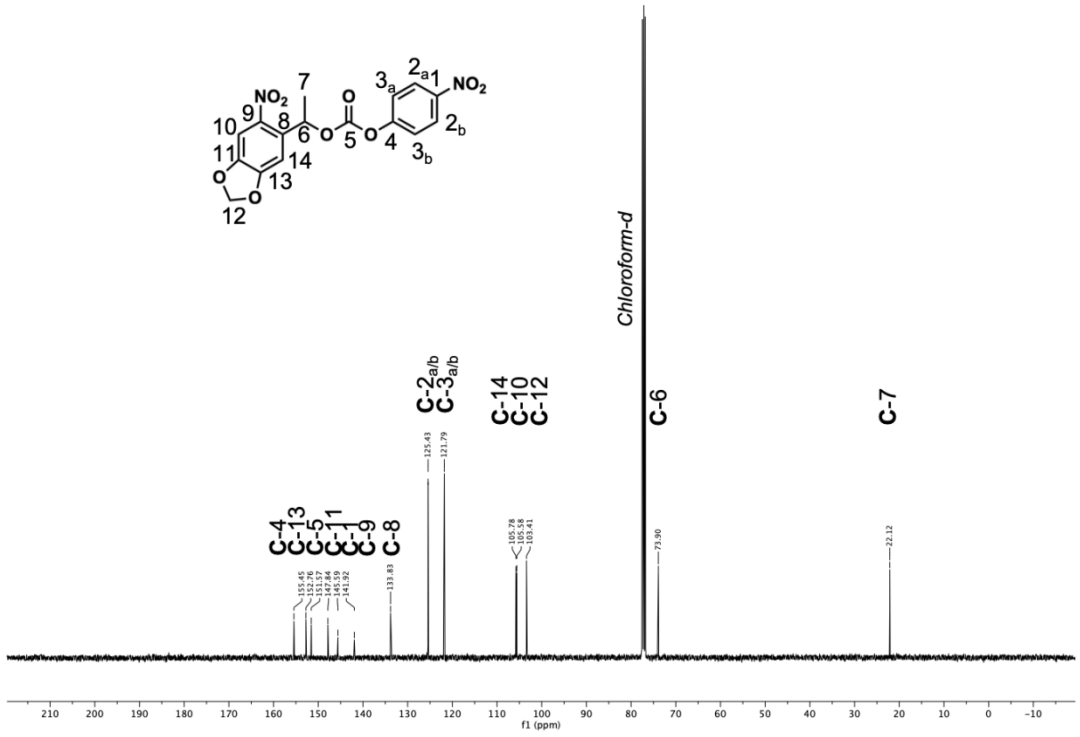

Compound 5

^{1}H NMR

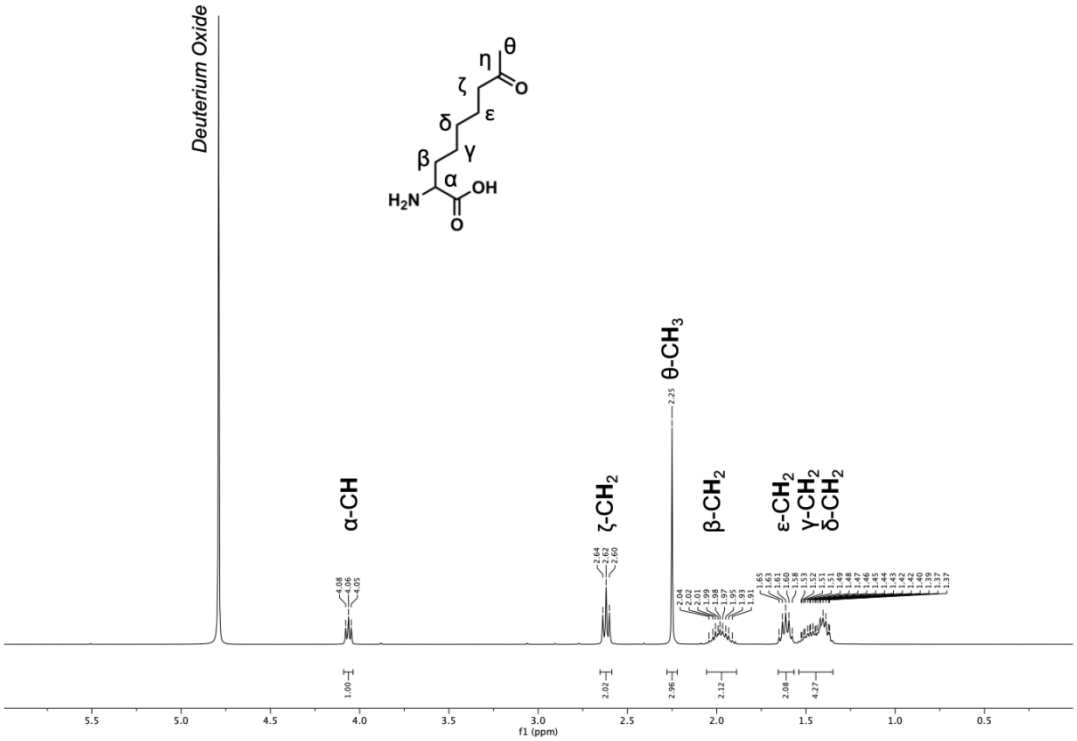

^{13}C NMR

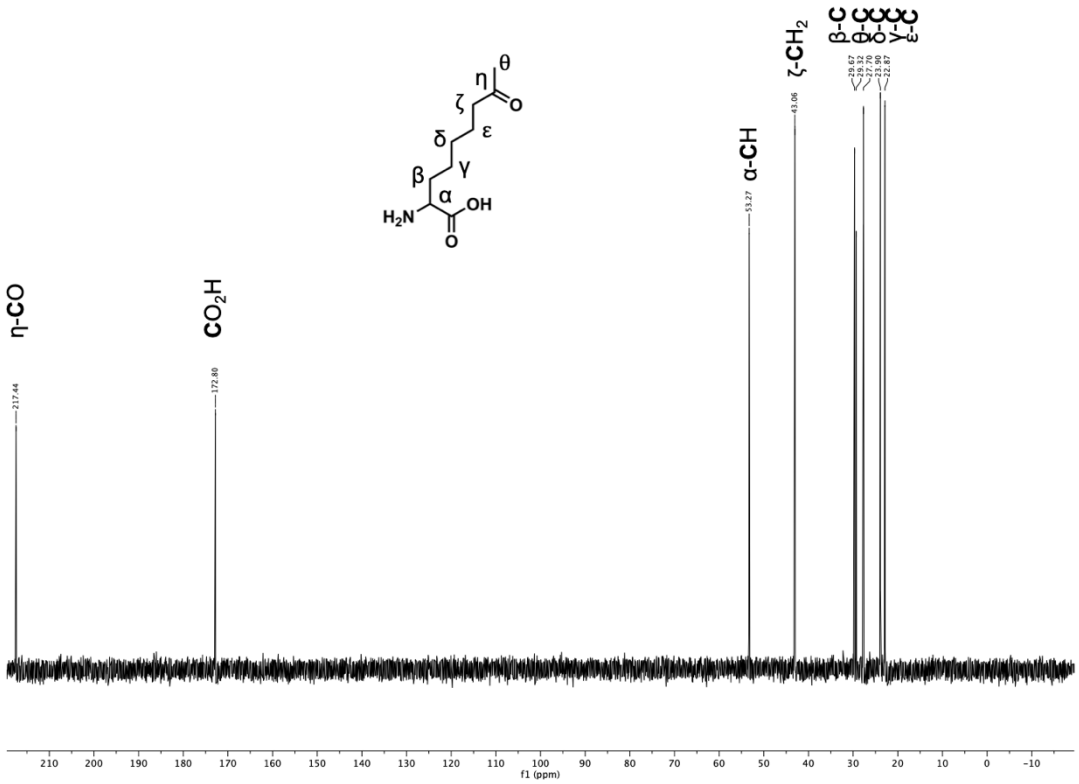

Compound 8

^{1}H NMR

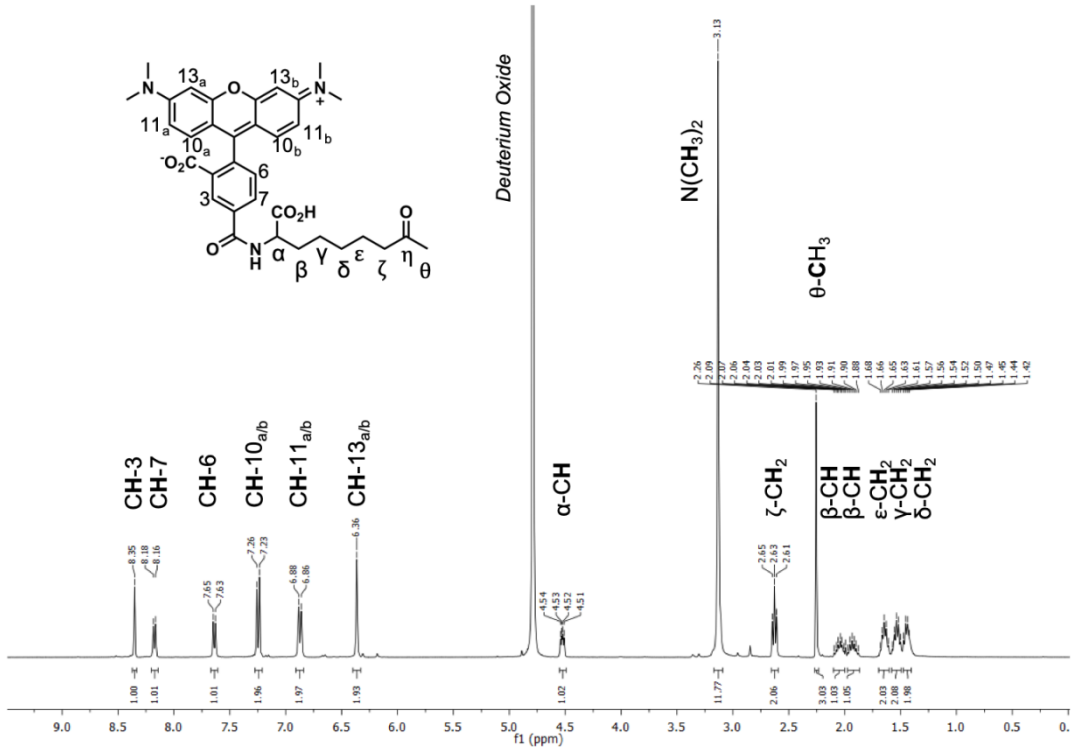

^{13}C NMR

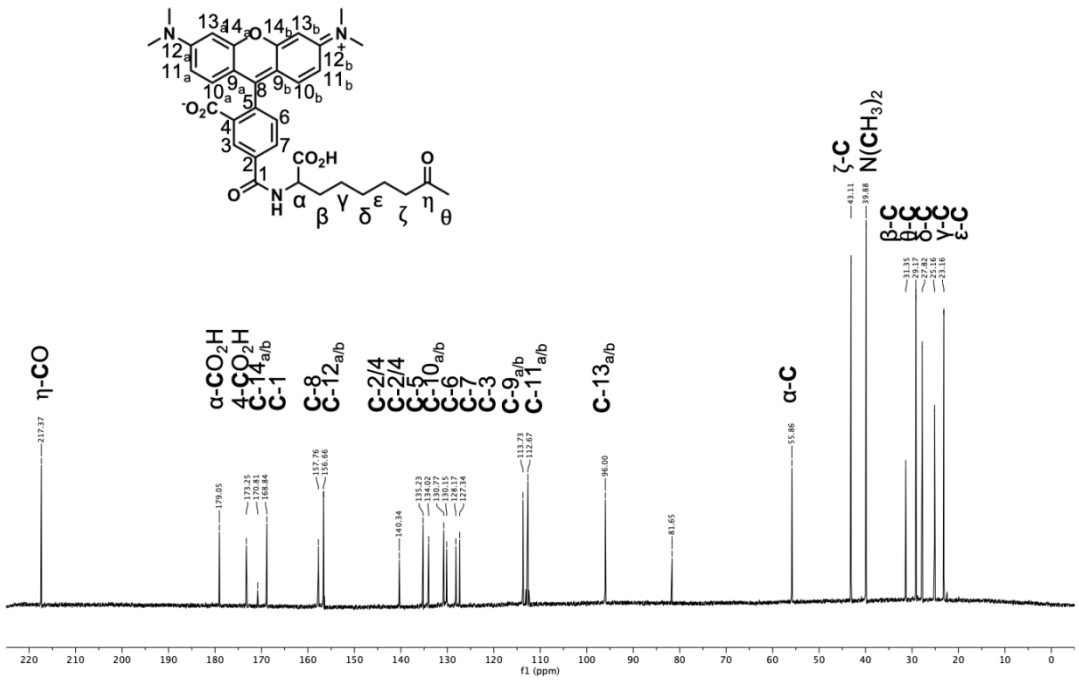

Compound 9

^{1}H NMR

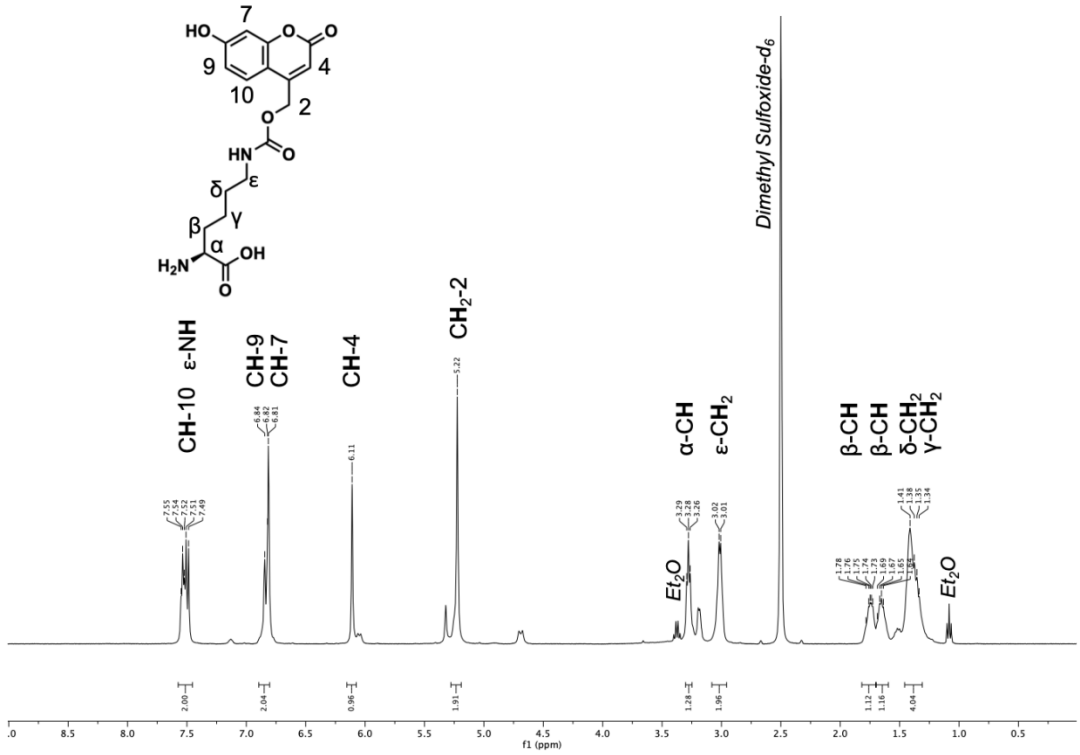

^{13}C NMR

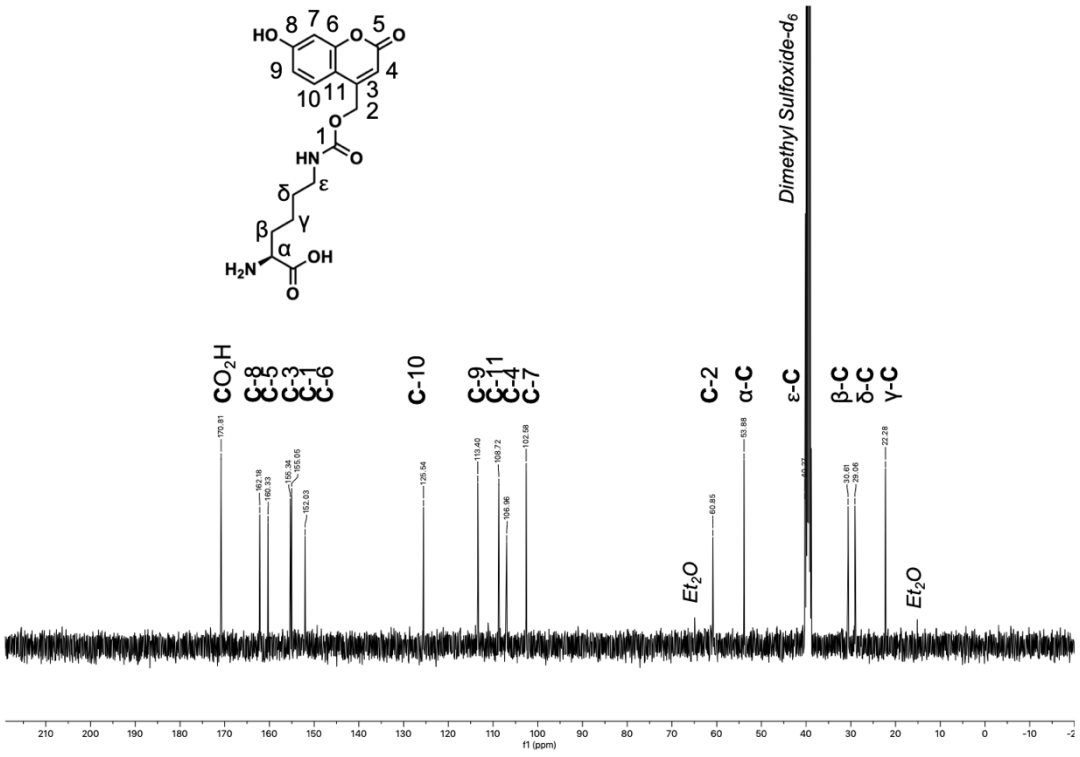

LC/MS Data

Irradiation of Ub 48U**3**

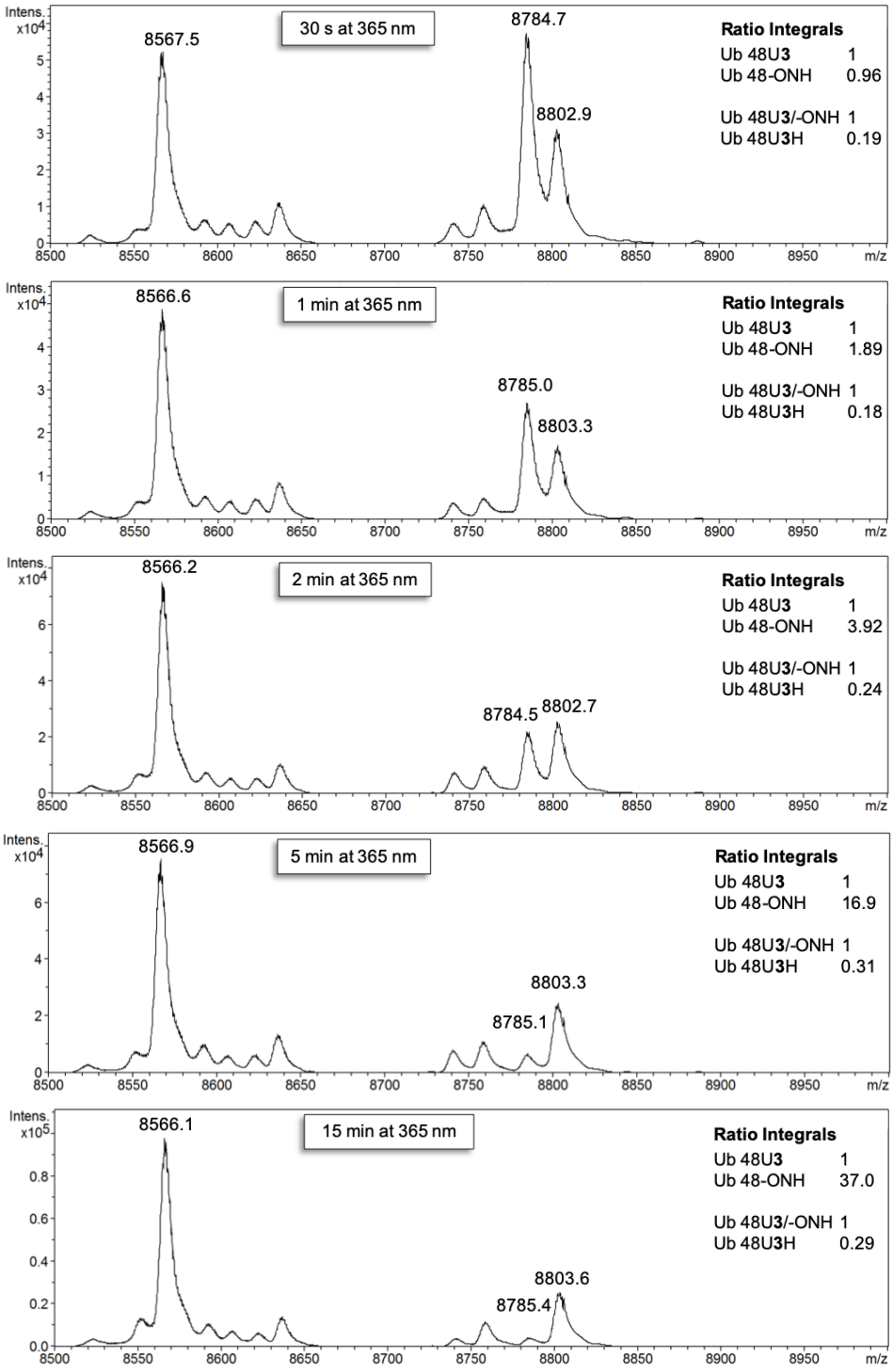

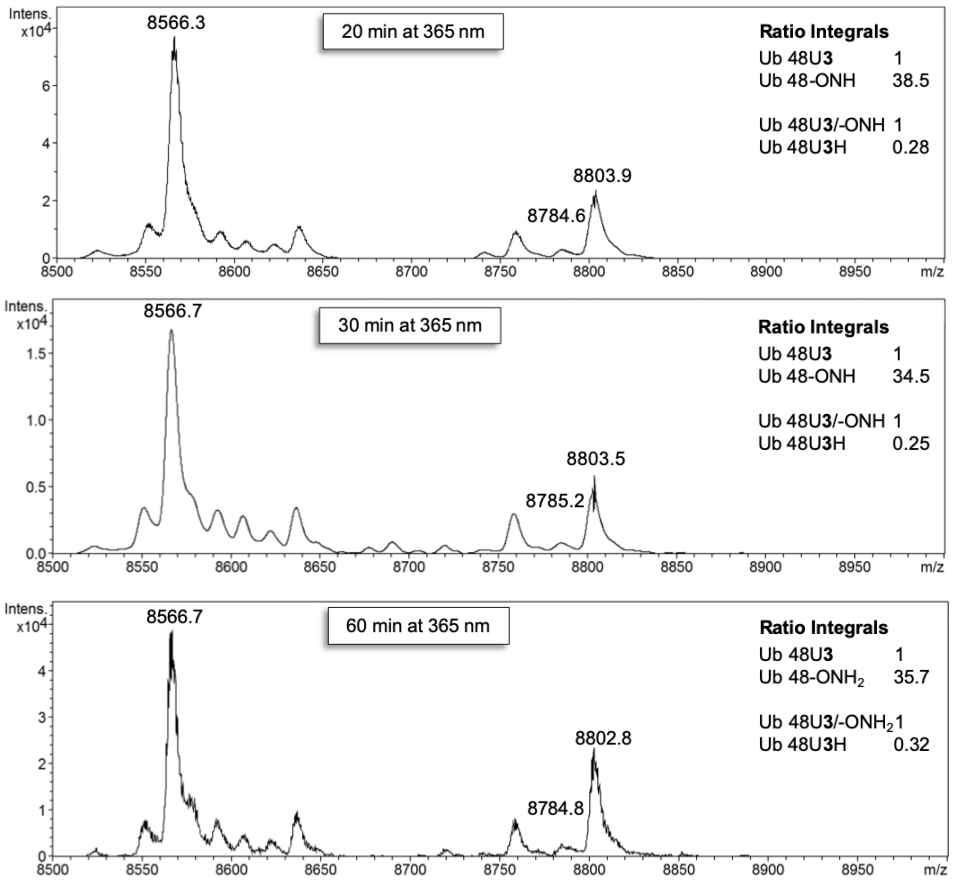

Ub 48U**3** – pH and Irradiation

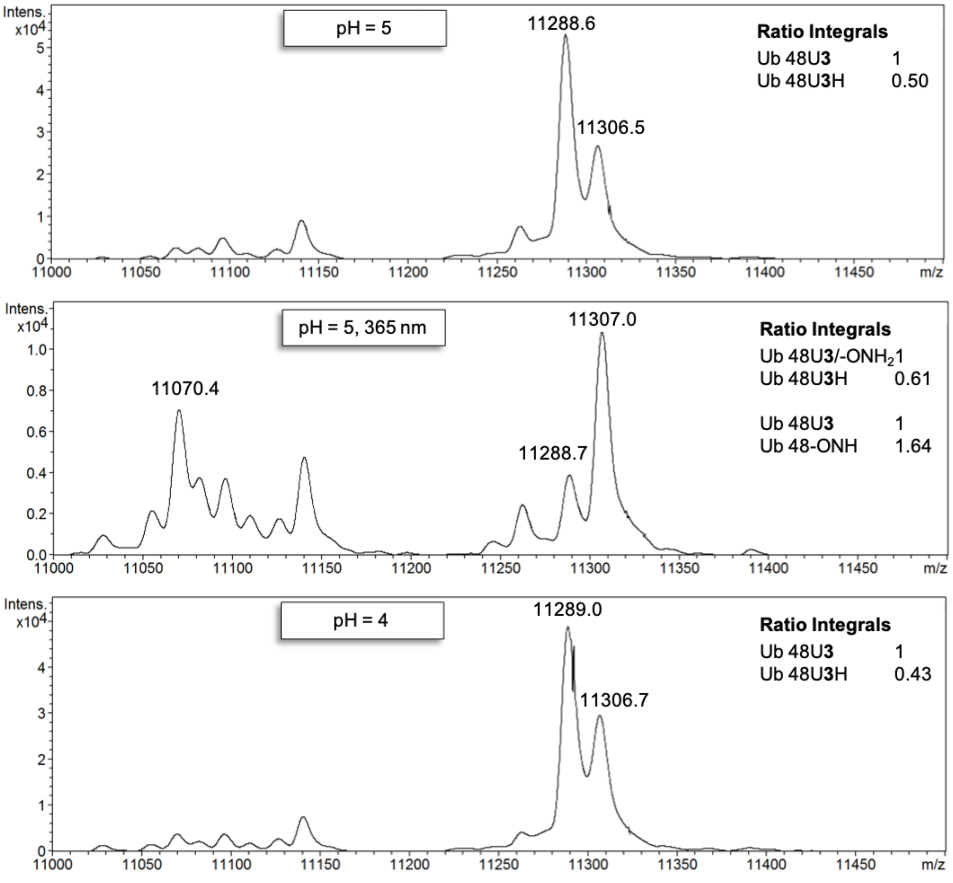

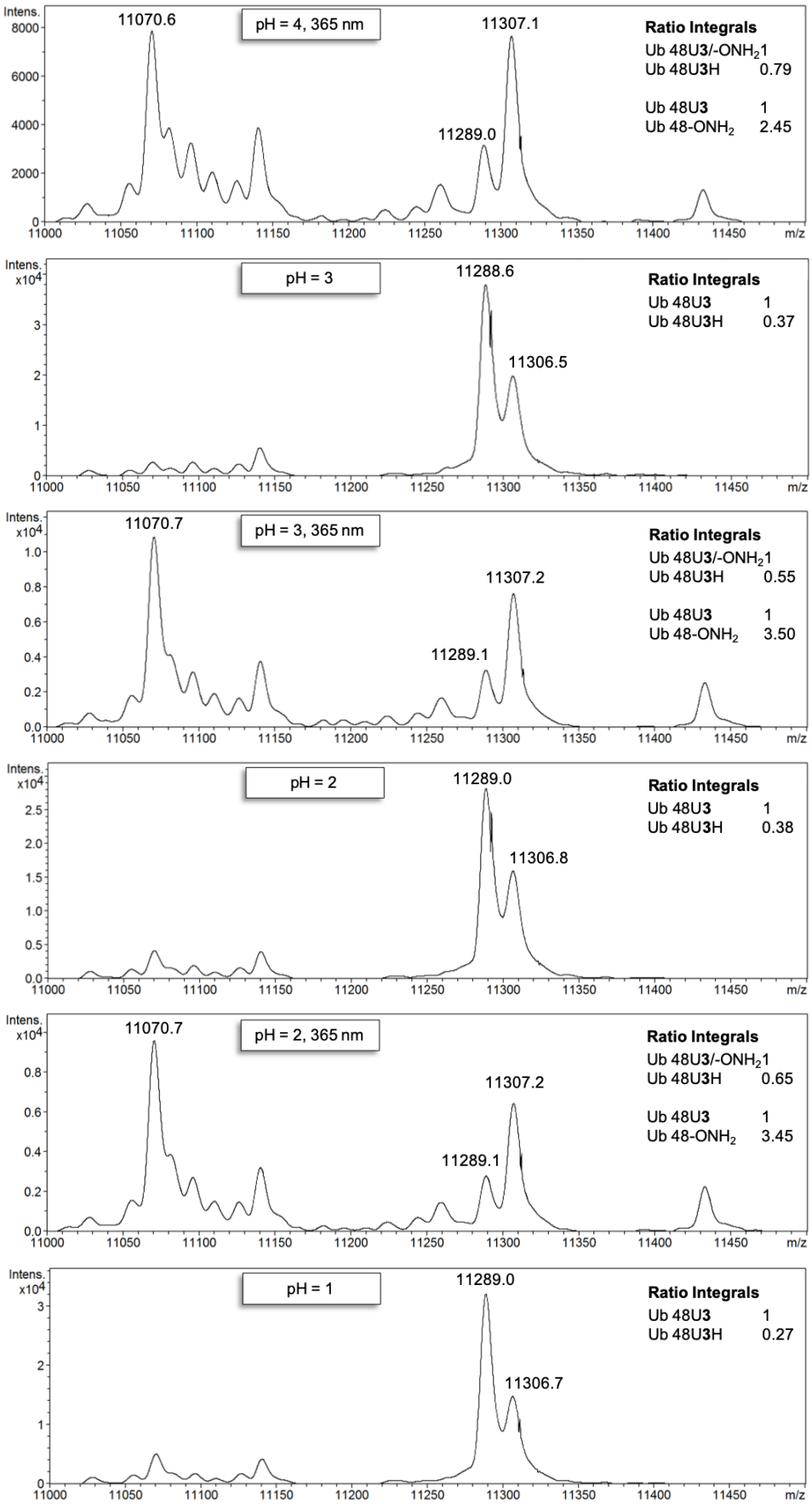
pH = 4, 365 nm
11070.6
11307.1
11289.0
Ratio Integrals
Ub 48U3/-ONH2 1
Ub 48U3H 0.79
Ub 48U3 1
Ub 48-ONH2 2.45
pH = 3
11288.6
11306.5
Ratio Integrals
Ub 48U3 1
Ub 48U3H 0.37
pH = 3, 365 nm
11070.7
11307.2
11289.1
Ratio Integrals
Ub 48U3/-ONH2 1
Ub 48U3H 0.55
Ub 48U3 1
Ub 48-ONH2 3.50
pH = 2
11289.0
11306.8
Ratio Integrals
Ub 48U3 1
Ub 48U3H 0.38
pH = 2, 365 nm
11070.7
11307.2
11289.1
Ratio Integrals
Ub 48U3/-ONH2 1
Ub 48U3H 0.65
Ub 48U3 1
Ub 48-ONH2 3.45
pH = 1
11289.0
11306.7
Ratio Integrals
Ub 48U3 1
Ub 48U3H 0.27
Intens.
m/z

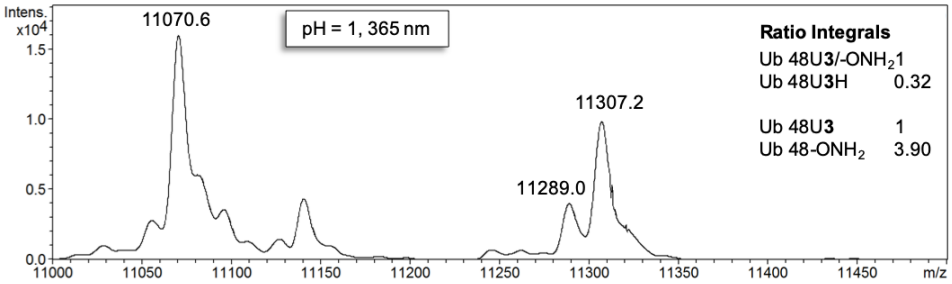

Ub 48U**3** – Expression in the presence of nicotinamide, without His tag

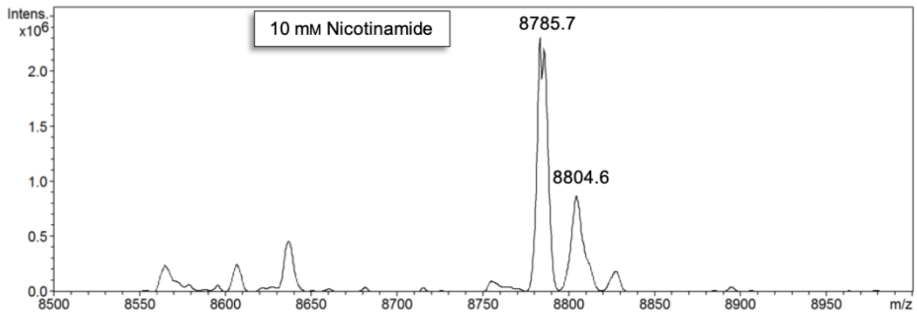

H1.2 206U**1**

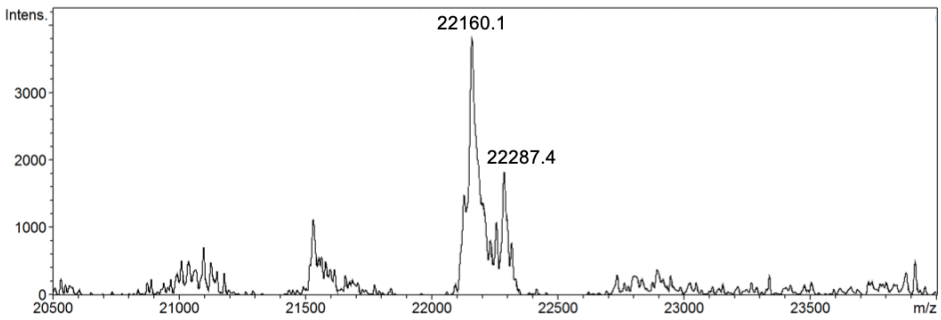

Cell growth (OD_{600}) of *E. coli* in the presence of coumarin and 7-hydroxycoumarin.